# The potential role of Rac signalling and the Planar Cell Polarity pathway in wiring of the Enteric Nervous System

Valentina Sasselli

February 2011

Division of Molecular Neurobiology
MRC National Institute for Medical Research
The Ridgeway
Mill Hill, London
NW7 1AA

Department of Cell and Developmental Biology
University College London

Thesis submitted to the University College London for the degree of Doctor of Philosophy

# Declaration of authenticity

This work has been completed in the laboratory of Vassilis Pachnis, in the Division of Molecular Neurobiology at the MRC National Institute for Medical Research, London. I, Valentina Sasselli declare that the work presented in this thesis is the result of my own independent investigation. Where information has been derived from other sources, I confirm that this has been indicated in the thesis. The analysis of Rac1 gene expression on *Sox10Cre;Rac1flox* embryos (section 3.1.1) was performed in collaboration with Dr Silvia Bogni (former post-doc in the laboratory, now at NeuroGlia Unit, San Raffaele Scientific Institute, Italy). I was supported by the Medical Research Council.

Valentina Sasselli

February, 2011

# Abstract

The functional development of the enteric nervous system (ENS) requires newly generated neurons and their progenitors to migrate to their appropriate sites, extend neurites, guide axons and dendrites to suitable locations and establish synaptic connections with the appropriate targets. Very little is known about the molecular mechanism underlying these processes.

Recent studies have suggested a potential role of Rho GTPases as intracellular regulators of several ENS developmental processes. However, the relative participation of specific members of the family in migration, neurogenesis and axonal guidance of enteric progenitors has not been addressed yet. Here, we investigate the *in vivo* role and genetic interaction of two members of the Rho-GTPase family, Rac1 and Rac3 in enteric neurogenesis. Taking advantage of the Cre/loxP recombination system and a Rac1 conditional inactivation mouse strain (*Rac1*$^{flox/flox}$), we generated a *Sox10Cre; Rac1*$^{flox/flox}$*;R26ReYFP* mouse line, where Rac1 gene is specifically ablated in the neural crest population which is also labeled by the expression of Yellow Fluorescent Protein. Secondly, we generated double Rac1;Rac3 mutant animals by crossing the *Sox10Cre;Rac1*$^{flox}$*;R26ReYFP* mouse line to a constitutive Rac3 KO strain (*Rac3*$^{-/-}$). *In vivo* and *in vitro* studies on Rac-deficient enteric neural crest cells and neurons showed distinctive roles for Rac1 and Rac3 in migration of enteric neural crest cells (ENCCs), in development of enteric neurons and in control of cell polarity within the developing ENS.

In addition, we also undertook a candidate gene approach to investigate the involvement of Wnt-signaling genes in enteric axon guidance and circuit formation. We found that two of the core components of the Planar Cell Polarity pathway, the Wnt receptor Frizzled 3 (Fzd3) and the Cadherin EGF LAG seven-pass G-type receptor 3 (Celsr3) are expressed specifically in ENCCs during embryonic development. Here we show, by using a combination of *in vivo* approaches that in mice deficient in either protein, enteric neurons had characteristic defects in neuronal tract formation and in patterning of individual axonal projections evident from early stages of ENS development. Furthermore, preliminary data show that these specific defects in ENS wiring might be the cause of impaired intestinal function and, therefore, provide the basis for understanding the aetiopathology of several idiopathic enteric neuropathies in humans.

# Table of contents

# List of figures

# List of tables

# Abbreviations

| | |
|---|---|
| **4-OHT** | 4-Hydroxytamoxifen |
| **5-HT** | 5-Hydroxytryptamine |
| **ACh** | Acetylcholine |
| **AChE** | Acetylcholinesterase |
| **ANS** | Autonomic nervous system |
| **AP** | Alkaline phosphatase |
| **ATP** | Adenosine triphosphate |
| **B-FABP** | Brain fatty acid binding protein |
| **BMN** | Branchiomotor neuron |
| **BMP** | Bone morphogenetic protein |
| **bp** | Base pair |
| **BSA** | Bovine serum albumine |
| **cDNA** | Complementary deoxyribonucleic acid |
| **Ca** | Calcium |
| **cds** | Coding determining region |
| **CGRP** | Calcitonin gene-related peptide |
| **ChAT** | Choline acetyltransferase |
| **CNS** | Central nervous system |
| **cRNA** | Complementary ribonucleaic acid |
| **DAPI** | 4’,6-diamino-2-phenylindole |
| **DiI** | 1,1'-dioctadecyl-3,3,3',3'-tetramethylindocarbocyanine perchlorate |
| **DMEM** | Dulbecco’s modified Eagle’s medium |
| **DMSO** | Dimethyl sulfoxide |
| **DNA** | Deoxyribonucleic acid |
| **dNTP** | Deoxyribonucleotide triphosphate |
| **D-PBS** | Dulbecco’s phosphate buffer saline |
| **DRG** | Dorsal root ganglion |
| **E** | Embryonic day |
| **ECM** | Extracellular matrix |
| **EDTA** | Ethylenediaminetetraacetic acid |
| **EdU** | 5-ethynyl-2´-deoxyuridine |
| **EGC** | Enteric glial cell |
| **EGF** | Epidermal growth factor |
| **ENCC** | Enteric neural crest cell |

| | |
|---|---|
| **ENK** | Enkephalin |
| **ENS** | Enteric nervous system |
| **FACS** | Fluorescent activated cell sorting |
| **FGF** | Fibroblast growth factor |
| **FN** | Fibronectin |
| **GABA** | Gamma (γ)-aminobutyric acid |
| **GAP** | GTPase-activating-protein |
| **GAPDH** | Glyceraldehyde 3-phosphate dehydrogenase |
| **GDI** | Guanine-nucleotide-dissociation inhibitors |
| **GDNF** | Glial cell line-derived neurotrophic factor |
| **GDP** | Guanosine diphosphate |
| **GEF** | Guanine-nucleotide-exchange factors |
| **GFAP** | Glial fibrillary acid protein |
| **GFP** | Green fluorescent protein |
| **gNCSC** | Gut neural crest stem cell |
| **GTP** | Guanosine triphosphate |
| **HISS** | Heat inactivated sheep serum |
| **HSCR** | Hirschsprung's disease |
| **ICC** | Interstitial cell of Cajal |
| **IPAN** | Intrinsic primary afferent neuron |
| **ISH** | *In situ* hybridisation |
| **LB** | Lysogeny broth |
| **KO** | Knock out |
| **MMC** | Migrating motor complex |
| **mRNA** | Messenger ribonucleic acid |
| **N** | Number of independent samples |
| **NAPDH-d** | Dihydronicotinamide adenine dinucleotide phosphate diaphorase |
| **NCAM** | Neural cell-adhesion molecule |
| **NC** | Neural crest |
| **NCC** | Neural crest cell |
| **NCSC** | Neural crest stem cell |
| **NO** | Nitric oxide |
| **(n)NOS** | (Neuronal) Nitric oxide synthase |
| **NPY** | Neuropeptide Y |
| **O/N** | Overnight |
| **PACAP** | Pituitary adenylyl cyclase activating peptide |

| | |
|---|---|
| **PBS** | Phosphate buffer saline |
| **PBT** | PBS/Triton or Tween |
| **PCP** | Planar cell polarity |
| **PCR** | Polymerase chain reaction |
| **PFA** | Paraformaldehyde |
| **PGP 9.5** | Protein gene product 9.5 (ubiquitin hydrolase) |
| **PNS** | Peripheral nervous system |
| **PSA** | Polysialic acid |
| **P** | Probability or postnatal day |
| **PTEN** | Phosphatase and tensin homolog |
| **RNA** | Ribonucleic acid |
| **RT** | Room temperature |
| **RT-PCR** | Reverse transcription polymerase chain reaction |
| **SDS** | Sodium dodecyl sulphate |
| **SEM** | Standard error of the mean |
| **SOM** | Somatostatin |
| **TAE** | Tris/Acetate/EDTA |
| **TH** | Tyrosine hydroxylase |
| **TK** | Tachykinins |
| **TNC** | Tenascin C |
| **TRITC** | Tetramethyl rhodamine iso-thiocyanate |
| **UK** | United Kingdom |
| **USA** | United States of America |
| **VIP** | Vasoactive intestinal peptide |
| **YFP** | Yellow fluorescent protein |

| | |
|---|---|
| **cm, mm, µm** | Centimetre, millimetre, micrometre |
| **g, mg, µg, ng** | Gram, milligram, microgram, nanogram |
| **ml, µl** | Millilitre, microlitre |
| **M, mM, µM** | Molar, millimolar, micromolar |
| **V** | Volt |
| **U** | Unit |
| **°C** | Celsius degree |
| **hr** | Hour |
| **‘, “** | Minute, second |

# Acknowledgements

"Why do you want to study the ENS?" Vassilis asked me when I first visited the lab in July 2006. I don't remember what I answered at that point (probably something diplomat-geek-ish), but I know that today I have more than a few reasons. And I really need to thank Vassilis for that, because by sharing his knowledge and passion for the ENS, he gave me strength, support and enthusiasm along my entire PhD.

I would also like to thank the members of my thesis committee, Iris Salecker and Patricia Salinas, for critical feedbacks on my project, and, especially Iris, for continuous support and *Drosophila* comments on my reports.

Thanks to Silvia for having shared her expertise and the Rac project with me.

Thanks to my "gut guru" Dipa for everything really, from the scientific to the "intimate" chats, for the support even thousands miles apart, for being such a positive and generous person. Your friendship means a lot to me.

Thanks to Nicole for having shared the "big" burden of being a *bfg* with me and being such a good thoughtful friend. Thanks also to little Ella and Hendrik, you are my favourite Germans.

Thanks to my housemates Ana and Emilie for having lived with me for so long, you should be writing a PhD thesis about it! Thanks, because we shared all the good and bad moments of all these years and you have always been ready to cheer up with a good pint of beer. Thanks also to Arnaud, for being part of our special London family.

Thanks to Catia and Reena, because you, ladies, made my everyday lab life. Thanks for your help, advices, jokes, *chai* breaks and your friendship.

Thanks to the Greeks (and Greek Cypriots!), you crazy bunch of people, thanks for sharing your humour and your way of doing, saying, seeing and eating things.

Thanks to all the other previous and present member of the lab, especially Rita and Tiffany for help and suggestions.

Thanks to Eileen for the invaluable help with formalities and for being so lovely and helpful.

Thanks to the people in MNB for feedbacks and technical help when I needed. And thanks for being such a friendly group of people, who I always enjoy to have a drink with.

Thanks to Colin, for all the weather and travel chats we had in the mornings.

Thanks to all the people taking care of my mouse lines. Thank you to Chloe for keeping up with the intense breeding schedule and to Pete for always cheering me up when staying until late.

Thanks to the NIMR bar, place of some of my deepest intellectual moments.

Thanks to my Nottingham friends, in particular Muriel and Juncal, because you are family for me and Ale, and you have always been so kind and supportive.

Thanks to my sister for always being there in all the small and big events of my life by giving me her support, advice and love, and thanks to Igor for sharing all the joys (and complaints) of the Sasselli's family.

Thanks to my dad, for continuously making me proud of having him as a parent. Thanks for the support and love you have always given me during the years.

Thanks to my mum, because she is, and always be, with me and my family.

Thanks to Ale, my love and happiness, my strength and safety. Thanks for your unconditional support and encouragement, your love and your caring during all these years. This thesis is dedicated to you.

# Chapter 1

# Introduction

## 1.1 Enteric nervous system anatomy and function

The enteric nervous system (ENS) is the largest and most complex division of the autonomic and peripheral nervous system (ANS and PNS) in vertebrates. The ENS contains a number of neurons (approximately 100 million in the human small intestine) comparable to that of the spinal cord and an array of neurotransmitters and neuromodulators similar to those found in the central nervous system (CNS). These components are organised in an integrating circuitry which controls motility of the intestine, exchange of fluids across the mucosal surface, blood flow and secretion of gut hormones. This highly integrated neural system is also referred to as the "brain-in-the-gut" (Wood, 1981) or the "second brain" (Gershon, 1998), because of its capability to function in the absence of input from the CNS.

### 1.1.1 Anatomy and organisation

The ENS is formed by an interconnected network of neurons, neuronal fibres and enteric glial cells embedded in the gut wall. Cell bodies of neurons and glial cells and neuronal processes are grouped into ganglia, which are organised into two major plexi: the myenteric plexus (or Auerbach's) and the submucosal plexus (or Meissner's) (Fig. 1.1). The structure of ganglia in both plexi is extremely compact and void of blood vessels, connective tissue or collagen fibrils, a structure highly reminiscent of that found within the CNS (Gabella, 1972). Myenteric ganglia are located in between the longitudinal and inner circular muscle layers and they are found around the circumference and along the length of the intestinal tube. Neuronal fibres are organized in thick interganglionic strands (primary plexus), finer parallel bundles lying below the primary plexus (secondary plexus) and thin neuronal processes innervating the gaps formed by the primary plexus (tertiary plexus). Secondary and tertiary fibres are those projecting to the effector systems such as musculature, glands and blood vessels (Furness *et al.*, 2000; Furness, 2006).

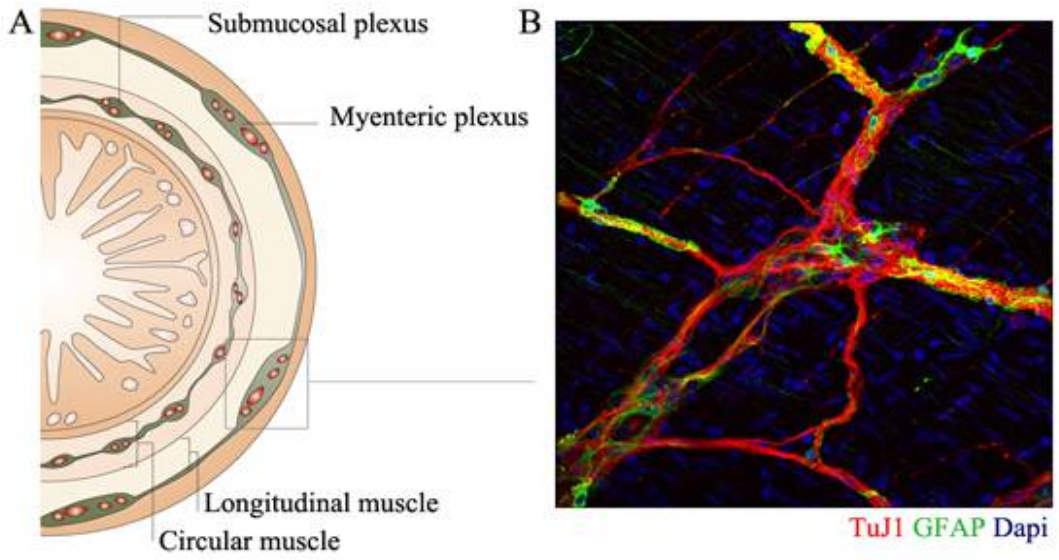


**Figure 1.1 The enteric nervous system anatomy**

**A**. Schematic representation of a cross section of the gastrointestinal tube showing the general organisation of tissues. Interconnected ganglia of the Myenteric plexus are localised between the longitudinal and circular muscle layers, whereas the submucosal plexus is found within the deeper submucosal layer. Image modified from (Heanue & Pachnis, 2007).

**B**. Immunofluorescence staining of a myenteric ganglion in adult mouse ENS. Neuronal ($Tuj1^+$, red) and glial ($GFAP^+$, green) cell bodies are compacted within the ganglia, while neuronal fibres, partially ensheathed by glial processes, interconnect ganglia and project to the underlying muscle cells ($TuJ1^-GFAP^-$). Nuclear counterstaining with DAPI (blue).

The morphology of the myenteric plexus, in terms of size and shape of ganglia and orientation of interganglionic strands, varies between different regions of the gut and between species (Gabella, 1990). Submucosal ganglia and fibres lie within the dense layer of connective tissue connecting the innermost mucosal tissue to the outer smooth muscle layers and they are generally smaller in size compared to their myenteric counterpart. The submucosal plexus is most prominent as a ganglionated network around the circumference and along the length of the small and large intestine. However, isolated ganglia occur also in the gastric and esophageal submucosa (Christensen & Rick, 1985). In large mammals, including humans, the submucosal plexus consists of an inner submucosal network (Meissner's) adjacent to the gut lumen and an outer plexus (Schabadasch's) in proximity of the circular muscle (Timmermans *et al.*, 2001).

Extrinsic innervation is also present within the gut tissue. Parasympathetic efferent and sensory afferent fibres of the vagus and pelvic nerves enter the gut at the esophagus/stomach and rectum respectively. They branch out at the level of the myenteric plexus forming a capillary network along the ENS (Aziz & Thompson, 1998; Powley, 2000). In addition celiac and mesenteric nerves, containing sympathetic efferent axons and sensory afferent fibres, follow the small arteries into the gut wall, branch alongside them until becoming undistinguishable within the enteric plexi (Furness, 2006).

### 1.1.2 Cellular components of the ENS: enteric glial cells

The ENS is formed by two major cellular populations: neurons and glial cells. Enteric glial cells (EGCs) are the most abundant cell type in the ENS, with a ratio close to 4:1 compared to neurons in large mammals (Gabella, 1981). EGCs create a widespread network along the gastrointestinal tract: they are found in close association with neurons within ganglia (Gabella, 1981), they accompany intrinsic and extrinsic fibres in the intestinal muscle and the mucosa (Bjorklund *et al.*, 1984; Gershon & Rothman, 1991) and they are also present around the epithelial crypt bases in the mucosa, where they are in close proximity with the epithelial cell layer (Ruhl, 2005) and they extend flat endfeet which ensheath the blood vessels supplying the ENS (Hanani & Reichenbach, 1994; Ruhl, 2005). Unlike Schwan cells of the PNS, EGCs do not form basal lamina and do not myelinate individual axons, instead they create a discontinuous sheath around multiaxonal bundles (Gabella, 1981). Morphologically, EGCs are small and irregular shaped with several cytosolic processes, which give them a star-shaped morphology similar to CNS astrocytes. Ultrastructurally, ECGs are packed with 10 nm intermediate filaments which cross the cell body and form longitudinal bundles within the glial processes. The main protein associated with these filaments is the glial fibrillary acid protein (GFAP) (Gabella, 1981; Jessen & Mirsky, 1980). In addition EGCs express the intermediate filament protein vimentin, the enzyme glutamine synthetase, the surface antigen Rat neural antigen 2 (Ran-2) (Jessen & Mirsky, 1983) and the calcium-binding protein S-100β (Ferri *et al.*, 1982). In mouse, it has also been shown that mature

EGCs specifically express brain fatty acid binding protein (B-FABP) and the transcription factor Sox10 (Young *et al.*, 2003), while, in human, also the low affinity neurotrophin receptor p75 (Kondyli *et al.*, 2005).

Physiologically, EGCs provide structural support to the ENS, since they stabilize ganglia and fibres by firmly anchoring them through $GFAP^+$ filaments, and they are also able to actively respond to mechanical stimulation by increasing the expression of the immediate early gene *c-fos* (Sharkey *et al.*, 1999) and the levels of intracellular calcium ($Ca^{2+}$) (Zhang *et al.*, 2003). In addition, the enteric glia have a role in the maintenance of neuronal and epithelial/vascular integrity, neurotransmission and immune responses. In murine models, EGC ablation led to neuronal degeneration (Bush *et al.*, 1998) and to changes in neurochemical coding and function of enteric neurons (Aube *et al.*, 2006). Moreover, loss of enteric glia resulted in vascular lesions in the mucosa and submucosa and fulminant intestinal inflammation, as a possible consequence of a breakdown in the intestinal epithelial cell layer (Bush *et al.*, 1998; Cornet *et al.*, 2001). Recent evidence suggests that EGCs are able to control intestinal barrier function and inflammation via release of S-nitrosoglutathione (Savidge *et al.*, 2007). Similarly, EGCs are able to produce (and respond to) cytokines (Ruhl *et al.*, 2001a; Ruhl *et al.*, 2001b), increase GFAP expression and actively proliferate in response to inflammatory insults of the mucosa (Bradley *et al.*, 1997), thus suggesting a role during immune responses. Enteric glia have also been implicated in neurotransmitter production and/or inactivation by immunohistochemical data which have shown that components of the glutamatergic signalling such as glutamine synthetase (Jessen & Mirsky, 1983), of the GABAergic signalling such as the high affinity γ-aminobutyric acid (GABA) transporter GAT 2 (Fletcher *et al.*, 2002) and of the nitrergic signalling such as the nitric oxide (NO) precursor L-arginine (Nagahama *et al.*, 2001) are almost exclusively expressed in EGCs. EGCs are further involved in responses to numerous neurotransmitters and neuroligands (Ruhl, 2005), indicating an active participation by enteric glia in information processing within the ENS.

### 1.1.3 Cellular components of the ENS: enteric neurons

Hundreds of thousands (in mouse) to millions (in human) of neurons are present along the gastrointestinal tract in different species (Gabella, 1987). Although organized in recognizable anatomical structures such as the ganglia, enteric neurons lack the morphological and functional segregation seen, for example, in the spinal cord, the medulla or the midbrain. Each enteric ganglion includes neurons of different morphology, biochemical nature and function within and along the intestinal wall. The absence of a precise functional topography has presented a major problem to scientists who tried in the past to unravel the enteric neural circuitry and function. A partial solution to this problem came from a combination of experimental approaches, namely morphology, physiological properties, histochemical and immohistochemical reactivity, primary transmitters and pattern of axonal projections (to targets and from presynaptic components). The ENS contains 14-20 types of neurons, depending on region and species. The most extensive data on enteric neuron classification has been obtained in guinea-pig, in which 15 neuronal subtypes have been identified (Brookes, 2001; Furness, 2006) (Table 1.1). However, there are several findings which suggest a conserved morphology, neurotransmitter biochemistry and projection pattern of similar functional subtypes of neurons in other mammals, such as mouse (Qu *et al.*, 2008), pig (Brehmer, 2006) and human (Anlauf *et al.*, 2003; Brehmer, 2006).

**Table 1.1 Classes of enteric neurons in guinea-pig small intestine**

| *myenteric neurons* | *Morp* | *Projection* | *EP* | *Chemical coding (primary transmitter in bold)* | *species differences* |
|---|---|---|---|---|---|
| primary afferent neuron (IPAN) | II | oral, anal, circumferential to the M, MP, SMP | AH | **ChAT**/**TK**/orexin/IB4/NeuNcyt/$NK_3$ receptor±Calb±Calr | CGRP found in many species |
| excitatory circular muscle neuron | I | short oral | S | **ChAT**/TK/ENK/GABA | ChAT/TK conserved |
| | I | long oral | S | **ChAT**/TK/ENK/NFP | |
| inhibitory circular muscle neuron | I | short anal | S | **NOS**/**VIP**/**PACAP**/ENK/NPY/GABA | NOS/VIP conserved |
| | I | long anal | S | **NOS**/**VIP**/**PACAP**/Dyn/GRP/NFP | |
| excitatory longitudinal muscle neuron | s/I | local | S | **ChAT**/Calr/TK | ChAT/TK conserved |
| inhibitory longitudinal muscle neuron | I | local | S | **NOS**/**VIP**/GABA | NOS/VIP conserved |
| ascending interneuron | I | oral | S | **ChAT**/Calr/TK/ENK | n/i |
| descending interneuron (local reflex) | I | anal to the MP/SMP | S | **ChAT**/NOS/VIP±GRP±NPY | n/i |
| (secretomotor and motility reflex) | I | anal to the MP/SMP | S | **ChAT**/**5-HT** | 5-HT conserved |
| (migrating mioelectric complex) | III | anal to the MP | S | **ChAT**/SOM | n/i |
| intestinofugal neuron | I | to the PS ganglia | S | **ChAT**/VIP/NOS/GRP/CCK/ENK | ChAT/VIP conserved |
| ***submucosal neurons*** | | | | | |
| primary afferent neuron (IPAN) | II | to the M, MP | AH | **ChAT**/TK/orexin/IB4/NeuNcyt/Calb | CGRP found in many species |
| secretomotor neuron | IV | short, local | S | **ChAT**/NPY/CCK/SOM/CGRP/Dyn/GAL/NMU | n/i |
| secretomotor/vasodilator neuron | I | short, local | S | **VIP**/CART/CRF/GAL/PACAP/NMU | VIP conserved |
| | stellate | short, local | S | **ChAT**/Calr/Dyn | n/i |
| interplexus interneuron | uniaxon | to the MP | S | **VIP**/GAL/NMU (NOS?) | n/i |

Abbreviations: I-III: Dogiel type I-III morphology, IV: type IV morphology, 5-HT: 5 hydroxytryptamine, AH: long after-hyperpolarization neuron, Calb: calbindin, Calr: calretinin, CART: cocaine and amphetamine-regulated transcript peptide, CCK: cholecystokinin, CGRP: calcitonin gene-related peptide, ChAT: choline acetiltransferase, CRF: corticotrophin-releasing factor, Dyn: dynorphin, ENK: enkephalin, EP: electrophysiology, GABA: gamma amino-butyric acid, GAL: galanin, GRP: gastrin-releasing peptide, IB4: isolectin B4, M: mucosa, Morp: morphology, MP: myenteric plexus, n/i: not investigated, NeuNcyt: cytoplasmic NeuN, NFP: neurofilament protein triplet, NK: neurokin, NMU: neuromedin U, NOS: nitric oxide synthase, NPY: neuropeptide Y, PACAP: pituitary adenylyl cyclase-activating peptide, PS: prevertebral sympathetic, s/I: small Dogiel type I morphology, S: fast excitatory postsynaptic potential neuron, SMP: submucosal plexus, SOM: somatostatin, TK: tachykinin (Substance P and neurokinin-A), VIP: vasoactive intestinal peptide (Bornstein, 2009; Brookes, 2001; Furness, 2006; Furness, 2009).

#### *1.1.3.1 Morphology*

Around the end of the 19th century the Russian histologist Alexander S. Dogiel was the first to provide a comprehensive description and classification of neurons in the myenteric and submucosal plexus of several large mammals. This morphological classification still remains in place and describes three neuron types referred as Dogiel types I, II and III. Dogiel type I and II are the principal morphological classes of neurons in the ENS. Dogiel type I neurons have flat, slightly elongated and stellate cell bodies with many (4-20) dendrites and one axon. Many functional subclasses of enteric neurons share this morphology and, depending on their targets, they have axons that project for relatively long distances through interganglionic strands. Dogiel type II neurons have large oval cell bodies with several axons arising directly from the cell soma (multipolar neurons) or from a single initial process (pseudo-unipolar neurons). The majority of myenteric and submucosal Dogiel type II neurons project to the mucosa and they represent a neurochemical and functional homogenous subclass of enteric neurons identified as intrinsic primary afferent neurons (IPAN, see below). In addition, myenteric Dogiel type II neurons have long processes which extend circumferentially through interganglionic strands and produce a varicose branching within their own or neighbouring ganglia, whereas submucosal Dogiel type II neurons have short processes supplying adjacent ganglia. Dogiel type III neurons, described also as filamentous neurons, have medium-short branched dendrites (2-10) which become thinner as they are followed from the cell body. Further refinements to this classification were made by W. Stach and A. Brehmen, who identified new morphologies designated as types IV to VII and small Dogiel type I (Brehmer, 2006; Stach, 1989; Stach *et al.*, 2000). In particular, Type IV neurons have a single axon that project vertically, short dendrites which do not branch as much as Dogiel type III neurons and they identify as secretomotor neurons.

#### *1.1.3.2 Electrophysiology*

Differences in electrical and synaptic behaviour provide a basis for classification of enteric neurons into two main subgroups defined as after-hyperpolarisation (AH) type and synaptic (S) type. Both classes are seen in guinea-pig, rat and human. AH neurons have prominent and

prolonged after-hyperpolarising potential that can last from about 2 to 30 seconds following their action potential. AH neurons do not exhibit fast excitatory postsynaptic potential (EPSP) and, when EPSPs are recorded, they are slow and small in amplitude. Conversely, S neurons have a short duration after-hyperpolarising potential lasting 20-100ms, followed by a fast EPSP which is of sufficient amplitude to evoke action potentials (Furness, 2006). AH type electrophysiological behaviour is characteristic of Dogiel type II cells, whereas S-type properties are typical of a variety of enteric neurons, including Dogiel type I and III neurons.

#### *1.1.3.3 Chemical coding*

Along with the morphological and electrophysiological investigation of enteric neurons, a useful approach to define specific neuronal classes is the identification of chemical attributes of enteric neurons. Immunohistochemical analyses have shown that unique combinations of neurotransmitters, their synthesising enzymes and other peptides (i.e. chemical code) is contained in functionally defined classes of neurons (Brookes, 2001; Furness, 2000). Furthermore, the chemical coding analysis has also proved that individual neurons are able to express and release several neurotransmitters (plurichemical transmission), although, usually, only one of them has a dominant role (primary transmitter). Some aspects of the chemical code, such as primary transmitters, are generally similar between gut regions and are highly conserved between different species (Furness *et al.*, 1995).

#### *1.1.3.4 Functional classes of enteric neurons*

As a result of the multidisciplinary efforts in classification of enteric neurons, at least 12 functional types of enteric neurons can be identified unambiguously in every mammal (Table 1.1). **Intrinsic primary afferent (or sensory) neurons (IPANs)** are AH-type multipolar neurons and they project to the mucosa where they detect chemistry (i.e. 5-hydroxytryptamine, 5-HT, and ATP release), texture and volume of intestinal contents (i.e. stress and tension of the mucosa) and they relay this information to neurons lying within the two ganglionated plexi. The chemical coding of IPANs relies mainly on acetylcholine (ACh) and its synthesising enzyme choline acetyltransferase (ChAT), on tachykinins (TK) such as Substance P and neurokinin A, and, in

many species, on calcitonin gene-related peptide (CGRP). **Motor neurons** have a single axon which innervates the outer muscle (longitudinal and circular muscle) and they subdivide into excitatory and inhibitory. In the circular muscle, the majority of excitatory motor neurons innervate the muscle orally to their cell bodies, whereas inhibitory motor neurons innervate anally. *Excitatory motor neurons* have as a primary neurotransmitter ACh, but transmission in these neurons is also mediated by TK. *Inhibitory motor neurons* utilise nitric oxide (NO) as a primary transmitter and they are identified by immunoreactivity for NO synthase (NOS). These neurons also release vasoactive intestinal peptide (VIP) and pituitary adenylyl cyclase-activating peptide (PACAP) as co-transmitters. **Interneurons** have long single axons which form chains that run either orally (ascending) or anally (descending) and they have consistent S cell electrophysiological characteristics. *Ascending interneurons* appear to be involved in local motility reflexes and they have a unique chemical coding containing immunoreactivity for ChAT, calretinin, TK, enkephalin (ENK) and neurofilament protein triplet (NFP). *Descending interneurons* also rely on ACh as their main neurotransmitter, but they are distinguished into three functional classes according to their co-trasmitters: NOS and VIP (control of local motility reflex), 5-HT (control of secretomotor and motility reflex) and somatostatin (SOM, control of migrating myoelectric complex). **Intestinofugal neurons** have Dogiel type I morphology and they send axons to sympathetic paravertebral ganglia, where they mediate reflexes, which start from the intestine and act back on the stomach or intestine (entero-enteric reflexes). Their coding is defined by ACh, VIP and NOS (only in the large intestine). **Secretomotor and vasodilator neurons** have a more diverse morphology and they project either to the mucosa and mucosal glands (secretomotor) or to submucous arterioles (vasodilator). Three main classes can be observed: *cholinergic* ($ChAT^+$) neurons, which are immunoreactive either for neuropeptide Y (NPY, secretomotor neuron) or calretinin (secretomotor/vasodilator neuron) and *non-cholinergic* secretomotor/vasodilator neurons, in which transmission is mediated principally by VIP, a potent stimulant of intestinal secretion and vasodilatation.

#### *1.1.3.5 Cellular targets*

The effector systems of the ENS are the musculature, secretory glands and blood vasculature. Innervation of the muscle coat (i.e. longitudinal and circular muscle layers) is exclusively provided by neurons residing within the myenteric plexus in small mammals, whereas submucosal neurons also contribute in larger animals. Although the smooth muscle is the target of the ENS function, smooth muscle cells are not the major cellular target of enteric neurons in the circular smooth muscle layer; rather, enteric motor neurons innervate a different cell type called interstitial cells of Cajal (ICCs). Although sharing a similar developmental origin with intestinal smooth muscle cells, ICCs are specialised electrical active/pacemaker-producing cells. They have fusiform cell bodies and multiple long processes and they are electrically coupled to each other as well as to the intestinal smooth muscle cells by gap junctions. Functional networks formed by ICCs transduce electrical activity to the smooth muscle and generate a slow wave pacemaker activity, which imposes an underlying rhythm and coordination on the muscle contractions evoked by the neural activity (Sanders, 2006). Mucosal efferent innervation (i.e. secretomotor and vasodilator neurons) is largely from submucosal neurons, whereas afferent neurons (i.e. IPANs) reside both in the submucosal and myenteric plexus. Secretomotor and secretomotor/vasodilator neurons branch within the mucosa and they provide innervation to mucosal glands, submucosal arterioles and the base of the villi in the small intestine, while, in the stomach, they also control some aspects of gastric acid secretion by acting on parietal cells (Furness, 2006).

### 1.1.4 Physiology of the ENS

The physiological function of the ENS is ultimately to control digestion and absorption of nutrients by the gastrointestinal tract. This requires a variety of enabling behaviours: intestinal motility to allow mechanical processing and movement of food (and waste); secretion of water, salt and digestive enzymes to facilitate breakdown and processing of intestinal contents; change in blood flow to enable absorption and transport of nutrients.

Intestinal motility is probably one of the most complex functions controlled by the ENS and this term refers to several movement behaviours of the intestine, including mixing movements (segmentation), propulsion (peristalsis) and migrating motor complexes (MMC). Segmentation involves localised contractions and relaxations repeated rhythmically at specific sites, where they mix intestinal contents with digestive enzymes and expose nutrients to the absorptive intestinal epithelium. Peristalsis consists of a propelling contractile activity which allows gut contents to move forward (anally) along the intestine. MMCs are slowly propagating contractions that travel along most of the gastrointestinal tract in fasted animals and they are thought to propel indigestible substances, epithelial debris, and mucus, to prevent accumulation of bacteria.

The special ENS status of "second brain" arises largely from the discovery that this complex array of motility behaviours is the result of morphologically defined neuronal circuits able to generate reflexes independent from any CNS intervention. In this perspective, intestinal peristalsis is a stereotypical response of a hardwired circuit similar to spinal motor reflexes (e.g. withdrawal reflexes; (Clarke & Harris, 2004). The peristaltic reflex (Fig. 1.2) is activated by IPANs which receive mechanical and/or chemical stimuli from the intestinal lumen or respond to release of serotonin (5-HT) from epithelial endocrine cells. Activated IPANs form a recurrent excitatory network around the intestinal circumference with outputs to two polarised feed-forward pathways of interneurons. Ascending interneurons ultimately activate excitatory motorneurons that project orally to the circular and the longitudinal muscle. Descending interneurons excite inhibitory motor neurons that project anally. The outcome is a polarised contraction of the circular muscle oral to the site of stimulation and a relaxation that occurs on the anal side, which generates a pressure gradient able to move the luminal contents along the intestine. Each of the patterns of motility, secretion and blood flow control, derives from the integrated activity of a hardwired ENS circuitry. In addition strength, repetition rate and coordination of different activities are also adjusted by several extrinsic reflexes involving symphatetic and parasympathetic fibres innervating the gut (Aziz & Thompson, 1998; Lomax *et al.*, 2010).

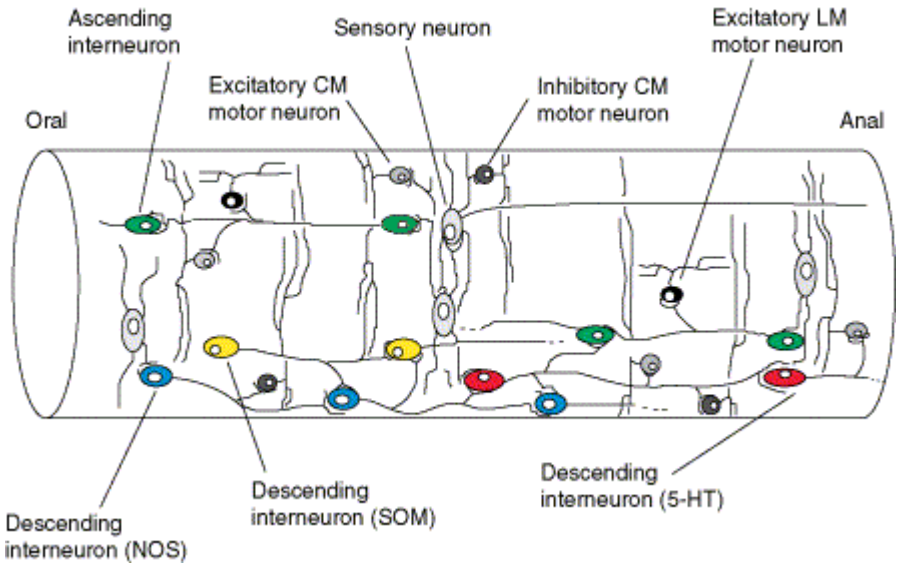


**Figure 1.2 The neuronal circuit underlying the peristaltic reflex**

Sensory neurons (light grey) provide excitatory inputs to interneurons. Ascending interneurons (green) excite other ascending interneurons and excitatory motor neurons to the circular muscle (CM, grey) and to the longitudinal muscle (LM, black). Descending interneurons, mainly $NOS^+$ (blue) activate a descending inhibitory reflex involving two other classes of descending interneurons ($SOM^+$, yellow, and $5\text{-}HT^+$, red) and inhibitory motor neurons (dark grey). Figure from (Bornstein, 2009).

## 1.2 Enteric nervous system development

### 1.2.1 Pre-enteric neural crest cells

The ENS, like the other components of the PNS, is a neural crest derivative. The neural crest (NC) is a transient cell population which is unique to vertebrates and is specified at the border of the neural plate and the non-neural ectoderm after gastrulation (Horstadius, 1950). When the borders of the neural plate converge dorsally to form the neural tube during neurulation, neural crest cells (NCCs) undergo an epithelial to mesenchymal transition, delaminate from the neuroepithelium and migrate extensively throughout the embryo following stereotypical trajectories. Migratory NCCs are a highly heterogeneous cell population, which includes multipotent progenitors (commonly referred as neural crest stem cells, NCSCs) (Stemple & Anderson, 1992) able to give rise to distinct sets of derivatives including: neurons and glia of

sympathetic and parasympathetic ganglia, adrenal chromaffin cells and melanocytes (trunk NCCs); cartilage, bone and connective tissue of the face (cranial NCCs); endothelium of the aortic arch arteries and the septum between the aorta and the pulmonary artery (cardiac NCCs); and enteric neurons and glia (vagal and sacral NCCs) (Le Douarin & Kalcheim, 1999). The neural crest origin of the ENS was first established by experiments performed by C. L. Yntema and W. S. Hammond in the 1950s. The two authors showed in avian embryos that, upon ablation of vagal regions of the neural crest, enteric ganglia failed to form throughout the length of the gastrointestinal tube (Yntema & Hammond, 1954). Subsequently, these results were confirmed and extended by the use of isotopic and isochronic grafting of quail pre-migratory neural crest into chick embryo neural axis (Le Douarin, 1973). Fate mapping of quail cells revealed a double NC origin of the ENS, in which NCCs emigrating from regions adjacent to somites 1-7 (vagal NCCs) were able to colonise the entire intestinal tract and NCCs arising caudally to the 28$^{th}$ somite (sacral NCCs) participated in the formation of ganglia of the post-umbilical gut (Le Douarin & Teillet, 1973). Cell lineage studies revealed a similar origin of the ENS in mammals (Anderson *et al.*, 2006a; Kapur, 2000; Serbedzija *et al.*, 1991) and they also identified a further subpopulation of NCCs at the interface between vagal and trunk NC able to colonise specifically proximal regions of the gut such as the esophagus (Durbec *et al.*, 1996).

Vagal NCCs emerge from the neural tube around embryonic day 8.5 (E8.5) in mouse and they migrate ventro-medially, until a subpopulation of them reaches the foregut at E9-E9.5 (Anderson *et al.*, 2006a; Durbec *et al.*, 1996). After this stage NCCs are termed enteric neural crest cells (ENCCs), they contain ENS-restricted progenitor cells and they migrate in a rostral-to-caudal fashion to colonise the developing gut, a process that is complete approximately in 5 days (E14.5-E15.5) (1.2.2). Sacral NCCs delaminate from the neural tube at E9-E9.5 (Serbedzija *et al.*, 1991) and they migrate ventrally to form pelvic ganglia and to give rise to enteric neurons and glia. Both in mouse and chick embryos, sacral NCCs migrate towards the distal hindgut, they coalesce in the proximity of the dorsal border and they only migrate into the gut upon arrival of vagal ENCCs in the same region (Burns & Douarin, 1998; Kapur, 2000). In mouse, this process starts after E13.5 and it is concluded by E15.5 (Anderson *et al.*, 2006a). The relative

contributions of vagal and sacral NCCs to the mature ENS have also been investigated. Vagal-derived ENCCs give rise to the majority of enteric neurons and glia, with different subsets of vagal neural crest contributing to the colonisation of different regions of the gut (Burns *et al.*, 2000; Epstein *et al.*, 1994; Peters-van der Sanden *et al.*, 1993). Sacral-derived ENCCs participate to a minor extent and they have been shown to generate neurons and glia of the most distal regions of the gut, such as caecum and colon (Burns & Douarin, 1998). Furthermore, migration of sacral-derived ENCCs into the gut, although strictly timed with that of the vagal-derived component, does not rely on it. In models of vagal ENCC ablation, sacral ENCCs still migrate into the gut and give rise to enteric neurons and glia in the most distal regions of the intestine (Anderson *et al.*, 2006a; Burns *et al.*, 2000; Durbec *et al.*, 1996; Kapur, 2000).

Several studies have also addressed cell autonomous properties of pre-enteric vagal and sacral NCCs, in order to identify whether these cells are pre-specified towards the ENS lineage or, rather, their fate depends on the microenvironment encountered along migratory pathways. Transplantation of quail vagal and sacral NC into new axial levels of chick embryos showed both hypotheses to be possibly true. Heterotopic grafted vagal and sacral NCCs are able to migrate to sites characteristic of their new axial level (Erickson & Goins, 2000; Le Douarin & Teillet, 1974; Le Douarin *et al.*, 1975), nevertheless, they seem to retain some of their original properties and to be able, to a certain extent, to reach the original target tissue (i.e. gut) (Barlow *et al.*, 2008; Burns *et al.*, 2002; Le Douarin & Teillet, 1974; Smith *et al.*, 1977). In addition, a rapidly expanding number of markers has been discovered that identify undifferentiated NCCs prior to their entry into the gut, which might point towards the existence of a pre-enteric specified subset of NCCs. Vagal and sacral NCCs express the transcription factor **Sox10** before the onset of migration and they maintain this expression until they reach the gut (Anderson *et al.*, 2006a; Southard-Smith *et al.*, 1998). In avian embryos, pre-migratory vagal NCCs have also been shown to express the endothelin receptor B (**EDNRB**) (Nataf *et al.*, 1996). Shortly after emigration from the neural tube, vagal NCCs express the low-affinity nerve growth receptor **p75** (Anderson *et al.*, 2006a; Wilson *et al.*, 2004) and, while they are migrating in proximity of dorsal aorta, they also induce the expression of the transcriptional regulator **Phox2b** (Pattyn *et al.*, 1999) and the receptor

tyrosine kinase **RET** (Anderson *et al.*, 2006a; Durbec *et al.*, 1996; Pachnis *et al.*, 1993). Interestingly, recent findings have suggested a similar phenotype also in sacral NCCs (Anderson *et al.*, 2006a; Burns *et al.*, 2002). However, it is not clear whether all cells express all the markers or whether different phenotypic classes exist. The markers identified are not exclusive to pre-enteric NCCs, but they are also largely found in NC precursors of sensory neurons and sympathetic neurons. An attempt to identify "pre-enteric" NCCs on the basis of concomitant or differential expression of markers has been made by Anderson et al. (2006), who identified a possible co-expression of $Sox10^{+}$ $p75^{+}$ in NCCs located around the rostral foregut, with a subpopulation of them also expressing Phox2b and RET (Anderson *et al.*, 2006a). Nevertheless, when cells enter the gut, a regional phenotypical restriction seems to be in place and undifferentiated ENCCs have a relatively defined expression of molecules (following section).

### 1.2.2 Enteric neural crest cells

Vagal ENCCs that have entered the embryonic gut at E9.5 follow a single wave of migration to sequentially colonise rostral-to-caudal regions of the developing gut (Kapur *et al.*, 1992; Young *et al.*, 1998a). Thus, in mouse, ENCCs migrate through the midgut at E10.5, the caecum at E11.5, the hindgut at E12.5 and, at E14.5, they complete the colonisation of the distal hindgut joined by sacral ENCCs (Fig. 1.3).

The mode of migration of ENCCs along the mouse gut has been examined by time-lapse imaging (Druckenbrod & Epstein, 2005; Druckenbrod & Epstein, 2007; Druckenbrod & Epstein, 2009; Young *et al.*, 2004). ENCCs migrate through the gut predominantly in strands of interconnected cells (chains). Although the net movement of the cell population has a clear rostrocaudal directionality, individual cells at the leading edge of chains follow complex and unpredictable trajectories (Young *et al.*, 2004). A further investigation into the dynamics of chain formation identified specific migratory behaviours of ENCCs at the wavefront, with the major contribution to chain extension from cells located 300 μm behind the leading edge and isolated cells caudal to the front (Druckenbrod & Epstein, 2007). In opposition to the advancing network

of chains observed in the developing midgut and hindgut, N. R. Druckenbrod and M. L. Epstein (2005) found that ENCCs migrating across the caecum pause for approximately 12 hrs before they separate from chains and they migrate as single cells into distinct areas of the caecum and proximal hindgut following invariable routes. These isolated cells form groups, which eventually contact other groups of cells and reform a network of chains able to progress towards the distal hindgut (Druckenbrod & Epstein, 2005). In addition, while ENCCs are migrating through the gut mesenchyme, a subpopulation of cells starts to differentiate into neurons and express pan-neuronal markers (Baetge & Gershon, 1989; Young *et al.*, 1999). Recent studies showed that many of these immature neurons are also migrating caudally, although at a lower speed and for limited distances compared to undifferentiated vagal ENCCs (Hao *et al.*, 2008).

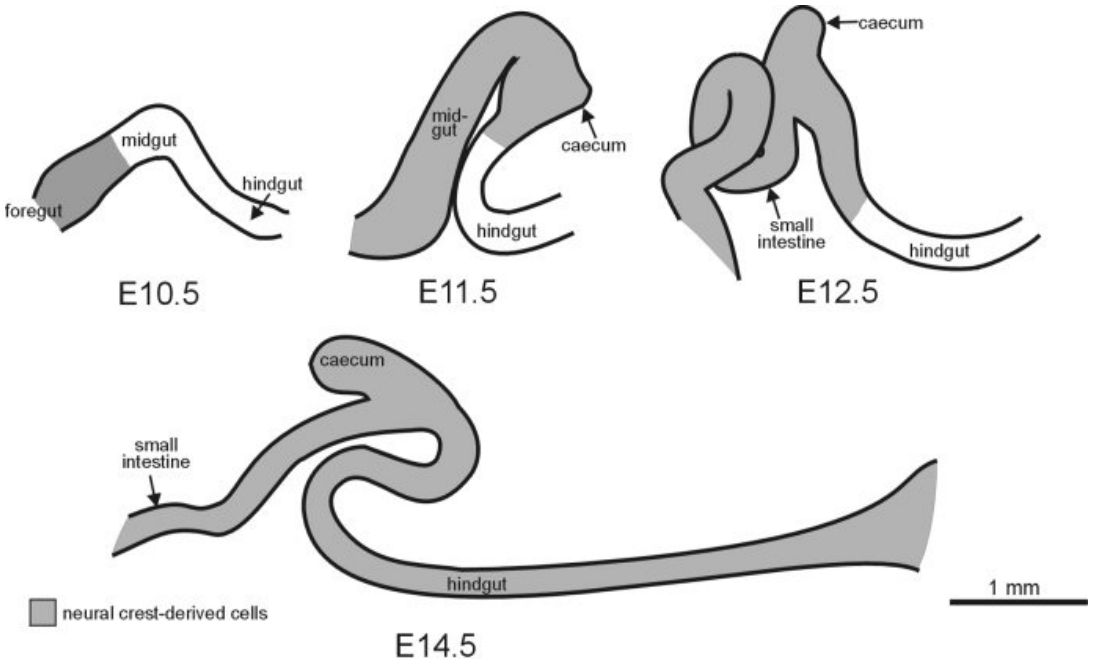


**Figure 1.3 Advance of ENCCs through the embryonic gut**

ENCCs (grey area) advance through the developing gut mesenchyme in a rostrocaudal fashion. In mouse at E10.5 ENCCs can be found in the midgut, approaching the ileocaecal junction. At E11.5 ENCCs have colonised the caecum, while, one day later (E12.5), they are advancing through the hindgut. Colonisation of the distal hindgut is completed around E14.5, where also sacral ENCCs participate. Figure from (Young & Newgreen, 2001).

A secondary wave of migration also appears several days after vagal and sacral ENCCs have formed a complete network around the gastrointestinal tube. In fact, in the small intestine, a subset of ENCCs which had migrated initially through the outer half of the mesenchyme (the projected position of the myenteric plexus), moves centripetally and colonises the submucosal region, where the submucosal plexus will form (Jiang *et al.*, 2003). In mouse, the process is similar in the hindgut (McKeown *et al.*, 2001), whereas, in avian embryos, ENCCs settle first within the submucosa at the inner margin of the developing circular muscle and then migrate outwards (Burns & Douarin, 1998).

During gut colonisation (E10.5-E13.5) the most caudal cells are undifferentiated ENCCs, which have been shown to co-express Sox10, RET, p75 and Phox2b (Young *et al.*, 1998a; Young *et al.*, 1999; Young *et al.*, 2003). Migrating ENCCs also express **EDNRB** (Barlow *et al.*, 2003; Gariepy *et al.*, 1998) and the transcriptional regulator **Mash 1** (Blaugrund *et al.*, 1996; Lo *et al.*, 1991); however, any overlap of expression with the previous markers has not been investigated. Furthermore, a recent study has also shown in chick embryos that sacral ENCCs share the same pool of markers including Sox10, EDNRB and RET (Delalande *et al.*, 2008). Behind the migratory front, ENCCs are at different stages of differentiation, with neurons differentiating before glial cells (Young *et al.*, 2003). Thus, differentiation of vagal-derived ENCCs into neurons takes place shortly after invasion of the foregut and is accompanied by downregulation of Sox10 and p75, maintenance of RET and Phox2b expression and upregulation of pan-neuronal markers such as the ubiquitin hydrolase **PGP 9.5**, neurofilament protein (**NF**), neuronal class III **β-tubulin** and the RNA-binding proteins **HuC** and **HuD** (Sato & Heuckeroth, 2008; Young *et al.*, 2002; Young *et al.*, 2003; Young *et al.*, 2005). A subset of $Mash1^{+}$ neuronal differentiating cells also transiently expresses the catecholaminergic marker tyrosine hydroxylase (**TH**) (Baetge & Gershon, 1989; Blaugrund *et al.*, 1996; Young *et al.*, 1999). All these neuronal-committed cells are considered to be progenitors at this stage, since they lack neuron-subtype specific markers and they are still mitotically active (Baetge & Gershon, 1989; Sato & Heuckeroth, 2008; Young *et al.*, 2003; Young *et al.*, 2005). Glial progenitors are first identified at E11.5 by expression of **B-FABP** and they locate mainly in the foregut and midgut, a long way from the migratory front

(Young *et al.*, 2003). These cells also maintain Sox10 and p75 expression and they upregulate **S100** and **GFAP** only at E14.5 and E16.5, respectively (Rothman *et al.*, 1986; Young *et al.*, 2003).

### 1.2.3 Molecular mechanisms controlling the colonisation of the gut by ENCCs

Development of the ENS is a complex and asynchronous process. As ENCCs migrate along the gut mesenchyme, they respond to proliferative signals which increase their number at the migratory front in order to colonise further empty regions and, behind the wavefront, to populate rapidly growing gut that has already been colonised. Concomitantly, subsets of ENCCs undergo lineage restriction to generate enteric neurons and glial cells. Appropriate orchestration of all these processes is essential for the formation of a complete functional network and it involves many molecular mechanisms which have begun to be unravelled.

#### *1.2.3.1 Cell number*

The population size of pre-enteric NCCs plays a role in determining the completion of invasion of the gastrointestinal tract. For example, reducing the initial number of vagal neural crest cells in avian embryos *in vivo* led to incomplete colonisation of the gut even though the remaining neural crest cells had no innate defect (Peters-van der Sanden *et al.*, 1993; Yntema & Hammond, 1954). It is now clear that a minimal number of NCCs emigrating from the neural tube is necessary for the complete rostrocaudal colonisation of the gastrointestinal tract (Barlow *et al.*, 2008). The pool size of ENCCs is also an important parameter for the speed of progression of the wavefront along the gut and the successful colonisation of the entire organ. When cells at the leading edge of the migratory front are isolated from the more rostral ENCC population, the rate of migration is dramatically reduced, unless a minimal number of wavefront ENCCs is maintained (Young *et al.*, 2004). Further mathematical modelling and grafting experiments in embryonic avian gut *in vitro* have shown that unidirectional invasion of the gut within a particular time frame is accomplished when cells at the wavefront act as a proliferative source to generate enough motile ENCCs to invade previously unoccupied tissues, while those behind the front are essentially non proliferative and do not participate directly in the invasion of unoccupied tissues (frontal

expansion model) (Simpson *et al.*, 2007). *In vivo*, this model also takes into account growth of the underlying intestinal tissue, which requires ENCCs behind the front to proliferate as well (as recorded in mouse by (Young *et al.*, 2005), but with no apparent consequence for the directed movement of the wavefront (Landman *et al.*, 2007).

#### *1.2.3.2 Proliferation and survival*

Several findings have confirmed that maintenance of the pool of proliferating undifferentiated ENCCs plays indeed a key role in colonisation of the gut. If this mechanism is impaired, caudal regions of the gut are devoid of enteric neurons and glial cells, a condition termed aganglionosis. Three major groups of molecules have been involved in control of ENCC proliferation and survival during ENS development, namely GDNF-RET, Endothelin 3 (ET3)-EDNRB and transcription factors such as Sox10 and Phox2b.

**RET** is a transmembrane tyrosine kinase which acts as a receptor for the glial cell line-derived neurotrophic factor (GDNF) family of ligands including GDNF, neurturin, artemin and persephin. Each ligand is able to activate RET through the binding to a preferred high-affinity glycosylphosphatidylinositol (GPI)-anchored co-receptor GFRα (GDNF family receptor α-component), which is **GFRα1** in the case of **GDNF** (Baloh *et al.*, 2000; Jing *et al.*, 1996). RET is expressed in migratory NCCs, it continues while cells migrate along the gut and, after that, it is maintained exclusively in the neuronal population (Durbec *et al.*, 1996; Pachnis *et al.*, 1993; Young *et al.*, 2003). On the other hand, GFRα1 expression has been found both in ENCCs and gut mesoderm (Chalazonitis *et al.*, 1998; Schiltz *et al.*, 1999), whereas GDNF has been shown to be specifically expressed by the gut mesoderm (Natarajan *et al.*, 2002; Young *et al.*, 2001). In mouse, mutation in the RET, GFRα1, GDNF genes leads to total intestinal aganglionosis, a condition where ENCCs fail to colonise the gastrointestinal tract beyond the esophagus (Cacalano *et al.*, 1998; Enomoto *et al.*, 1998; Manié *et al.*, 2001; Moore *et al.*, 1996; Pichel *et al.*, 1996; Sanchez *et al.*, 1996; Schuchardt *et al.*, 1994). *In vitro* and *in vivo* investigations on the effects of the targeted mutation of the gene encoding RET (*c-Ret*) have revealed that the activation of the receptor by GDNF is required at early stages of gut colonisation for survival of

the majority of ENCCs. In absence of RET, progenitors undergo an extensive apoptosis, which depletes dramatically the pool of cells able to progress along the gastrointestinal tract (Taraviras *et al.*, 1999). In addition to its role in cell survival, RET-GDNF signalling generates a strong proliferative signal for ENCCs in a time-dependent manner. *In vitro* studies have shown that GDNF is able to enhance cell proliferation and induce an increase in number of neuronal progenitors in early migratory ENCCs (Chalazonitis *et al.*, 1998; Hearn *et al.*, 1998; Heuckeroth *et al.*, 1998; Taraviras *et al.*, 1999). In accordance with these studies, depletion of GDNF *in vivo*, as reported in mice heterozygous for mutation in the *Gdnf* gene (*Gdnf* $^{+/-}$*)*, leads to a reduced number of enteric neurons along the intestine (hypoganglionosis) as a result of diminished proliferative capacity of progenitor ENCCs (Gianino *et al.*, 2003). However, at later post-migratory stages, GDNF seems to mainly promote survival and neuronal differentiation (Chalazonitis *et al.*, 1998; Taraviras *et al.*, 1999; Uesaka *et al.*, 2007; Wang *et al.*, 2010). GDNF-RET signalling has also additional roles in control of ENCC migration and development of enteric neurons (1.2.3.3 and 1.2.4.1).

**EDNRB** is a G protein-coupled receptor for the small peptides endothelin-1 (ET-1), ET-2 and ET-3 (Inoue *et al.*, 1989). In the embryonic mouse gut, **ET-3** is the only ligand expressed by the gut mesenchyme, with its highest levels in the caecum (Barlow *et al.*, 2003; Leibl *et al.*, 1999), while EDNRB is expressed by both ENCCs and non-neural crest gut tissue (Barlow *et al.*, 2003; Woodward *et al.*, 2000; Wu *et al.*, 1999). Spontaneous or targeted mutations of the *Ednrb* or *Et-3* locus lead to identical phenotypes, characterised by the absence of enteric neurons from the terminal region of the gut (colonic aganglionosis) (Baynash *et al.*, 1994; Hosoda *et al.*, 1994; Kapur *et al.*, 1995). *In vitro* studies in mouse and bird showed that ET-3 inhibits or delays neuronal differentiation of ENCCs (Hearn *et al.*, 1998; Wu *et al.*, 1999), with little or no effect on proliferation on its own (Chalazonitis *et al.*, 1998; Heuckeroth *et al.*, 1998; Kruger *et al.*, 2003; Wu *et al.*, 1999). Further studies on clonogenic cultures of isolated ENS progenitor cells (EPCs) have confirmed that ET-3 is able to inhibit reversibly the commitment of these cells towards neuronal and glial lineages, maintaining them in an uncommitted state (Bondurand *et al.*, 2006). Therefore, it has been suggested that the ET-3-EDNRB signalling provides a halt to

ENCC differentiation, promoting the maintenance of a pool of undifferentiated and uncommitted progenitors able to fully colonise all regions of the developing gut. In accordance with this hypothesis, absence of ET-3 *in vivo* results in migratory delay in colonisation of the gut (Barlow *et al.*, 2003), associated with a reduced pool of proliferative progenitors and with premature neuronal differentiation at the front of migration (Bondurand *et al.*, 2006). In addition, several interactions of the ET3-EDNRB signalling with other signalling pathways have been reported to cooperate in control of proliferation and/or differentiation of ENCCs. For example, ET-3 is able to synergistically increase the proliferative effect induced by GDNF-RET signalling *in vitro* (Barlow *et al.*, 2003), while *in vivo*, mutations in the *Et-3* or *EdnrB* locus are able to increase the severity of aganglionosis in $Sox10^{Dom/+}$ mice (Cantrell *et al.*, 2004; Stanchina *et al.*, 2006) and in mice carrying only the monoisoformic *c-Ret* allele $Ret^{51}$ (Barlow *et al.*, 2003).

**Sox10** is a member of the SRY-box containing (Sox) family of transcription factors, defined by sequence similarity of its members to the high-mobility group (HMG) DNA-binding motif of the mammalian sex-determining gene *Sry* (Bowles *et al.*, 2000). *Sox10* is expressed in NCCs as they emigrate from the neural tube and it continues to be expressed as these cells migrate towards their target tissues (Kuhlbrodt *et al.*, 1998). In post-migratory target tissues such as dorsal root ganglia (DRG) and the ENS, Sox10 expression is present in undifferentiated multipotent progenitors, until, upon lineage segregation, it is only maintained by the glial cell lineage (Anderson *et al.*, 2006a; Kuhlbrodt *et al.*, 1998; Paratore *et al.*, 2001; Southard-Smith *et al.*, 1998; Young *et al.*, 2003). In mouse, a spontaneous (*dominant megacolon, $Sox10^{Dom}$)* and a targeted (*$Sox10^{LacZ}$*) mutation of *Sox10* lead to colonic aganglionosis in heterozygosity and to total intestinal aganglionosis in homozygosity in addition to several other defects in multiple neural crest derivatives (Britsch *et al.*, 2001; Herbarth *et al.*, 1998; Lane & Liu, 1984; Southard-Smith *et al.*, 1998). From *in vivo* studies, the transcription regulator Sox10 is thought to play a primary role in sustaining the survival of multipotent undifferentiated NCCs. In absence of Sox10, a dramatic increase in apoptotic death has been reported both in vagal NCCs prior to their entry into the rostral foregut (Kapur, 1999) and in undifferentiated trunk NCCs within the DRGs (Paratore *et al.*, 2001). Premature death seems therefore to preclude the entrance of ENCCs into

the gut, since investigation of progenitor markers failed to find any positive cell during early stages of gut colonisation (Kapur, 1999). A combination of *in vivo* and *in vitro* studies has also implicated Sox10 in maintenance of ENCCs in an undifferentiated state. Paratore et al. (2002) reported that, in the case of Sox10 hyploinsufficiency, as seen in $Sox^{LacZ/+}$ mice, the pool of ENCCs expressing progenitor markers such as Sox10 and p75 is reduced along the gastrointestinal tract, with concomitant increase in cells expressing neuronal precursor markers (Paratore *et al.*, 2002). On the other hand, Bondurand et al. (2006) showed that overexpression of Sox10 is able to reduce the number of neurons and glial cells differentiated from EPCs *in vitro* (Bondurand *et al.*, 2006). Thus, these findings demonstrate that Sox10 levels are indeed critical for maintenance of the ENS progenitor pool. Furthermore, Sox10 is part of a molecular cascade which controls spatial and temporal commitment and differentiation of ENS by interacting with other signalling pathways. In fact, genetic studies have shown that Sox10-binding sites exist at the *Ednrb* enhancer and these are required for appropriate spatiotemporal regulation of the gene in the developing ENS (Zhu *et al.*, 2004). In addition, other studies have implicated Sox10 in the regulation of the expression of *c-Ret* (Lang *et al.*, 2000; Lang & Epstein, 2003) and *Phox2b* (Elworthy *et al.*, 2005; Kim *et al.*, 2003).

**Phox2b** is a paired-homeodomain transcription factor which is widely expressed in the developing autonomic nervous system (Pattyn *et al.*, 1997). Phox2b expression in vagal NCCs occurs after the expression of Sox10 and it is maintained by all ENCCs within the embryonic mouse gut, including both neuronal and glial precursors (Anderson *et al.*, 2006a; Young *et al.*, 1998a). Recently, a transgenic line driving the cerulean fluorescent protein (CFP) under control of the Phox2b promoter has shown that there are differential levels of Phox2b expression at the front of migrating ENCCs and, also, that Phox2b expression persists both in mature enteric neurons and glial cells (Corpening *et al.*, 2008). Mice with targeted mutation of the *Phox2b* locus ($Phox2b^{LacZ}$) lack autonomic ganglia, including the ENS in all regions of the gastrointestinal tract (Pattyn *et al.*, 1999). In absence of Phox2b, vagal NCCs enter the foregut but fail to express markers such as RET, Mash 1 and TH and they coalesce around the esophageal-gastric junction before undergoing extensive apoptotic death which leads to total intestinal aganglionosis (Pattyn

*et al.*, 1999). These studies suggest a role for Phox2b in control of ENCC survival by direct regulation of RET expression.

Besides the major molecular mechanism just described, recent evidence pointed also towards the role of other signalling cascades in control of gut colonisation by maintaining the pool of undifferentiated and proliferative ENCCs. For example, ablation of a core component of the **Notch** signalling pathway resulted in deficits in the number of ENS progenitor cells accompanied by loss of Sox10 expression and precocious neuronal differentiation (Okamura & Saga, 2008; Taylor *et al.*, 2007). Furthermore, maintenance of enteric NCSCs has been reported to rely also on the mitogenic role of the epidermal growth factor (**EGF**) through the activity of members of the Rho family of GTPases (Fuchs *et al.*, 2009), section 1.4.3).

#### *1.2.3.3 Migration*

Several processes involving responses to diffusible molecules, extra-cellular matrix interactions, cell-cell interactions and intracellular reorganisation control motility and directionality of ENCCs migrating through the gut mesenchyme. Increasing evidence suggests that control of all these events contributes to the successful colonisation of the gastrointestinal tract by neural crest derivatives.

Mechanisms that confer directionality to ENCCs along the gut have been explored by different groups. Direction of migration seems not to be an intrinsic property of ENCCs, since experiments, where colonised regions (donor) of embryonic gut where added to the caudal end of an aganglionic gut (host), showed that ENCCs present in the donor graft were able to colonise the host graft in an opposite direction to that of endogenous ENCCs (Anderson *et al.*, 2007; Simpson *et al.*, 2007; Young *et al.*, 2002). Mathematical modelling suggested that frontal expansion of the proliferating migrating wavefront is able to justify rostro-caudal migration of vagal-derived ENCCs (Simpson *et al.*, 2007) (1.2.3.1). However, this model is unable to explain how vagal NCCs migrate into the foregut anlage in the first place and how sacral-derived ENCCs are capable of colonising gut regions where vagal-derived ENCCs are already present. Furthermore, some earlier studies have shown that single $RET^{+}$ cell injected into the stomach of aganglionic

guts were still able to migrate extensively as individual cells, with little or no cell interaction with other proliferating cells (Natarajan *et al.*, 1999). Therefore, it is clear that molecular mechanisms other than cell number and proliferation might indeed play a key role in directing ENCC migration, such as the presence of diffusible chemoattractive molecule. **GDNF** mRNA is expressed by the gut mesenchyme in a time-dependent fashion, with high levels initially in the foregut mesenchyme and later in the caecum, which precede the colonisation of those regions by ENCCs (Natarajan *et al.*, 2002). *In vitro* studies have shown that GDNF acts as chemoattractant to vagal NCCs prior to their entry into the gut and to ENCCs within the gut, thus the GDNF-RET signalling pathway seems to play a key role in retaining neural crest cells within the gut mesenchyme, and also in inducing their rostro-caudal migration (Natarajan *et al.*, 2002; Young *et al.*, 2001). Nevertheless, attempts to identify a GDNF gradient within the gastrointestinal tube were unsuccessful (Anderson *et al.*, 2007) and it is not known how ENCCs are able to pass the caecum and proceed through the hindgut, since no other sources of GDNF have been found in the most caudal regions of the gut. Experimental evidence points towards a GDNF-opposing role of **ET-3**, which is specifically expressed in the caecum prior to ENCC arrival in the region (Barlow *et al.*, 2003). Addition of ET-3 *in vitro* enables ENCCs present in the proximal hindgut of ET-3 deficient mice to fully colonise the distal aganglionic regions (Wu *et al.*, 1999) and specifically reduces the chemoattractive effect of GDNF on ENCCs migrating in a collagen matrix from gut explants (Barlow *et al.*, 2003; Kruger *et al.*, 2003). In addition, Druckenbrod and Epstein (2009) have recently shown, by pharmacological inhibition of the receptor EDNRB in organ cultures, that the migratory behaviour of ENCCs is directly affected, resulting in retraction of cellular processes and loss of chain migration (Druckenbrod & Epstein, 2009). Thus, ET-3 might be able to relieve GNDF attraction and enhance migratory properties of ENCCs across the caecal region, allowing the cells to progress further instead of stalling.

Delayed entry into the gut and caudal-rostral migration of sacral-derived ENCCs is an issue that requires further investigation. Some early speculation suggested that sacral NCCs might be inhibited by temporal regulated expression of molecules in the hindgut, such as semaphorins. In avian embryos, **Sema3A** is transiently expressed in the hindgut and it acts as a

chemorepellent for axons of neurons present in the nerve of Remark (Shepherd & Raper, 1999). When Sema3A expression decreases, axons enter the hindgut and sacral NCCs migrate along with them, therefore it has been suggested that Sema3A might account indirectly for the delayed entry in the gut of the sacral-derived ENCCs (Burns, 2005). In mouse, Sema3A is also expressed in the most caudal regions of the gut and, when absent, some sacral ENCCs and extrinsic axons enter prematurely into the distal hindgut (Anderson *et al.*, 2007). However, it is still not clear whether Sema3A acts directly on ENCCs, and it is likely that other molecular mechanisms are involved in the directed migration of sacral NCCs into the gut mesenchyme. A recent study in chick embryos from Delalande et al. (2008) reported that sacral ENCCs express almost a 4-fold less mRNA transcript for RET than vagal ENCCs. When RET is over-expressed in sacral ENCCs, increased number of cells enter the hindgut and earlier during development, thus suggesting a differential control of similar molecular mechanism underlying directed migration in vagal- and sacral-derived ENCCs (Delalande *et al.*, 2008).

In addition to molecules involved in guidance of migration of ENCCs along the gut, a class of molecules such as **netrins** has been implicated in chemoattraction of enteric progenitors to give rise to the submucosal and pancreatic plexi (Jiang *et al.*, 2003). In mouse, Netrin-1 and Netrin-3 are expressed by the gut endoderm and pancreas, while the netrin receptor, deleted in colorectal cancer (DCC), is expressed by ENCCs. *In vivo* deletion of DCC leads to absence of submucosal and pancreatic ganglia. This phenotype has been explained by *in vitro* analysis showing that ENCCs can migrate toward explants of gut endoderm and pancreas, but this chemoattractive response can be specifically blocked by antibodies to DCC, thus proving the role of netrins in guiding secondary migration of ENCCs (Jiang *et al.*, 2003).

ENCC migration involves the control of cell adhesion to extracellular matrix (ECM) components as well as between migrating cells themselves. The intestinal ECM is a dynamic environment, with temporal regulated expression of several molecules affecting the migratory behaviour of ENCCs during development. Thus, altered expression of defined ECM components or impairment in adhesive properties of ENCCs might lead to incomplete colonisation of the gastrointestinal tract. Studies from Breau et al. (2009) have reported the existence of a gradient of

ECM components in the developing gut. In instance, **fibronectin** (FN) and **tenascin C** (TNC) are expressed by the mesenchyme of E11.5 mouse guts more abundantly in the caecum and hindgut compared to the wall of the midgut, whereas other components, such as vitronectin, found in all pericellular spaces around epithelial and mesenchymal cells, or laminin α1, laminin α5 and collagen V, found mainly in the basal laminae, were expressed at similar levels in all regions of the gut (Breau *et al.*, 2009). The high levels of expression of FN and TNC in the caecum and proximal hindgut coincide with the timing of crossing of these regions by ENCCs, which show opposing migratory responses to them. *In vitro* TNC inhibits ENCC migration (Breau *et al.*, 2009), which correlates with the temporary arrest of migration observed when ENCCs reach the base of the caecum (Druckenbrod & Epstein, 2005). Conversely, FN promotes migration, cell adhesion and spreading through a mechanism involving **β1 integrins** expressed on the surface of ENCCs (Breau *et al.*, 2006; Breau *et al.*, 2009). In accordance, *in vivo* ablation of β1 integrin leads to a delay in ENCC migration with an altered colonisation of the caecum and hindgut, which ultimately results in colonic aganglionosis (Breau *et al.*, 2006; Breau *et al.*, 2009). These findings suggest that expression of β1 integrin is essential for ENCCs to interact with fibronectin and overcome the TNC-mediated migratory inhibition during the invasion of the caecum and proximal hindgut and they suggest that alteration of adhesive properties of ENCCs might represent *per se* a molecular basis for incomplete colonisation of the gut. In addition to these findings, recent studies have also shown how physiological or pathological changes occurring during development in the structure of the intestinal wall might account for defects in colonisation of distal segments of the gut reported in several mutants. In fact, the intestinal mesenchyme undergoes dramatical changes during embryonic development (Young, 2008), such as differentiation into specific cells types (i.e. smooth muscle, mucosal and epithelial cells) and production of specific ECM components. *In vitro* recombination of E11.5 caecum grafts into aganglionic hindgut explants of different developmental ages demonstrated an age-dependent efficiency in colonisation of the host gut, with the oldest (E16.5) explant to be the least colonised by E11.5 donor ENCCs (Hotta *et al.*, 2010). Accordingly, a study from Druckenbrod and Epstein (2009) showed decreased permissiveness to ENCC migration in the hindgut between E13.5 and

E14.5, a change possibly connected to an increase in ECM deposition of **laminin**, a potent pro-differentiative for enteric neurons (Druckenbrod & Epstein, 2009). It is also suggested that this change in the gut environment, which is normally occurring during development, might create a physical obstacle to a delayed wavefront of ENCCs, as reported by the same authors for *Ednrb* mutant ENCCs (Druckenbrod & Epstein, 2009). On the other hand, studies have also shown that ET-3 mutations are able to alter directly the expression of laminin by the gut mesoderm and, along with the cell-autonomous effects of the mutation, lead to terminal aganglionosis (Rothman *et al.*, 1996; Tennyson *et al.*, 1986; Wu *et al.*, 1999).

Transient cell-cell interactions play a key role in migration of neural crest cells. Directional migration of cranial NCCs has been shown to rely on contact inhibition of locomotion (CIL), a molecular mechanism for which, within a population of migrating cells, a cell becomes polarised and initiates sustained directional migration away from contact with another neural crest cell (Carmona-Fontaine *et al.*, 2008). In this system, therefore, multiple transient cell interactions are necessary for collective migration of the entire population of cells, whereas loss of contact and cell isolation results in diminished chemotaxis and directionality (Carmona-Fontaine *et al.*, 2008; Theveneau *et al.*, 2010). In the developing ENS, it is likely that a similar mechanism acts on migrating ENCCs. *In vitro* blocking of the **cell adhesion molecule L1** expressed on ENCCs leads to partial disruption of the chains of cells at the wavefront with increased numbers of isolated cells and consequent incomplete colonisation of the distal gut, thus suggesting that L1 dependent cell-cell contact is important for migration of ENCCs (Anderson *et al.*, 2006b). However, *in vivo* deletion of L1 only results in transient delay of ENCCs, which does not lead to aganglionosis (Anderson *et al.*, 2006b), indicating that other cell adhesion molecules might be accountable for cell-cell interactions within chains of migrating ENCCs. A study from Fu et al. (2006) has suggested that addition of the polysialic acid (PSA) to the neural cell adhesion molecule 1 (NCAM1) might affect the migration of ENCCs into the hindgut in E11.5 gut explants *in vitro*. Expression of **PSA-NCAM1** is found in both ENCCs and the underlying muscle layer during fetal life, with a consistent increase on maturing neurons and neurites as development proceeds (Fu *et al.*, 2006). *In vitro*, bone morphogenetic protein 4 (BMP 4) is

shown to increase PSA-NCAM1 expression on isolated ENCC, as previously reported (Chalazonitis *et al.*, 2004), but also to reduce the rate of migration of ENCCs into the hindgut of cultured gut explants. Treatment of explants with endo-*N*-acylneuraminidase (endo-N), an enzyme that specifically removes PSA from NCAM1, is able to reverse the effects of BMP 4 on ENCC migration, thus suggesting that BMP induced modifications of NCAM1 is one of the molecular mechanisms controlling the migratory behaviour of ENCCs.

Cell migration requires polarisation and coordinated activation of proteins, which ultimately control cytoskeleton remodelling. There are some indirect data showing that inhibition of polarisation of ENCCs leads to delayed colonisation of the hindgut in organotypic cultures of E11.5 guts (Vohra *et al.*, 2007). *In vitro*, retinoic acid has been shown to facilitate ENCC migration by reducing the levels of the phosphatase and tensin homolog **PTEN**, whose function affects the polarised and coordinated activity of proteins that regulate the actin cytoskeleton (Fu *et al.*, 2010). Candidate molecules suggested to regulate the intracellular actin dynamics in response to chemotactic signals such as GDNF are the **Rho GTPases** (Chapter 1.4).

### 1.2.4 Development of enteric neurons and ENS patterning

#### *1.2.4.1 Neuronal subtype specification*

Enteric neurons are born and mature throughout fetal life and after birth. As early as E10-E10.5, neuronal progenitors can be identified in the developing gut by expression of pan-neuronal markers, such as Hu, β-tubulin, neurofilament protein and PGP9.5, along with maintenance or increase in RET expression (Baetge & Gershon, 1989; Young *et al.*, 1999). Differentiation into distinct neuronal subtypes is an asynchronous and heterogeneous process. Subtype-specific neuronal progenitors exit the cell cycle during defined developmental windows; however, immunoreactivity for the related neurotransmitters or subtype markers might not appear until several days later (Table 1.2). Moreover, as in other parts of the nervous system, immature enteric neurons may express combinations of neurotransmitters and neurotransmitter synthetic enzymes that are not observed in mature neurons, while the full spectrum of enteric chemical

coding is only developed after birth. For example, transient expression of the catecholamine synthetic enzyme tyrosine hydroxylase (TH) is found in the majority of developing neurons between E10 and E12.5 (Baetge & Gershon, 1989; Young *et al.*, 1999). These cells, which also co-express Mash 1 and are still proliferative (Baetge & Gershon, 1989; Blaugrund *et al.*, 1996), have been suggested to be neuronal progenitors of serotonergic neurons (Blaugrund *et al.*, 1996) and NOS neurons (Young *et al.*, 2002), but this issue still remains controversial. Certainly, transiently expressing $TH^+$ progenitors do not seem to generate the small population of catecholaminergic neurons present in the adult mouse (Li *et al.*, 2004). The first enteric neurons to express a neurotransmitter synthetic enzyme present in mature enteric neurons are the NOS (nitrergic) neurons around E12-E12.5 (Baetge & Gershon, 1989; Young *et al.*, 2002). Serotonergic neurons are also believed to develop around the same time, since uptake of radioactively labelled 5-HT can be recorded at E12 in neurites present in the midgut; however, immunoreactivity for the neurotransmitter can only be found at E18 (Rothman & Gershon, 1982). Analogously, cholinergic neurons are thought to develop around E10 and E12, when conversion of radioactive choline into acetylcholine (ACh) can be recorded within the ENS (Rothman & Gershon, 1982), although, only at E18.5 have the synthetic enzyme and the vesicular transporter for ACh been detected by immunolabelling (Vannucchi & Faussone-Pellegrini, 1996). In addition, VIP and NYP immunoreactivity are firstly found around E13.5 (Branchek & Gershon, 1989; Rothman *et al.*, 1984), substance P at E14-E14.5 (Rothman *et al.*, 1984), CGRP at E17 (Branchek & Gershon, 1989), while calretinin has been recorded only at P0 (Young *et al.*, 1998b).

Several molecular mechanisms underlie differentiation of enteric neurons and they implicate maintenance of number of neurons, control of neuronal commitment and regulation of neuronal subtype specification. Two major signalling pathways have been shown to regulate the relative abundance of neuronal classes within the developing ENS by controlling proliferation of neuronal progenitors: GDNF and BMP. The **GDNF-GFRα1-RET** signalling has a pleiotropic effect on ENCCs during early and late stages of development by controlling several steps of neuronal maturation such as proliferation, differentiation and survival of enteric neurons

(Chalazonitis *et al.*, 1998; Hearn *et al.*, 1998; Uesaka *et al.*, 2007). However, a recent study has shown how temporal control of GDNF expression regulates the proliferation of specific precursors and thus the abundance of specific subclasses of postmitotic enteric neurons (Wang *et al.*, 2010). When GDNF is over-expressed at late stages of development under control of the GFAP promoter (approximately from E17 onwards), the number of neurons expressing NADPH-d, a marker for NOS activity, was increased, whereas neurons expressing ChAT/Substance P remained unaffected. Since NO progenitors proliferate up to P1, in contrast to ChAT progenitors that undergo cell cycle exit by E15, this result suggests a selective mitogenic effect of GDNF based on the stage enteric neuronal precursors exit the cell cycle (Wang *et al.*, 2010). Partially consistent with these findings, *in vivo* GDNF hyploinsufficiency leads to a reduction in number of myenteric neurons (Gianino *et al.*, 2003), with some studies indicating concomitant reduction in the proportion of NOS and ChAT myenteric neurons in the small intestine (Wang *et al.*, 2010), and others revealing unaffected proportion of NOS myenteric neurons in the colon (Roberts *et al.*, 2008). Bone morphogenetic proteins (**BMPs**) play a role in enteric neuronal development by possibly acting on several molecular processes similar to those controlled by GDNF. *In vitro* concentration-dependent activity of BMP 2 and BMP 4 increases neuronal differentiation and affects neuronal survival of purified enteric progenitors (Chalazonitis *et al.*, 2004). *In vivo*, over-expression of the BMP inhibitor noggin under control of the neuron specific enolase (NSE) is associated with a significant increase in number of enteric neurons in both enteric plexi with different effect on specific neuronal subtypes. Noggin-mediated BMP antagonism leads to an increase in number of neurons derived from precursors that exit the cell cycle early in neurogenesis (serotonin, calretinin and calbindin neurons), whereas those that exit the cell cycle late (CGRP, GABA, TH, DAT neurons) were decreased, and NOS neurons remained unaffected (Chalazonitis *et al.*, 2004; Chalazonitis *et al.*, 2008). Thus, BMP signalling might contribute to enteric neuronal phenotypic diversity by promoting cell cycle exit of neuronal precursors at appropriate developmental times.

Neuronal commitment of ENCC progenitors is a process that is strictly connected to maintenance of their undifferentiated state. Thus, the function of transcription factors such as

**Sox10**, which have been found to inhibit neuronal differentiation, needs to be down regulated during neuronal specification (Bondurand *et al.*, 2006). Therefore, it has been proposed that Mash1, a transcription factor that belongs to the basic helix-loop-helix (bHLH) family and promotes several aspects of neurogenesis in the CNS, suppresses Sox10 expression in some of the enteric progenitors which give rise to neurons (Okamura & Saga, 2008). Another bHLH transcription factor, **Hand2**, has been found to modulate neuronal development by promoting terminal differentiation of enteric neuronal progenitors (D'Autreaux *et al.*, 2007; Hendershot *et al.*, 2007). In fact, conditional ablation of Hand2 results in affected neuronal differentiation of ENCCs *in vitro* and *in vivo* and in absence of subtype-specific markers such as NOS and VIP in the gut of embryonic mice *in vivo* (D'Autreaux *et al.*, 2007; Hendershot *et al.*, 2007).

Additionally, some studies have also implicated **ET-3** in late events of neuronal differentiation. In fact, in ET3 null mice, an increase in the proportion of $NOS^+$ myenteric neurons has been recorded in the region rostral to the aganglionic colon (Roberts *et al.*, 2008) and in the small intestine (Sandgren *et al.*, 2002), thus suggesting a subtle effect of this mutation on the phenotype of enteric neurons.

Genetic control of neuronal subtype specification is still a key issue in ENS development. To date, few genetic mutations result in loss of specific neuronal subtypes, suggesting that neuronal differentiation might be the result of combinatorial activity of one or more genetic factors. **Mash1** is the only transcription factor that has been unequivocally associated with the development of a defined neuronal population such as the serotonergic subtype. Targeted ablation of *Mash1* leads to lack of neurons in the esophagus in addition to a failure to develop $TH^+$ progenitors and 5-HT neurons along the entire gastrointestinal tract (Blaugrund *et al.*, 1996). Similarly, mice lacking the tyrosine kinase receptor C (**TkrC**) or its ligand neurotrophin-3 (**NT-3**) show reduction in myenteric neuron number and have a dramatic decrease in CGRP positive submucosal neurons (Chalazonitis *et al.*, 2001).

**Table 1.2 Timing of cell cycle exit (birth date) of neuronal progenitors and earliest developmental appearance of subtype-specific markers of myenteric neurons in mouse small intestine**

| *Subtype-specific markers* | *Birthdates (peak)* | *Earliest immunoreactivity* | *References* |
|---|---|---|---|
| 5-HT | E8-E14 (E10) | (E12[a]) E18 | (Branchek & Gershon, 1989; Pham *et al.*, 1991; Rothman & Gershon, 1982) |
| ChAT or vChAT | E8-E15 (E12) | (E11[b]) E18.5 | (Pham *et al.*, 1991; Rothman & Gershon, 1982; Vannucchi & Faussone-Pellegrini, 1996) |
| CGRP | E10-P3 (E17) | E17-E17.5 | (Branchek & Gershon, 1989; Pham *et al.*, 1991; Young *et al.*, 1999) |
| ENK | E10-E18 (E14) | n/d | (Pham *et al.*, 1991) |
| NOS | E12.5-P1[c] (E14.5) | E12-E12.5 | (Branchek & Gershon, 1989; Chalazonitis *et al.*, 2008; Young *et al.*, 2002) |
| NPY | E10-E18 (E15) | E13-E13.5 | (Branchek & Gershon, 1989; Pham *et al.*, 1991) |
| VIP | E10-P5 (E15) | E13.5 | (Pham *et al.*, 1991; Rothman *et al.*, 1984) |

[a] radioactively labelled 5-HT neurites can be detected in mouse midgut at E12; however, immunoreactivity is not present until E18.
[b] radioactively labelled ACh uptake from enteric neurons can be first detected from E10 to E12; however, immunoreactivity for the choline acetyltransferase (ChAT) and the vesicular acetylcoline transporter (vAChT) are not present until E18.5.
[c] birth date of NOS neurons is likely to be earlier than E12.5, since immunoreactivity for NOS is detected already at E12, but earlier developmental ages have not been investigated in the reported study.
See Table 1.1 for abbreviations of markers. (Peak): age at which the majority of progenitors have exited the cell cycle. Modified from (Hao & Young, 2009).

### *1.2.4.2 Morphological development of enteric neurons*

Most classes of enteric neurons possess a characteristic morphology with the presence of one or more axons, different shape of dendrites and several degrees of branching (1.1.3.1). Development of specific neuronal morphologies involves in first place growth of neurites and specification of axons and dendrites. From *in vivo* studies involving the use of the lipophilic dye 1,1'-dioctadecyl-3,3,3',3'-tetramethylindocarbocyanine perchlorate (DiI) to retrogradely label neuronal projection and cell bodies, Young et al. (2002) found that the majority of neurons present in E11.5-E16.5 mouse gut, including early born NOS neurons, had one single long process and multiple short neurites, suggesting the establishment of neuronal polarity at early stages of ENS development (Young *et al.*, 2002). Interestingly, the morphology of mature NOS neurons is similar to that

found in their embryonic counterpart, with one long axon and several short lamellar dendrites (Dogiel type I); however, it remains to be determined whether the mature neuronal morphology is determined as soon as specification occurs or whether it is defined at later stages, for example upon synaptic connection with the final targets. Few studies have addressed the molecular mechanisms underlying neuritogenesis and determination of neuronal polarity in the developing ENS. Evidence emerging from the work of Vohra et al (2007) showed a role for protein kinase C zeta (**PKCζ**) and glycogen synthase kinase 3β (**GSK3β**) in axon specification of enteric neurons. In culture, the majority of neurons developing from immunoselected rat ENCCs produce a single axon. PKCζ and GSK3β transiently localise at the tip of growing axons and pharmacological inhibition of their activity results in an increase in both the number of multi-axonal neurons and the number of neurons without any axons, indicating that PKCζ and GSK3β are able to influence neuronal polarity and are likely to influence the number of axons in enteric neurons. Furthermore, the authors showed that PKCζ and GSK3β activity is also implicated in neurite growth, a mechanism that most likely involves recruitment of SMURF1 protein, which, in turn, promotes RhoA degradation (Vohra *et al.*, 2007). Conversely, retinoic acid (**RA**) reduces neurite length in cultured enteric neurons by decreasing the levels of expression of *smurf1* and, consequently, increasing the abundance of RhoA protein, especially at the tip of neurites (Sato & Heuckeroth, 2008). Nevertheless, there is currently no information on the relevance of genetic programmes and environmental cues on the morphological maturation of enteric neurons and on the expression of intracellular components and regulators of cytoskeleton dynamics during development.

#### *1.2.4.3 Axon guidance*

Mature enteric neurons differ in their axon projection patterns and target cells. Some classes of neurons project orally, others project anally, circumferentially and locally (1.1.3.4). Very little is known about the mechanisms controlling navigation of axons of developing enteric neurons to their correct targets and in their correct direction. DiI tracing of neuronal projections in E11.5-E12.5 mouse gut revealed that many of the first differentiating neurons have a long longitudinal

process which projects anally, whereas oral projecting neurons appear to develop only at later stages (Young *et al.*, 2002). By immunofluorescence analysis, it is possible to identify many of the caudal projecting neurons as TH and NOS positive (at E11.5 and E12.5 respectively), with cell bodies located between tens to hundreds of microns behind the wavefront and their processes often in contact with migrating ENCCs at the leading edge (Breau *et al.*, 2006; Hao & Young, 2009; Young *et al.*, 1999; Young *et al.*, 2002). Furthermore, the longitudinal processes of individual neurons are observed forming prominent bundles of fibres shortly after each gut region is colonised by ENCCs (Hao & Young, 2009; Young *et al.*, 2002). Thus, there must be some neural guidance cues allowing growing axons to sense the polarity of the gut (oral vs anal along the longitudinal axis, but also circumferential) and also, some molecular mechanisms that mediate interaction of axons for the formation of longitudinal fibres. In co-culture experiments in which vagal ENCCs were forced to migrate caudo-rostrally, most of the neurons projected rostrally, suggesting that migration and axon guidance are associated at least during early stages of colonisation of the gut (Young *et al.*, 2002). However, the molecular mechanism linking neuronal processes to undifferentiated ENCCs is not clear and, moreover, this hypothesis cannot explain the onset of oral/circumferential projecting neurons or the patterning of projections after ENCC migration is concluded.

To date, there have been no defects in enteric axon targeting described in mice lacking any of the major neural guidance molecules. Nevertheless, it has been reported that mice, in which **neurturin** (NRTN, one of the members of the GDNF family of ligands) or **GFRα2** (NRT high affinity co-receptor) have been genetically ablated, have a drastic reduction of cholinergic fibres projecting to the circular muscle, whereas there are no changes in NO-containing nerve fibres (Heuckeroth *et al.*, 1999; Rossi *et al.*, 1999). Since density of neurons is unaffected by the mutations (Gianino *et al.*, 2003), it has been suggested that NRTN produced by the circular muscle layer acts as a chemoattractant or a trophic cue for axons of a sub-population of myenteric neurons. Recently, transgenic mice overexpressing **GDNF** under control of the regulatory regions of the glial marker GFAP have shown an increase in NADPH-d fibres surrounding and connecting ganglia, without similar changes in TH or ChAT positive fibres. This

accumulation matched the distribution of GFAP-expressing glial cells, thus suggesting that the spatial expression of GDNF can attract specific subsets of neuronal processes (Wang *et al.*, 2010).

Some studies have also implicated **BMP** signalling in fasciculation and patterning of neurites within the developing gut. BMP 4 treatment results in markedly fasciculated neuronal processes within the wall and from the edge of gut explants *in vitro* (Fu *et al.*, 2006). Furthermore, BMP induced fasciculated fibres were found to extend increasingly more parallel to the main axis of the gut than in control cultures. These specific effects of BMP 4 were attributed to increase in PSA addition on the cell adhesion molecule NCAM1 and they were selectively abolished when PSA was removed by treatment of explants with endo-N. Thus, PSA-NCAM1 might have important functions in controlling neurite association and directionality by regulating homo- or heterophilic cell interactions or by altering responsiveness of neural precursors to specific neurotrophic factors, as shown in other systems (Durbec & Cremer, 2001; Muller *et al.*, 2000; Yin *et al.*, 1995).

### 1.2.5 Development of gut motility

In adult animals, intestinal motility arises from the interaction of enteric neurons, interstitial cells of Cajal (ICC) and intrinsic smooth muscle cells. Synapse-like contacts containing synaptic vesicles in the presynaptic nerve terminal can be identified ultrastructurally already in the stomach of E12.5 mice (Vannucchi & Faussone-Pellegrini, 2000). However, the functional development of these connections and their cellular components occurs throughout fetal life and early stages of postnatal life and intestinal motility complexes similar to those present in mature animals can only be recorded several days after birth. Onset of motility has been studied extensively in mouse by using spatiotemporal mappings, in which video recordings of segments of duodenum and colon *in vitro* were used to generate maps of gut diameter as function of intestinal length and time (Roberts *et al.*, 2007; Roberts *et al.*, 2008; Roberts *et al.*, 2010). Spontaneous shallow contractions that propagate orally and anally (ripples) are present in the

mouse gut before birth and they are first detected in the duodenum at E13.5 and in the colon at E14.5 (Roberts *et al.*, 2010). However, this primitive motility pattern is not dependent on neural activity, as it persists after tetrodoxin (TTX) treatment and it is present in mutant mice that lack enteric neurons (i.e. $Ret^{-/-}$ mice) (Roberts *et al.*, 2007; Roberts *et al.*, 2010). Furthermore, ripples cannot be attributed to the intrinsic contractile activity of ICCs, since morphologically mature networks of ICCs and slow wave transmission are only detected in the mouse duodenum around E18.5-E19 (Roberts *et al.*, 2010; Torihashi *et al.*, 1997), thus suggesting that the first pattern of intestinal motility is generated primarily by smooth muscle cells. The first neurally mediated propagating contraction complexes appear in the duodenum at E18.5 and in the colon at postnatal day 6 (P6) (Roberts *et al.*, 2007; Roberts *et al.*, 2010). Hence, neural control of intestinal motility arises well after neuron precursors have colonised the gastrointestinal tract, but approximately before the onset of feeding. Nevertheless, these primitive ENS-dependent contractions still differ in control, frequency and coordination from the adult pattern of motility and they seem to fully mature only several days after birth. Only from P10 duodenal contractile complexes occur upon increase in intraluminal pressure, in contrast to E18.5-P0 complexes which were triggered also at resting pressure (Roberts *et al.*, 2010), and colonic migrating motor complexes (CMMCs) propagate the entire length of the colon and have similar properties to the adult counterparts (Roberts *et al.*, 2007). Little is known about the development of circuits underlying motility reflexes. In accordance with the early appearance of NOS neurons in the ENS (Branchek & Gershon, 1989), NO is one of the earliest modulators of intestinal motility, as shown by the induction and the increase in frequency of contractile complexes produced by the nitric oxide synthase inhibitor NOLA, as early as E18.5 and P6, in duodenum and colon preparations respectively (Roberts *et al.*, 2007; Roberts *et al.*, 2010). Interestingly, this early role of NO transmission seems to be conserved in between species (Holmberg *et al.*, 2006; Sundqvist & Holmgren, 2006).

Recent studies have been able to show functional consequences of specific gene mutations involved in the cellular and molecular development of the ENS. In colon of $Gdnf^{+/-}$ mice spatiotemporal mapping has reported disorganised CMMCs at least until P14, which appear

abnormal (i.e. reduced frequency and length of propagation) and unaffected by NOS inhibition and serotonin receptor antagonism (Roberts *et al.*, 2008). In accordance, a study from Gianino et al. (2003) showed that, in *Gdnf*$^{+/-}$, *Gfrα1*$^{+/-}$ and *Ret* $^{+/-}$ mice, electrically evoked contractions of the colonic circular and longitudinal muscle and VIP and substance P release are dramatically reduced (Gianino *et al.*, 2003). Conversely, mice overexpressing GDNF (*GFAP-Gdnf*) revealed increased contractility of the smooth muscle and enhanced release of neurotransmitters *in vitro* and shorter intestinal transit time *in vivo* (Wang *et al.*, 2010). In *Et-3*$^{-/-}$ and *Ednrb*$^{-/-}$ mice, CMMCs are absent from the ganglionic region of the colon, whereas in *Ednrb*$^{+/-}$ and *Et-3*$^{+/-}$ mice, CMMCs are present, but abnormal in the former and comparable to wild-type in the latter (Roberts *et al.*, 2008). Lastly, mice overexpressing the BMP antagonist noggin (*NSE-noggin*) showed an increase in stool frequency, weight and water content, observations consistent with a shorter gastrointestinal transit time (Chalazonitis *et al.*, 2008). Together these studies suggest that impaired intestinal motility can result from a significant change in neuron density (*Gdnf*$^{+/-}$, *Ednrb*$^{+/-}$, *NSE-noggin*), from altered proportion of neuronal subclasses (*GFAP-Gdnf*, *Et-3*$^{-/-}$, *NSE-noggin)* and from yet unknown subtle changes in the ENS network (*Gfrα1*$^{+/-}$, *Ret*$^{+/-}$).

## 1.3 Enteric neuropathies

The mature ENS is involved in controlling a complex array of digestive functions. Thus, it is not surprising that damage to the ENS circuitries may result in a wide array of gut disorders, including motor abnormalities, which are characterised by high morbidity, markedly compromised patient's quality of life depending on the clinical severity, and occasional fatal outcomes. Along with defects in enteric neurons and innervation (enteric neuropathies) (De Giorgio *et al.*, 2000), alterations in smooth muscle layers (Kapur & Correa, 2009) or ICC networks (Vanderwinden & Rumessen, 1999) have also been associated with abnormal motility patterns. Current evidence indicates that enteric neuropathies arise from loss, degeneration, and functional impairment of enteric neurons resulting from congenital developmental defects of the ENS, the action of known agents (i.e. toxic, infectious) or secondary to pathological conditions

such as chronic inflammation, diabetic neuropathy, amyloidosis and Parkinson's disease. Nevertheless, for many of the primary enteric neuropathies, the aetiology is still unclear and it may involve multiple causes (Table 1.3).

**Table 1.3 Neuropathological features and proposed aetiological factors of primary enteric neuropathies**

| *Disease* | *Neuropathological features* | *Proposed aetiological factors* |
|---|---|---|
| Achalasia | Defective inhibitory innervation ± inflammatory neuropathy | Immune-mediated<br>Neurotropic viruses |
| | Complete loss of myenteric ganglia | Genetic factors |
| Gastroparesis | Degenerative neuropathy<br>Inflammatory neuropathy | Immune-mediated<br>Genetic factors |
| Congenital hypertrophic pyloric stenosis | Defective inhibitory innervation | Genetic factors |
| Chronic idiopathic intestinal pseudo-obstruction (CIP) | Degenerative neuropathy<br>Inflammatory neuropathy | Immune-mediated<br>Genetic factors |
| Slow transit constipation | Impairment in neurotransmission without evidence of neuronal damage<br>Degenerative neuropathy<br>Inflammatory neuropathy | Immune-mediated<br>Genetic factors |
| Hirschsprung's disease (HSCR) | Absence of enteric ganglia (aganglionosis) | Genetic factors |

Modified from (Di Nardo *et al.*, 2008)

### 1.3.1 Congenital enteric neuropathies

In the developing human gut, ENCC colonisation, differentiation of the muscle layers and the development of ICCs occur in a similar sequence to that described in laboratory animals. ENCCs complete their rostro-caudal migration between week 4 and 7 (Wallace & Burns, 2005), and by week 24 fetuses seem to have a full complement of enteric neurotransmitters (Rauch *et al.*, 2006; Timmermans *et al.*, 1994; Walters *et al.*, 1993), while ENS function develops during gestation and after birth (Berseth, 1996). Since enteric neurons are required for normal intestinal motility soon after birth, several developmental disorders of the ENS resulting in impaired gastrointestinal function are commonly diagnosed in neonates and infants (Chitkara & Di Lorenzo, 2006; Gariepy, 2004).

The best known form of enteric neuropathy is **Hirschsprung's disease** (HSCR), a congenital condition associated with the absence of myenteric and submucosal neurons in the

distal colon and rectum, along with hypertrophic nerve bundles in the submucosa, representing projections of extrinsic nerve fibres into the muscularis mucosa and lamina propria (Hamoudi *et al.*, 1982; Meier-Ruge, 1974). In addition, the area proximal to the aganglionic segment, the transition zone, can exhibit features of neuronal dysplasia (i.e. hypo- or hyperganglionosis) (Meier-Ruge, 1992). The lack of enteric neurons leads to tonic contraction of the aganglionic gut segment, with a concomitant functional obstruction, which is responsible for a dramatic distension of the proximal bowel (condition often referred as "megacolon"). HSCR prevalence is one case in 5000 neonates per year (Goldberg, 1984), generally diagnosed within 48 hrs from birth by failure to pass meconium, abdominal distension, vomiting or enterocolitis. Survival with this condition depends on surgical resection of the aganglionic segment and rejoining of the remaining gut to the anus, with usually variable functional outcomes, such as persisting severe constipation or fecal incontinence (Haricharan & Georgeson, 2008; Thapar, 2009). In fact, increasing evidence suggests that also the normoganglionic region of HSCR patient might be characterised by subtle alteration of the structure and function of the ENS (Baillie *et al.*, 1999; Facer *et al.*, 2001).

HSCR has a strong genetic component and it can occur as sporadic or familiar; in the latter, inheritance can be polygenic, dominant or recessive. Additionally, HSCR can exist as a single alteration or be a component of clinical syndromes such as Down's, central hypoventilation and Waanderburg syndromes (Farndon & Bianchi, 1983; Goldberg, 1984; Hamilton & Bodurtha, 1989). Several HSCR susceptibility loci have been discovered during the years by combining genetic linkage studies on familiar cases of HSCR (Brooks *et al.*, 2005) and studies on animal models reproducing the aganglionic phenotype (1.2.3). Thus, gene mutations affecting the control of ENCC proliferation, differentiation and migration have unequivocally associated with the onset of HSCR. In accordance to its pleiotropic role in ENS development, *RET* has been identified has one of the key genetic factors involved in the genesis of HSCR, with heterozygous mutations in its locus accounting for up to 50% of familiar cases (Brooks *et al.*, 2005; Chakravarti, 2001). Mutations in *EDNRB*, *ET-3* and *SOX10* genes have also been implicated in syndromic forms of HSCR associated to pigmentation defects and sensorineural

deafness, a clinical condition that is termed Waardenburg syndrome type 4 (WS4) (Hofstra *et al.*, 1996; Pingault *et al.*, 1998; Puffenberger *et al.*, 1994). Although the aetiology of HSCR is now well established, there is still no clear explanation of the motor dysfunction observed in pre- and post-operatory HSCR patients. Studies from mouse models have shown that abnormalities in the transition zone, such as decrease in neuronal density and changes in neurotransmitter release, might account for abnormal patterns of motility within and around the aganglionic segment (Roberts *et al.*, 2008).

Other common intestinal disorders have also shown some genetic inheritance, but the lack of defined neuropathological features and the absence to date of animal models in which these specific motility disturbances could be reproduced, have hindered the research of their aetiology and successful treatments. **Achalasia** is an esophageal disorder marked by the prominent defect in intrinsic inhibitory neurons releasing NO, VIP and PACAP (Park & Vaezi, 2005). The majority of cases are sporadic and findings suggest that infectious and immune agents are likely to play a role in the genesis of this pathology. However, rare cases of familial achalasia within the clinical condition termed AAA syndrome (i.e. Alacrima-Achalasia-Adrenocorticotropinresistant adrenal insufficiency syndrome) have been linked to mutations in a gene coding for a regulatory protein involved in nucleo-cytoplasmatic signalling, named ALADIN (Weber *et al.*, 1996). Defective nitrergic innervation is also a characteristic feature of congenital **hypertrophic pyloric stenosis** (Vanderwinden *et al.*, 1992). In this rare form of gastroparesis, absence of myenteric NO terminals in the pyloric region results in absence of relaxation and promotes a sustained tonic contraction of the pylorus followed by muscle hypertrophy. The pathogenic role of NO innervation defects is supported by a mouse model in which NOS ablation results in functional gastric obstruction comparable to hypertrophic pyloric stenosis (Mashimo *et al.*, 2000). However it is not clear, in both achalasia and hypertrophic pyloric stenosis, what are the molecular mechanisms affecting specifically the inhibitory innervation and sparing the excitatory component. **Chronic idiopathic intestinal pseudo-obstruction** (CIIP) represents another rare and highly morbid syndrome characterised by impaired gastrointestinal propulsion, together with symptoms and signs of intestinal functional

obstruction in absence of any lesion or physical impediment occluding the gut lumen (Coulie & Camilleri, 1999; Di Lorenzo, 1999). Typical neuropathological findings in familial cases of CIIP include reduction of neurons in myenteric and submucosal plexus, nuclear inclusions and axonal degeneration; however, these features are not found consistently in all regions of the gut and in all patients. Some genes and loci have been associated with forms of CIIP including *SOX10*, the DNA polymerase gamma (*POLG*), *FILAMIN A* and a locus on chromosome 8 (De Giorgio *et al.*, 2001; Deglincerti *et al.*, 2007; Gargiulo *et al.*, 2007). Nevertheless, the mechanism through which these factors might be involved in CIIP aetiology during and after ENS development is still unknown. Similarly, the molecular mechanisms leading to another condition termed as **slow transit constipation** (STC) remain obscure. STC is characterised by persistent inhibition of propulsive contractile activity in the colon, which is often unresponsive to high doses of laxatives and, in the most severe cases, requires surgical intervention (colectomy). Subtle alterations of the ENS, not obvious to conventional histological examination, are often associated to STC (Bassotti & Villanacci, 2006). These ENS abnormalities include altered number of neurons and defects in excitatory and/or inhibitory innervation of the circular muscle, such as reduced axonal density and changes in neurotransmitter content (Cortesini *et al.*, 1995; Krishnamurthy *et al.*, 1985; Porter *et al.*, 1998). However, the functional meaning of these findings is still a matter of debate. Indeed, the absence of an experimental model in which enteric neuropathies such as CIIP and STC can be reliably reproduced has made difficult any investigation on underlying pathophysiological and aetiological mechanisms.

## 1.4 Rho GTPases and nervous system development

### 1.4.1 Rho and Rac GTPases

GTPases are hydrolase enzymes able to bind to guanosine triphosphate (GTP) and hydrolyse it into guanosine diphosphate (GDP). Rho GTPases mostly function as molecular switches cycling between an active GTP-bound and an inactive GDP-bound conformation (Fig. 1.4). In their GTP-bound state they interact and activate effector molecules to initiate downstream responses, until GTP hydrolysis returns the protein into its inactive state (Schmidt & Hall, 2002). Nucleotide exchange and hydrolysis of GTP are catalysed by guanine-nucleotide-exchange factors (GEFs) and GTPase-activating-proteins (GAPs), respectively (Bernards & Settleman, 2004; Schmidt & Hall, 2002). In addition, Rho GTPases can bind to proteins known as guanine-nucleotide-dissociation inhibitors (GDIs), which prevent their interaction with the plasma membrane, but not necessarily with downstream targets (Zalcman *et al.*, 1999). Most Rho proteins are post-translationally modified at their C-termini by prenylation of a conserved cysteine and this is required for their interaction with membranes and function (Seabra, 1998).

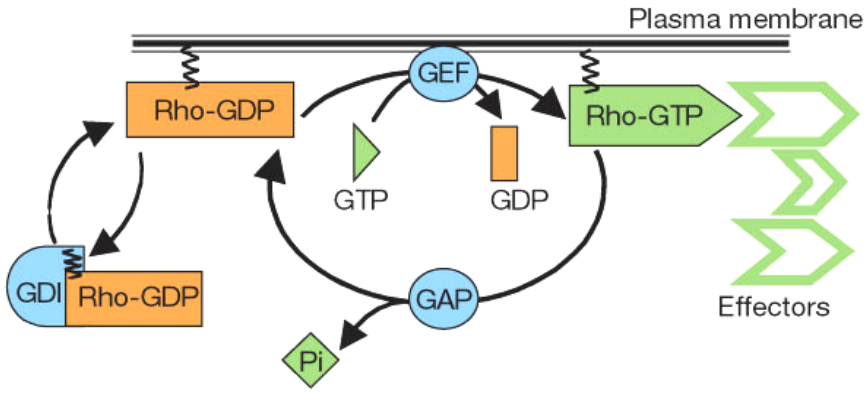


**Figure 1.4 The Rho GTPase cycle and regulation**

Almost all the members of the Rho GTPases cycle between a GTP-bound ('active state') and a GDP-bound ('inactive state'). In their active conformation they are able to interact with downstream effectors. Three classes of regulatory proteins control the cycle: GEFs (guanine-nucleoside-exchange factors) promoting exchange of GDP with GTP, GAPs (GTPase-activating proteins) stimulating GTP hydrolysis and GDIs (guanine-nucleoside-dissociation inhibitors) extracting the inactive GTPase from the membrane. Interaction with membranes is mediated by prenylation of the C-terminus of the protein. Figure from (Etienne-Manneville & Hall, 2002).

Mammalian Rho GTPases comprise a family of 20 members, of which RhoA (Ras homologous member A), Rac1 (Ras-related C3 botulinum toxin substrate 1) and Cdc42 (cell division cycle 42) have been characterised most extensively (Heasman & Ridley, 2008). Based on sequence similarity to Rac1, a subfamily of Rac GTPases can be identified and it comprises four members: Rac1, Rac2, Rac3 (sharing 88-92% sequence identity) and RhoG (the most divergent, with approximately 70% sequence homology with Rac1) (Heasman & Ridley, 2008). The four genes have specific expression patterns: *Rac1* is expressed ubiquitously (Moll *et al.*, 1991), *Rac2* expression is mainly restricted to cells of hemopoietic lineages (Shirsat *et al.*, 1990), *Rac3* is enriched in the developing and adult nervous system (Haataja *et al.*, 1997; Malosio *et al.*, 1997) and *RhoG* is expressed at varying levels in a variety of organs including the brain (O'Kane *et al.*, 2003; Vincent *et al.*, 1992). Rac GTPases, along with many of the other Rho GTPases, are critical regulators of the actin cytoskeleton in several physiological and developmental processes such as control of cell morphology and polarity, cell motility, cell-cell and cell-ECM interactions. In addition, some Rho GTPases members have also been shown to play a role in transcriptional activation, secretion, phagocytosis and proliferation (Etienne-Manneville & Hall, 2002; Jaffe & Hall, 2005).

### 1.4.2 Rac GTPases and neuronal development

Studies *in vitro* in mammalian cultured cell lines and *in vivo* in *Drosophila melanogaster* and *Xenopus laevis* have described a variety of functions for Rho GTPases in neural development, such as control of neuronal migration, neurite and dendrite formation, polarization, axon growth, branching and axon guidance (Govek *et al.*, 2005). However, the *in vivo* role of these proteins in mammalian neuronal development has always been elusive, although recent generation of knock-out mice for several members of the Rho family, including Rac proteins, has provided some new insights (Heasman & Ridley, 2008). Rac1 knock-out mice show a range of defects in germ-layer formation and die at gastrulation (Sugihara *et al.*, 1998). To bypass the early lethality of Rac1-deficient embryos, conditional knock-out mice have been generated, which allow the cell and tissue-specific ablation of Rac1 (Chrostek *et al.*, 2006; Glogauer *et al.*, 2003; Walmsley *et al.*,

2003). Global knockout mice for Rac2 (Roberts *et al.*, 1999), Rac3 (Cho *et al.*, 2005; Corbetta *et al.*, 2005) and RhoG (Vigorito *et al.*, 2004) are viable and do not show obvious developmental defects, but they do have cell-type-specific functional impairments.

#### *1.4.2.1 Migration of progenitor cells and neurons*

It is known that *in vitro* cell migration requires the formation of membrane protrusions at the leading edge of the cell, membrane adhesive interactions with the extracellular substrate and the coordinated dynamics of the cytoskeleton (Ridley *et al.*, 2003). Rho GTPases (Rac, Rho and Cdc42) are well-known modulators of several of these activities (Jaffe & Hall, 2005; Ridley *et al.*, 2003). Moreover, it has been shown that directional migration *in vitro* in the absence of extrinsic chemoattractants is controlled by the level of Rac activity (Pankov *et al.*, 2005). Rac promotes the formation of peripheral lamellipodia during random migration, while slightly lower levels of Rac favour the formation of a polarized cell with lamellipodia specifically at the leading edge (Pankov *et al.*, 2005). Directed collective migration is a feature of neural crest cell derivatives in the embryo. *In vivo* fluorescence resonance energy transfer (FRET) microscopy in migrating cranial neural crest cells in *Xenopus* has revealed that directed migration of NCCs is the result of the coordinated polarisation and activity of small GTPases. Cell-cell interactions within the migrating cell population lead to increase RhoA activity at the site of contact, which inhibits Rac1 activity locally and promotes protrusion retraction (Carmona-Fontaine *et al.*, 2008; Matthews *et al.*, 2008). At the same time, Rac1 activity increases at the juxtamembrane promoting the extension of cell protrusions, which are stabilised by the presence of an extracellular chemokine gradient (i.e. the stromal-cell derived factor, Sdf1), thus leading to directed migration towards the chemoattractive source (Theveneau *et al.*, 2010). Extensive migration is also characteristic of neuronal progenitors within the developing cortex in mammals. Findings suggest that Rac 1 GTPase is able to control several aspect of this process. Overexpression of a dominant-negative form of Rac1 in cortical progenitors in the subventricular zone (SV) *in vivo* severely retards the radial migration of neurons without affecting their

differentiation (Kawauchi *et al.*, 2003). In accordance, *in vivo* ablation of p35 protein, a downstream effector of Rac1, alters the "inside-out" migration pattern of cortical projection neurons (Chae *et al.*, 1997; Nikolic *et al.*, 1998). Furthermore, when Rac1 is conditionally ablated in the entire ventricular zone (VZ) of the telencephalon (using a Foxg1-Cre transgene), tangential migration of olfactory and cortical interneurons is disrupted (Chen *et al.*, 2007).

#### *1.4.2.2 Neuronal morphology and neuritogenesis*

Rac GTPases have been implicated in promotion of cell-ECM adhesion complexes, important for both migration of progenitors and neurite outgrowth. *In vitro* studies on mammalian neuroblastoma cells have shown an opposing role of Rac1 and Rac3 on cell adhesion and neuronal differentiation. In this system, Rac1 stimulates cell spreading and neurite outgrowth by promoting the assembly of integrin adhesion complexes, whereas Rac3 induces cell rounding and poor cell adhesion by inhibiting Rac1-mediated adhesive effects (Hajdo-Milasinovic *et al.*, 2007; Hajdo-Milasinovic *et al.*, 2009). Nevertheless, neurite outgrowth also requires a coordinated growth of the actin cytoskeleton, a process that appears to be highly dependent on the activity of all three neuron-expressed Rac GTPases (i.e. Rac1, Rac3 and RhoG) (de Curtis, 2008). However, the control of neuritogenesis by GTPases seems complex, with distinct effects of individual members and differential effects of the same GTPase on different neuronal compartments. For example, in *Drosophila* Rac1 mutants disrupt axon growth, leaving dendritic morphology intact in sensory neurons (Luo *et al.*, 1994), whereas the same mutants show axon guidance, but not growth, defects in motor neurons (Kaufmann *et al.*, 1998). Furthermore, the progressive loss of the combined activity of Rac genes leads to distinct effects on neurite development in mushroom body neurons, where branching is the first process to be affected, followed by guidance and finally growth (Ng *et al.*, 2002). In mammals, perturbance of Rac1 activity by expression of a constitutively active form of the protein in mouse Purkinje cells *in vivo* leads to axonal growth defects with apparently normal dendritic arbor growth (Luo *et al.*, 1996). Conversely, treatment of hippocampal neurons with siRNA (small interfering RNA) for Rac1 specifically impairs dendrite growth, without affecting neuronal polarity, branching and axonal growth (Gualdoni *et*

*al.*, 2007), and, furthermore, conditional knockout of Rac1 in telencephalic neurons shows normal axonal outgrowth and branching (Chen *et al.*, 2007). Hence, the requirement for Rac1 activity in neuritogenesis is specific in various neuronal types and structures.

During development, Rac3 expression is particularly abundant during the time of intense neurite branching and synaptogenesis within the CNS, which highly suggests a role for the protein in neuronal maturation (Albertinazzi *et al.*, 1998; Bolis *et al.*, 2003). In accordance, *in vitro* overexpression of Rac3 potentiated neuritogenesis and branching in avian retinal neurons (Albertinazzi *et al.*, 1998). Surprisingly, Rac3-deficient hippocampal neurons have normal morphology and polarity and Rac3-null mice have no gross anatomical defects in brain structure or in the organisation of neurons (Corbetta *et al.*, 2005; Gualdoni *et al.*, 2007). Nevertheless, behavioural studies revealed hyperactivity to novel stimuli and changes in motor learning, suggesting a subtle effect of Rac3 deletion in neuron network structure and function (Corbetta *et al.*, 2008). In accordance, generation of double mutant Rac1/Rac3 mice (*SynI-Cre;Rac1*$^{f/f}$*;Rac3*$^{-/-}$) (Corbetta *et al.*, 2009) has revealed a synergistic activity of the two Rac GTPases in hippocampus development, including branching and synaptogenesis of mossy cells, and dendritic spine development (Corbetta *et al.*, 2009). Dendritic spines are special protrusions receiving synaptic inputs from axons and they are the basic units of synaptic integration. Some earlier studies had shown that expression of constitutive active Rac1 in mice results in increased number (but smaller size) of dendritic spines in Purkinje cells (Luo *et al.*, 1996), whereas a dominant negative form of Rac1 is able to reduce the formation of dendritic spines in rat cortical neurons *in vitro* (Threadgill *et al.*, 1997). In hippocampal neurons, Rac1 depletion leads to mild effects on spine formation and only the concomitant ablation of Rac3 results in severe defects in number and shape of dendritic spines, thus suggesting a cooperative role of Rac1 and Rac3 in dendritic remodelling (Corbetta *et al.*, 2009).

#### *1.4.2.3 Axon guidance*

Axon guidance can be thought of as a specialised form of directed migration, where the growth cone at the axon tip responds to attractive and repulsive extracellular cues as it extends to its

target site. Thus, Rho GTPases activity, regulating actin filament assembly and disassembly and actin-myosin-dependent contractility, underlies the growth cone dynamics in response to extracellular cues (Dickson, 2001). Evidence for a specific role of Rac GTPases in axon guidance comes from several organisms. In *Caenorhabditis Elegans* the mutation of the Rac-like GTPase Mig-2 causes occasional guidance defects (Zipkin *et al.*, 1997). Similarly, in *Drosophila*, perturbation of Rac activity leads to axon guidance errors at specific choice points in motor neurons (Kaufmann *et al.*, 1998) and aberrant accumulation of misguided axons in mushroom body neurons (Ng *et al.*, 2002). In mouse, conditional deletion of *Rac1* in telencephalic neurons results in failure of axons to form commissural fibres and corpus callosum (Chen *et al.*, 2007; Kassai *et al.*, 2008). Furthermore, genetic loss-of-function of the triple functional domain protein (TRIO) has shown, in several animal models, that this GEF, which is able to activate Rac1 and RhoG, is required for axon guidance. In *Drosophila* TRIO homologue is genetically required for the growth and guidance of sensory neurons and central nervous system neurons (Awasaki *et al.*, 2000; Bateman *et al.*, 2000; Liebl *et al.*, 2000; Newsome *et al.*, 2000). Similarly, mice that lack TRIO display an aberrant organisation in several regions of the CNS, including absence of anterior commissural axons, defasciculated spinal commissural axon projections and defective corpus callosum and internal capsule (Briancon-Marjollet *et al.*, 2008; O'Brien *et al.*, 2000). An outstanding issue remains on whether Rac GTPases only provide regulation of cellular structures (i.e. lamellipodia) necessary for the progression of the growth cone (permissive role) or whether they also interpret the guidance signals directly (instructive role). The investigation of the intracellular cascades downstream of known guidance cues has supported the idea of an instructive role for Rho GTPases. In fact, Rac1 has been found to specifically mediate the effects of semaphorins (Vastrik *et al.*, 1999) and netrins (Briancon-Marjollet *et al.*, 2008), whereas another member of the Rho family, RhoA was shown to be downstream of the ephrin-induced growth cone collapse (Wahl *et al.*, 2000).

### 1.4.3 Rac GTPases in ENS development

The role of Rac GTPases in ENS development has just started to be unveiled, although the relevance of these molecular mediators in enteric axon guidance has not yet been addressed.

RET receptor kinase and the co-receptor GFRα1 are expressed by migrating ENCCs and they mediate responses to GDNF that is produced by embryonic gut mesenchyme. Several studies have demonstrated that the signalling complex GDNF-GFRα1-Ret plays a crucial role for the proliferation, survival and differentiation of ENS progenitors and that it is also involved in the chemoattraction and migration of ENCCs (1.2.3). Biochemical studies have shown that the phosphorylation of the serine residue at codon 696 (S696) of RET is required for Rac1-GEF activation and lamellipodia formation in a human neuroectodermal tumor cell line (Fukuda *et al.*, 2002) and that *in vitro* and *in vivo* targeted mutation of S696 leads to abnormal colonization of the gut by ENCCs (Asai *et al.*, 2006). Furthermore, some recent studies have dealt with the dissection of possible signalling pathways downstream of RET which may control migration and neurite outgrowth (Fu *et al.*, 2010; Vohra *et al.*, 2007). It was speculated that Rac1 is activated at the leading edge of migrating ENCCs by the GDNF-mediated localised activity of phosphatidylinositol 3 kinase (PI3K) and it is inhibited by accumulation of PTEN (Fu *et al.*, 2010). In addition, during enteric neuritogenesis, activation of the protein kinase Cζ and glycogen synthase kinase-3β downstream of RET are thought to be part of a positive feedback loop involving Rac1/Cdc42 activation (Vohra *et al.*, 2007). Although conceptually interesting, these studies did not present any evidence of a direct involvement of Rho GTPases in ENS development *in vivo*.

A first attempt to address this issue has been reported by Stewart et al. (2007), who pharmacologically inhibited the activity of Rac/Cdc42 and Rho kinases, Rock-I and Rock-II in intact gut explants (Stewart *et al.*, 2007). The authors found that inhibition of both Rac/Cdc42 and Rho signalling led to retarded migration of ENCCs and extension of axons along the developing hindgut, without affecting cell proliferation and differentiation. In addition, both treatments increased the frequency of uncoupled undifferentiated cells and axonal $Tuj1^{+}$ ends at

the front of migration, whereas inhibition of Rac1/Cdc42 also led to reduced protrusions and cell-cell contacts in wavefront ENCCs. These effects were shown to be possibly RET-dependent, since ENCCs in explants of guts from embryos that were haploinsufficient for RET were more sensitive to the inhibitors (Stewart *et al.*, 2007). On the other hand, the first attempt to address the specific function of Rac1 and Cdc42 in the neural crest development *in vivo* has recently been reported (Fuchs *et al.*, 2009). Ablation of either one of the two genes by using the NC specific Wnt1-Cre line (Danielian *et al.*, 1998) led to morphological defects in NC target tissues, such as defects in craniofacial structures, heart septation, size of dorsal root ganglia and colonization of the distal parts of the gut. The phenotype was correlated to increased cell cycle exit in NCCs within target tissues, with no recorded defects in NCC migration or differentiation. Neural crest stem cell proliferation and self-renewal are suggested to a have a stage-specific requirement for mitogenic growth factors, such as the epidermal growth factor (EGF), which acts intracellularly through Rac1/Cdc42. Thus, during early stages, emigrating NCCs are dependent on the mitogenic activity of the fibroblast growth factor (FGF), whereas, upon reaching target tissues, such as the gut, they also acquire sensitivity to EGF by expressing its receptor (EGFR). EGF and FGF were shown to be able to promote enteric NCSC proliferation from explants of E11.5 guts, although only EGF-mediated proliferation seemed dependent on the presence of Rac1 and Cdc42. In accordance, enteric NCSCs generated from Rac1 and Cdc42 mutant guts showed decreased proliferation and self-renewal in sphere assays *in vitro* (Fuchs *et al.*, 2009). Interestingly, a recent report has also dealt with the defects arising from Rac1 mutation in craniofacial and cardiovascular development in the same genetic mouse model (Rac1|Wnt1-Cre) (Thomas *et al.*, 2010). Rac1-mutant NCCs were reported to fail to migrate from neural tube explants and NCCs within the pharyngeal arches showed poor spreading and impaired formation of focal adhesion complexes *in vitro*, thus suggesting that Rac1 might also be involved in controlling adhesive properties of NCCs within their target tissues (Thomas *et al.*, 2010).

Taken together, these observations demonstrate that Rac1 GTPase is required for the normal development and colonization of the gut by NCCs, however it is unclear what is its real *in vivo* contribution in processes such as proliferation, migration and axonal growth and whether

any of these is secondary to the other/s. Moreover, there is no information at the present on whether axon guidance and connectivity between enteric neurons may rely on Rac activity. Nevertheless, the signalling pathways that lead to Rac1 activation and the effector mechanisms regulated by this GTPase are poorly understood. Finally, the relative contributions of the other members of the Rac subfamily of GTPases (such as Rac3) on ENS development are currently unexplored.

## 1.5 Wnt signalling in neural circuit development

### 1.5.1 Canonical and non-canonical Wnt pathways

The Drosophila Wingless (Wg) and their vertebrate homologues Wingless-type (Wnt) proteins consist of a family of molecules able to initiate several intracellular pathways (Nusse, 2005). The first to be discovered was the molecular cascade leading to the stabilisation and subsequent nuclear translocation of β-catenin (canonical pathway) (Cadigan & Liu, 2006). However, more recent work has identified at least two additional pathways, referred as "non-canonical", which are mediated through Rho GTPases and calcium signalling (Veeman *et al.*, 2003). In vertebrates, there are 19 identified Wnt genes and at least 10 genes encoding for Frizzled (Fzd) family of seven-pass trans-membrane receptors capable of binding Wnt proteins. In the canonical pathway (Fig. 1.5 A), the binding of Wnt to a Fzd receptor, in association with a coreceptor (i.e. low-density-lipoprotein-related protein, LRP5 or LRP6), triggers the phosphorylation and activation of a cytoplasmic signalling molecule, Disheveled (Dvl), which inhibits the ability of GSK-3β to target β-catenin for degradation. Increased cytoplasmic β-catenin is subsequently translocated into the nucleus, where it complexes with members of the TCF/LEF (ternary complex factor/lymphoid enhancer factor) family, leading to transcriptional changes important in embryonic patterning, cell fate determination and cell proliferation (Cadigan & Liu, 2006). In the non-canonical signalling pathway, Fzd-mediated Dvl activation is maintained, but the downstream pathways do not involve GSK-3β or β-catenin. In the Wnt-calcium pathway (Fig. 1.5 B) certain combinations of Wnts and Fzds can increase intracellular calcium and activate the calcium/calmodulin-dependent kinase (CAMKII) and the protein kinase C (PKC), which mediates various intracellular responses (Kohn & Moon, 2005). Finally, a second non-canonical pathway (Fig. 1.5 C) utilises Fzds and Dvl, along with a number of other molecules, to activate Rho GTPases, the heterotrimeric G proteins, and in some cases, C-Jun N-terminal kinase (JNK), which modulate cytoskeletal elements including actin and microtubules. This pathway has been discovered, and extensively studied, in *Drosophila*, where it controls the uniform orientation of epithelial cells along a plane orthogonal to their apicobasal axes and, therefore, it has been

referred to as Planar Cell Polarity (PCP) pathway (Zallen, 2007). Analysis of mutants revealed that a similar pathway is also involved in control of cell polarity in vertebrates, where the best examples come from sensory hair cells of the inner ear and progenitors undergoing convergent extension during neural tube closure (Montcouquiol *et al.*, 2006; Wang & Nathans, 2007). These studies strongly support the presence of core PCP genes highly conserved across species and tissues. These include ***Fz*** (encoding for Fzd proteins), ***Dvl***, ***Celsr*** (cadherin, epidermal growth factor (EGF)-like, laminin globular (LAG)-like and seven pass receptor; the vertebrate hortholog of *Drosophila* flamingo, fmi), ***Vangl*** (Van-Gogh like; vertebrate hortholog of *Drosophila* Vang gogh/strabismus, Vang/stbm) and ***Pk*** (Prickle). The specific roles of these factors in vertebrates have not yet been fully determined, but data from *Drosophila* suggest that Celsr might mediate homophilic cell-cell interactions which lead to asymmetric distribution of Fzd and Vangl (Chen *et al.*, 2008), whereas Vangl-Pk complexes might play a role in inhibition or degradation of Dvl (Park & Moon, 2002). Interestingly, although the PCP pathway utilises Fzd and Dvl, the requirement for Wnt proteins is variable. In *Drosophila*, for example, Wg is not required for activation of Frizzled during PCP, whereas, there is strong evidence that vertebrates have retained a role for Wnts in this pathway (Mlodzik, 2002; Wang & Nathans, 2007). Therefore, it is intriguing how Wnt-Fzd interactions are able to activate multiple downstream pathways in different contexts. Findings suggest that there is some level of specificity in the Wnt and Fzd members, where Wnt4, Wnt5a, Wnt7a, Wnt11 appear to signal preferentially through the non-canonical pathways (Du *et al.*, 1995) and, similarly, Fzd3 and Fzd6 appear to be involved specifically in PCP-related processes (Wang *et al.*, 2006).

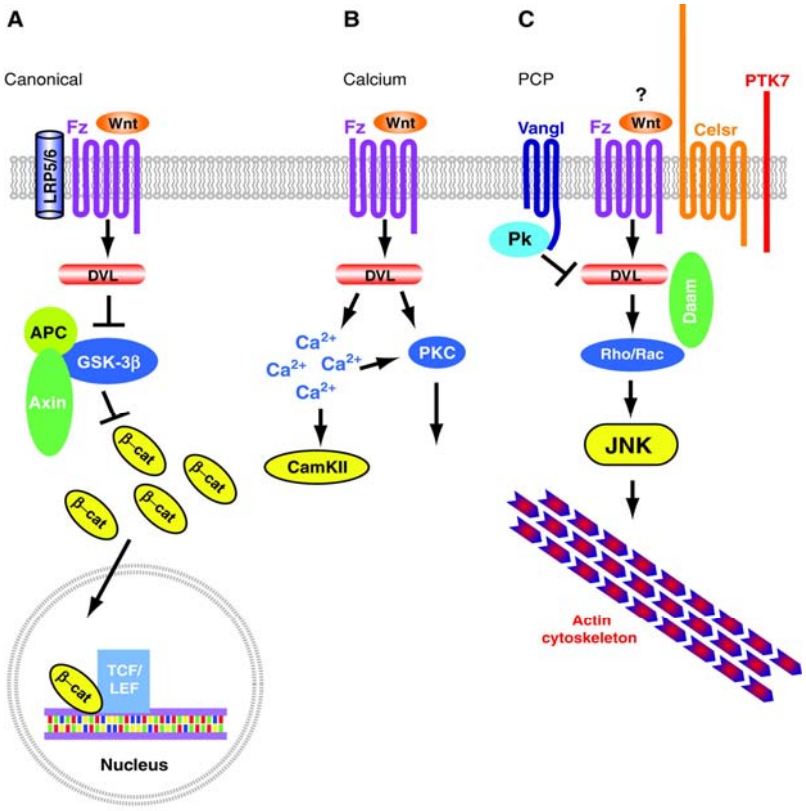


**Figure 1.5 Wnt signalling pathways**

**A**. The canonical Wnt signalling pathway. **B**. The Wnt-calcium pathway. **C**. The Wnt-PCP pathway. See text for description and abbreviations. Figure from (Montcouquiol *et al.*, 2006)

### 1.5.2 PCP genes and neuronal development

Although studies with mice have confirmed the presence in vertebrates of conserved PCP pathways in maintenance of polarity within the epithelium, they also illustrated novel and broader functions of PCP genes in several aspects of neuronal development, such as migration, neuronal polarity, axon guidance and dendrite morphogenesis (Goodrich, 2008; Wada & Okamoto, 2009). It is still not clear whether these functions occur in response to already established PCP polarisation events or whether they result from acquired new functions of PCP genes which exploit properties that are fundamental to the PCP signalling (i.e. cytoskeleton remodelling). Nevertheless, a general theme of these developmental processes is the proper positioning of cells and their processes in response to directional cues, therefore it is likely that common molecular mechanisms are shared.

#### *1.5.2.1 Migration*

PCP genes have been firmly involved in the control of directed migration of groups of cells along stereotypical trajectories, such as neurons in the developing brain and neural crest cells along their migratory routes. In this context, PCP components seem to regulate cytoskeletal changes, membrane protrusions, cell-cell interactions and directionality.

Facial branchiomotor neurons (BMNs) within the embryonic hindbrain undergo tangential migrations along the mediolateral axis such that specific BMN subtypes occupy distinct dorsolateral locations (Chandrasekhar, 2004). In zebrafish, mutants in *Vangl*, *Pk1*, *Fz3* and *fmi/Celsr2* show migration defects in BMNs, consistent with a failure for these cells to generate and maintain caudally directed protrusions (Bingham *et al.*, 2002; Carreira-Barbosa *et al.*, 2003; Jessen *et al.*, 2002; Wada *et al.*, 2006). Mosaic analysis has shown that these PCP components act both cell-autonomously and non-cell autonomously, thus suggesting that cell-cell interactions, possibly mediated by homophilic interactions of Celsr proteins, may direct the trajectory of migrating BMNs (Jessen *et al.*, 2002). Interestingly, no Wnt ligands have been so far linked to BMN migration in zebrafish (Chandrasekhar, 2004), unlike in mouse, where a recent study has revealed a chemoattractive role for Wnt5a, which acts on a conserved network of PCP genes, including Fzd3 and Vangl2 (Vivancos *et al.*, 2009). In addition, a recent study has reported a role also for Celsr proteins in BMN migration. In particular, Celsr1 appears to provide, non-cell autonomously, a directional cue to neuronal progenitors, while Celsr 2 and Celsr 3, along with Fzd3 would be required for rostrocaudal migration and maintenance of BMNs (Qu *et al.*, 2010). In accordance with this putative role of Celsr genes in neuronal migration, Celsr3 has been recently implicated in tangential and radial migration of specific subclasses of interneurons in the developing mouse brain (Ying *et al.*, 2009).

Neural crest cell migration represents a second interesting example, where canonical Wnt signalling is required for specification of neural crest, whereas the non-canonical pathway seems to play a fundamental role in control of migration. In earlier studies in *Xenopus*, De Calisto et al. (2005) showed that overexpression of non-canonical Dvl mutants did not affect neural crest

induction, but severely impaired the migration of NCCs, which did not move away from their site of formation and showed reduced size of cellular protrusions (De Calisto *et al.*, 2005). In addition, a gradient of Wnt11 produced by the ectoderm just adjacent to premigratory NCCs has been shown to be required for neural crest migration and to possibly activate the non-canonical Wnt pathway through Fzd7 and the protein kinase 7 (Ptk7) (De Calisto *et al.*, 2005; Shnitsar & Borchers, 2008). Further studies into the molecular mechanism of PCP signalling in neural crest migration revealed that the pathway is able to activate RhoA and, by doing so, to mediate contact inhibition of locomotion (CIL), a phenomenon in which a cell changes direction of polarisation and migration upon contact with another cell (Carmona-Fontaine *et al.*, 2008; Matthews *et al.*, 2008). In *Xenopus* migratory neural crest cells, Wnt11, Fzd7 and Dvl accumulate at contacting surfaces, where RhoA is activated and lamellipodia are locally inhibited, producing a polarised cell (Carmona-Fontaine *et al.*, 2008). Thus, core PCP genes might contribute to NCC migration by indicating cell-cell contacts and inducing transient cell repulsion. According to this model, Wnt11 is required for polarisation but does not provide directionality (i.e. it is not a chemoattractant). Additionally, CIL has been shown to be also dependent on cell-cell contact mediated by N-cadherins, which inhibits Rac1 activity at the site of contact and further polarise the migrating cells (Theveneau *et al.*, 2010). However, the precise mechanism of interaction between N-cadherin and Wnt/PCP during CIL remains to be investigated.

#### *1.5.2.2 Neuronal morphology and neuritogenesis*

In the mouse CNS, many PCP genes are expressed in regionalised patterns throughout fetal life, suggesting the possibility that these genes are involved in aspects of brain development other than migration (Tissir *et al.*, 2002; Tissir & Goffinet, 2006). Indeed, in *Drosophila*, flamingo regulates dendritic morphology and growth (Gao *et al.*, 2000), and, in vertebrates, Celsr 2 and Celsr 3 affect neurite growth *in vitro* by promoting and inhibiting it, respectively (Shima *et al.*, 2007). However, little is known about the molecular mechanisms underlying these Celsr functions and it has been suggested that fmi/Celsr might operate independently from other PCP genes (Gao *et al.*, 2000; Shima *et al.*, 2004). A role for Wnt5a in control of polarity and growth

of neurites has been highlighted recently. *In vitro*, Wnt5a is able to induce multiple axons in cultured hippocampal neurons, promote axonal growth in cortical neurons and potentiate the nerve growth factor (NGF)-mediated axonal branching and growth in developing sympathetic neurons (Bodmer *et al.*, 2009; Li *et al.*, 2009; Zhang *et al.*, 2007). In these contexts, Wnt5a activity appears to be mediated by non-canonical pathways (Li *et al.*, 2009) and, possibly, by intersection with other intracellular signalling pathways (i.e. apico-basal polarity Par pathway) (Zhang *et al.*, 2007), however the precise molecular effectors are still unknown. Similarly, Wnt7a has been reported to promote dendritic branching through Dvl-dependent activation of Rac and JNK (Rosso *et al.*, 2005)

#### *1.5.2.3 Axon guidance*

Studies in both vertebrates and invertebrates have shown that both Wnt proteins and PCP genes have a role in axon guidance. In *Drosophila*, *flamingo* null mutations are embryonically lethal as a result of defective longitudinal tracts in the CNS; likewise, fmi ablation within the visual system leads to mistargeting of photoreceptor axons (Chae *et al.*, 1999; Chen & Clandinin, 2008; Lee *et al.*, 2003; Usui *et al.*, 1999). Analysis of Fzd3 and Celsr3 knockout mice has revealed remarkably similar defects in axonal tract formation, including loss of anterior commissure, and thalamocortical and corticothalamic tracts, without affecting proliferation or differentiation of neuronal progenitors (Tissir *et al.*, 2005; Wang *et al.*, 2002). To test the cell/non cell-autonomous effects of the mutation in the Celsr 3 locus, a series of conditional mutant mice were also analysed (Zhou *et al.*, 2008). Results suggest that Celsr expression is required both in axons and in cells that possibly guide axons through a specific region ("guidepost" cells) to mediate cell-cell interactions (Zhou *et al.*, 2008). Although there is no evidence of genetic interaction between Fzd3 and Celsr3 in axonal tract formation, it appears that they function together in the same PCP pathway. For example, within the developing CNS, Celsr3 expression has been found concomitantly with that of Fzd3, Dvl3 and Pk2, thus indicating a favourable position for all these genes to interact (Tissir & Goffinet, 2006). Additionally, Fenstermaker et al. (2010) have reported that core PCP genes, such as Fzd3, Celsr3 and Vangl2 are expressed in monoaminergic

neurons in the brainstem and, when mutated, they lead to anterior-posterior (A-P) axon guidance defects associated with aberrant orientation of neuronal cell bodies (Fenstermaker *et al.*, 2010). The same authors have also shown that this set of PCP core genes might function by mediating the attractive and repulsive effects of gradients of Wnt proteins (i.e. Wnt5a and Wnt7a) (Fenstermaker *et al.*, 2010). These findings suggest that the Wnt/PCP pathway is indeed a guidance mechanism for patterning of axons within the CNS. Further support for this hypothesis has been provided by studies showing that Fzd3 mediates the anterior-directed growth of spinal cord commissural axons in response to the Wnt4 gradient present within the floor plate (Lyuksyutova *et al.*, 2003). Similarly, corticospinal tract axons, which project in the opposite direction, were found to be repelled and directed posteriorly by a gradient of Wnt1 and Wnt5a within the spinal cord grey matter (Liu *et al.*, 2005), and callosal commissural axons were repelled by Wnt5a produced at the midline (Keeble *et al.*, 2006). This Wnt repulsion has been reported to be mediated by a newly identified atypical tyrosine-kinase receptor Ryk (related to tyrosine kinase, the vertebrate homologue of *Drosophila Derailed*) (Keeble *et al.*, 2006; Liu *et al.*, 2005; Yoshikawa *et al.*, 2003).

It is still unclear how Wnt-mediated attraction and repulsion is transduced by Fzd and Ryk receptors. Wnt-calcium and PCP signalling are the best candidates, since their strong involvement in Wnt-mediated cell migration, a process that has many similarities with axon guidance. Furthermore, there is increasing evidence that GTPase activation is necessary to control the response of the growth cone to different guidance cues (Schlessinger *et al.*, 2009).

### 1.5.3 Wnt signalling in ENS development

To date there is no evidence that implicates Wnt-signalling related molecules in any aspect of ENS development. Earlier studies have reported temporal- and spatial-restricted expression of several Wnt proteins in the gut wall during development, such as Wnt4, Wnt5a and Wnt11 (Lickert *et al.*, 2001). These genes have been mainly implicated in the morphogenesis of the intestinal tube so far. For example, Wnt5a knockout mice present several defects along their gastrointestinal tract; the A-P gut axis is shortened and the midgut has a bifurcated lumen instead

of a single tube (Cervantes *et al.*, 2009). Detailed analysis has suggested that Wnt5a acts through a non-canonical Wnt pathway to regulate proliferation and intercalation of epithelial cells (Cervantes *et al.*, 2009). Nevertheless, no investigation of specific abnormalities in the ENS has been reported on mice lacking Wnt proteins or PCP genes. Thus, it is possible that these molecules used to regulate tissue morphogenesis in early patterning of the gastrointestinal tract, can be also used to control axon growth, directionality and connectivity at later stages, as it has been shown in the CNS (Ciani & Salinas, 2005).

## 1.6 Aims of the present work

The functional development of the enteric nervous system (ENS) requires enteric neural crest cells (ENCCs) and newly generated neurons to migrate to their appropriate sites, extend neurites, guide axons and dendrites to suitable locations and establish synaptic connections with the appropriate targets. Currently there is very little evidence about the molecular mechanisms underlying these processes. Therefore, the overall aim of this work is to dissect the role of molecular candidates in specific aspects of enteric circuitry development, such as migration, cell polarity, neuritogenesis and axon guidance.

Recent findings have suggested that Rho GTPases might control different aspect of ENS development; however, their relative participation in ENCC migration and enteric neuron maturation is still elusive. Thus, we wish to determine whether Rac1 and Rac3 functions are required *in vivo* for guidance of migratory ENCCs and/or enteric neuronal processes. Furthemore, by using a combination of *in vitro* assays, we intend to dissect some of the molecular pathways involving the activation of these Rac GTPases.

On the other hand, unlike in the developing central nervous system, in the ENS no studies to date have shown the existence of molecular pathways specifically responsible for axonal pathfinding in enteric neurons. We wish, therefore, to identify potential candidates involved in neuronal maturation and axon guidance of enteric neurons. To address this aim, we will explore the expression pattern of members of the Wnt-signalling pathway and their potential role in enteric circuitry formation *in vivo* and *in vitro*.

# Chapter 2

# Materials and Methods

## 2.1 Materials

### 2.1.1 Solutions and buffers

General solutions and buffers were prepared by in-house facilities at the MRC National Institute for Medical Research using reagents from Sigma-Aldrich and Fisher Scientific as follow:

| | |
|---|---|
| **Phosphate Buffer Saline (PBS), 1X** | 137 mM NaCl, 3mM KCl, 8mM $Na_2HPO_4$, 1.5 mM $KH_2PO_4$ in $dH_2O$, pH 7.4 |
| **Tris-acetate EDTA (TAE), 1X** | 40mM Tris-acetate, 1mM EDTA in $dH_2O$ |
| **Tris-borate EDTA (TBE), 1X** | 100mM Tris-borate, 5mM EDTA in $dH_2O$ |
| **Sodium chloride-citrate buffer (SSC), 1X** | 150 mM NaCl, 15mM trisodium citrate in $dH_2O$ |
| **Lysogeny Broth (LB) medium, 1X** | 1% w/v Bactotryptone, 0.5% w/v yeast extract, 1% w/v NaCl |
| **Lysogeny Broth (LB) agar, 1X** | 1% w/v Bactotryptone, 0.5% w/v yeast extract, 1% w/v NaCl, 2% w/v agar |

Specialised solution and reagents will be described in the relevant sections.

### 2.1.2 Chemicals

All general chemicals were obtained from Sigma-Aldrich, unless otherwise stated.

| | |
|---|---|
| **Agarose** | Roche 11 388 991 001 |
| **Sodium Dodecyl Sulfate, SDS** | Biorad 1610418 |
| **Triethanolamine** | Fluka 90279 |
| **Vectashield mounting medium with DAPI** | Vector Laboratories H1200 |
| **Glycergel Mounting Medium** | DAKO C0563 |
| **GelRed™** | Biotium BT41003 |
| **Sylgard 184 silicone elastomer kit** | Dow Corning |

### 2.1.3 Enzymes

| | |
|---|---|
| **Proteinase K** | Roche 3 115 879 |
| **Collagenase/Dispase** | Roche 10 269 638 |

### 2.1.4 Tissue culture and detection reagents

Leibovitz's L-15 medium (E15-821) was from PAA. Dulbecco´s Modified Eagles Medium (DMEM, D5671) was from Sigma-Aldrich. OptiMEM (31985), Neurobasal medium (211030-049) and Dulbecco's Phosphate Buffer Saline (D-PBS, 14190-094) were purchased from Gibco. Penicillin-Streptomycin mix, L-Glutamine, N2 and B27 supplements were purchased from Gibco. Sodium pyruvate solution was from Sigma-Aldrich.

All sterile flasks and dishes, including LabTek chamber slides (177445), were supplied by Nunc. Sterile bottles, tubes and pipettes were purchased from Corning.

Blocking solutions for *in situ* hybridization (2.2.5.1) and immunofluorescence (2.2.5.2) were prepared by using sheep serum (Biosera, SH650), inactivated for 30 minutes at 60°C on a water bath (heat inactivated sheep serum or HISS). HISS was stored in aliquots at -20°C.

### 2.1.5 Laboratory equipment

| | |
|---|---|
| **Walker class II microbiological safety cabinet** | Walker safety cabinets Ltd |
| **Sanyo MCO-18AIC $CO_2$ incubator** | Sanyo Electric Co. Ltd |
| **Leica MZ6 stereoscope** | Leica |
| **Axiovert 35 inverted optical microscope** | Zeiss |
| **Leica MZ16F fluorescence stereoscope** fitted with | Leica |
| **Retiga Exi Fast 1394 camera** | QImaging |
| **Axioplan 2 fluorescence microscope** fitted with | Zeiss |
| **ProgRes C14 camera** | Jenoptik |
| **BioRad Radiance confocal** | BioRad |
| **Leica TCS SP5 MP confocal** | Leica |
| **Microm HM 560 cryostat** | Zeiss |
| **Innova U725 -86°C Freezer** | New Brunswick (Eppendorf) |
| **Heraeus Pico centifruge (24x 1.5/2.0 rotor)** | Thermo Fisher Scientific |
| **5702R centrifuge (4x400g or 24x 3.75g rotor)** | Eppendorf |
| **Innova 4200 incubator shaker** | New Brunswick (Eppendorf) |
| **Hybaid Mini 10 oven** | Thermo Fisher Scientific |
| **BioDoc-IT gel imaging system** | Ultra-Violet products Ltd. |
| **DNA Engine Dyad Thermal Cycler Chassis** | Biorad |

| | |
|---|---|
| **7500 Fast Real-Time PCR system** | Applied Biosystems |
| **MultiSub horizontal electrophoresis units** | Geneflow |
| **NanoDrop micro-volume spectrophotometer** | Thermo Fisher Scientific |

### 2.1.6 Companies

| | |
|---|---|
| Abcam | Cambridge, UK |
| AbD Serotech, Serotech Ltd | Oxford, UK |
| Adobe Systems | San Jose, CA, USA |
| Agar Scientific | Stansted, UK |
| Ambion, Inc. | Foster City, CA, USA |
| Anachem | Luton, UK |
| Applied Biosystems Europe | Warrington, UK |
| BD UK Ltd | Oxford, UK |
| Bio-Rad Laboratories | Hemel Hempstead, UK |
| BioSera | Ringmer, UK |
| Biotium Inc. | Hayward, CA, USA |
| Carl Zeiss GA | Oberkochen, Germany |
| Cell Signaling Technology, Inc. | Beverly MA, USA |
| Chemicon International Inc. | Temecula, CA, USA |
| Corning Inc. | Corning, NY, USA |
| Covance | Berkeley, CA, USA |
| Cytoskeleton, Inc. | Denver, CO, USA |
| DAKO UK Ltd | Cambridge, UK |
| Dow Corning | Seneffe, Belgium |
| Eppendorf UK Ltd. | Cambridge, UK |
| Fisher Scientific UK Ltd | Loughborough, UK |
| Fluka Chemie GmbH | Buchs, Switzerland |
| Invitrogen Corporation | Paisley, UK |
| Jenoptik AG | Jena, Germany |
| Leica Microsystems (UK) Ltd | Milton Keynes, UK |
| MathWorks Inc. | Solms, Germany |
| Millipore | Billerica, MA, USA |
| Molecular Probes, Inc. | Eugene, OR, USA |
| Nacalai Tesque, Inc. | Kyoto, Japan |
| Nalge Nunc International | Rochester, NY, USA |

| | |
|---|---|
| New England Biolabs (UK) Ltd. | Hitchin, UK |
| OriGene Technologies Inc. | Rockville, MD, USA |
| PAA laboratories GmbH | Pasching, Austria |
| PeproTech, Inc. | Rocky Hill, NJ, USA |
| PerkinElmer, Inc. | Seer Green, UK |
| Promega Corporation | Southampton, UK |
| Qiagen Ltd. | Crawley, UK |
| QImaging | Burnaby, BC, Canada |
| R&D Systems Europe Ltd. | Abingdon, UK |
| Roche Diagnostics Ltd. | Burgess Hill, UK |
| Santa Cruz Biotechnology, Inc. | Santa Cruz, CA, USA |
| Sanyo Electric Co. Ltd. | Osaka, Japan |
| Sigma-Aldrich Company Ltd. | Gillingham, UK |
| Sigma-Genosys Ltd | Haverhill, UK |
| Thermo Fisher Scientific | Loughborough, UK |
| Ultra-Violet products Ltd. | Cambridge, UK |
| Vector Laboratories Ltd | Peterborough, UK |
| VWR International | Lutterworth, UK |
| Walker safety cabinets Ltd. | Glossop, UK |
| Zymed laboratories Inc | San Francisco, CA, USA |
| Jackson ImmunoResearch Laboratories, Inc. | West Grove, PA, USA |

## 2.2 Methods

### 2.2.1 Animals

#### *2.2.1.1 Mouse lines*

Transgenic mice used in our studies have been kindly provided and generated as follows: *Sox10Cre* (N. Kessaris, UCL, UK; Matsuoka *et al.*, 2005), *Sox10iCreER$^{T2}$* (C. Laranjeira, NIMR, UK; Laranjeira, 2010), *Wnt1Cre* (Danielian *et al.*, 1998), *R26ReYFP* (S. Srinivas, University of Oxford, UK; Srinivas *et al.*, 2001), *Rac1flox* (V. Tybulewicz, NIMR, UK; Walmsley *et al.*, 2003), *Rac3$^{-}$* (I. De Curtis, S. Raffaele Scientific Institute, Italy; Corbetta *et al.*, 2005), *Fzd3$^{-}$* (A. Goffinet, UCL, Belgium; Wang *et al.*, 2002), *Celsr3$^{-}$* (A. Goffinet, Université Catholique de Louvain, Belgium; Tissir *et al.*, 2005) and *Celsr3flox* (A. Goffinet, Université Catholique de Louvain, Belgium; Zhou *et al.*, 2008). Experimental genotypes were obtained by crossing these individual transgenic mouse lines as described in sections 3.1.1, 4.1.2, 4.1.6 and 4.1.8. Transgenes were identified by PCR on genomic DNA as described in sections 2.2.2.1 and 2.2.2.8.

Purified wild type YFP$^{+}$ ENCCs were obtained from embryos generated by *Sox10Cre;R26ReYFP* (3.1.1) or *Wnt1Cre;R26ReYFP* (4.1.1) double transgenics crossed to Parkes (outbred) mice.

For all embryonic studies the midday at the date at which the vaginal plug was observed was designated as embryonic day 0.5 (E0.5).

Mice were housed, bred and treated according to the guidelines approved by the UK Home Office under the Animals (Scientific Procedures) Act 1986.

#### *2.2.1.2 In vivo administration of EdU and 4-OHT*

5-ethynyl-2´-deoxyuridine (EdU; Invitrogen, E10187) was dissolved in sterile D-PBS (Gibco) at a concentration of 10 mg/ml and stored in aliquots at -20°C. To study cell proliferation *in vivo* (3.1.3), E11.5 pregnant females were injected intraperitoneally with 30 µg/g EdU 1 hr before harvesting the embryos.

4-hydroxytamoxifen (4-OHT; Sigma, H-6278) was dissolved in ethanol/sunflower oil (1:9) mixture at the concentration of 10 mg/ml and stored at 4°C for short term (up to 2 weeks) or -20°C for long term (months) usage. To label single neurons *in vivo* (4.1.6), E10.5 pregnant females carrying the *Sox10iCreER$^{T2}$;R26ReYFP* transgenes were injected intraperitoneally with 3 μg/g 4-OHT and embryos were harvested at E12.5.

## 2.2.2 Molecular biology techniques

### *2.2.2.1 Extraction of DNA*

*Genomic DNA* was extracted from ear biopsies or yolk sacs using 500 μl of Proteinase K lysis buffer (100 mM Tris-HCl pH 8.5, 5 mM EDTA pH 8.0, 0.2% SDS, 200 mM NaCl, Proteinase K 0.1 mg/ml) overnight (O/N) at 55°C. The DNA was precipitated by adding 500μl of isopropanol and then centrifuged at 13000 rpm for 10 minutes at room temperature (RT) and the supernatant was discarded. DNA pellets were air dried and resuspended in 50 μl of distilled $H_2O$ (d $H_2O$). 1-1.5 μl of the DNA preparation were used for the PCR-based screening (2.2.2.8).

*Plasmid DNA* was isolated using PowerPrep Express Plasmid Miniprep System (OriGene, 11453-024) following manufacturer's instructions. Briefly, after an alkaline/SDS-mediated lysis of pelleted transformed E. Coli cells (2.2.2.6), DNA was allowed to bind to a silica-based membrane, followed by a series of washes to eliminate RNA, proteins and cellular waste. DNA was eluted from the silica membrane in 50 μl of pre-warmed (65°C) TE buffer (10mM Tris-HCl pH 8.0, 1mM EDTA) and then stored at -20°C.

### *2.2.2.2 Restriction enzyme digestion*

Restriction enzymes were supplied by New England Biolabs and Roche. Diagnostic digestions of plasmid DNA were performed in 20 μl final volume containing: 1 μg of DNA, 2 μl enzyme-specific 10× digestion buffer, 0.5 μl of each 10 U/μl restriction enzyme and d$H_2O$ up to 20 μl. Digestion reaction was incubated for 1 hour in a water bath at 37°C and then used for DNA electrophoresis (2.2.2.4).

#### 2.2.2.3 Extraction of RNA

RNA was extracted from FACS purified cells (2.2.3.3) using Ambion RNAqueous Micro Kit (Applied Biosystems, AM1931) following manufacturer's instructions. Briefly, sorted cells were centrifuged at 900 rpm for 5 minutes at RT and the supernatant removed. Cell pellet was resuspended in 100 µl of lysis solution and the lysate was then diluted with an ethanol solution and applied to an RNA-binding silica filter. Proteins, DNA, and other contaminants were removed in a series of washing steps, and the bound RNA was eluted in 15 µl of elution solution.

To avoid any contamination of genomic DNA, eluted RNA samples were also treated with DNAse I for 20 minutes at 37°C. After digestion, DNAse I was removed by using an inactivation resin (DNAse and inactivation resin both provided with the RNAqueous Micro Kit) and RNA solution transferred to a fresh RNAse-free tube and stored at -20°C.

#### 2.2.2.4 Quantification of nucleic acids

Concentration and purity of DNA and RNA samples were quantified by measuring the adsorbance of 1 µl of undiluted samples at 260 and 280 nm in a micro-volume spectrophotometer (NanoDrop). Considering that conventional absorbance reading at $A_{260}$ of 1 optical density (O.D.) corresponds to 50 µg/ml of dsDNA and 40 µg/ml of RNA, nucleotide concentration in µg/ml was calculated as $A_{260}$ (O.D.) x 50 for DNA samples and A260 (O.D.) x 40 for RNA samples. Purity of samples was determined by the ratio of adsorbances at 260 nm and 280 nm ($A_{260/280}$), where pure DNA and RNA samples have a $A_{260/280} \geq 1.8$ and $\geq 2$, respectively.

#### 2.2.2.5 Agarose gel electrophoresis

Electrophoresis was performed in horizontal units (MultiSub). Gels were prepared by dissolving agarose (typically 1-2% w/v) in TAE for DNA or TBE for RNA electrophoresis and heating the solution in a microwave oven until the agarose was completely dissolved. The fluorescent nucleic acid dye GelRed™ was then added to the agarose solution (1:10,000), before being poured into a casting plate with the appropriate comb.

DNA and RNA samples were mixed in a 9:1 ratio with 10× Orange G DNA loading buffer (20% Ficoll, 0.1M EDTA, 1% SDS, 0.25% Orange G) before loading and being electrophoresed in 1× TAE or 1× TBE running buffer at 100-120V. The size of nucleic acids was determined by comparison against a 1 Kb DNA ladder (Invitrogen, 1561 016) also loaded into the gel. Nucleic acids were visualised in a light proof cabinet containing an ultraviolet transilluminator at 302 nm and a CCD camera (BioDoc-It).

#### *2.2.2.6 Amplification of plasmid DNA*

Plasmid DNA was amplified in One Shot® TOP10 chemically competent *E. Coli* cells (Invitrogen, C4040). A 50 µl aliquot of chemically competent cells was thawed on ice, mixed to 100 ng of plasmid DNA and then incubated for 30 minutes on ice. Uptake of DNA from the cells was induced by 30 seconds heat-shock in water bath at 37°C followed by 2 minutes incubation on ice. The cells were allowed to recover by the addition of 250 µl of LB medium in a shaking incubator at 37°C and 225 rpm for 1 hour. Two aliquots of the suspension (20 µl and 100 µl) were then plated onto pre-warmed (37°C) LB agar plates containing 100 µg/ml ampicillin. The plates were incubated overnight at 37°C and they were examined on the following day for the formation of antibiotic-resistant colonies.

A single colony isolated from a fresh LB plate was used to inoculate 4 ml of LB medium containing 100 µg/ml ampicillin; the cells were then incubated at 37°C in a shaking incubator at 225 rpm overnight (no more than 15 hours). On the following day, bacteria were collected by centrifugation (6000 rpm for 5 minutes) and processed for plasmid DNA extraction (2.2.2.1). When long-term storage of clones was needed, glycerol was added to an aliquot of O/N cultures at a final concentration of 15% v/v, and the stocks were stored in 1 ml aliquots at -80°C.

#### *2.2.2.7 Reverse transcriptase polymerase chain reaction (RT-PCR)*

RT-PCR was performed using the High-Capacity cDNA Reverse Transcription kit (Applied Biosystems, 4374966) following manufacturer's instructions. Briefly, a reaction containing 15 ng RNA, 2 µl 10× RT reaction buffer, 0.8 µl 25× dNTPs, 2 µl 10× random primers, 1 µl RNAse

inhibitor, 1 µl MultiScribe™ MuLV reverse transcriptase and sterile RNAse-free $H_2O$ up to 20 µl was prepared in a RNAse-free tube. A control reaction was set up for each RNA sample by omitting the MuLV reverse transcriptase (No RT reaction or NRT).

Reactions were incubated at 37°C for 60 minutes, stopped by heating to 85°C for 5 minutes and then stored at -20°C and used for subsequent PCR analysis (2.2.2.8 and 2.2.2.9).

#### *2.2.2.8 Polymerase chain reaction (PCR)*

PCR reactions were performed using *Taq* DNA polymerase, including 10X buffer and $MgCl_2$, from Invitrogen (18038-18) and 10mM stock of mixed single dNTPs purchased from Promega (dATP, U1205; dCTP, U1225; dGTP, U1215; dTTP, U1235). All primers were provided lyophilised by Sigma-Genosys and they were resuspended in $dH_2O$ at a concentration of 100 µM for stock solutions and 20 µM for working solutions and both stored at -20°C.

PCR genotyping of transgenic lines was performed using primers and cycling settings listed in Table 2.1. Reactions were performed in a final volume of 20 or 25 µl using 1 µl of non-quantified extracted genomic DNA (2.2.2.1) and 0.2 µl of *Taq* polymerase. dNTPs and $MgCl_2$ were used at a final concentration of 200 µM and 1.5 mM, respectively, with the exception of the Rac1 PCR reaction (160 mM dNTPs and 2mM $MgCl_2$). Primers were added at a final concentration of 0.2 µM (Celsr3, Fzd3 and Sox10iCreER$^{T2}$), 0.4 µM (Rac1, R26ReYFP and Sox10/Wnt1Cre) and 0.6 µM (Rac3).

PCR for analysis of cDNA expression (3.1.1) was carried out by using primers and cycling settings listed in Table 2.2. Reactions were performed in a final volume of 40 µl using 0.5 µl of the template cDNA produced by RT-PCR (2.2.2.7) and 0.2 µl of *Taq* polymerase. Final concentrations of dNTPs, $MgCl_2$ and primers were 250 mM, 1.8 mM and 0.5 µM, respectively.

Presence and size of PCR products was determined by gel electrophoresis (2.2.2.5).

**Table 2.1 Primers sequences and PCR cycling parameters used for genotyping**

| | **Primers sequence (5'- 3')** | **PCR settings** | | | | | | | **Exp band size (bp)** |
|---|---|---|---|---|---|---|---|---|---|
| | | Step 1 1 cycle | | Step 2 # cycles | | | Step 3 1 cycle | | |
| | | °C | T | °C | T | # | °C | T | |
| Celsr3 | (**F**) AGCCAAGATGTCCGAGTCAC<br>(**R**) GCCCACAAGTGTCCTGTCTC<br>(**R**) AGCATGGAGGTAGTGGAAGG | 94 | 4' | 94<br>60<br>72 | 30"<br>1'<br>1' | 30 | 72 | 10' | 598 (KO)<br>500 (flox)<br>416 (wt) |
| Fzd3 | ($\mathbf{F_{ko}}$) ACTGAGGAGCCTAACAGATAAGGG<br>($\mathbf{R_{ko}}$) CATCAACATTAAATGTGAGCGAGT<br>($\mathbf{F_{wt}}$) TGTGAGCTGGATTGTCTTTGATCT<br>($\mathbf{R_{wt}}$) GTTCAGAAGATTAGGCATGAAGGTA | 94 | 4' | 94<br>65<br>72 | 30"<br>1'<br>1' | 35 | 72 | 10' | 520 (KO)<br>200 (wt) |
| R26ReYFP | (**F**) GCTCTGAGTTGTTATCAGTAAGG<br>(**R**) GCGAAGAGTTTGTCCTCAACC<br>(**R**) GGAGCGGGAGAAATGGATAGT | 95 | 6' | 95<br>55<br>72 | 30"<br>30"<br>45" | 35 | 72 | 10' | 500 (wt)<br>350 (stop) |
| Rac1 | (**F**) GAAGGAGAAGAAGCTGACTCCCATC<br>(**R**) CAGCCACAGGCAATGACAGATGTC | 94 | 2' | 94<br>54<br>72 | 30"<br>30"<br>30" | 30 | 72 | 10' | 300 (flox)<br>250 (wt) |
| Rac3 | (**F**) CATTTCTGTGGCGTCGCCAAC<br>(**R**) CACGCGGCCGAGCTGTGGTG<br>(**R**) TTGCTGGTGTCCAGACCAAT | 94 | 1' | 98<br>66<br>72 | 20"<br>1'<br>1' | 30 | 72 | 10' | 460 (wt)<br>370 (KO) |
| Sox10Cre<br>Wnt1Cre | (**F**) ATCCGAAAAGAAAACGTTGA<br>(**R**) ATCCAGGTTACGGATATAGT | 94 | 3' | 94<br>53<br>72 | 30"<br>1'<br>90" | 35 | 72 | 5' | 550 |
| Sox10iCre<br>$ER^{T2}$ | (**F**) GAGGGACTACCTCCTGTACC<br>(**R**) TGCCCAGAGTCATCCTTGGC | 94 | 3' | 94<br>53<br>72 | 30"<br>1'<br>90" | 35 | 72 | 5' | 630 |

**F**, forward primer; **R**, reverse primer; **°C**, temperature in Celsius degrees; **T**, incubation time; **#**, number of cycles, **bp**, base pairs; **wt**, wild type allele; **KO**, null allele, **flox**, flox allele.

**Table 2.2 Primer sequences and PCR cycling parameters used for cDNA expression analysis**

| | **Primers sequence (5'- 3')** | **PCR settings** | | | | | | | **Exp band size (bp)** |
|---|---|---|---|---|---|---|---|---|---|
| | | Step 1 1 cycle | | Step 2 # cycles | | | Step 3 1 cycle | | |
| | | °C | T | °C | T | # | °C | T | |
| Rac1§ | (**F**) CCCAATACTCCTATCATCCTCG<br>(**R**) CAGCAGGCATTTTCTCTTCC | 94 | 2' | 94<br>55<br>72 | 30"<br>30"<br>1' | 30 | 72 | 10' | 240 |
| Rac2§ | (**F**) CCAGCACCCCCATCATCCTGG<br>(**R**) GGGGCGCTTCTGCTGTCGTGTG | 94 | 2' | 94<br>55<br>72 | 30"<br>30"<br>1' | 30 | 72 | 10' | 240 |
| Rac3§ | (**F**) CACACACCCATCCTTCTGGTG<br>(**R**) CAGTGCACTTCTTGCCTGGC | 94 | 2' | 94<br>52<br>72 | 30"<br>30"<br>1' | 33 | 72 | 10' | 250 |
| GAPDH‡ | (**F**) TGGAAAGCTGTGGCGTGAT<br>(**R**) CCCTGTTGCTGTAGCCGTAT | 94 | 5' | 94<br>58<br>72 | 1'<br>45"<br>1' | 30 | 72 | 5' | 395 |

primer sequences § from (Wells *et al.*, 2004) or ‡ custom designed**. F**, forward primer; **R**, reverse primer; **°C**, temperature in Celsius degrees; **T**, incubation time; **#**, number of cycles, **bp**, base pairs.

*2.2.2.9 Real Time PCR*

Gene expression was quantified by Real-Time PCR (4.1.1). Quantitative PCR was performed by using the TaqMan Gene Expression technology (Applied Biosystems) which provides a mix of pre-made fluorescence TaqMan probe and primers for specific gene of interest. Real Time PCR reactions were prepared in triplicates in nuclease-free multi-well plates for each cDNA template and negative control (NRT). TaqMan Gene Expression assays ID: Fzd3 Mm00445423_m1, Celsr3 Mm00466861_m1 and β-actin Mm02619580_g1.

| | |
|---|---|
| 20× TaqMan Gene Expression assays (containing probe and primers) | 1 µl |
| 10× TaqMan Fast Universal Master Mix | 10 µl |
| cDNA (diluted 1:2 or 1:3 in $H_20$) | 2 µl |
| nuclease-free $dH_20$ | up to 20 µl |

Reactions were performed in a 7500 Real-Time PCR System (Applied Biosystems). An initial denaturation step of 10 minutes at 95°C, was followed by 40 cycles of denaturation (95°C for 15 seconds), annealing (60°C for 1 minute) and elongation (72°C for 1 minute).

Transcript levels of genes of interest were normalised to the levels of the housekeeping gene actin, as an internal control. Relative quantities of cDNA were finally quantified automatically by the 7500 System SDS Software v1.4 using the $2^{-\Delta\Delta CT}$ method. Data is shown as the mean of triplicates values ± standard deviation of the mean (Fig. 4.3).

*2.2.2.10 Riboprobe synthesis*

Riboprobes for *in situ* hybridisation (2.2.5.1) were generated by *in vitro* RNA transcription of linearised plasmid DNA containing complete or partial coding sequences (cds) of the gene of interest. Details of sequences, restriction enzymes and RNA polymerases used for the generation of antisense riboprobes are provided in table 2.3.

Linearisation of plasmids was performed in a final volume of 50 µl mixing 20 µl of Miniprep plasmid DNA (approximately 10 µg), 2 µl of restriction enzyme, 5 µl of enzyme-specific buffer and $dH_2O$ (up to volume). Reactions were incubated for 1 hour at 37°C in a water

bath, then an additional 0.5 µl of enzyme was added and they were incubated for further 30 minutes at 37°C. At the end of the incubation time, a small aliquot of the reaction was run on a gel (2.2.2.5) to check that linearisation of the plasmid was completed. DNA was then extracted by using a phenol/chloroform protocol and purified by ethanol precipitation. Briefly, 1:1 volume of phenol was added to the restriction reaction, centrifuged for 2' at 13000 rpm and the upper aqueous phase transferred to a fresh tube. The same step was then repeated by adding 1:1 volume of chloroform. The aqueous phase, containing the DNA, was then precipitated by addition of 1:2 ethanol (EtOH) and 10:1 of 3M sodium acetate (NaAC) followed by incubation for 1 hour at -80°C. DNA was then centrifuged for 10 minutes at 13000 rpm, supernatant removed, washed twice in 70% EtOH and pellet left to dry at RT. DNA pellets were dissolved in 10 µl of $dH_2O$ and stored at -20°C.

Generation of digoxigenin (DIG)-labelled riboprobes was performed by using RNA polymerases obtained from Promega (T3, P208C; T7, P207B) and Roche (SP6, 11996427). The reaction was set up in a final volume of 20 µl including 1× transcription buffer (Promega, P1181), 10mM DTT (Promega, P1171), 1× DIG labelling mix (Roche, 1 277 073), RNAse inhibitor (Promega, M610A), 1.5 µg linearised plasmid and 1.5 µl of RNA polymerase (10 units/µl). The reagents were incubated for 30 minutes at 37°C in a water bath, after which, a 1 µl of reaction was run on an agarose gel to check for the presence of RNA (2.2.2.5). 2 µl of RQ1 DNAse I (Promega, M610A) were added to the reaction solution and incubated for 30 minutes at 37°C to eliminate any trace of plasmid DNA. RNA probes were precipitated by adding 10:1 4M lithium chloride ($LiCl_2$) and 1:3 EtOH at -20°C for at least 30 minutes and centrifuged for 10 minutes at 13000 rpm. RNA pellets were washed with 70% EtOH, air dried and dissolved in 50 µl of TE buffer (10 mM Tris-HCl pH 7.5, 1 mM EDTA) and stored at -20°C.

**Table 2.3 Sequences, restriction enzymes and RNA polymerases used for generation of antisense riboprobes for *in situ* hybridization**

| | vector | Sequence details | Enzyme to linearize | RNA pol |
|---|---|---|---|---|
| Celsr3[a] | pCRII | partial cds | HindIII | T7 |
| Fzd2[b] | pBS-SK | partial cds | EcoRI | T7 |
| Fzd3[a] | pCRII | partial cds | EcoRV | SP6 |
| Fzd4[b] | pBS-SK | partial cds | EcoRI | T7 |
| Fzd6[b] | pBS-KS | complete cds | HindIII | T3 |
| Fzd7[b] | pBS-SK | complete cds | KpnI | T3 |
| Fzd8[b] | pBS-KS | complete cds | SphI | T3 |
| Rac1[c] | pBS-KS | 3' cDNA | EcoRI | T3 |
| Rac3[c] | pBS-KS | 3' cDNA | NotI | T3 |
| Ret | pBS-SK | partial cds | NotI | T7 |
| Ryk | pCMV-SPORT6 | complete cds | SalI | T7 |

Plasmids were kindly provided by: [a] A. Goffinet (UCL, Brussels, Belgium), [b] J. Nathans (John Hopkins University, Baltimore, USA), [c] I. De Curtis (S. Raffaele Scientific Institute, Milan, Italy). Ret plasmid was produced in the lab and Ryk plasmid was purchased from Source Bioscience LifeSciences (I.M.A.G.E. clone #5370100). Cds, coding determining region.

### 2.2.3 Tissue manipulation

#### *2.2.3.1 Dissection of embryos and embryonic guts*

Dissection of embryos was done in pre-chilled L15 medium (PAA Laboratories, E15821). Embryos were dissected out of the uterus and any embryonic membrane, including the yolk sac, removed. When required, a portion of the yolk sac or of the tail was collected to isolate DNA for genotyping (2.2.2.1). Embryos were stored in L15 medium on ice, while embryonic guts were individually dissected in L15 medium.

Whole-mount embryos were used for cryosectioning, upon fixation and freezing (2.2.3.4), dissected embryonic guts were cultured (2.2.4) or processed for DiI labelling (2.2.6) or immunofluorescence (2.2.5.2).

#### *2.2.3.2 Dissection of adult gut muscle strips with adherent myenteric plexus*

Adult mice (P21 and P35) were sacrificed by cervical dislocation and their intestinal tract removed from the abdominal cavity and washed in ice-cold PBS. The small intestine was dissected in pieces of 1 cm length and placed (stretched) over a 1 ml pipette. A small incision was made longitudinally on the outer muscle layer and a cotton swab soaked in PBS was used to

strip away the longitudinal muscle and the adherent myenteric plexus from the underlying tissue. Tissue strips were then stretched and pinned flat onto a dish coated with Sylgard using stainless steel 0.2 mm insect pins (Agar Scientific, L4494). Tissues were fixed for 20 minutes at RT and then processed for immunofluorescence staining (2.2.5.2).

#### *2.2.3.3 Fluorescence Activated Cell Sorting (FACS)*

Dissected embryonic E11.5 and E12.5 guts were collected into sterile 0.5 ml tube containing sterile D-PBS. The D-PBS was removed and 100 µl of 1 mg/ml collagenase/dispase solution was added and incubated for 5' at 37°C in a water bath. At the end of the incubation, samples were washed with 500 µl D-PBS, resuspended in 500 µl of OptiMEM containing 1mM L-glutamine and 100 U/ml penicillin-streptomycin mix and mechanically dissociated by pipetting. The cell suspension was transferred to a flow cytometry conical bottom tube provided with a cell strainer cap (BD, 352235), through which it was filtered to ensure single cell suspension. Tubes were kept in ice and processed for FACS in a Beckman Coulter MoFlo Cell Sorter. $YFP^+$ and $YFP^-$ cells were collected into individual RNAse-free tubes and immediately processed for RNA extraction (2.2.2.3).

#### *2.2.3.4 Freezing of embryos and cryosectioning*

Whole embryos were washed in PBS to remove any excess of blood and extra-embryonic tissue and fixed in 4% PFA in PBS for 2 hours at 4°C on a rocking shaker. Fixed embryos were cryoprotected in 30% sucrose in PBS O/N at 4°C, embedded in 15% sucrose; 7.5% gelatine (Sigma, GS2500) in PBS for 1 hour at 4°C (or until set) and then frozen in dry ice-cooled isopentane (-60°C) Serial cryosections were acquired on a cryostat (Microm HM 560) at a thickness of 12 µm and placed on Superfrost Plus glass slides (Thermo Scientific, 2011-07). Sections were air dried for 1 hr at RT and then directly processed for ISH (2.2.5.1) or stored at -80°C.

## 2.2.4 Tissue and cell culture

### *2.2.4.1 Coating of plates*

Lab-Tek permanox 8-well chamber slides (Thermo Fisher Scientific, 177445) were coated with fibronectin (2.2.4.3 and 2.2.4.4) or poly-D-lysine (PDL) and laminin (2.2.4.5).

Fibronectin (Sigma-Aldrich, F1141) was diluted in PBS at 20 µl/ml. The solution was added 100 µl/well and incubated for 10 minutes at RT. The surfaces were then washed once with D-PBS and used directly for seeding.

When PDL/laminin coating was performed, 1 mg/ml poly-D-lysine (Sigma-Aldrich, P6407) in PBS was added to each surface and incubated for 10 minutes at RT. Slides were then washed three times for 5 minutes with D-PBS. Surfaces were covered with 1 µg/µl laminin (Sigma-Aldrich, L2020) for 30 minutes at 37°C in a $CO_2$ incubator. Laminin solution was removed; slides washed once with D-PBS and used for seeding.

### *2.2.4.2 Explant cultures in collagen matrix (3D cultures)*

1-2 mm long segments from the midgut region of E11.5 and E12.5 guts were dissected in L15 medium and embedded in collagen matrix. 1 mL of collagen working solution was prepared by first mixing 500 µl of collagen from rat tails and 400 µl 1× DMEM (Sigma-Aldrich, D5523). Then 100 µl 10× DMEM was mixed to the solution and 0.8 M sodium bicarbonate ($NaHCO_3$) was added until the solution turned to a dark yellow/orange colour (2 µl/100 µl). 25 µl droplets of collagen were placed directly on the surface of four well dishes (Termo Fisher Scientific, 176740) and explants embedded within them with the help of forceps. Collagen was set for 1.5-2 hrs at RT, before adding OptiMEM supplemented with 1 mM L-glutamine and 100 U/ml penicillin-streptomycin mix. Explants were cultured for 24-48 hrs in an atmosphere of 5% $CO_2$. Human recombinant GDNF (hrGDNF, Peprotech, Rocky Hill, NJ, USA) was supplemented at 20 ng/ml.

#### *2.2.4.3 Explant cultures on fibronectin substrate (2D cultures)*

Rings (200-500 μm thick) of E11.5-E12.5 midgut were placed on fibronectin-coated 8 chamber wells by using cloning cylinders (Sigma-Aldrich, CLS31668). Briefly, after coating, a cloning cylinder was placed inside each well and filled with 400 μl of culturing medium (OptiMEM with 1mM L-glutamine and 100U/ml penicillin-streptomycin mix, 20 ng/ml hrGDNF). Gut rings (4-5 per cylinder) were then gently placed with forceps within the medium, dropped to the bottom and adhered to the fibronectin-coated surface. Explants were cultured for 24 hrs in an atmosphere of 5% $CO_2$.

#### *2.2.4.4 Short term cultures of embryonic dissociated guts*

Whole guts from E11.5 and E12.5 embryos were washed with D-PBS and digested for 5 minutes with 1 mg/ml collagenase/dispase solution (100 μl/gut) at 37°C on a water bath. Tissues were washed in D-PBS and 500 μl of OptiMEM was added by pipetting a few times up and down to generate a single cell suspension. Cells were then centrifuged for 5 minutes at 900 rpm at RT and resuspended in fresh culturing medium containing OptiMEM, 1 mM L-glutamine and 100 U/ml penicillin-streptomycin mix. Cell suspension was plated in 2 wells (for E11.5 guts) and 3 wells (for E12.5 guts) of fibronectin-coated chamber slides (2.2.4.1) and additional medium was added up to 300 μl per well. Cultures were maintained for up to 4 hours in an atmosphere of 5% $CO_2$.

For EdU incorporation *in vitro*, 10 μM EdU was added to the culturing medium.

#### *2.2.4.5 Culture of primary enteric neurons*

E11.5 and E12.5 guts were dissociated as described in section 2.2.4.4. After centrifugation, cells were resuspended in neurobasal medium supplemented with 1 mM L-glutamine, 100 U/ml penicillin-streptomycin mix, 1X B27 and N2 supplements. Cell suspension was plated in 2 wells (for E11.5 guts) and 3 wells (for E12.5 guts) of PDL/laminin-coated chamber slides (2.2.4.1) and additional medium was added up to 400 μl per well. Neurons were cultured for 4 days in an atmosphere of 5% $CO_2$ and medium changed after 2 days.

## 2.2.5 Histo- and cyto-chemistry

### *2.2.5.1 RNA in situ hybridisation*

*In situ* hybridisation was performed using digoxigenin-labelled cRNA probes (2.2.2.10) on transverse cryosections of whole mount embryos as previously described (Schaeren-Wiemers & Gerfin-Moser, 1993). Sections were fixed in 4% PFA in PBS for 10 minutes at RT. After three 10 minutes washes in PBT (1× PBS, 0.1% Tween 20), sections were incubated in acetylation solution (0.1 M Triethanolamine, 0.65% of 37% HCl, 0.375% v/v acetic anhydride in $dH_2O$) for 10 minutes at RT in a fume hood, then washed three times for 5 minutes in PBT. Sections were then incubated in pre-hybridisation solution (50% v/v de-ionised formamide; 5× SSC; 5× Denhardt's, Invitrogen 750018; 250 µg/ml yeast tRNA, Sigma, R6750; 500 µg/ml herring sperm DNA, Promega, D1816) for 45 minutes at RT and. After this incubation, hybridisation solution was prepared by adding 200-400 ng/ml of DIG-labelled RNA probe into pre-hybridisation solution, incubating the solution at 80°C for 5 minutes and then putting it on ice. Hybridisation solution was applied to each slide (100 µl) and covered with a glass coverslip. Slides were incubated O/N at 72°C inside a humidified chamber in a mini oven. On the following day, slides were immersed in 5× SSC to remove coverslips, then washed in 0.2× SSC (1 hour at 72°C followed 5 minutes at RT) and equilibrated in B1 buffer (150 mM NaCl, 100mM Tris-HCl pH 7.5) for 5 minutes at RT. Slides were then pre-blocked in B2 solution (10% heat inactivated sheep serum, HISS, in B1) and then incubated with an alkaline phosphatase (AP) conjugated sheep anti-DIG antibody (Roche, 11 093 274 910) diluted 1:5000 in 1% HISS in B1 solution O/N in a humidified chamber, at 4°C. Sections were washed in B1 solution three times of 5 minutes at RT and then equilibrated in B3 buffer (100 mM NaCl, 50 mM $MgCl_2$, 100 mM Tris-HCl pH 9.5) for 10 minutes at RT. Colorimetric detection of AP-DIG-antibody was performed by incubating slides in the dark at RT in a developing reaction prepared by mixing in 2 ml of B3 solution 6.75 µl of 75 mg/ml Nitrotetrazolium Blue chloride (NBT; Sigma-Aldrich, N6639) in 70% dimethylformamide and 5.25 µl of 50 mg/ml 5-Bromo-4-chloro-3-indolyl phosphate disodium

salt (BCIP; Sigma-Aldrich, B6149) in $dH_20$. To stop the reaction, slides were quickly washed in PBS and then mounted and coverslipped with glycerol mounting medium (Glycergel).

#### *2.2.5.2 Immunofluorescence*

Immunostaining was performed on embryonic (whole-mount guts, gut explants and dissociated gut cells) and adult (strips of muscle and adherent myenteric plexus) gut tissues.

Embryonic guts (whole-mount or explants) and adult tissues were fixed in 4% PFA in PBS for 2 hours at 4°C on a rocking shaker. After washing twice in PBT (0.1% Triton-X100 in PBS), samples were incubated in blocking solution (10% HISS in PBT) for 1 hour at RT rocking. Primary antibodies were diluted in blocking solution and applied O/N at 4°C. After three 5 minutes washes with PBT, samples were incubated with secondary antibodies for 2 hours at RT. After three washes of 10 minutes in PBT, samples were placed on a glass slide with mounting media with DAPI (Vectashield), coverslipped and the edges sealed with nail polish.

Dissociated gut cells (short term cultures and primary neurons) were fixed in 4% PFA in PBS for 10 minutes at RT. After washing twice for 5 minutes in PBT, they were incubated in blocking solution (1% BSA, 0.15% glycine in PBT) 1 hr at RT. Primary antibodies were diluted in blocking solution and incubated O/N at 4°C. After washing three times for 5 minutes with PBT, samples were incubated with secondary antibodies for 2 hrs at RT. After washing several times with PBT, samples were mounted with mounting media containing DAPI (Vectashield), covered with a glass coverslip and the edges sealed with nail polish.

Source and dilution of primary antibodies are listed in Table 2.4. Secondary antibodies were goat or donkey Alexa Fluor 488- or 568-conjugated (Molecular Probes) and used at 1:500 dilution. TRITC-phalloidin (Sigma, P1951) was added with secondary antibodies incubation at a dilution of 1:500.

**Table 2.4 List of primary antibodies used for immunofluorescence**

| Antiserum | Host | Dilution | Source |
|---|---|---|---|
| β-tubulin (TuJ1) | mouse | 1:1000 | Covance MMS-435P |
| GFP | rabbit | 1:1000 | Molecular Probes A11122 |
| GFP | rat | 1:1000 | Nacalai Tesque 0440484 |
| nNOS | rabbit | 1:200 | Invitrogen 61-7000 |
| PGP 9.5 | rabbit | 1:1000 | Biogenesis 22101802 |

#### *2.2.5.3 EdU labelling*

Detection of 5-ethynyl-2´-deoxyuridine (EdU) was performed by using the Click-iT EdU Alexa Fluor 594 Imaging kit (Invitrogen, C10339). Cultured cells (2.2.4.4) were fixed with 4% PFA in PBS for 10' at RT, then washed with PBT (0.1% Triton X-100 in PBS) three times for 5 minutes. Cells were then incubated for 30 minutes at RT in EdU developing solution, prepared fresh just before use by mixing 25 µl of solution F (1×), 215 µl of reaction buffer (1×), 10 µl of 100 mM copper sulphate ($CuSO_4$) and 0.6 µl of 594 Alexa Fluor dye, for a final volume of 250 µl (enough for a 8 well-chamber slide). Slides were washed three times 5 minutes at RT, before proceeding to the immunofluorescence protocol by blocking and incubating with GFP primary antisera (2.2.5.2).

#### *2.2.5.4 Acetylcholinesterase staining*

Acetylcholinesterase (AChE) staining was performed on small intestine of adult mice (4.1.8). Details of solutions are provided at the end of the section. 1.5 cm long pieces of small intestine were cut longitudinally and flat pinned (lumen-side down) on Sylgard-coated plates. Samples were fixed in 4% PFA, 0.5% glutaraldehyde in 0.1 M phosphate buffer ($PO_4$) O/N at 4°C rocking. Tissues were washed three times for 10 minutes in 0.1 M maleate buffer, before being incubated for 5 hours in the dark at RT in incubation solution. Following several washes in 0.05 M Tris-HCl pH 7.6, the tissues were placed in developing solution and incubated for up to 20 minutes. When the reaction was completed, the outer muscle with the adherent myenteric plexus were removed and mounted flat on a glass slide with glycerol mounting medium (Glycergel).

Incubation solution (50 ml): 50 ml 0.1 M maleate buffer pH 6.0, 30 µl 0.0865 M acethylcoline-iodine (Sigma, A5751), 100 µl 0.03M Iso-OMPA (Sigma, T-1505), 500 µl K&R solution.

K&R solution (50 ml): 5 ml 0.03 cupric sulphate, 2.5 ml 0.1 M sodium citrate, 42.4 ml 0.1 M maleate buffer pH 6.0, 8 mg potassium ferricyanide.

Developing solution (25 ml): 10 mg 3,3'-Diaminobenzidine tetrahydrochloride, DAB, (Sigma, D5905), 25 ml 0.05M Tris-HCl pH 7.6, 50 mg nickelammonium sulphate, 2.5 µl 30% $H_2O_2$

### 2.2.6 DiI labelling of neuronal projections

Dissected guts from E12.5 mice were fixed in 4% paraformaldehyde (PFA) in 0.1% EDTA/PBS for 2 hrs at 4°C rocking. Tissues were anchored to Sylgard plates using 0.2 mm insect pins by pinning the stomach and the caecum to the dish. One further pin which had been previously dipped in DiI tissue-labelling paste (Molecular Probes, N 22883) was applied in the central region of the midgut. Tissues were covered in 4% PFA/0.1% EDTA/PBS and placed in a 37°C oven for 7 days. DiI retrograde tracing was monitored every day and, at the end of the incubation time, tissues were washed and mounted in PBS and promptly examined using a confocal microscope.

### 2.2.7 Image processing and analysis

eYFP expression in double transgenic embryos *Sox10Cre;R26ReYFP* or *Wnt1Cre;R26ReYFP* was analysed using a fluorescent stereomicroscope (Zeiss, M2-Bio) and images acquired with a monochrome camera (Retiga Exi Fast 1394) and Improvision Openlab software (PerkinElmer). Immunostained whole-mount guts, explants, cell cultures and adult tissues were examined with a fluorescence microscope (Zeiss Axioplan) and images acquired through a colour camera (Prog Res C14) and Openlab software. Confocal microscopy was performed on two confocal laser scanning microscopes (Bio-Rad Radiance and Leica TCS SP5 MP), using standard excitation and emission filters for visualising DAPI, Alexa Fluor 488, Alexa Fluor 568, TRITC and DiI.

All fluorescence images were processed with Adobe Photoshop CS2 (Adobe Systems), while analyses were performed in ImageJ (Wayne Rasband, NIH). Analysis of neuron morphology (3.1.5 and 4.1.5) was performed by using the plug-in for ImageJ, NeuronJ (http://www.imagescience.org/meijering/software/neuronj/).

### 2.2.8 Statistical analysis

All cell counting was performed on a sample of cells (numbers specified in the text) coming from at least three independent embryos per genotype. Data are expressed as means ± standard error of the mean (SEM). Differences between data sets were determined by using the Student's t-test function (two-tailed distribution, two-sample equal variance) in Excel (Microsoft) and they were considered significant when $P<0.05$ (*), 0.01 (**) and 0.001 (***). Histograms and survival curves were generated in GraphPad Prism (GraphPad Softwares) and rose plot graphs were generated in Matlab (MathWorks).

# Chapter 3

# Rac1 and Rac3 GTPases are involved in control of migration and neuronal development of enteric neural crest cells

## 3.1 Results

### 3.1.1 Rac1 and Rac3 expression in developing ENS and genetic ablation *in vivo*

To start investigating the potential role of Rac GTPases in ENS development, we first examined the mRNA expression of the three members (i.e. *Rac1*, *2* and *3*) by RT-PCR on $YFP^+$ ENCCs purified from *Sox10Cre;R26ReYFP* guts at E11.5. In this double transgenic line the bacterial Cre recombinase is expressed by early neural crest cells (Matsuoka *et al.*, 2005) and it mediates recombination of the reporter allele *R26ReYFP* (Srinivas *et al.*, 2001). This allows permanent labelling by YFP fluorescence of all NC derivatives, including the enteric nervous system.

*Rac1*, *2* and *3* expression was analysed by RT-PCR on FACS-purified $YFP^+$ cells (ENCCs) and $YFP^-$ cells (all non-ectodermal-derived cells of the gut) from E11.5 guts and on control samples derived from E13.5 brain and lung (Fig. 3.1 A). In accordance with the patterns of expression already reported (Malosio *et al.*, 1997; Moll *et al.*, 1991; Shirsat *et al.*, 1990), we found that Rac1 mRNA was present in all samples, including $YFP^+$ ENCCs, whereas Rac2 was absent in $YFP^+$ gut cell population but expressed in $YFP^-$ cells and lung, possibly because of the presence of cells of hematopoietic origin within these tissues. Additionally, we found that *Rac3* was also expressed in ENCCs (Fig. 3.1 A). We confirmed *Rac1* and *Rac3* expression in the developing ENS by mRNA *in situ* hybridization (ISH) on cryosections of E12.5 wild type embryos (Fig. 3.1 B-D). In fact, Rac1 and Rac3 signals were particularly enriched in regions where ENCCs are present at this stage (Fig. 3.1 D).

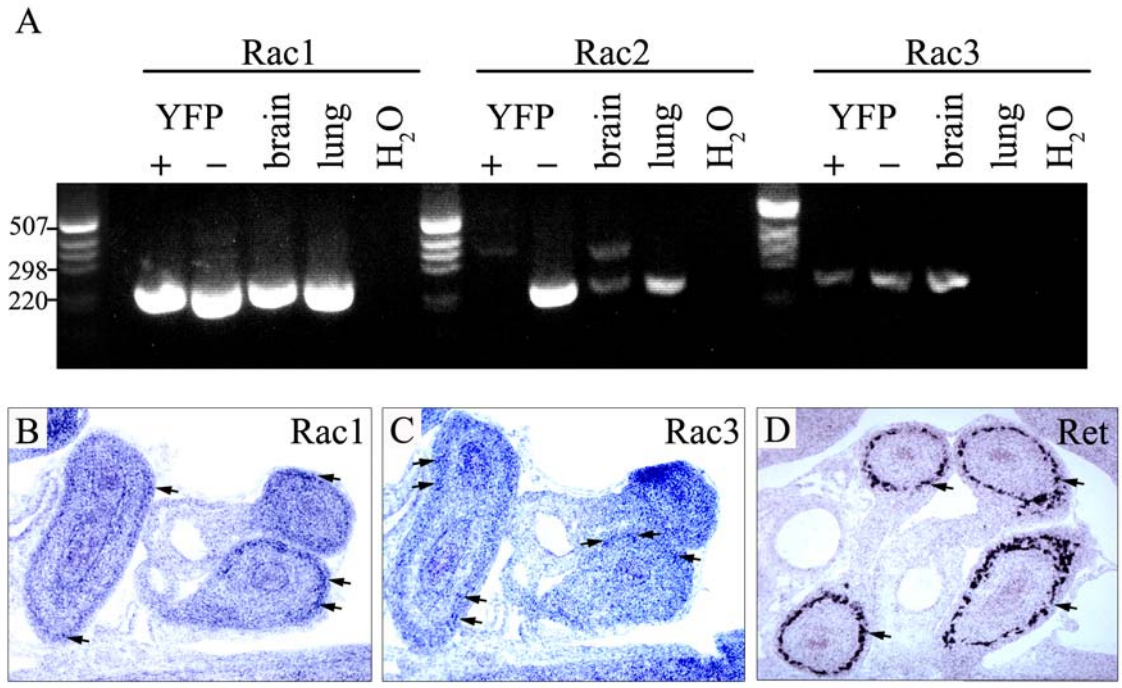


**Figure 3.1 Expression of Rac genes in the developing ENS**

(**A**) RT-PCR analysis for *Rac1*, *Rac2* and *Rac3* expression on FACS-purified ENCCs ($YFP^+$) and the rest of non-neural crest derived cells of the gut ($YFP^-$) from E11.5 guts of *Sox10Cre;R26ReYFP* double transgenic embryos. Samples derived from E13.5 whole brain and lung were used as positive controls and water ($H_2O$) was used as a negative control for contaminations. The expected PCR product for *Rac1* (240 bp) was found in all samples, whereas a specific band for *Rac2* (240 bp) was detected only in $YFP^-$, brain and lung and for *Rac3* (250 bp) in both $YFP^+$ and $YFP^-$ cells and brain. (**B-D**) mRNA *in situ* hybridization for *Rac1*, *Rac3* and *c-Ret* on transversal cryosections of E12.5 wild type embryos. Signals for *Rac1* (**B**) and *Rac3* (**C**) probes were found enriched in regions of the gut where ENCCs are located (arrows), as shown by reactivity for *Ret* (**D**, arrows), which is expressed by all ENCCs at this stage.

Given the expression of *Rac1* and *Rac3* as early as E11.5 in the developing ENS, we wished to explore the role of these proteins in the migration of ENCCs and the projection pattern of enteric neurons during enteric neurogenesis. For this, we adopted a genetic ablation approach *in vivo*. We combined the *Sox10Cre* transgene and the *R26ReYFP* reporter with a *Rac1* conditional mutant allele, $Rac1^{flox}$ (Walmsley *et al.*, 2003), in order to target the deletion of *Rac1* to the NC derivatives in the gut and, simultaneously, trace ENCCs by YFP expression. We confirmed successful ablation of *Rac1* by RT-PCR on FACS-purified $YFP^+$ ENCCs from E11.5 guts of $Rac1^{+/f};Sox10^{+/Cre};R26ReYFP^{+/st}$ (controls) and $Rac1^{f/f};Sox10^{+/Cre};R26ReYFP^{+/st}$ (Rac1 mutants) embryos (Fig. 3.2). A PCR product specific for the Rac1 transcript was not detected in $YFP^+$ ENCCs in Rac1 mutant embryos, whereas it was present in control samples. Conversely, Rac1 expression was detected in the remaining gut $YFP^-$ gut cells both in mutant and control samples, thus proving the targeted deletion of the gene only within the Sox10 expression domain and its derivatives.

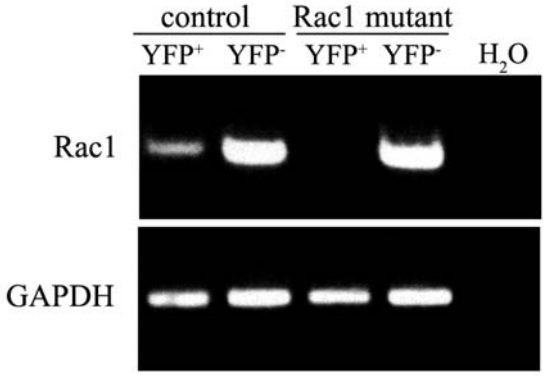


**Figure 3.2 Successful ablation of *Rac1* is confirmed by RT-PCR**

RT-PCR analysis on FACS-purified $YFP^+$ (ENCCs) and $YFP^-$ (rest of gut cells) from $Rac1^{flox/flox};Sox10^{+/Cre};R26ReYFP^{+/st}$ (Rac1 mutant) and $Rac1^{+/flox};Sox10^{+/Cre};R26ReYFP^{+/st}$ (control) E11.5 guts. The expected band amplified by *Rac1*-specific primers is absent from $YFP^+$ ENCCs dissociated from Rac1 mutant guts, whereas it can be still detected in the $YFP^-$ cell population, confirming the conditional ablation of the gene only within neural crest cell population. In control samples, the Rac1 gene product is still present both in $YFP^+$ and $YFP^-$ cells. The transcript for the housekeeping gene GAPDH has been used as a positive control. $H_2O$ has been used as a negative control against contaminations.

Preliminary analyses showed that Rac3 knockout mice have no detectable deficit in the development of the ENS. This is consistent with published reports (Corbetta *et al.*, 2005) as well as with the normal morphology, life span and fertility of *Rac3*$^{-/-}$ animals (detail of this analysis will be presented in the context of our studies on double Rac1 and Rac3 mutants). Therefore, we introduced the Rac3 null mutation into the *Rac1flox;Sox10Cre* background to test the possible genetic interaction between *Rac1* and *Rac3*. A summary of the breeding strategy is presented in Figure 3.3 A and experimental genotypes in Figure 3.3. B. These genotypes will be referred in the text as Rac3 mutant (*Rac3*$^{-/-}$*;Rac1*$^{+/flox}$*; Sox10*$^{+/Cre}$*;R26ReYFP*$^{+/st}$*)*, Rac1 mutant (*Rac3*$^{+/-}$*;Rac1*$^{flox/flox}$*;Sox10*$^{+/Cre}$*;R26ReYFP*$^{+/st}$), Rac1/3 or double mutant (*Rac3*$^{-/-}$*;Rac1*$^{flox/flox}$*;Sox10*$^{+/Cre}$*;R26ReYFP*$^{+/st}$) and control (*Rac3*$^{+/-}$*;Rac1*$^{+/flox}$*;Sox10*$^{+/Cre}$*;R26ReYFP*$^{+/st}$).

All the experimental genotypes were recovered in the expected mendelian ratio of 1:1:1:1 only up to E12.5-E13.5. Subsequent to these stages, Rac1 and Rac1/3 mutant genotypes were rarely observed, while they were never recovered at birth. At E11.5, Rac1 mutants presented severe craniofacial dysmorphologies such as facial clefting (Fig. 3.3 E) and cardiac defects, a phenotype similar to that reported in mice with an independently generated conditional allele of *Rac1* combined with the *Wnt1Cre* transgene (Fuchs *et al.*, 2009; Thomas *et al.*, 2010). Rac3 mutant embryos showed no defect at any stage we analysed (Fig. 3.3 D). Interestingly, Rac1/3 mutant embryos showed anatomical defects and embryonic lethality indistinguishable to that of Rac1 mutants (Fig. 3.3 F).

### 3.1.2 Rac1 and Rac1/3 mutant ENCCs fail to colonize the embryonic gut

Early migration of neural crest cells (NCCs) to their target tissues did not appear to be affected by the single or combined Rac mutations. YFP$^{+}$ cells could be found in branchial arches, cranial sensory ganglia, dorsal root ganglia and sympathetic chains both in controls and mutants in whole-mount preparations of E11.5 embryos immunolabelled with GFP antibody (Fig. 3.3 G-J).

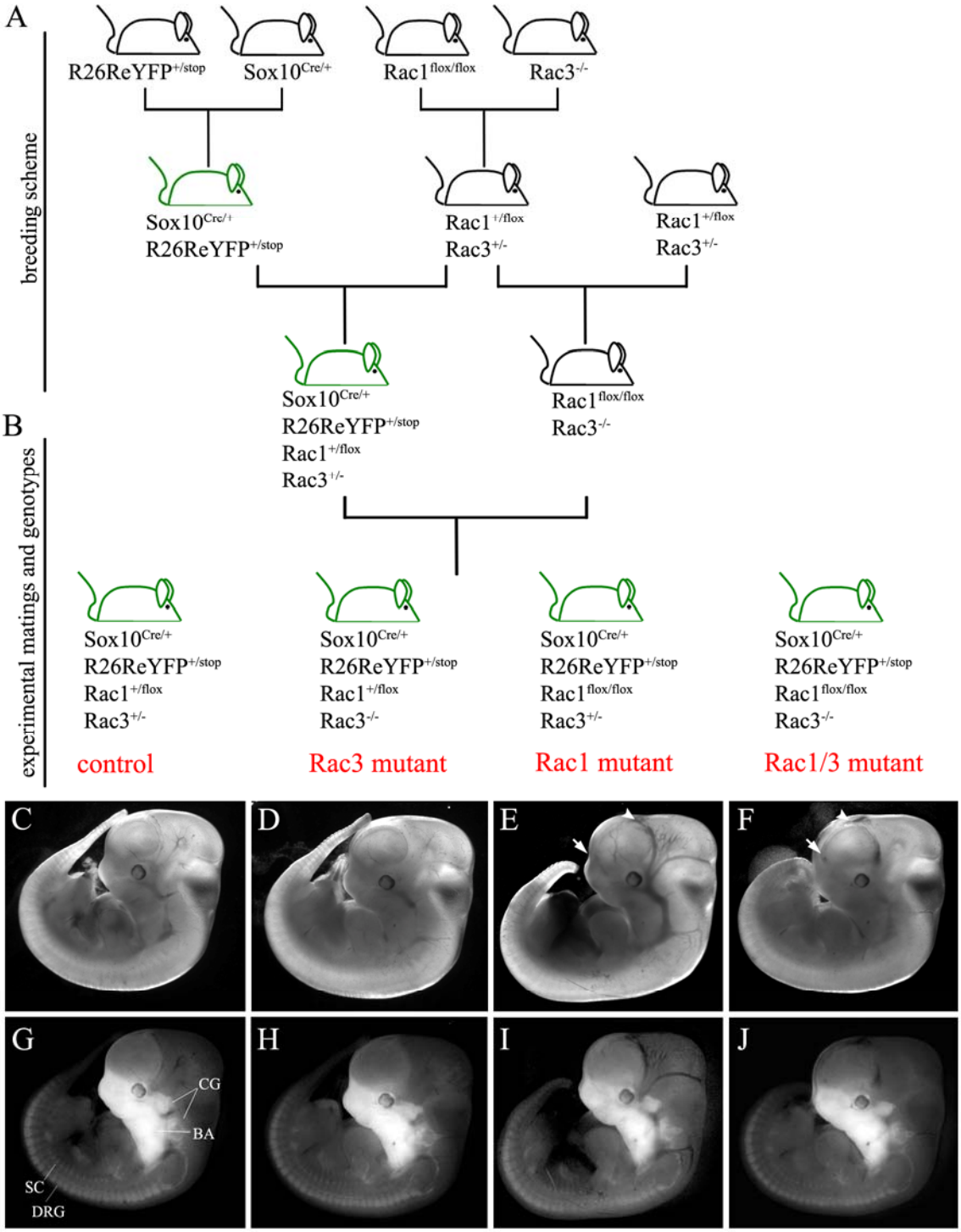


**Figure 3.3 (legend next page)**

**Figure 3.3 Generation of experimental genotypes and analysis of anatomy and *R26ReYFP* transgene expression of Rac mutant embryos**

(**A**) Schematic of the crossings used to generate the experimental genotypes. The *Sox10Cre* transgenic line (Matsuoka *et al.*, 2005), was crossed to the reporter line *R26ReYFP* (Srinivas *et al.*, 2001), where it mediates permanent labelling of NCCs and their derivatives (green mouse). Concomitantly the conditional allele for *Rac1* (Walmsley *et al.*, 2003) and the null allele for *Rac3* (Corbetta *et al.*, 2005) were combined within the same background. Finally, the two sets of double transgenics were intercrossed to generate the experimental control genotype $Sox10^{+/Cre};R26ReYFP^{+/st};Rac1^{+/f};Rac3^{+/-}$. (**B**) Generation of experimental genotypes was achieved by crossing double homozygous *Rac1flox;Rac3KO* to $Sox10^{+/Cre};R26ReYFP^{+/st};Rac1^{+/f};Rac3^{+/-}$ transgenics, thus producing, within the same crossing, control, Rac3 mutant, Rac1 mutant and Rac1/3 mutant embryos (see figure for detailed genotypes). (**C-F**) Representative brightfield pictures of E11.5 embryos for each experimental genotype. Rac1 mutant (**E**) and Rac1/3 mutant (**F**) embryos presented visible craniofacial defects such as facial cleft (arrows) and diffuse haemorrhages (arrowheads), whereas Rac3 mutant embryos (**D**) appeared morphologically indistinguishable from controls (**C**). (**G-J**) YFP fluorescence micrograph of the same preparations shown in C-F (greyscale). The *Sox10Cre* transgene mediates the permanent labelling of all neural crest cells by YFP fluorescence as soon as they emigrate from the neural tube at E8.5. (**G**) In control embryos at E11.5, $YFP^+$ NCCs can be detected in cranial ganglia (CG), branchial arches (BA), dorsal root ganglia (DRG) and sympathetic chains (SC). (**H-J**) Similarly, in Rac3 (H), Rac1 (I), Rac1/3 (J) mutant embryos, YFP fluorescence can be detected at comparable locations and intensity, indicating that ablation of Rac genes does not affect emigration of NCCs to their target tissues.

Similarly, mutant NCCs were also able to reach and invade the embryonic foregut as indicated by GFP fluorescence in whole-mount preparations of E10.5 guts (Fig. 3.4 A-D). However, in Rac1 and Rac1/3 mutants, colonisation of more distal regions of the gastrointestinal tract by ENCCs was delayed relative to controls. In control and Rac3 mutant animals, the front of migrating ENCCs was positioned in the caecum area and halfway along the hindgut at E11.5 and E12.5 respectively (Fig. 3.4 E-F, I-J). In contrast, in Rac1 and Rac1/3 mutants, the front of ENCCs, at E11.5, was still located in the midgut region and, at E12.5, it had progressed minimally and appeared to stall around the caecum area (Fig. 3.4 G-H, K-L).

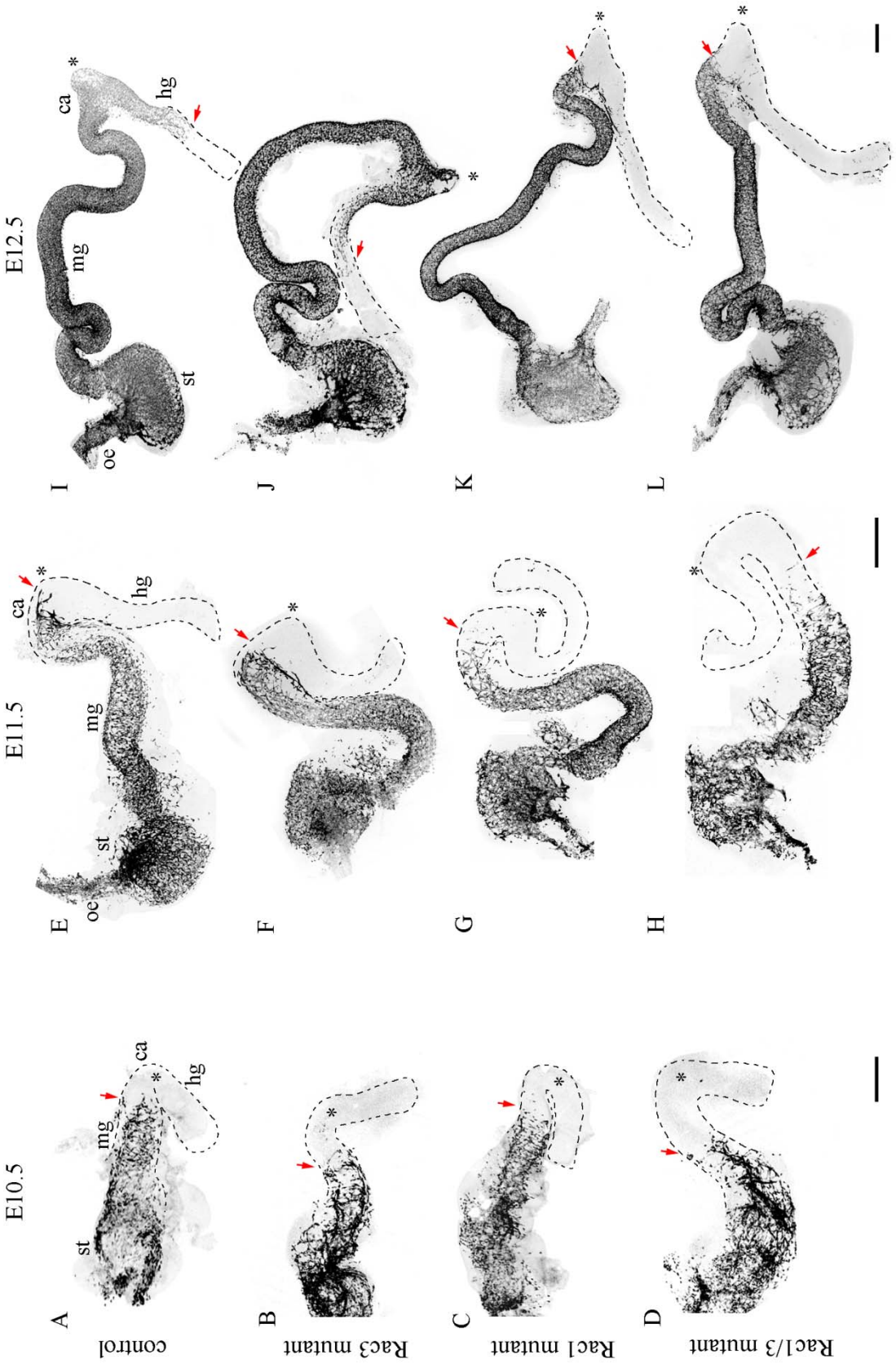


**Figure 3.4 (legend next page)**

**Figure 3.4 Gut colonisation by ENCCs is defective in Rac1 and Rac1/3 mutant embryos**
Inverted confocal micrographs of whole mount gut preparations immunostained for GFP, indicating the distribution of ENCCs within the developing gut. Red arrows indicate the position of the front of migration of ENCCs, while the caecal curvature (asterisk) has been used as an anatomical landmark. (**A-D**) At E10.5 ENCCs can be observed progressing through the midgut both in control (A) and Rac mutant (B-D) preparations. (**E-H**) At E11.5, in control (E) and Rac3 mutant (F) animals the front of ENCCs is approaching the caecum area. At equivalent stages, Rac1 (G) and Rac1/3 (H) mutant ENCCs can be found delayed in the midgut region.(**I-J**) At one of the latest stages at which Rac1 and Rac1/3 mutant embryos can be found alive, E12.5, control ENCCs have invaded the hindgut (I), whereas the migratory front in Rac1 and Rac1/3 mutant guts is still located in the proximal caecum (K-L). No differences were observed in the extent of gut colonisation between Rac3 mutants (J) and controls (I) also at this stage. Hg, hindgut; mg, midgut; oe, oesophagus; st, stomach. Scale bars 500 μm.

To investigate neuronal differentiation, we immunolabeled whole-mount preparations of E11.5 guts with a monoclonal antibody for the pan-neuronal marker β-tubulin (TuJ1) (Fig. 3.5). $TuJ1^{+}$ enteric neurons were found in all samples, distributed from proximal regions to the most distal colonized areas of the gut at this stage, suggesting that there is no primary deficit in neuronal differentiation upon ablation of Rac genes. However, in Rac1 and Rac1/3 mutants, the density of neurons in the pyloric antrum was often decreased and the network of neuronal processes within the midgut was generally less organised than in controls (Fig. 3.5 C-D).

Therefore, our phenotypic analysis suggests that Rac1 is required for the normal colonisation of the mammalian gut by neural crest cells and enteric neurons. In contrast, no discernible role for Rac3 was revealed by these studies.

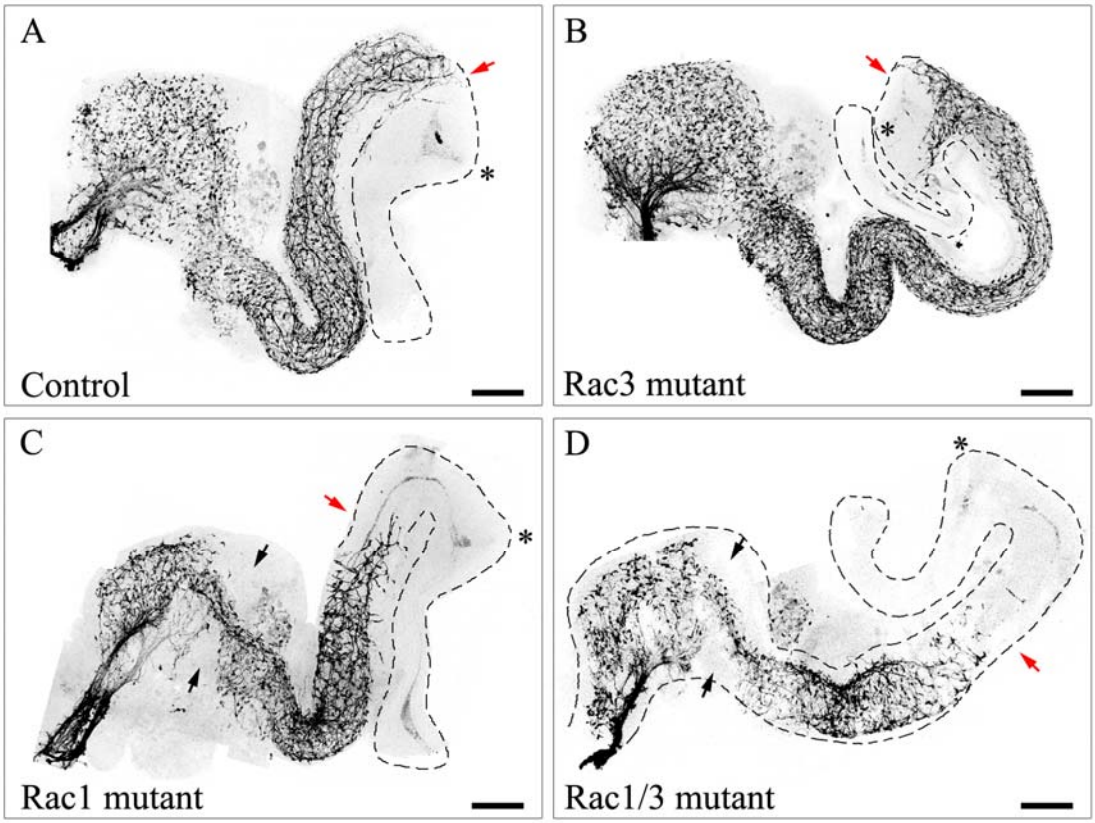


**Figure 3.5 Rac ablation does not prevent neuronal differentiation**

Inverted confocal micrographs of whole mount E11.5 guts immunolabelled for the neuronal marker TuJ1. In control preparations (**A**) TuJ1$^{+}$ cell bodies and processes are present from rostral regions of the gut to the proximal caecum (red arrow). Rac3 mutant embryos (**B**) present an analogous distribution of enteric neurons. In Rac1 and Rac1/3 mutants (**C-D**), enteric neurons are only present to the most distal colonised area at this stage (i.e. midgut, red arrow). In addition, the density of neurons appears defective in the distal stomach (black arrows) and processes and cell bodies seem not homogenously distributed within the midgut. Scale bars 300 μm.

### 3.1.3 Proliferation of ENCCs in Rac mutants

Next we wished to explore the molecular and cellular mechanisms by which Rac GTPases control the development of the ENS. Cell proliferation and maintenance of ENS progenitors have been shown to be critical for the successful colonisation of the embryonic gut. To test the possibility that ablation of Rac genes might affect the mitotic activity of ENCCs and lead to a reduced number of ENS progenitors, we assayed 5-ethynyl-2´-deoxyuridine (EdU) incorporation in ENCCs *in vivo*. EdU is a modified nucleoside analog to thymidine that is incorporated into newly replicated DNA during the S phase of the cell cycle, thus labeling replicating cells at a given time.

We performed EdU pulse labelling for 1 hr at E11.5, followed by immunofluorescence analysis on short-term cultures of dissociated embryonic guts (Fig. 3.6 A-D, A'-D'). ENCCs were identified by GFP immunolabelling and proliferating cells were defined as the proportion of $GFP^+$ cells labelled by EdU. We found that the percentage of ENCCs at the S phase did not differ significantly between controls and Rac mutants. In controls, proliferating cells were 33.6±3.2%, in Rac3 mutants 27.5±2.0%, in Rac1 mutants 29.1±1.7% and in Rac1/3 mutants 31.5±2.6% (counting performed on a total of ≥760 cells from at least 3 independent guts per genotype. Fig. 3.6 E).

Thus, these data suggest that the incomplete colonisation of the gut observed in Rac1 and Rac1/3 mutants cannot be accounted by an altered number of migrating ENCCs resulting from proliferation defects in ENS progenitors.

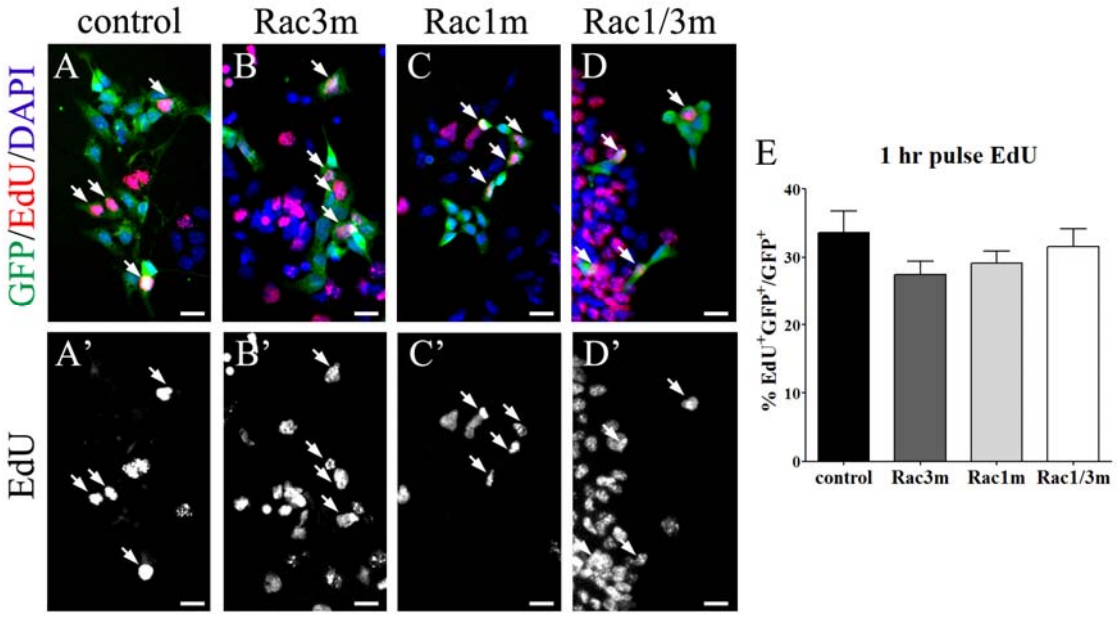


**Figure 3.6 Proliferation is not affected in Rac mutant ENCCs**

*In vitro* analysis of cell proliferation. Following a short EdU pulse *in vivo*, E11.5 guts were dissociated and cultured for 4 hrs *in vitro* and then processed for EdU and GFP reactivity. (**A-D**) Proliferating ENCCs were identified by double fluorescence for GFP (green) and EdU (red) (arrows). (**A'-D'**) Greyscale panels of the red channel (EdU) shown in A-D. Nuclei counterstained with DAPI (blue). Scale bars 20 µm. (**E**) Quantification of proliferating cells in the $GFP^+$ ENCC population. Cells counted≥760. N=3. Error bars, SEM.

### 3.1.4 Ablation of *Rac1* greatly reduces response to GDNF *in vitro*

The delay in the colonisation of the gut observed *in vivo* could be due to a primary migratory defect of ENCCs in Rac1 and Rac1/3 mutant embryos. To explore this possibility, we adopted two separate *in vitro* assays. First, we compared the response of ENCCs within the gut of Rac-deficient and control embryos to GDNF using a 3D collagen matrix (3D cultures, Fig. 3.7). GDNF has been suggested to play a major role in the migration of ENS progenitors and induces dramatic chemotactic responses of these cells in collagen gel assays (Natarajan *et al.*, 2002; Young *et al.*, 2001). In these conditions, control and Rac3 mutant explants showed a massive invasion of the collagen matrix by ENCCs and neuronal processes (Fig. 3.7 B-B", C-C"). However, under similar conditions, Rac1 and Rac1/3 mutant explants showed no response of both ENCCs and neuronal processes (Fig. 3.7 D-D", E-E"). These findings are in contrast to the colonisation phenotype observed *in vivo* in Rac mutants. In fact, Rac1 and Rac1/3 mutant ENCCs migrate through the embryonic midgut *in vivo* (albeit with some delay), thus suggesting that migration of cells and axons *in vivo* is not driven solely by GDNF activity. On the other hand, these data indicate that under the conditions of the 3D cultures, GDNF activity is critically dependent on Rac1 function, whereas Rac3 function seems dispensable. Taken together, these data suggest that other signalling pathways and interactions with extracellular matrix (ECM) proteins and/or mesenchymal cells might be implicated in the *in vivo* migration of endogenous ENCCs.

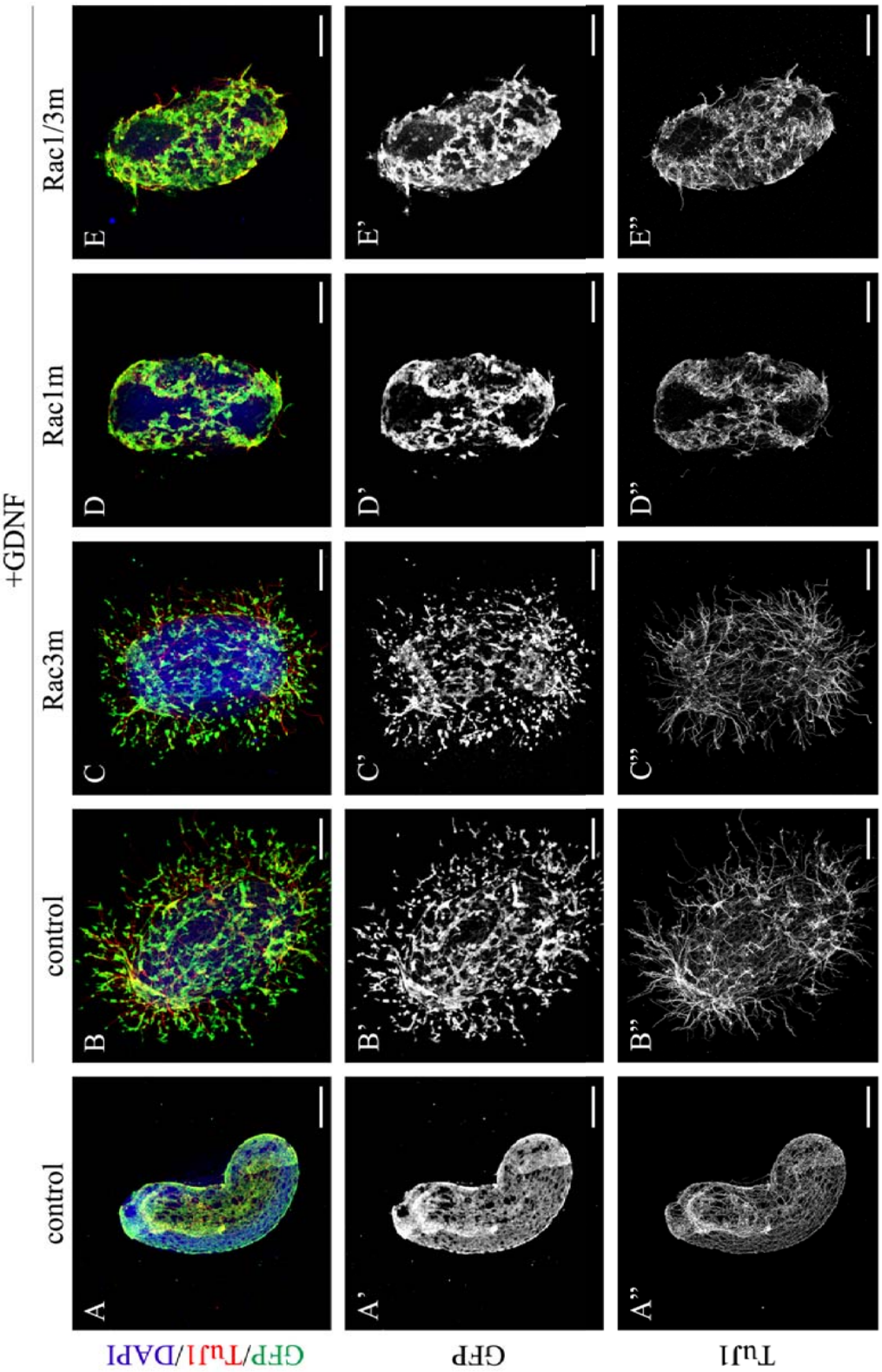


**Figure 3.7 (legend next page)**

**Figure 3.7 Rac1 and Rac1/3 mutant ENCCs fail to respond to GDNF in 3D cultures**
(**A-E**) E11.5 gut explants set in collagen matrix and immunostained for GFP (green) to identify ENCCs, TuJ1 (red) to label neuronal processes and DAPI (blue) for identification of tissue boundaries. (**A'-E'**) Greyscale panels for the green channel (GFP) shown in A-E. (**A"-E"**) Greyscale panels for the red channel (TuJ1) shown in A-E. In presence of GDNF, control explants show invasion of the matrix by $GFP^+$ ENCCs (**B** green, **B'**) and $TuJ1^+$ neuronal processes (**B** red, **B"**), which were absent when GDNF was not applied to the cultures (**A-A"'**). In the same conditions, Rac1 (**D'**) and Rac1/3 (**E'**) mutant ENCCs and neuronal processes (**D"**, **E"**) fail to show any response to GDNF. Conversely, Rac3 mutant ENCCs and neuronal processes present a response to GDNF comparable to controls (**C-C"**). Scale bars 200 μm.

To further examine the migratory and adhesive properties of Rac mutant ENCCs we used a second assay that had been reported previously (Breau *et al.*, 2006). This assay involves the culturing of transverse slices of gut in fibronectin-coated tissue culture dishes (2D cultures, Fig. 3.8). Fibronectin is one of the major ECM molecules and it has been shown to be abundantly expressed in neural crest migration pathways *in vivo* (Newgreen & Thiery, 1980). As early as 24 hrs in culture, control explants showed a scattered network of $GFP^+$ ENCCs and $GFP^-$ mesenchymal cells (also identified by α-actin staining) around the gut tissue. The $GFP^+$ cells were found either close to the slice, in which case they were resting on top of mesenchymal gut cells, or farther away migrating onto the fibronectin substrate (Fig. 3.8 A-A'). In contrast to control explants, far fewer ENCCs were found outside Rac1 and Rac1/3 mutant gut slices, and the majority of those that had migrated, were restricted on top of mesenchymal cells and often formed aggregates (Fig. 3.8 C-C', D-D'). We quantified these observations by measuring the average distance migrated by ENCCs and mesenchymal cells relative to the border of the explant (Fig. 3.8 E). Migration of ENCCs was significantly reduced in Rac1 and Rac1/3 mutants compared to controls. Control ENCCs were able to cover a significant distance on top of the fibronectin substrate, unlike Rac1 and Rac1/3 mutant cells, which migrated as far as the mesenchymal cells (*control*: ENCCs 346.8±23.6 μm, mesenchymal cells 175.3±8.6 μm. *Rac1 mutant*: ENCCs 143.1±17.8 μm, mesenchymal cells 178.7±22.9 μm. *Rac1/3 mutant*: ENCCs 183.3±16.2 μm, mesenchymal cells 197.7±17.4 μm. $P<0.001$. Total of ≥200 cells measured from

at least 4 independent explants per genotype). Rac3 mutants showed a migratory behaviour similar to controls (ENCCs 403.4±19.3 μm, mesenchymal cells 199.6±3.0 μm. Fig. 3.8 B-B', E), thus suggesting, along with the absence of a specific phenotype in Rac1/3 mutants compared to Rac1 mutants, a minimal role of the Rac3 protein in control of ENCC migration.

**Figure 3.8 Rac1 and Rac1/3 mutant ENCCs show a migratory defect and aberrant morphology on a 2D culture assay (figure next page)**

(**A-D**) Transverse slices of E12.5 guts were cultured on a fibronectin substrate for 24 hrs and then stained for GFP (green) and α-actin (red) to identify ENCCs and the actin cytoskeleton of all cells present in the explants, respectively. (**A'-D'**) Greyscale panels of the green channel (GFP) shown in A-D. (**A-A'**) In control slices, $GFP^+$ ENCCs formed a scattered network on top of mesenchymal cells ($YFP^-$ $\alpha\text{-actin}^+$) and beyond them directly on the fibronectin substrate (dashed line indicates the border formed by mesenchymal cells). Fewer Rac1 (**C-C'**) and Rac1/3 (**D-D'**) mutant ENCCs were found outside the explant and the majority of them migrated on top of mesenchymal cells (**C-D**). Scale bars 200 μm. (**E**) Quantification of the average distance migrated by ENCCs and mesenchymal cells away from the border of the explant. Cells measured≥200. N≥4. *** indicates P<0.001. Error bars, SEM.

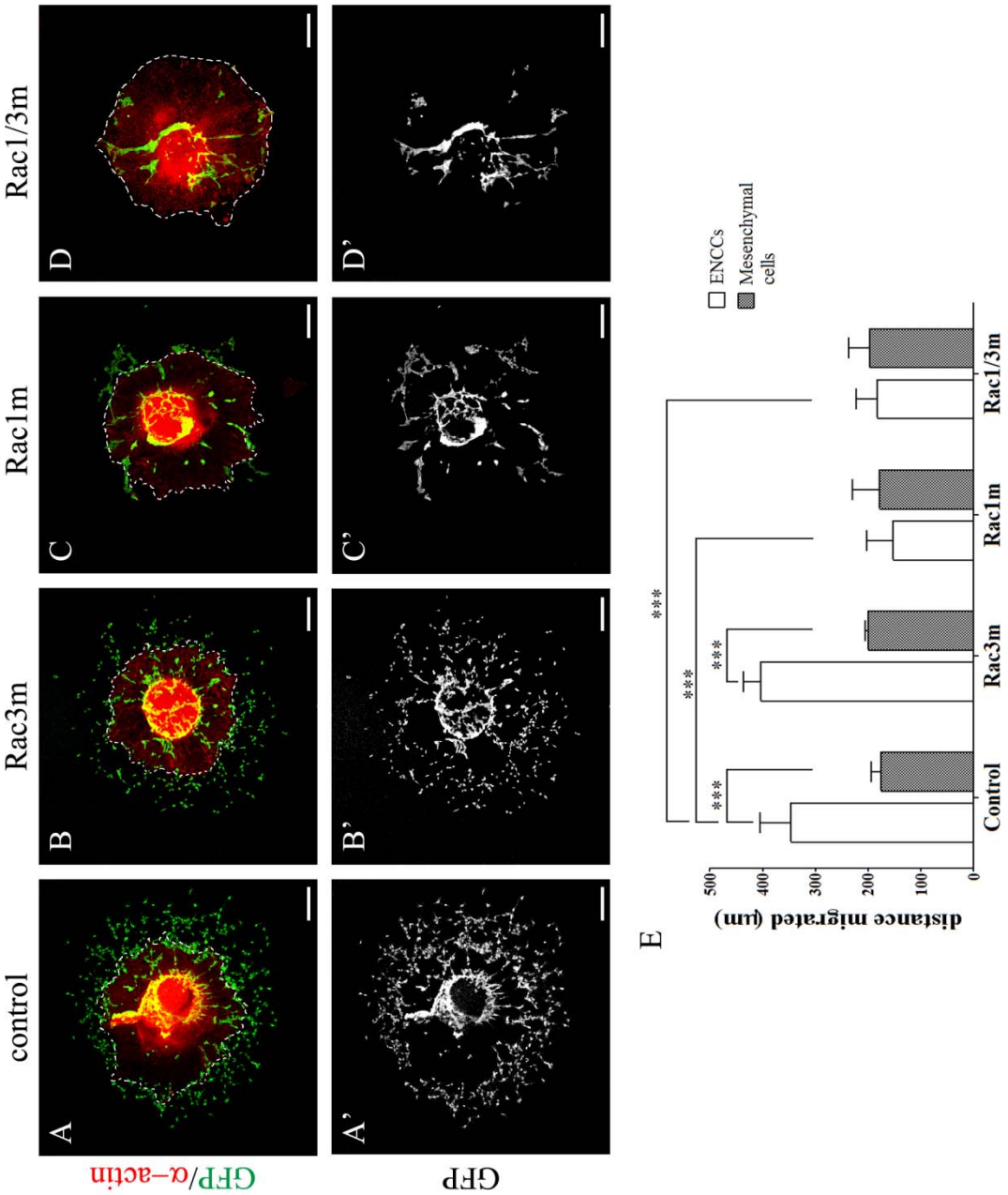


**Figure 3.8 (legend previous page)**

We also analysed the morphology of ENCCs migrating onto the fibronectin substrate by visualising the actin cytoskeleton with phalloidin staining (Fig. 3.9). Control ENCCs had spread-out morphology with a dynamic cytoplasmic structure characterized by lamellipodia and filipodia. However, we could also observe, especially behind the front migrating cells, several adherent cells with prominent stress fibres anchoring the cell membrane to the fibronectin substrate (Fig. 3.9 A-A'). Conversely, Rac1 and Rac1/3 mutant cells showed mainly a rounded morphology lacking lamellipodia. Additionally, small actin filaments, such as filipodia, were greatly reduced and there was a prevalence of stress fibres (Fig. 3.9 C-C', D-D'). Rac3 mutant ENCCs appeared morphologically comparable to control cells (Fig. 3.9 B-B').

Taken together, our data showed an altered response of Rac1 null cells to extracellular signals. Also, absence of Rac1 protein *in vitro* leads to an alteration in cell-cell and cell-matrix interactions, suggesting that this could be the mechanism behind the migratory delay observed in Rac1 mutants *in vivo*.

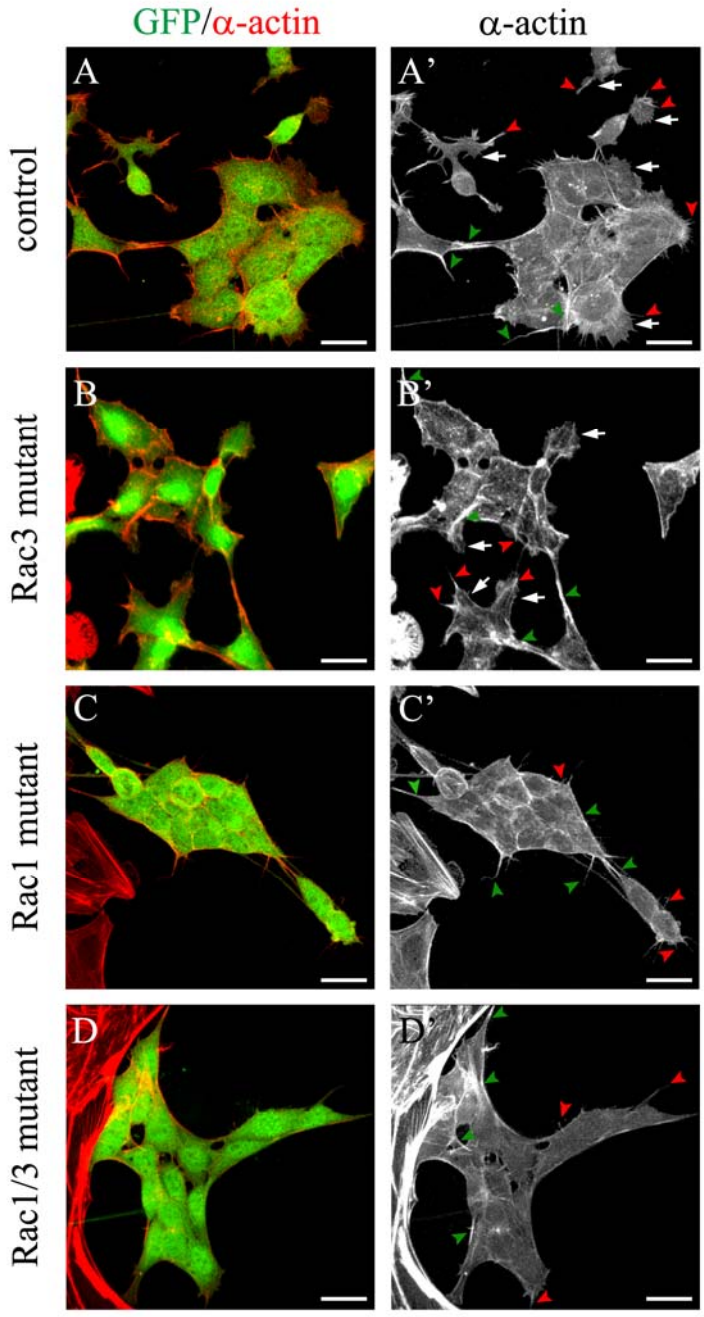


**Figure 3.9 Rac1 deficiency leads to altered cell morphology of migrating ENCCs**

Morphology of migrating ENCCs on fibronectin substrate in 2D cultures. (**A-D**) GFP immunofluorescence (green) identifies ENCCs and α-actin (red) highlights the structure of the cellular cytoskeleton. (**A'-D'**) Greyscale panels of the red channel (α-actin) shown in A-D. (**A-A'**) Migrating ENCCs from control explants show lamellipodia (white arrows) and filipodia (red arrowheads) at their leading edge, whereas cells behind the front have a spread and stable morphology characterised by the presence of several cortical stress fibres (green arrowheads). (**B-B'**) Rac3 mutant ENCCs do not differ in their morphology from control counterparts. Conversely, both Rac1 (**C-C'**) and Rac1/3 (**D-D'**) mutant ENCCs lack lamellipodia, they present sporadic filipodia and abundance of stress fibres. In addition, these cells are always found tightly aggregated. Scale bars 20 µm.

### 3.1.5 Rac proteins control neuritogenesis and morphology of enteric neurons

Having established that Rac1 mutation leads to a clear migratory deficit, we investigated the possible role of Rac GTPases in development of enteric neurons.

We first addressed whether the ablation of Rac genes might lead to impaired neuronal specification by analysing dissociated cells from E11.5 guts immunolabelled with GFP and TuJ1 antibodies (Fig. 3.10 A-D, A'-D'). We found similar fractions of $GFP^+$ ENCCs expressing the neuronal marker TuJ1 in control, Rac3 mutant and Rac1 mutant samples (control 23.1±1.5%, Rac3 mutant 23.4±1.2%, Rac1 mutant 25.0±0.3%. Total of ≥1100 cells from at least 3 guts per genotype. Fig. 3.10 E). Interestingly, Rac1/3 mutant ENCCs showed a small, but significant, increase in the proportion of neuronal committed cells (28.4±1.0%. N≥3. P<0.05. Fig. 3.10 E).

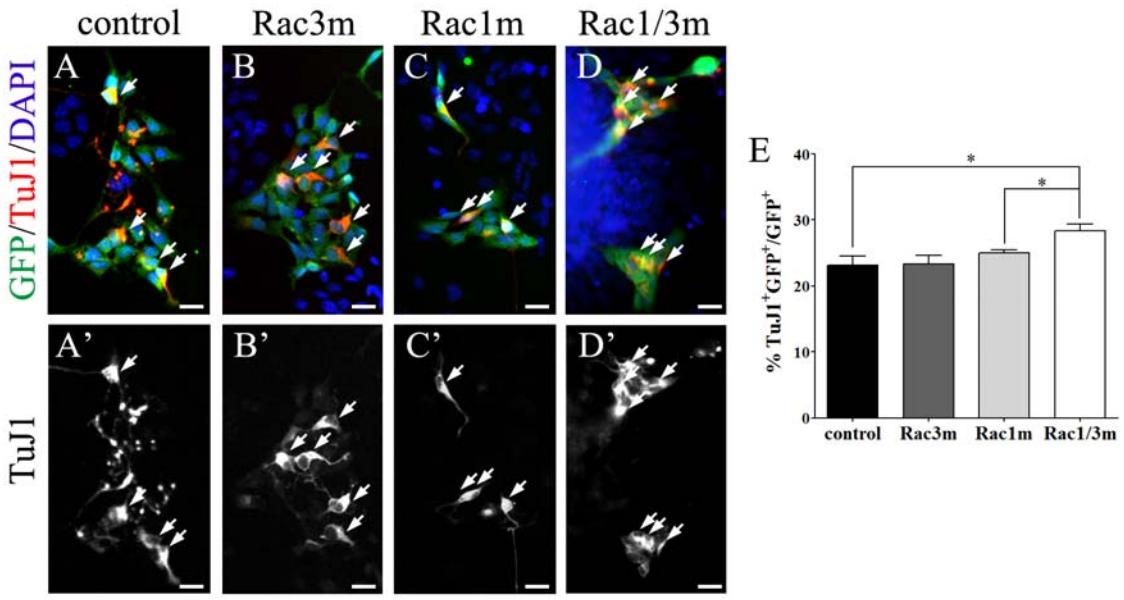


**Figure 3.10 Rac deficiency does not prevent neuronal differentiation**

*In vitro* analysis of neuronal differentiation. Short term cultures of E11.5 guts were immunolabelled for GFP (green), TuJ1 (red) and DAPI (nuclear counterstaining, blue). (**A-D**) ENCCs committed to the neuronal lineage were identified by double GFP and TuJ1 fluorescence (arrows). (**A'-D'**) Greyscale panels of the red (TuJ1) channels shown in A-D. Scale bars 20 µm. (**E**) Quantification of neuronal progenitors and neurons within the $GFP^+$ population. Total cells counted≥1100. N≥3. * indicates P<0.05. Error bars, SEM.

Since Rac mutations do not prevent neuronal differentiation, we next tested the intrinsic ability of mutant neurons to grow and maintain neurites. For this, we cultured primary enteric neurons from E11.5 guts and we investigated their morphology by immunostaining the cultures with a TuJ1 antibody (Fig. 3.11 A-D). Neuronal branches were considered to be primary when directly connected to the cell body, secondary and tertiary when linked to primary and secondary branches respectively. We measured for each neuron the longest primary and secondary branch and the sum of the lengths of all neurites and we compared these values between the experimental genotypes. We found that neurons deriving from Rac1 and Rac1/3 mutants generated primary neurites significantly shorter than their control counterparts (control 478.3±53.0 μm, Rac1 mutant 220.7±31.7 μm, Rac1/3 mutant 239.5±14.8 μm. Neurons measured≥290. N≥5. P<0.01. Fig. 3.11 E). In fact, the proportion of neurons with short (20-200 μm) and long (>400 μm) primary neurites were significantly increased and reduced respectively, in Rac1 and Rac1/3 mutant cultures (*20-200 μm*: control 11.8±1.4%, Rac1 mutant 60.8±7.6%, Rac1/3 mutant 48.2±2.7%. P<0.01. *>400 μm*: control 49.2±7.0%, Rac1 mutant 12.4±4.4%, Rac1/3 mutant 15.3±3.2%. P<0.01. Fig. 3.11 F). Moreover, neurons in both mutant samples also presented a significant reduction in length of secondary neurites and of the entire neurite arbour (*2ry branching*: control 133.6±16.6 μm, Rac1 mutant 74.8±10.0 μm, Rac1/3mutant 84.7±7.1 μm. P<0.05. *Total length*: control: 591.2±80.1 μm, Rac1 mutant 271.2±57.4 μm, Rac1/3 mutant 235.6±39.2 μm. P<0.05. Fig. 3.11 G, H). Hence, Rac1 ablation has a dramatic effect on neurite extension of enteric neurons. Interestingly, we also observed that Rac3 mutant neurons had a clear trend to have shorter neurites compared to controls (*1ry branching* 401.8±36.1 μm. P=0.26. *2ry branching* 97.6±9.1 μm. P=0.08. *total length* 430.5±39.5 μm. P=0.09. Fig 3.11 E, G, H), thus suggesting a redundant function of Rac3 in the process of neuritogenesis.

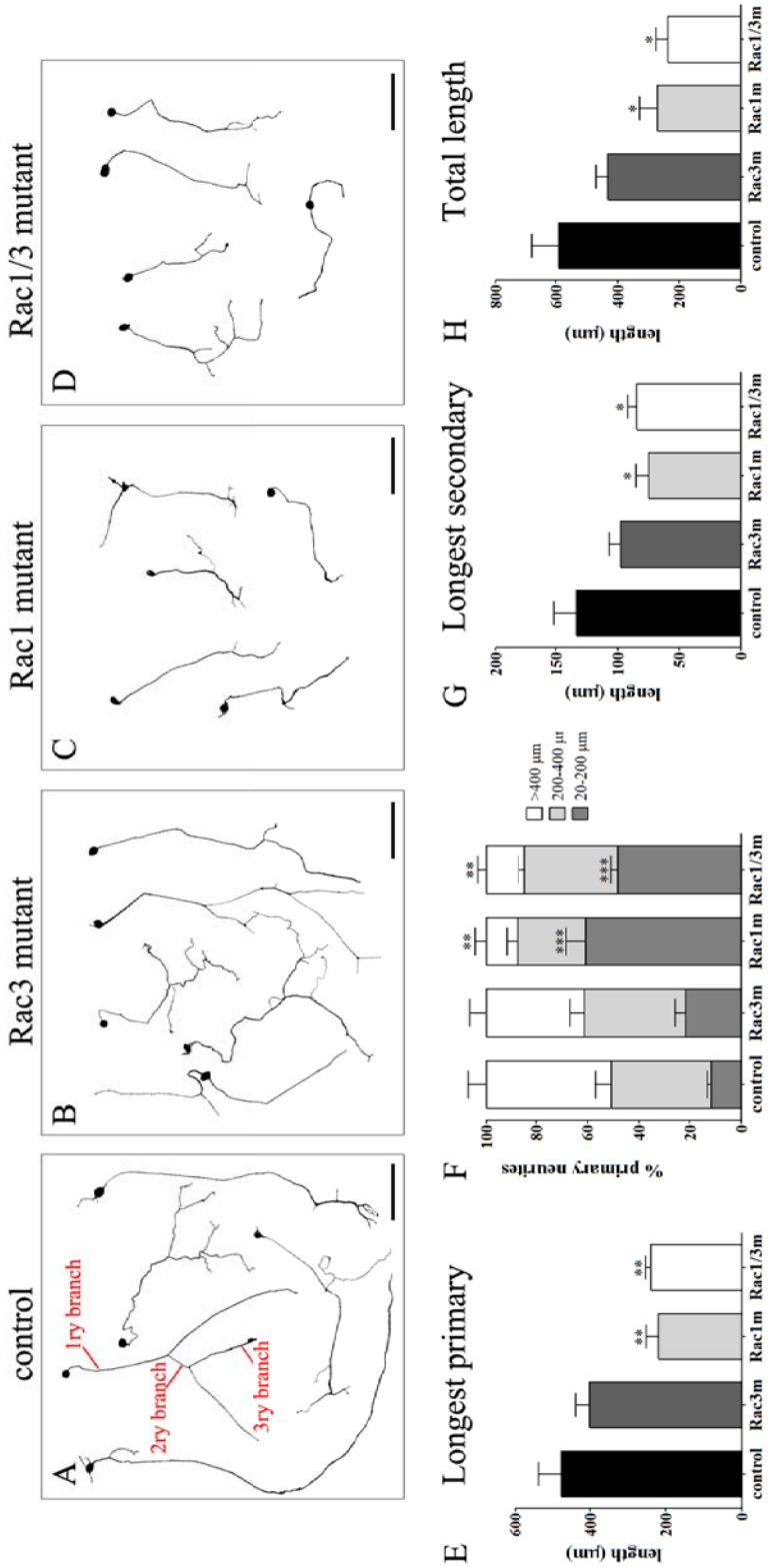


**Figure 3.11 (legend next page)**

**Figure 3.11 Analysis of neuritogenesis in primary enteric neurons *in vitro***
Primary enteric neurons from E11.5 guts were cultured for 4 days *in vitro* and then immunolabelled for the pan-neuronal marker TuJ1 to assess neurite extension and branching. (**A**-**D**) Inverted fluorescence images of $TuJ1^+$ enteric neurons. Neurites were defined as primary if directly connected to the cell body and secondary and tertiary if branched from primary and secondary neurites, respectively. Scale bars 100 μm. (**E**) Quantification of the average length in μm of the longest primary neurite per neuron. (**F**) Distribution of longest primary neurites according to their length. (**G**) Quantification of the average length in μm of the longest secondary neurite per neuron. (**F**) Average of the sum of lengths of all neurites per neuron (total neurite length). Total neurons measured ≥290. N≥5. * indicates P<0.05. ** indicates P<0.01. *** indicates P<0.001. Error bars, SEM.

Rac proteins have been shown to also be able to control the complexity of the neurite arbour by regulating the branching process (Ng *et al.*, 2002). Therefore, we tested the role of Rac1 and Rac3 in the branching of enteric neurons by measuring the proportion of neurons with only primary (1ry), with secondary (1-2ry) and with tertiary (1-2-3ry) neurites (Fig. 3.12 A). Notably, we found that the "1-2-3ry" morphology was significantly under-represented in Rac1 and Rac1/3 mutant neuronal cultures (control 12.2±1.8%, Rac1 mutant 5.3±2.2%, P<0.05, Rac1/3 mutant 5.0±1.2%. P<0.01. Fig. 3.12 A). Additionally, Rac1 mutant samples also presented a decreased number of neurons with secondary neurites (*1-2ry*: control 42.6±2.4%, Rac1 mutant 27.6±2.2%. P<0.05), with a concomitant expansion of the neuronal population with only primary branches (1ry). On the other hand, Rac3 mutant neurons appeared to have a neurite organization comparable to that found in controls.

Morphology of neurons is determined not only by the presence of 1ry, 2ry and 3ry branches, but also by their number. For example, a single primary branch denotes unipolar neurons, whereas two or three primary neurites are feature of bipolar and multipolar neurons respectively. To assess whether Rac function might be implicated in this process, we quantified the amount of primary and secondary neurites for each individual neuron. As a result, we found no difference in the number of neurons with 1, 2 or more than 2 primary or secondary neurites between mutants and controls (Fig. 3.12 B, C).

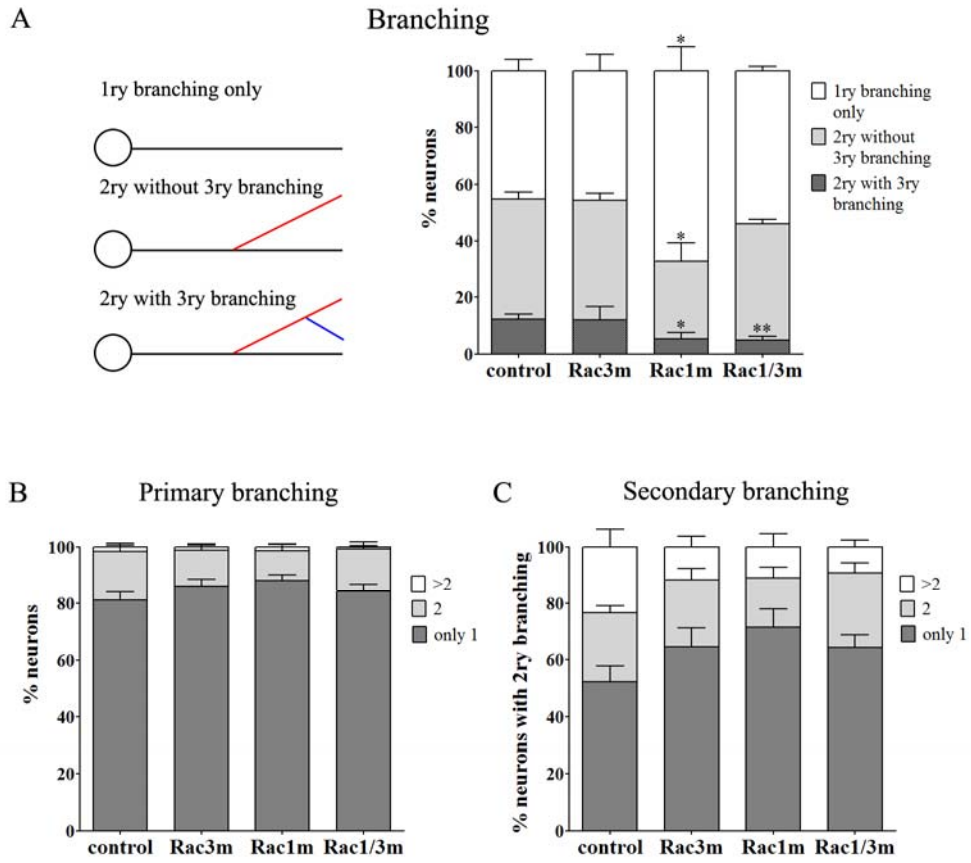


**Figure 3.12 Analysis of branching of primary enteric neurons *in vitro***

(**A**) Extent of branching of E11.5 primary enteric neurons cultured *in vitro* was assessed by quantifying the proportion of neurons with only primary branches and with secondary neurites with and without tertiary branches. Additionally, the number of primary (**B**) and secondary (**C**) branches per neurons was also measured. Total neurons measured ≥290. N≥5. * indicates P<0.05. ** indicates P<0.01. Error bars, SEM.

These data suggest that several aspects of neuritogenesis of ENS neurons are controlled by Rac proteins. In particular, Rac1 ablation results in an almost a two-fold decrease in length of primary and secondary neurites and a reduction in the proportion of neurons bearing 2ry and 3ry branches. Furthermore, the role of Rac3 in the control of neurite length appears to be redundant, since ablation of both Rac proteins does not lead to a worsening of the phenotype already observed in Rac1 mutants.

### 3.1.6 Rac mutant ENCCs and projections have an aberrant orientation *in vivo*

Given the altered neuritogenesis found in Rac1- and Rac1/3-deficient neurons *in vitro*, we next wished to investigate the development and organisation of enteric neuronal processes *in vivo*. For this, we considered individual neurites and neuronal tracts clearly identifiable at the front of migration and we investigated their orientation in whole mount preparation of E11.0-E11.5 guts immunolabelled with TuJ1 antibody (Fig. 3.13). More specifically, we measured the angles between neuronal tracts and the long axis of the gut, and we analysed their distribution and average size. We considered only the first 15 tracts at the migratory front that were at least 100 μm long and had a constant orientation along this length (Fig. 3.13 A-D, A'-D'). In control samples, $TuJ1^+$ tracts were mostly longitudinal (70.0±5.1% of tracts fell between 0 and 30°). In contrast, in all Rac mutants the fraction of angles measured between 0-30° (0-30° angles) was reduced. Concomitantly, more tracts formed angles that were above 30° (30-60°angles and 60-90° angles). Specifically, in Rac3 mutants we observed a statistically significant decrease of 0-30° angles. On the other hand, in Rac1 and Rac1/3 mutants, both the decrease of the 0-30° angles and the increase of the proportion of 60-90° angles was statistically significant (*0-30° angles*: Rac3 mutant 48.0±6.4% $P<0.05$, Rac1 mutant 44.8±4.0% $P<0.01$, Rac1/3 mutant 40.0±4.1% $P<0.001$. *60°-90° angles*: control 7.8±3.0%, Rac3 mutant 21.3±3.8%, Rac1 mutant 19.0±4.8%, Rac1/3 mutant 26.7±4.8%. $P<0.05$. Tracts measured ≥75. N≥5. Fig. 3.13 E-H). Average size of angles followed the same trend (control 25.6±1.9%, Rac3 mutant 36.2±3.1% $P<0.05$, Rac1 mutant 36.7±2.9% $P<0.01$, Rac1/3 mutant 40.5±4.6% $P<0.001$. Fig. 3.13 I).

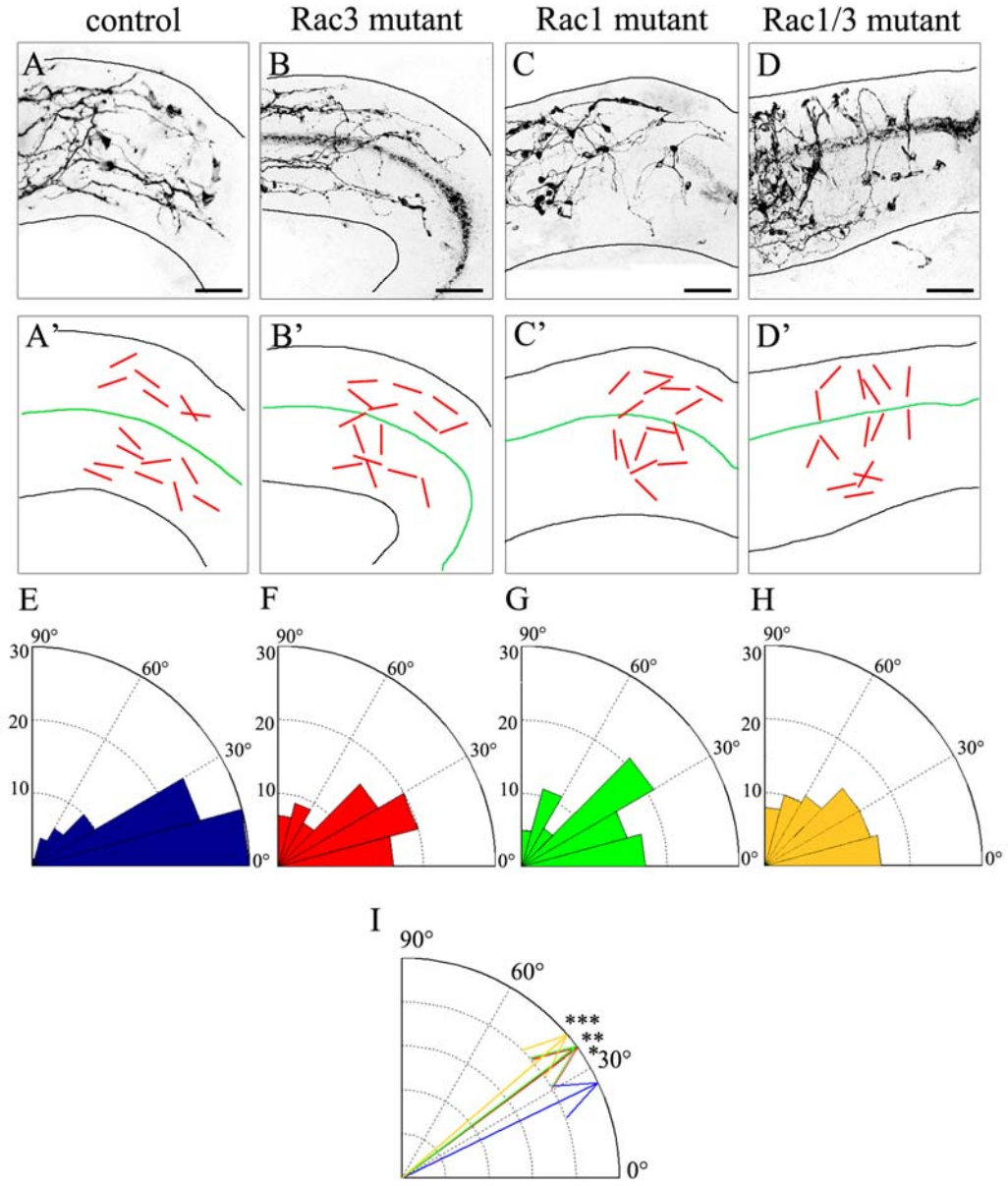


**Figure 3.13 Orientation of neuronal tracts is aberrant in Rac mutants *in vivo***

(**A-D**) Inverted confocal microscope images of migratory fronts in whole mount preparations of E11.0-11.5 guts immunolabelled for the neuronal marker TuJ1. Scale bars 100 µm. (**A'-D'**) Schematic representation of images shown in A-D, where the first 15 neuronal tracts with constant orientation for at least 100 µm were drawn as straight lines (red) and the longitudinal axis of the gut with a green line. Orientation of tracts was measured by quantifying the angle between straight lines and the main axis of the gut. (**E-H**) Rose plots showing the distribution of 75 representative angles. The area of each bin represents the number of neuronal tracts oriented in that direction (**E**) Control. (**F**) Rac3 mutant. (**G**) Rac1 mutant. (**H**) Rac1/3 mutant. (**I**) Rose plot showing the average angles of control (blue arrow), Rac3 mutant (red arrow), Rac1 mutant (green arrow) and Rac1/3 mutant (orange arrow) neuronal tracts. N≥75. * indicates P<0.05. ** indicates P<0.01. *** indicates P<0.001.

To examine whether such orientation defects are restricted to neuronal processes, we measured the angle forming between the long axis of the cellular body of the first 15 $GFP^+$ ENCCs located at the leading edge of the migratory front and the longitudinal axis of the gut (Fig. 3.14 A-D, A'-D'). By doing so, we were able to observe an increasing tendency in misoriented cells in Rac mutant samples (Rac3>Rac1>Rac1Rac3). Hence, angles formed by controls ENCCs were mainly distributed within 0° and 30°, while those found in Rac3 and Rac1 mutants mainly between 15° and 45° and those in Rac1/3 mutants between 60° and 90° (Fig. 3.14 E-H). However, the average size of angles was consistently and significantly increased only in Rac1 and Rac1Rac3 mutants, while Rac3 mutants samples showed a similar, almost significant, tendency (control 27.5±2.7°, Rac3 mutant 36.4±3.1° $P=0.07$, Rac1 mutant 43.9±3.5° $P<0.01$, Rac1Rac3 mutant 47.3±3.7° $P<0.01$. Cells measured≥60. N≥4. Fig. 3.14 I). These data suggest that both Rac1 and Rac3 might play a key role in orienting neuronal processes and migrating neural crest cells along the developing gut *in vivo*. Interestingly, these processes appear to involve a dose-dependent activity of Rac genes, since the consequent ablation of Rac3, Rac1 and both proteins produced an increasing worsening of the phenotype.

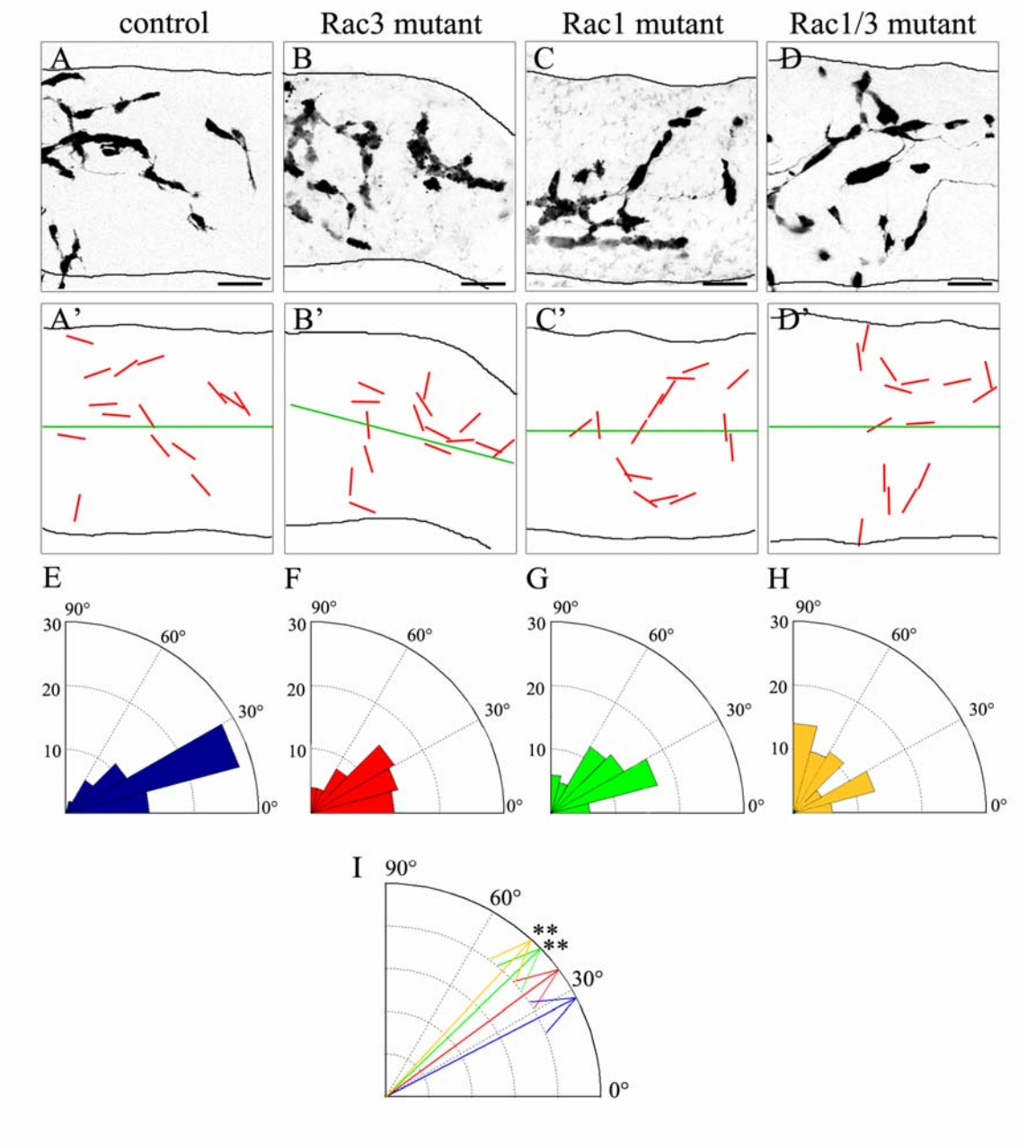


**Figure 3.14 Orientation of ENCCs is aberrant in Rac1 and Rac1/3 mutants *in vivo***

(**A-D**) Inverted confocal microscope images of migratory fronts in whole mount preparations of E11.0-11.5 guts immunolabelled with a GFP antibody. GFP fluorescence is highly detected within the cell bodies of ENCCs. Scale bars 100 µm. (**A'-D'**) Schematic representation of images shown in A-D, where the longest axis of the first 15 $GFP^+$ cell bodies was drawn as straight lines (red) and the longitudinal axis of the gut with a green line. Orientation of tracts was measured by quantifying the angle between straight lines and the main axis of the gut. (**E-H**) Rose plots showing the distribution of 60 representative angles. The area of each bin represents the number of cell bodies oriented in that direction (**E**) Control. (**F**) Rac3 mutant. (**G**) Rac1 mutant. (**H**) Rac1/3 mutant. (**I**) Rose plot showing the average angles of control (blue arrow), Rac3 mutant (red arrow), Rac1 mutant (green arrow) and Rac1/3 mutant (orange arrow) $GFP^+$ ENCC cell bodies. N≥60. ** indicates P<0.01.

It has been previously reported that undifferentiated ENCCs migrate in close contact with developing neuronal projections while colonising the gut, in such a way that caudal migrating cells might give directionality to axons or vice versa (Young *et al.*, 2002). Therefore, it is unclear whether the observed changes in orientation of axons and cells are due to the uncoupling of ENCC progression from the elongation of neuronal processes. To address this, we looked at E11.5 guts labeled for GFP and TuJ1 for the relationship between undifferentiated $TuJ1^{-}GFP^{+}$ ENCCs and $TuJ1^{+}GFP^{+}$ neuronal processes (Fig. 3.15). In control guts, tips of $TuJ1^{+}$ processes were always found in contact with undifferentiated ($GFP^{+}TuJ1^{-}$) ENCCs located at the migratory front (Fig. 3.15 A-A" arrows). Interestingly, in Rac1 and Rac1/3 mutant samples, $TuJ1^{+}$ processes still contacted undifferentiated ENCCs. However, these cells were often found delayed behind the front of migration and, instead, ectopic differentiating neurons were observed at the leading edge especially in Rac1/3 mutant preparations (Fig. 3.15 C-C", D-D" arrowheads). Rac3 mutants did not appear to have such a dramatic phenotype and relationship between ENCCs and neuronal processes appeared comparable to controls (Fig. 3.15 B-B").

We conclude that contact between neuronal fibres and migrating ENCCs has not been lost in Rac mutants and, therefore, it cannot account for the changes in orientation observed in neuronal processes and ENCCs in Rac1 and Rac1/3 mutant guts. However, we observed that undifferentiated ENCCs tended to be misplaced relative to the leading edge in Rac1 and Rac1/3 mutant samples, possibly because of delayed migration or altered orientation, thus suggesting that the correct positioning of ENCCs at the migratory front is important for the patterning of developing neuronal processes.

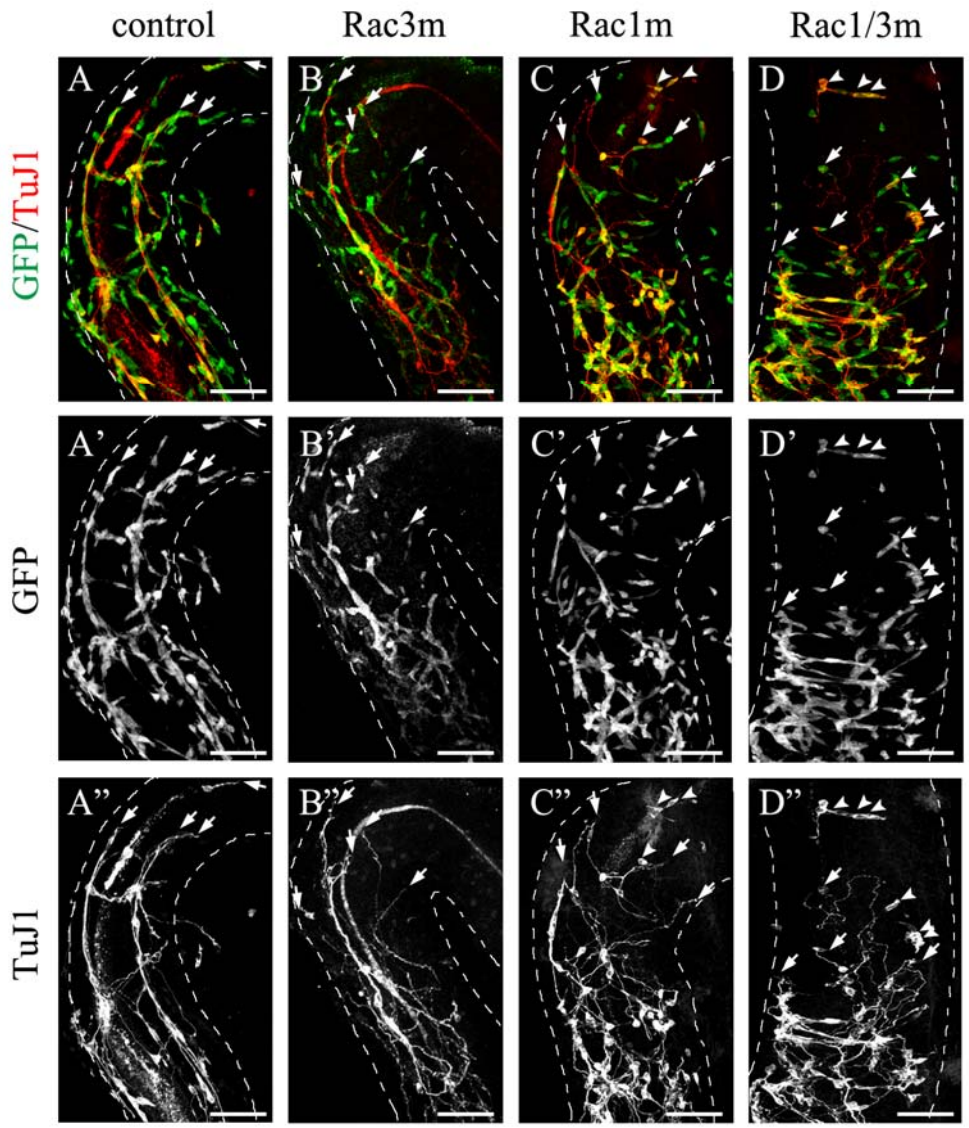


**Figure 3.15 Contact between migrating ENCCs and axons is maintained in Rac mutant guts**
(**A-D**) Fronts of migration in whole mount preparations of E11.0-11.5 guts immunolabelled with GFP and TuJ1 antibodies to identify ENCC cell bodies (GFP, green) and neuronal cells and processes (TuJ1, red). (**A'-D'**) Greyscale panels of the green (GFP) channels shown in A-D. (**A"-D"**) Greyscale panels of the red (TuJ1) channels shown in A-D. (**A**) In control preparations undifferentiated ENCCs ($GFP^{+}TuJ1^{-}$) have migrated the farthest and they are always in contact with caudal extending neuronal processes ($GFP^{+}TuJ1^{+}$) (arrows). (**C-D**) In Rac1 and Rac1/3 mutant guts, the contact between undifferentiated ENCCs and neuronal processes is maintained (arrows), but several $TuJ1^{+}$ cell bodies are found ectopically at the leading edge of the migratory front (arrowheads). (**B**) Rac3 mutant preparations did not show any obvious differences compared to controls. Scale bars 100 μm.

## 3.2 Discussion

The wiring of the ENS requires the directed migration of neural crest progenitors and enteric neurons to specific locations in the developing gut and the concomitant growth and guidance of axons towards their synaptic targets. Despite studies that implicate several members of the Rho family of GTPases in all these developmental processes within the central nervous system (Govek *et al.*, 2005), in the ENS, little is known about the role of this subfamily of GTPases in the maturation of the enteric neuronal network.

By using the conditional inactivation of the Rac1 gene within the neural crest population *in vivo*, we demonstrated that this small Rho GTPase controls migration of ENCCs, neuritogenesis and axon guidance of early born neurons, without affecting the proliferative and differentiative potential of enteric progenitors. In addition, by ablating the other member of the Rac family expressed in ENCCs, Rac3, we have been able to discover a redundant role for Rac1 and Rac3 in orientation of cell and neuronal processes along the developing gut.

### 3.2.1 Rac1 controls migration and adhesion of ENCCs

*In vivo*, Rac1 mutant ENCCs show a delay in colonisation of the gut mesenchyme from E11.5 and they appear to be increasingly retarded in their progression while approaching the caecum area. *In vitro*, Rac1-null ENCCs fail to invade the collagen matrix in response to GDNF in 3D assays and they show reduced migration on fibronectin substrate in 2D cultures. Furthermore, migrating Rac1 mutant ENCCs present an abnormal cytoskeletal organisation characterised by lack of lamellipodial protrusions and occurrence of several stress fibres. These data are corroborated by previous published studies, in which site specific mutagenesis of the RET putative binding sites results in decreased Rac1-GEF activity and impaired lamellipodia formation in a neuroectodermal tumor cell line *in vitro*, and in incomplete gut colonisation *in vivo* (Asai *et al.*, 2006; Fukuda *et al.*, 2002). Furthermore, our data are consistent with studies showing that pharmacological inhibition of Rac1 and Cdc42 in ENCCs leads to altered migration in gut organ cultures and impaired response to GDNF in collagen assays (Stewart *et al.*, 2007).

Together these findings strongly suggest that GDNF-mediated migration is regulated by Rac1 and that the GDNF-RET-Rac1 signalling pathway represents one of the guiding forces for gut colonisation by ENCCs.

Nevertheless, Rho GTPases can also be intracellular mediators of other signalling pathways implicated in cell migration. For example, it is evident that Rac1 deficiency leads to altered cell-cell and cell-ECM contacts, since, *in vitro*, mutant ENCCs tend to form aggregates and they do not spread and migrate efficiently onto fibronectin substrate. This phenotype is highly reminiscent of what has been reported for ENCCs in mice lacking β1-integrin (Breau *et al.*, 2006; Breau *et al.*, 2009). Indeed, in fibroblasts, coordinated engagement of cell adhesion receptors, such as β1-integrin and syndecan 4, is necessary for activation of Rac1 in response to fibronectin (Morgan *et al.*, 2007). Interestingly, syndecan-4/Rac1 signalling has also been implicated in control of directional migration both in fibroblasts *in vitro* (Bass *et al.*, 2007) and neural crest cells *in vivo* (Matthews *et al.*, 2008). Thus, it is likely that several signalling pathways, other than the GDNF-RET pathway, modulate Rac1 activity in cell adhesion and migration. In accordance, Rac1 mutant ENCCs are particularly delayed when approaching the caecum; an area expressing increasing gradients of ECM molecules capable of challenging the advance of ENCCs also in normal physiological conditions (Breau *et al.*, 2009; Druckenbrod & Epstein, 2005).

### 3.2.2 Rac GTPases and proliferation of ENS progenitors

A recent report from Fuchs et al. (2009) has also brought to attention that Rac1 ablation within the neural crest affects fundamental processes such as cell proliferation and, as a consequence, it might result in incomplete colonization of target tissues by NCCs (Fuchs *et al.*, 2009). In this study, proliferation of gut neural crest stem cells (gNCSCs), upon exposure to epidermal growth factor (EGF) *in vitro*, is shown to be dependent on Rac1 function. In contrast, our data and those of others (Stewart *et al.*, 2007) showed that Rac1 deficiency does not lead to any reduction in

percentage of the pool of ENCCs at the S phase. This apparent discrepancy may be explained by the different approaches undertaken by the two studies.

Under control conditions (i.e. in absence of any growth factor), Fuchs et al. found that approximately 4% of cells were proliferating, whereas in our study about 30% of all ENCCs were found to be mitotically active, in accordance with other published studies (Breau *et al.*, 2006; Stewart *et al.*, 2007). This suggests that it is likely that the two studies have considered different cell populations. In accordance with this hypothesis, different strategies were used to indentify ENS progenitors: in the case of Fuchs et al., progenitors were identified on the basis of p75 expression, while in our case they were identified by using the YFP lineage reporter. Our approach would include both undifferentiated ENCCs and committed progenitors actively proliferating, whereas that of Fuchs et al. mainly undifferentiated ENS progenitors, thus explaining the higher proportion of mitotically active cells recorded in our analysis, but also suggesting that the dependency on Rac1 of proliferating ENS progenitors might be restricted only to the small percentage of undifferentiated cells, likely to be overlooked in our study.

Different methods were also used to evaluate the percentages of proliferating ENS progenitors. In our study, we used a short pulse EdU incorporation to identify cells in S phase, whereas Fuchs et al. took advantage of an antibody against phospho-histone H3 (pH3), which is detected mainly during G2 to M transition of the cell cycle (Hendzel *et al.*, 1997). Therefore, it is possible that the discrepancy between the two studies relates to a differential requirement of Rho GTPases in distinct phases of the cell cycle.

Nevertheless, the dependency of ENS progenitor proliferation on Rho GTPases reported by Fuchs et al. might be related to the culturing conditions used. The authors clearly showed that this molecular mechanism was true on gNCSCs upon exposure to EGF *in vitro*. However the same dependency was not shown in explants cultured in absence of the growth factor, a condition similar to the experimental set up used in our study and that would mimic more closely the normal physiological conditions found in the developing gut *in vivo*.

### 3.2.3 Rac function is required for development of enteric neurons

Rac1 ablation does not only alter migration of ENCCs, but it also affects enteric neuronal development. We showed that within the Rac1 mutant ENCC population, the proportion of differentiating neurons is similar to controls, although their distribution *in vivo* appears to be defective. In fact, colonisation of the developing gut by enteric neurons and processes is delayed (due to the ENCC migratory delay) and in some areas, such as the stomach and the midgut, not as homogenous as seen in controls. These observations suggest that, similar to what we observed in migrating ENCCs, the adhesive properties of enteric neurons are impaired, resulting either in delayed neuronal migration or aberrant distribution of cell bodies and processes within the gut mesenchyme. By a systematic *in vitro* analysis, we identified specific defects in neurite growth and in branching of enteric neurons upon ablation of *Rac1*. Rac1 seems to have a key role in controlling the extension of enteric neurites, so that, when absent, the average length of primary and secondary branches is almost two-fold shorter than that of control counterparts. This appears to be due mainly to a dramatic reduction in number of long branches and concomitant increase in those with short neurites, leaving almost unaffected the proportion of branches of intermediate length. In addition, we have also shown that, upon ablation of Rac1, the branching of secondary and tertiary neurites is reduced, indicating a less complex neuronal morphology. Nevertheless, the polarity of Rac1 mutant enteric neurons seems not affected, in accordance with the involvement of other members of the Rho family of GTPases (i.e. Cdc42) in control of this cellular process (Etienne-Manneville, 2004).

### 3.2.4 Patterning of projections *in vivo*

Extension of neurites and branching are fundamental processes that underlie the projection of axons to their final targets, the development of the mature architecture of the enteric network and, ultimately, the coordinated function of the ENS. In accordance with our *in vitro* data, we found that early patterning of the developing ENS is aberrant in Rac1 mutant embryos *in vivo*. While ENCCs progress through the gut mesenchyme, neuronal processes of neurons differentiating

behind the migratory front extend caudally and their tips are always found in close contact with migrating undifferentiated ENCCs at the leading edge (Hao & Young, 2009; Young *et al.*, 2002). Notably, in our study, the majority of Rac1 mutant processes found at the migratory front were not oriented caudally anymore, instead they had a clear tendency to project circumferentially, indicating that not only axon growth but also axon guidance and positioning might be dependent on Rac1 function. Similarly, we found that cell bodies of Rac1 mutant ENCCs at the leading edge were misoriented compared to the direction of migration, thus suggesting that Rac1 might be involved in control of motility and directionality of migrating ENCCs, as shown, for example, in cranial neural crest cells (Theveneau *et al.*, 2010). It has been suggested that migrating ENCCs might provide some guidance for caudal projecting axons (Young *et al.*, 2002). However, this hypothesis is still lacking substantial experimental evidence. In precerebellar neurons, inhibition of different small Rho GTPases uncouples neuron migration from axon extension (Causeret *et al.*, 2004). However, in the developing ENS, pharmacological inhibition of Rac1/Cdc42 or Rho effectors ROCKI/II in explants of embryonic guts *in vitro* has been unable to find a similar mechanism, since ENCC migration and axon extension could not be uncoupled and they appeared to be controlled by a common set of Rho GTPases (Stewart *et al.*, 2007). Similarly, in our study, undifferentiated ENCCs did not lose their contacts with neuronal processes. However, in Rac1 mutant guts, several single ENCCs, often differentiating into neurons, were found beyond the migratory front of undifferentiated ENCCs. Therefore, it is possible that ENCCs represent the primary source of guidance for neuronal processes and, if misplaced behind the farthest differentiating neurons because of delayed migration, they prevent the axons from extending caudally. Alternatively, it is also possible that, *in vivo*, neuronal processes are the guidance cue to migrating ENCCs, and because of defects in neurite extension and response to GDNF (as shown by our data in 3D cultures), they are unable to extend caudally. Nevertheless, defects in patterning of neuronal tracts are also observed in Rac3 mutants, which do not show any obvious delay in colonisation of the gut by ENCCs and no significant misplacement of cells at the migratory front, thus suggesting the existence of different intracellular mechanisms controlling migration of ENCCs and axon extension.

### 3.2.5 Redundancy and specific roles of Rac proteins in ENS development

We showed that along with Rac1, the other member of the Rac GTPases, Rac3, is expressed in the developing ENS. However, the role of Rac3 in all the developmental processes analysed appears to be minor. Although published reports have suggested an opposing role of Rac3 and Rac1 in cell adhesion (Hajdo-Milasinovic *et al.*, 2007; Hajdo-Milasinovic *et al.*, 2009), ablation of *Rac3* does not lead to any obvious defect in ENCC migration both *in vivo* and *in vitro*, as expected by the absence of any detectable anatomical and morphological phenotype in Rac3 null mice (Corbetta *et al.*, 2005). Analogously, simultaneous ablation of Rac1 and Rac3 does not worsen the delay in gut colonisation already reported in Rac1 mutants, confirming no discernible role for Rac3 in ENCC migration.

It has been suggested that Rac3 might play a role in late stages of neuronal development, given its peak of expression in postmitotic neurons at developmental stages involving intense branching and synaptogenesis within the CNS (Albertinazzi *et al.*, 1998; Bolis *et al.*, 2003). Interestingly, the combined Rac1 and Rac3 deficiency resulted in a small but significant increase in the proportion of neurons within the ENCC population *in vitro*. This change appears to reflect an increase in the presence of ENCCs differentiating into neurons at the migratory front in double mutants compared to Rac1 single mutants. In addition, we found that Rac3 ablation in enteric neurons had a milder effect compared to Rac1 ablation on extension of neurites. Length of Rac3 mutant primary and secondary neurites was generally reduced relative to controls, but not significantly, indicating that the Rac1 function preserved in these mutants is able to at least partially compensate for the lack of Rac3 during neuritogenesis. Furthermore, it appears that regulation of neurite growth by Rac3 is mainly redundant to that of Rac1, since combined ablation of both proteins does not increase the growth defects already observed in Rac1 mutants. Additionally, no specific effects of Rac3 ablation were observed on branching and polarity of neurons. Therefore, the function of this small Rac GTPase appears dispensable in development of enteric neurons *in vitro*.

Nevertheless, we found that, *in vivo,* patterning of neuronal tracts is clearly affected to a similar extent in Rac3 and Rac1 mutants and it becomes even more defective when both genes are ablated. It has been previously suggested in *Drosophila* that axon growth, guidance and branching require an increasing amount of combined Rac GTPase activity *in vivo* (Ng *et al.*, 2002). In accordance with this hypothesis, our data show that Rac1 function is sufficient to control aspects of neuritogenesis such as growth and branching, whereas the coordinated function of both Rac1 and Rac3 is required for axon patterning of enteric neurons (Fig. 3.16).

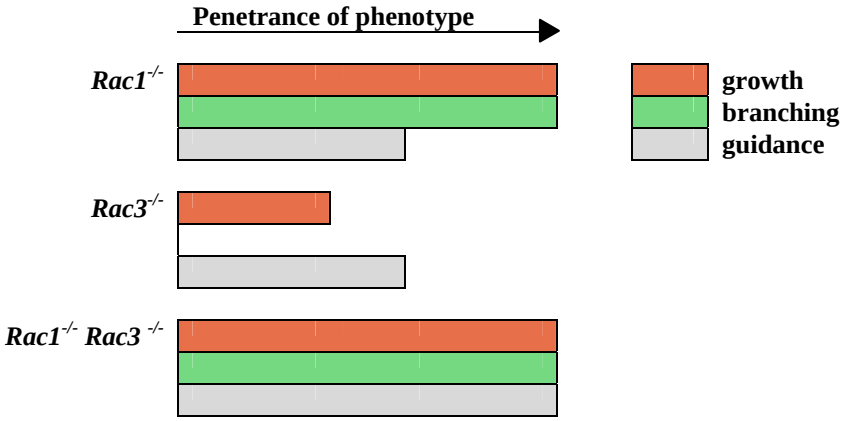


**Figure 3.16 Effects of Rac mutations on maturation of enteric neurons**
Growth, branching and guidance of enteric neurons have a differential requirement for Rac proteins function, which might explain the different penetrance of phenotypes observed in Rac mutants. Growth and branching of enteric neurons require Rac1, whereas axon guidance is co-ordinately controlled by Rac1 and Rac3 function.

Our results demonstrate the requirement for Rac GTPases in migration of ENCCs and maturation of enteric neurons and they provide evidence for the existence of Rac1/Rac3-mediated intracellular pathways underlying wiring of the ENS. On the other hand, the signalling pathways involved in activation of these small GTPases in all the developmental processes described are still largely unknown. Intriguingly, the specific defects found in Rac mutants in patterning of neuronal tracts and in orientation of cell bodies along the axis of the gut are suggestive of defects in control of cell polarity. Members of the PCP pathways have been recently shown to play a major role in control of directional migration and axon guidance (Carmona-Fontaine *et al.*, 2008; Vivancos *et al.*, 2009), it is therefore attractive to speculate that a similar molecular mechanism might also underlie the genetic hardwiring of the ENS.

# Chapter 4

# Novel role for Fzd3 and Celsr3 in enteric neuronal network formation

## 4.1 Results

### 4.1.1 *Fzd3* and *Celsr3* are expressed within the developing ENS

To establish a role for members of the Wnt signalling pathway in enteric network formation, we investigated the pattern of expression of candidate molecules using mRNA *in situ* hybridization (ISH) on embryonic gut tissue. Initially, we examined the expression pattern of transmembrane proteins that are thought to mediate canonical and non-canonical Wnt signalling using ISH on transverse cryosections of E13.5 wild type embryos. This group of genes included the Frizzled (Fzd) receptors, EGF LAG seven-pass G-type (Celsr) receptors and the atypical tyrosine kinase Ryk (Fig. 4.1). We used as a control for localization and identification of ENCCs a probe for the tyrosine receptor RET, which is expressed at this stage by all ENCCs and newly differentiated neurons (Pachnis *et al.*, 1993; Young *et al.*, 1999) (Fig. 4.1 I). We found that, within the Fzd receptor members, the expression of *Fzd3* was specifically restricted to the ENCC population (Fig. 4.1 G), whereas *Fzd2*, *Fzd4*, *Fzd6* and *Fzd8* were expressed broadly in the outer mesodermal layer (Fig. 4.1 A-C, E) and *Fzd7* did not show any expression (Fig. 4.1 D). Interestingly, we also detected *Celsr3* expression in a pattern similar to that of *Fzd3* (Fig. 4.1 H), whereas Ryk probe failed to produce any distinct signal within the developing gut (Fig. 4.1 F). Given the expression of *Fzd3* and *Celsr3* in the gut of E13.5 embryos, we performed a time course ISH analysis for both genes on cryosections of E12.5, E14.5 and E15.5 wild type embryos (Fig. 4-1 J-R). We were able to show that Fzd3 and Celsr3 are expressed in similar pattern within the ENCC population throughout ENS development (Fig. 4.1 J-K, M-N, P-Q), although *Fzd3* signal at E15.5 was weaker than earlier stages (Fig. 4.1 P). At all time points investigated, when adjacent serial sections were compared, the number of cells positive for Fzd3 and Celsr3 appeared smaller relative to those expressing RET, suggesting that only a subgroup of ENCCs express one or both genes (Fig. 4.1 J-L, M-O, P-R).

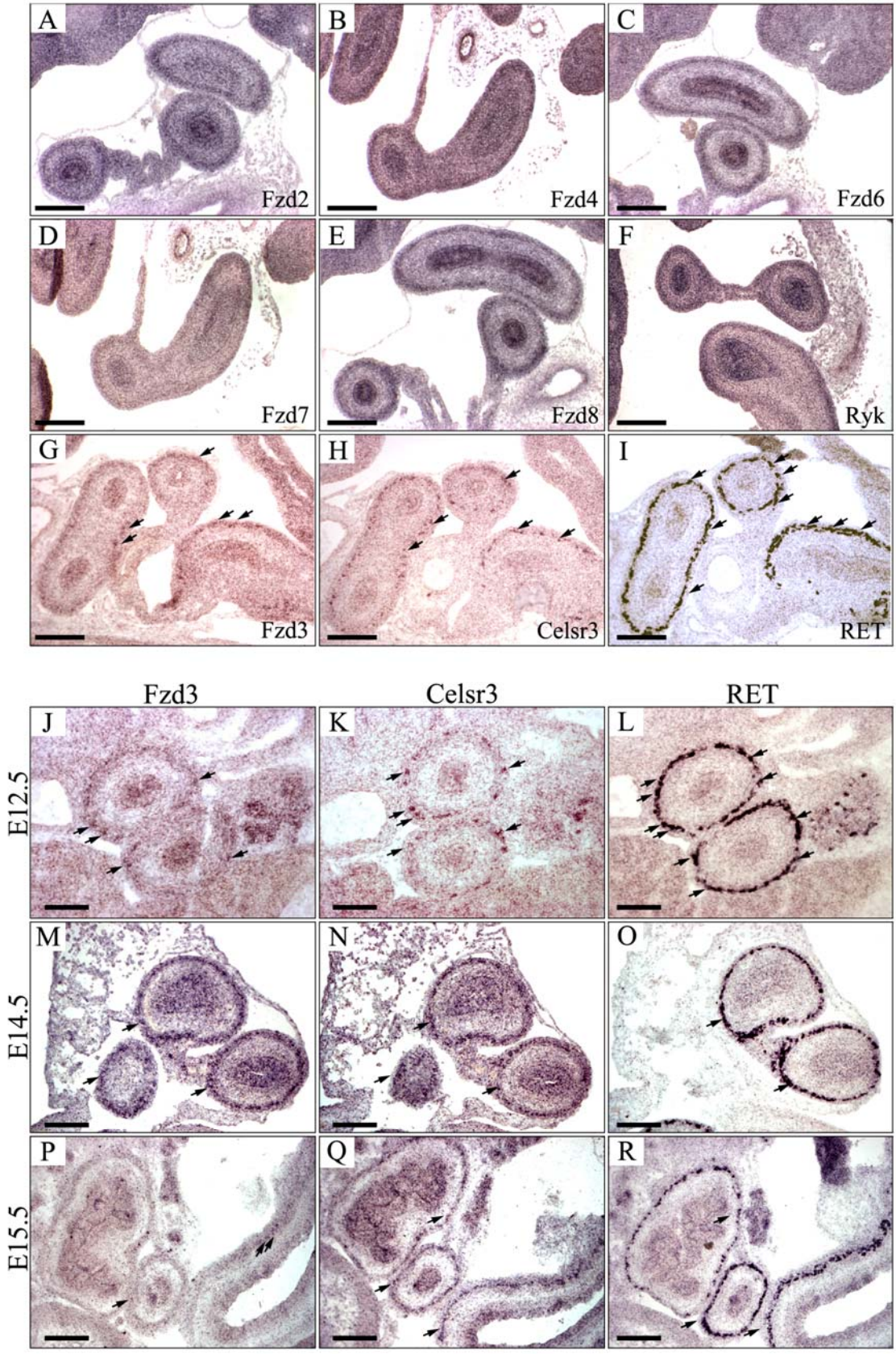


**Figure 4.1 (legend next page)**

**Figure 4.1 *Fzd3* and *Celsr3* are expressed in the developing ENS**

(**A-H**) Expression of Fzd receptors, Celsr3 and Ryk (gene symbol indicated in the bottom right corners) was investigated by mRNA *in situ* hybridisation (ISH) on transversal sections from E13.5 wild type embryos. Ret probe was used as a control to localise ENCCs at this stage (**I**, arrows). *Fzd3* (**G**) and *Celsr3* (**H**) are the only genes to show a pattern of expression compatible to the presence of ENCCs within the gut mesenchyme (arrows). Scale bars 200 μm.

(**J-R**) Time course ISH analysis of *Fzd3*, *Celsr3* and *Ret* expression on sequential transversal sections of E12.5 (**J-L**), E14.5 (**M-O**) and E15.5 (**P-R**) wild type embryos. *Fzd3* positive cells are found at all stages investigated (**J**, **M**, **P** arrows); however, in reduced number and intensity at E15.5 (**P**). Celsr3 reactivity was detected within ENCCs at all stages investigated (**K**, **N**, **Q**). By comparison with expression of the *Ret* probe (**L**, **O**, **R** arrows), both *Fzd3* and *Celsr3* appear to be expressed only in a subset of $Ret^+$ ENCCs. Scale bars 100 μm.

Since detection of probes was generally difficult (leading to low signals or high background even after several troubleshooting steps) and probes for some of the members of Fzd and Celsr families were not available to us, we decided to search for the expression pattern of the genes we were interested in publicly available databases. Genepaint.org and Eurexpress.org offer an atlas of gene expression at E14.5 investigated by ISH on sagittal sections of whole mount embryos. We searched in these databases for pattern of expression of the entire range of Frizzled receptors, Celsr proteins and Ryk and Ror2 receptors (Fig. 4.2). Consistent with our results, this independent approach confirmed that only Fzd3 and Celsr3 are expressed in an ENS-restricted pattern (Fig. 4.2 C, L).

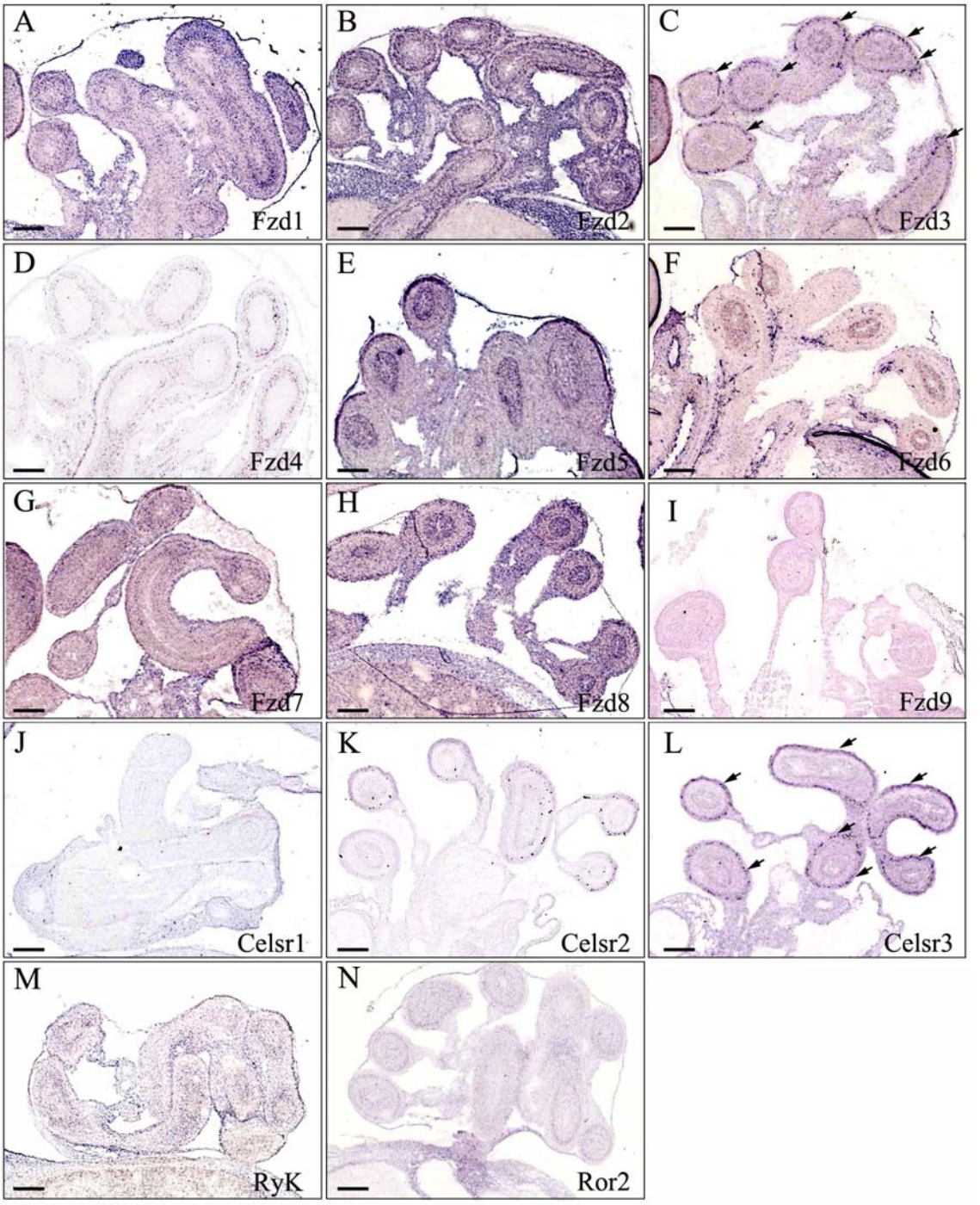


**Figure 4.2 Patterns of expression of Fzd, Celsr, Ryk, Ror genes in E14.5 guts retrieved from digital atlas of gene expression in the mouse**

Pattern of expression of Wnt-signalling genes indicated by symbols in the bottom right corners is shown in sagittal sections of E14.5 wild type embryos (only gut loops shown). Images are taken from the transcriptome atlas databases www.genepaint.org (**E**, **F**, **M**) and www.eurexpress.org (**A-D**, **G-L**, **N**). *Fzd3* (C) and *Celsr3* (L) are the only genes expressed in a pattern compatible with ENCCs at this developmental age (arrows). Scale bars 200 μm.

Lastly, we performed analysis of mRNA expression by Real Time PCR on ENCCs FACS-purified from double transgenic *Wnt1Cre;R26ReYFP* embryos at E12.5. These experiments established that Fzd3 and Celsr3 transcripts are enriched in the ENCC population (Fig. 4.3). Unfortunately, we were unable to investigate cellular expression and subcellular localization of Fzd3 and Celsr3 proteins due to a lack of reliable antibodies for immunofluorescence analysis.

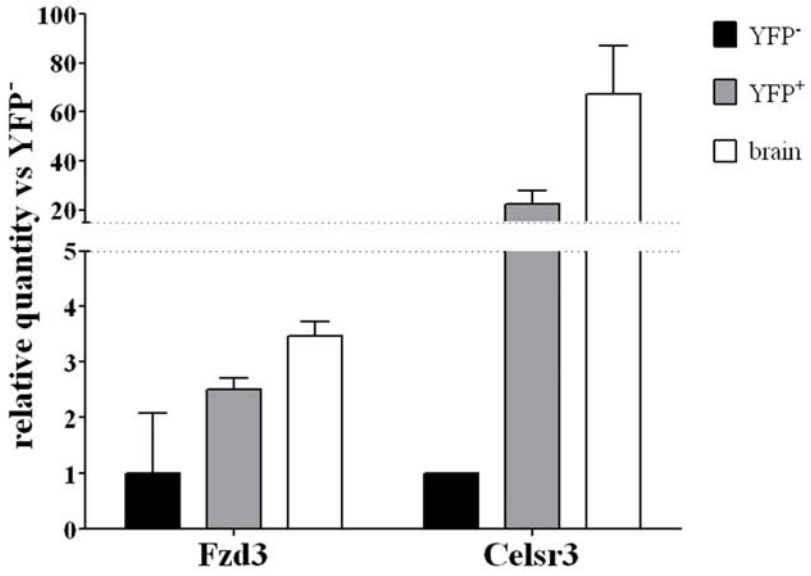


**Figure 4.3 *Fzd3* and *Celsr3* mRNA expression in ENCCs is confirmed by Real Time PCR**
Analysis of gene expression by Real Time PCR was carried out on cDNAs from FACS purified ENCCs ($YFP^+$) and non-ectodermal gut cells ($YFP^-$) derived from E12.5 dissociated guts of *Wnt1Cre;R26ReYFP* embryos. cDNA from E14.5 brain was used as a positive control. The relative amount of mRNA transcript for Fzd3 and Celsr3 is enriched in $YFP^+$ ENCCs relative to $YFP^-$ gut cells. Data is shown as the mean of triplicate values for each sample. Error bars, standard deviation of the mean.

### 4.1.2 Colonisation of the gut by enteric progenitors and neurons occurs normally in Fzd3 and Celsr3 mutant mice

Gene inactivation of *Fzd3* and *Celsr3* has been previously reported (Tissir *et al.*, 2005; Wang *et al.*, 2002). Fzd3KO and Celsr3KO mice have been generated by targeted deletion of exons 1-2 of the Fzd3 gene (*Fzd3*$^{-}$) and exons 19-27 of the Celsr3 gene (*Celsr3*$^{-}$). *Fzd3*$^{-/-}$ and *Celsr3*$^{-/-}$ mice die shortly after birth due to a failure in central control of ventilation. These animals show an almost indistinguishable phenotype, characterised by defects in the development of commissural and longitudinal neural tracts within the forebrain, leaving other aspects of the CNS development mostly unaffected.

Given the expression of *Fzd3* and *Celsr3* in ENCCs, we addressed their possible role in ENS development by studying both mutant mouse lines. In order to be able to trace all neural crest cells and their derivatives (including the ENS), we introduced into the Fzd3 and Celsr3 mutant background the *Wnt1Cre* transgene (Danielian *et al.*, 1998) and the *R26ReYFP* reporter (Srinivas *et al.*, 2001). Wnt1 regulatory regions drive Cre expression in the dorsal neural tube and early emigrating NCCs (Danielian *et al.*, 1998; Echelard *et al.*, 1994), leading to recombination of the *R26ReYFP* locus and consequent permanent expression of YFP in all NCCs and their derivatives.

Also, since heterozygous (*Fzd3*$^{+/-}$ and *Celsr3*$^{+/-}$) mice are indistinguishable from their wild type (*Fzd3*$^{+/+}$ and *Celsr3*$^{+/+}$) littermates in viability, growth, appearance, fertility and the gross anatomy and structure of central and enteric nervous system, we will refer to both genotypes as controls.

To characterise the effect of *Fzd3* and *Celsr3* deletions on ENS development and network formation, we analysed various aspects of ENS development. Initially we investigated the ability of ENCCs to migrate and colonise the developing gut of mutant embryos in the appropriate time frame. We assessed the extent of migration of YFP$^{+}$ ENCCs in whole mount preparations of E12.5 guts by immunolabeling the samples with an anti-GFP antibody (Fig. 4.4). In control embryos at E12.5, migrating ENCCs have colonised most of the developing gut,

including the midgut, caecum and proximal hindgut (Fig. 4.4 A). In mutant samples, ENCCs were found in similar positions along the gut axis and they had colonised all gut regions as observed in controls (Fig. 4.4 B-C), indicating that inactivation of *Fzd3* or *Celsr3* has little or no effect on ENCC migration.

We subsequently looked specifically into neuronal development. Migrating ENCCs are a heterogeneous population of cells, in which neurons positive for the neuron-specific β-tubulin can be found up to the farthest colonised areas of the gut already as early as E10.5, and they increase in number and organization as development proceeds. Whole mount preparations of E12.5 guts were immunolabelled with a monoclonal antibody for β-tubulin (TuJ1) in order to evaluate the extent of neuronal differentiation and the features of the forming neuronal network. In control guts, neurons have fully colonised all gut regions all the way to the front of migrating ENCCs in the hindgut (Fig. 4.4 D). Similar to controls, Fzd3 mutant samples were $TuJ1^+$ immunoreactive within the stomach, along the midgut and in the proximal hindgut (Fig. 4.4 E). A similar distribution of enteric neurons was found in Celsr3-deficient gut preparations (Fig. 4.4 F).

These data suggest that migration and neuronal specification of ENCCs is not affected by the ablation of either Fzd3 or Celsr3 gene *in vivo*.

**Figure 4.4 Gut colonisation by ENCCs and neurons is not affected by Fzd3 and Celsr3 deficiency (figure next page)**

Inverted confocal images of whole mount preparations of E12.5 guts immunolabeled for GFP (**A-C**) to identify $YFP^+$ ENCCs and the neuronal marker TuJ1 (**D-F**) to identify enteric neurons. The extent of migration of ENCCs in *Fzd3*$^{-/-}$ (B) and *Celsr3*$^{-/-}$ (C) guts is comparable to that of ENCCs in control samples (A), as indicated by the most distal cells invading the hindgut (A-C, arrow). Similarly, colonisation of the gut by $TuJ1^+$ neurons is indistinguishable between control (D) and mutant (E-F) preparations. Arrows in D-F indicate the farthermost differentiating neuron. Ca, caecum; hg, hindgut; mg, midgut; st, stomach. Scale bars 500 μm.

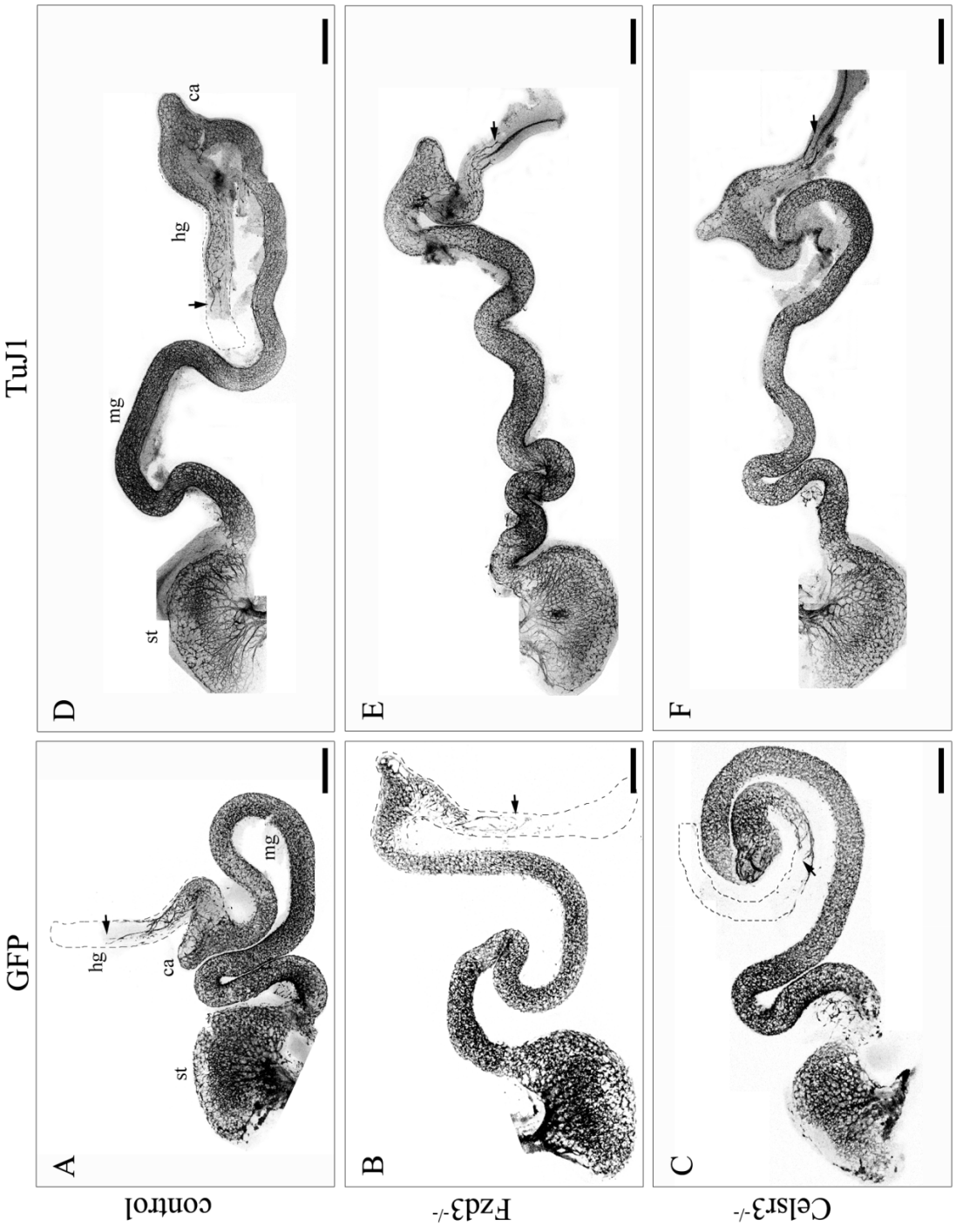


**Figure 4.4 (legend previous page)**

### 4.1.3 Ablation of Fzd3 or Celsr3 proteins affects specifically organization and morphology of neuronal tracts

Although neuronal colonisation in the gut of Fzd3 and Celsr3 mutants appeared normal, we decided to investigate whether we could observe subtle changes in the morphology and organization of the immature neuronal plexus. For this, E12.5 midgut regions from whole mount preparations immunolabelled for TuJ1 were examined at higher magnification by confocal microscopy (Fig. 4.5). In control guts, we could observe prominent longitudinal TuJ1$^{+}$ thick fibres running through proximal, central and distal midgut, and evenly distributed around the circumference of the intestinal tube (Fig. 4.5 A-C). The thickness of these tracts indicated that several single neuronal processes fasciculated in forming such structures. Nevertheless, individual fibres could still be observed in the space between bundles. This specific neuronal patterning was consistently observed in control preparations between E11.5 and E12.5. Strikingly, when we analysed mutant preparations this stereotypical pattern of neuronal tracts was mostly absent. In Fzd3-null guts the thick longitudinal neuronal tracts were greatly reduced and in some cases totally absent. However, individual neuronal processes and cell bodies were still present throughout the area of the midgut (Fig. 4.5 D-F). Similarly, Celsr3 mutant preparations showed a highly disorganised network of neuronal processes, with almost complete absence of neuronal bundles projecting longitudinally along the entire length of the midgut (Fig. 4.5 G-I). These observations suggest a similar role for Fzd3 and Celsr3 in patterning and organisation of enteric neuronal processes.

To examine the combined effect of Fzd3 and Celsr3 mutations, we also generated *Fzd3*$^{-/-}$*;Celsr3*$^{-/-}$ animals. In E12.5 guts of double mutant animals, longitudinal neuronal tracts were dramatically reduced and no other major defect was identified by using TuJ1 immunolabelling (Fig. 4.5 J-L). This indicates that Fzd3 and Celsr3 mutations do not have an additive effect and suggests that they are components of the same pathway. Therefore, we decided to focus our subsequent analyses on single Fzd3 and Celsr3 mutant animals.

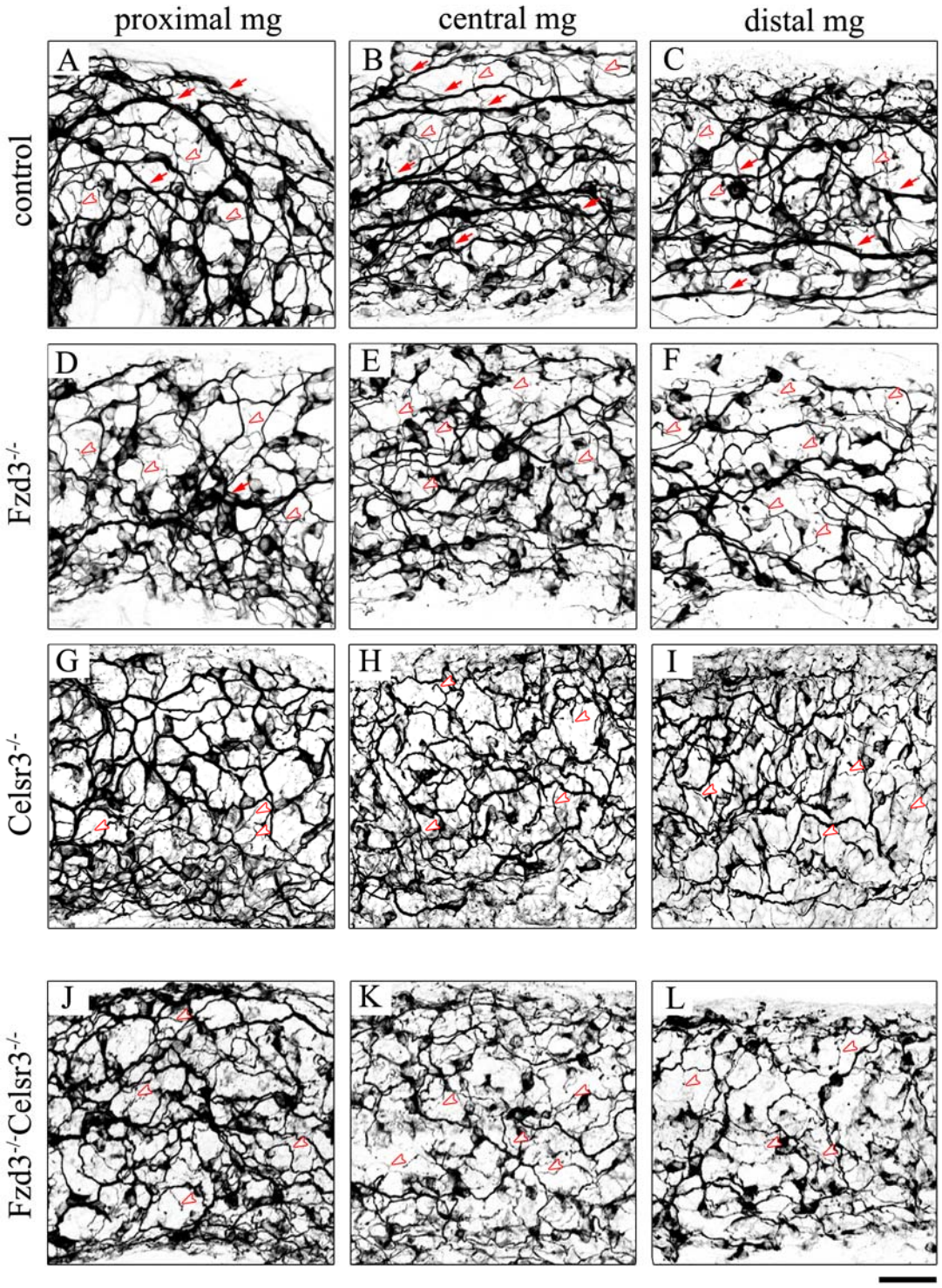


**Figure 4.5 (legend next page)**

**Figure 4.5 Organisation of the forming neuronal network is altered in Fzd3 and Celsr3 mutant guts**

Inverted confocal images of the proximal (**A**, **D**, **G**, **J**), mid (**B**, **E**, **H**, **K**) and distal (**C**, **F**, **I**, **L**) regions of E12.5 midgut immunolabelled for the neuronal marker TuJ1. Control samples (**A-C**) show an intricate network of neuronal processes characterised by obvious longitudinal tracts (arrows) and individual neurites (empty arrowheads). In the corresponding regions of *Fzd3* (**D-F**) and *Celsr3* (**G-I**) mutants the longitudinal tracts are almost completely absent and several single neurites and their terminal endings can be observed (empty arrowheads). Similar changes are also observed in the midgut of double mutant embryos (**J-L**). Mg, midgut. Scale bar 50 μm.

The failure to observe longitudinal tracts in mutant guts may be explained by two hypotheses. One of these is that longitudinal neuronal processes are present but fail to fasciculate and form prominent bundles. Alternatively, there could be a reduction of individual longitudinal processes, which is reflected secondarily in the absence of longitudinal fibres. To address these issues, we applied the lipophilic dye 1,1'-dioctadecyl-3,3,3',3'-tetramethylindocarbocyanine (DiI) on to the midgut region of fixed E12.5 gut preparations (Fig. 4.6). DiI diffuses readily through aldehyde-fixed plasma membranes and marks axons that happen to project at or go through a given labelling site and their cell bodies. In control guts, individual axonal processes could be observed projecting mainly longitudinally and some of them also for some distance within the gut. Additionally, all cell bodies were found exclusively oral to the labelling site, whereas growth cones were localised mainly on the opposite side (Fig. 4.6 A-B). This confirmed the presence in controls of several longitudinal individual processes and that the majority of enteric neurons at this stage projected caudally (aborally), as reported previously (Young *et al.*, 2002). Conversely, DiI labelling in *Fzd3*$^{-/-}$ or *Celsr3*$^{-/-}$ guts failed to produce a similar pattern. In all preparations the area of diffusion of the dye was reduced in comparison to controls. In particular, we found that DiI diffused mainly along short projections around the labelling site and along very few long longitudinal processes both rostrally and caudally (Fig. 4.6 C-D, E-F). Moreover, when we looked at ENCC cell bodies, we could also record in one *Celsr3*$^{-/-}$ sample a neuronal process terminating rostrally to the labelling site, indicating an oral projecting neuron (Fig. 4.6 E).

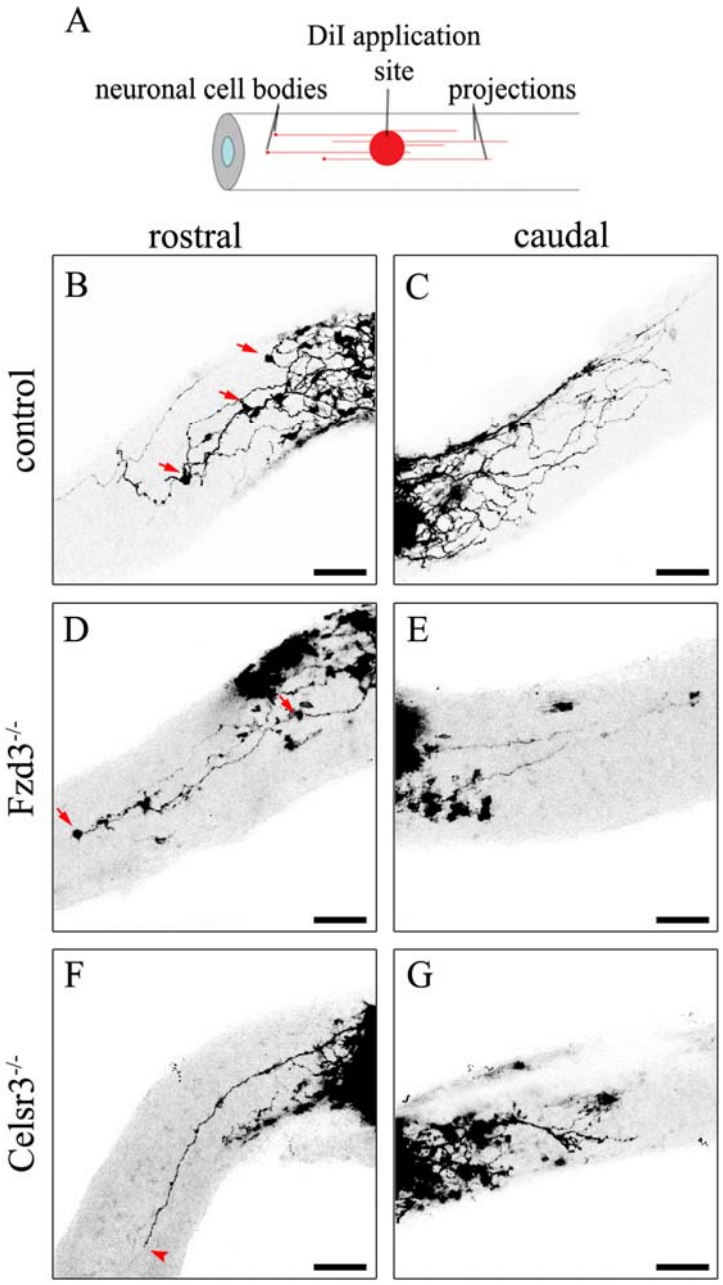


**Figure 4.6 Longitudinal projections are reduced in the gut of *Fzd3*$^{-/-}$ and *Celsr3*$^{-/-}$ mutants**

DiI retrograde labelling of enteric neurons and their processes in E12.5 gut preparations. (**A)** Schematic of the experimental protocol. DiI is applied in the midgut of fixed gut preparations and it diffuses and labels neurons whose processes happen to cross the point of application. (**B-G**) Inverted confocal images of regions rostral (B, D, F) and caudal (C, E, G) to the DiI labelling site. (B-C) In control samples many longitudinal projections are dyed. Cell bodies are found mostly rostral to the DiI labelling site (**B**, red arrows), indicating that at this stage the majority of neurons are projecting caudally. (**D-G)** In mutant preparations DiI diffusion reveals a substantial reduction in the overall number of stained projections and cell bodies. The number of longitudinally running axons is greatly reduced compared to controls, and, in one mutant preparation, an oral projecting neurons has also been detected (F, arrowhead). N≥3. Scale bars 100 μm.

These observations indicate that, in mutant guts, individual longitudinal neuronal processes are reduced in number and those that are remaining seem to have the same length, but, possibly, an aberrant orientation.

These data show that ablation of *Fzd3* and *Celsr3* leads to changes in the organisation of longitudinal processes and suggest this phenotype is due to altered directionality of enteric neuronal processes.

### 4.1.4 No defects in cell proliferation and neuronal differentiation of *Fzd3*$^{-/-}$ and *Celsr3*$^{-/-}$ ENCCs

It is possible that the absence of longitudinal neuronal processes is the result of neuronal loss in *Fzd3*$^{-/-}$ and *Celsr3*$^{-/-}$ animals. To examine this possibility, we first analysed cell proliferation of enteric progenitors by incorporation of 5-ethynyl-2´-deoxyuridine (EdU) in dissociated E12.5 guts *in vitro*. For this, ENCCs were identified by GFP fluorescence and proliferating cells were counted as a proportion of the GFP$^{+}$ population labelled by EdU (Fig. 4.7 A-D). We found that the percentage of EdU$^{+}$ cells in mutant ENCCs was comparable to that found in controls (Control 28.4±5.1%, *Fzd3*$^{-/-}$ 27.4 ±4.5%, *Celsr3*$^{-/-}$ 28.8 ±3.5%. Total cells counted ≥1900 from at least 4 independent guts per genotype. Fig. 4.7 D), indicating that a change in the proportion of proliferating progenitors could not be responsible for the severe reduction of axonal tracts in the gut of mutant embryos.

We then looked into neuronal specification of ENCCs by counting TuJ1$^{+}$GFP$^{+}$ cells within dissociated guts from E12.5 embryos (Fig. 4.7 E-H). Interestingly, the proportion of neurons in *Celsr3*$^{-/-}$ guts did not differ significantly from that recorded in controls, while in cultures from *Fzd3*$^{-/-}$ guts there was a modest significant increase (Control 25.4±4.7%, *Celsr3*$^{-/-}$ 23.2±4.3%, *Fzd3*$^{-/-}$ 32.6±2.2%. $P<0.05$. Cells counted ≥2000. N≥4. Fig. 4.7 H). In E12.5 guts, some of the first detectable neurons are the neuronal nitric oxide synthase (nNOS) producing neurons (Baetge & Gershon, 1989; Young *et al.*, 2002). To examine whether mutant guts have changes in the subtype specification of enteric neurons, we examined the proportion of

TuJ1$^{+}$GFP$^{+}$ ENCCs co-expressing the nitrinergic marker nNOS (Fig. 4.7 I-L). We could not find any significant difference in the number of nNOS neurons between controls and Fzd3 and Celsr3 mutants (controls 14.5±5.8%, *Fzd3*$^{-/-}$ 13.7±6.9%, *Celsr3*$^{-/-}$ 15.3±0.7%. Cells counted≥600, N≥3. Fig. 4.7 L).

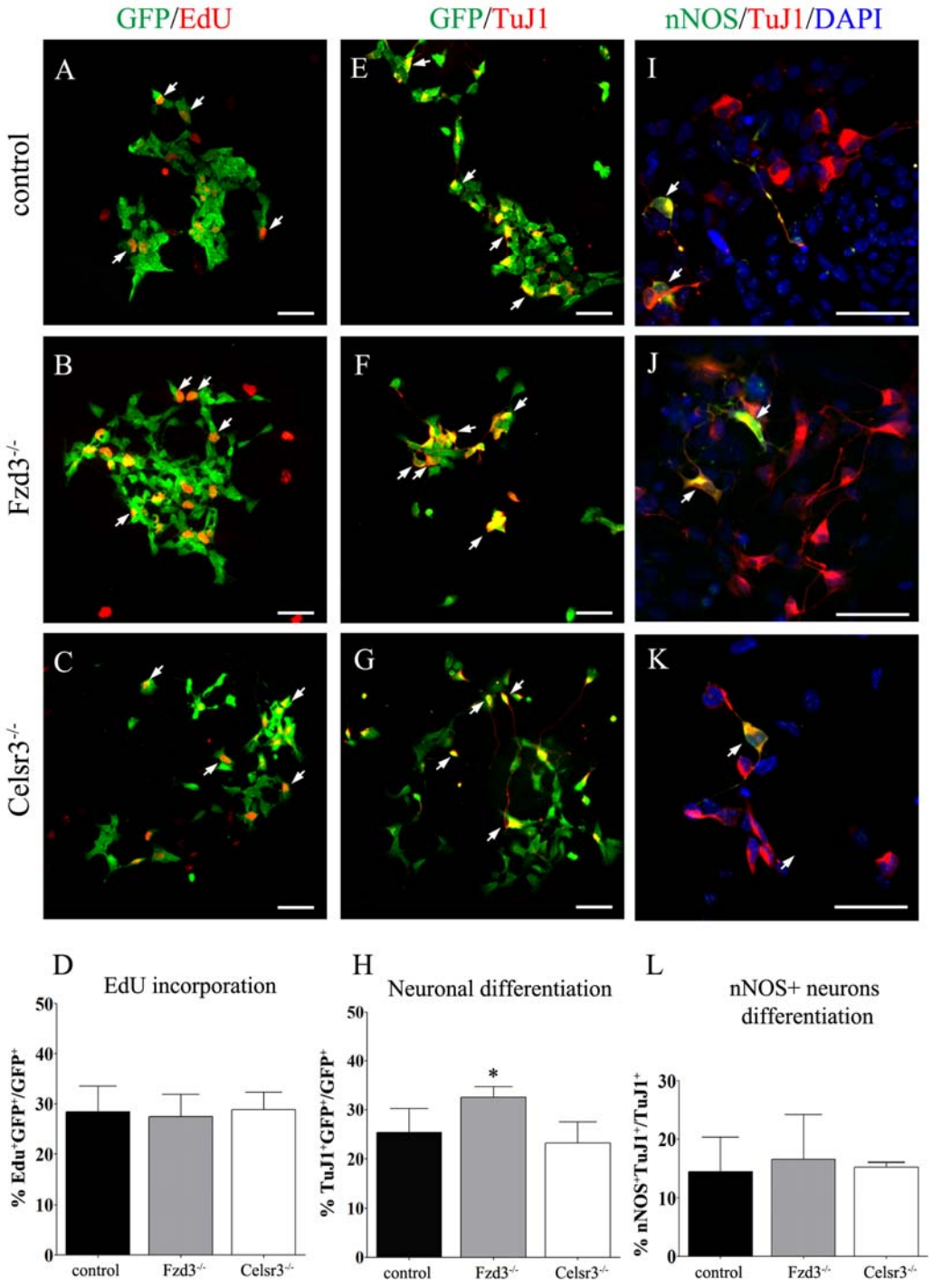


**Figure 4.7 (legend next page)**

**Figure 4.7 Proliferation and neuronal differentiation of ENCCs is normal in the absence of Fzd3 and Celsr3**

(**A-C**) Analysis of cell proliferation by EdU incorporation *in vitro*. E12.5 guts were dissociated and cultured for 4 hrs *in vitro* in presence of EdU and then processed for EdU and GFP reactivity. Proliferating ENCCs were identified by double fluorescence for GFP (green) and EdU (red) (arrows). Scale bars 50 μm. (**D**) Quantification of proliferating cells in the $GFP^+$ ENCC population. Cells counted≥1900. N≥4. Error bars, SEM.

(**E-G**) Analysis of neuronal differentiation on short term cultures of dissociated E12.5 guts *in vitro*. Cultures were processed for GFP (green) and the neuronal marker TuJ1 (red) staining and differentiating neurons were identified by double GFP and TuJ1 fluorescence (arrows). Scale bars 50 μm. (**H**) Quantification of $TuJ1^+$ neurons/neuronal progenitors in the $GFP^+$ ENCC population. Cells counted≥2000. N≥4. * indicates $P<0.05$. Error bars, SEM.

(**I-K**) Analysis of specification of $NOS^+$ neurons in short term cultures of dissociated E12.5 guts *in vitro*. Cultures were processed for TuJ1 (red) and the nitrinergic marker NOS (green) immunostaining. Nuclei were counterstained with DAPI (blue). $NOS^+$ neurons were identified by double immunoreactivity for TuJ1 and NOS (arrows). Scale bars 50 μm. (**L**) Quantification of proportion of $NOS^+$ neurons within the entire $TuJ1^+$ enteric neuronal population. Cells counted≥600. N≥3. Error bars, SEM.

Therefore, our data show that *Fzd3* and *Celsr3* mutations do not prevent proliferation or neuronal differentiation of ENS progenitors.

### 4.1.5 Neuritogenesis is unaffected in mutant neurons *in vitro*

The dramatic decrease in neuronal tracts *in vivo* could also be explained by a defect in several aspects of neurite development of enteric neurons, such as generation, growth, organization and maintenance of neurites. To test this hypothesis we cultured primary enteric neurons from dissociated guts at E12.5 and investigated their survival and morphology after 4 days in culture (Fig. 4.8 A-I). Mutant neurons (*Fzd3*$^{-/-}$ or *Celsr3*$^{-/-}$) were found in similar proportions as controls in culture, indicating similar neuronal survival. We then assessed the extent of neuritogenesis by measuring for each neuron the length of the longest primary and secondary neurite and the sum of lengths of all neurites. No differences were recorded between control and Fzd3- or Celsr3-deficient neurons. (*Longest primary*: control 306.2±19.6 μm, *Fzd3*$^{-/-}$ 336.5±36.4 μm, *Celsr3*$^{-/-}$

274.5±17.0 μm. Neurites measured≥230. N≥4. Fig. 4.8 D. *Longest secondary*: control 89.6±2.3 μm, *Fzd3*$^{-/-}$ 100.8±8.3 μm, *Celsr3*$^{-/-}$ 81.4±3.8 μm. Neurites measured≥140. N≥4. Fig. 4.8 E. *Total length per neuron*: control 442.0±32.0 μm, *Fzd3*$^{-/-}$ 475.1±55.8 μm, *Celsr3*$^{-/-}$ 389.7±20.8μm. Neurons measured≥230. N≥4. Fig. 4.8 F).

Extensive neurite arborisation and branching is a distinctive feature of enteric neurons, therefore we examined whether absence of Fzd3 and Celsr3 could affect this particular aspect of neuronal development. We investigated the degree of branching by measuring the proportion of neurons in culture with primary, secondary and tertiary neurites (Fig. 4.8 G). In control neuronal cultures we found that 57.3±3.6% of neurons had secondary branches and 12.8±2.9% had formed secondary and tertiary branching (neurons counted≥230. N≥4). These proportions did not differ in Fzd3 (secondary without tertiary branching 53.5±3.7%, secondary with tertiary branching 15.7±3.0%) and Celsr3 mutant cultures (secondary without tertiary branching 47.3±2.3%, secondary with tertiary branching 9.2±1.3%). Nevertheless, when we considered the total number of neurons with secondary branching (with or without tertiary branching), we found that in *Celsr3*$^{-/-}$ samples the proportion was significantly reduced to 56.5±2.0%, compared to control 70.2±4.5% ($P<0.05$), while *Fzd3*$^{-/-}$ samples did not show any difference (69.2±3.7%).

We also examined the complexity and architecture of the neurite arborisation by defining how many primary and secondary neurites where present for each individual neuron (Fig. 4.8 H-I). Proportion of neurons with one (monopolar), two (bipolar) and more than two (multipolar) primary neurites were unaffected by Fzd3 and Celsr3 mutations (control: one 72.8±4.3%, two 22.9±3.1%, more than two 4.3±1.5%; *Fzd3*$^{-/-}$: one 80.5±4.5%, two 17.2±3.7%, more than two 2.3±1.3%; *Celsr3*$^{-/-}$: one 62.3±1.4%, two 30.9±2.2%, more than two 6.8±1.2%. Neurons measured≥230. N≥4). Similarly, the architecture of secondary branching was unchanged between controls and Fzd3 null samples. However, Celsr3 mutant samples appeared to have significantly less neurons with only two secondary branches, with a concomitant tendency to have neurons with a more complex branching (i.e. more than two secondary neurites) (control: one 52.0±2.5%, two 31.0±5.2%, more than two 17.0±5.2%; *Fzd3*$^{-/-}$: one 52.3±4.1%, two 31.6±4.1%, more than

two 16.1±5.9%; *Celsr3*$^{-/-}$: one 56.5±2.7%, two 20.7±2.5%, more than two 23.3±2.5%. P<0.05. Neurons counted>140. N≥4).

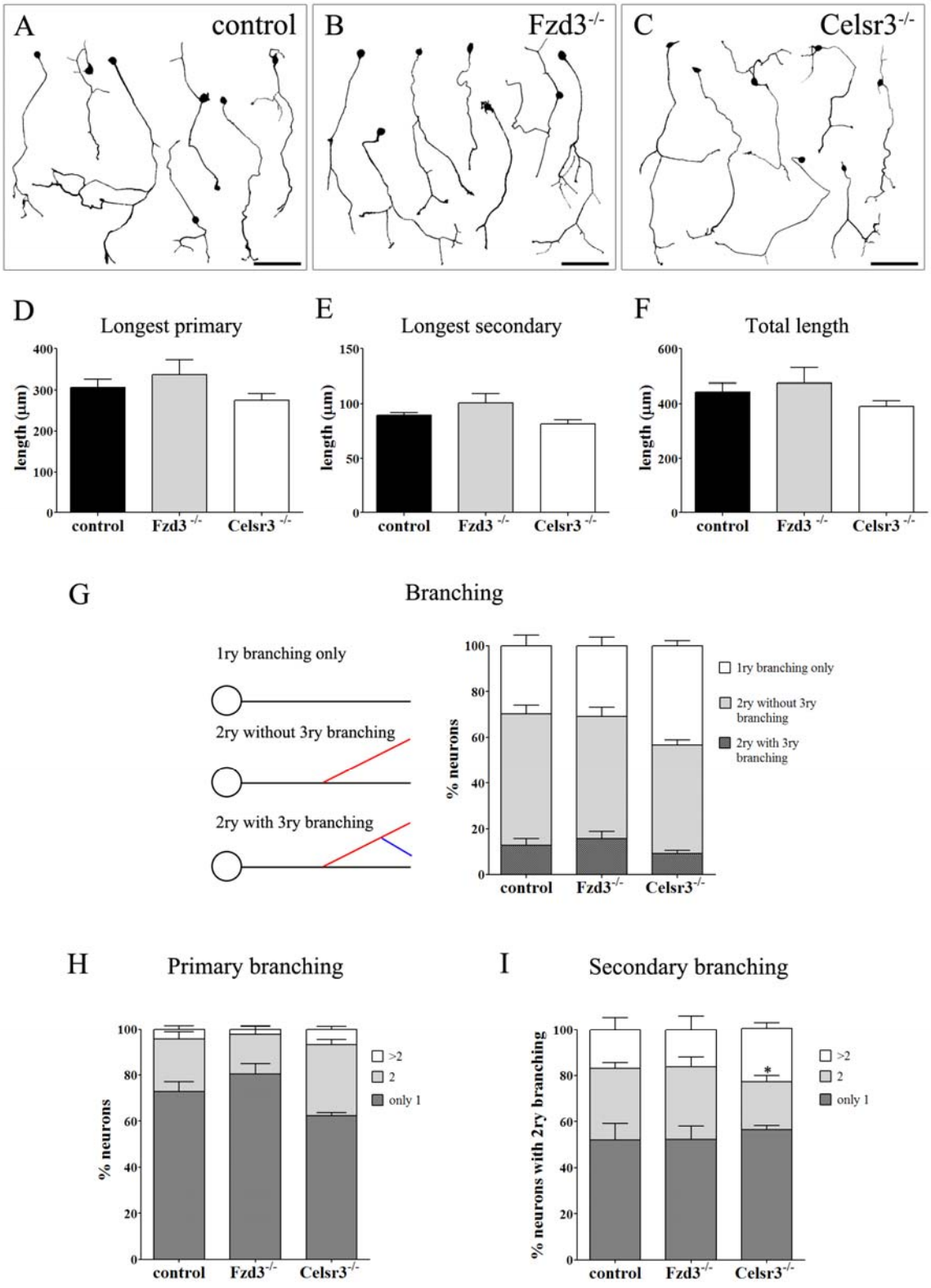


**Figure 4.8 (legend next page)**

**Figure 4.8 Fzd3 and Celsr3 deficiency does not affect morphological development of enteric neurons *in vitro***

Primary enteric neurons derived from dissociated E12.5 guts were cultured *in vitro* for 4 days and their morphology analysed upon staining with a TuJ1 antibody. (**A-C**) Inverted confocal images of representative control (A), *Fzd3*$^{-/-}$ (B) and *Celsr3*$^{-/-}$ (C) primary enteric neurons. Scale bars 100 μm. (**D-F**) Studies of neurite length of enteric neurons. Quantification of the average length in μm of the longest primary (D) and secondary (E) neurite per neuron, and average of the sum of lengths of all neurites per neuron (total neurite length, F). (**G-I**) Studies of branching pattern of enteric neurons. Extent of branching was assessed by quantifying the proportion of neurons with only primary branches and with secondary neurites with and without tertiary branches (G). Additionally, the number of primary (**H**) and secondary (**I**) branches per neuron was also assessed. Total neurons measured≥230. N≥4. * indicates P<0.05. Error bars, SEM.

These results showed that *Fzd3* and *Celsr3* mutation did not affect neuritogenesis *per se*. Nevertheless, we found that the degree of branching was affected in *Celsr3*$^{-/-}$ neurons. However, this evidence was not sufficient to explain the major phenotype observed *in vivo* in both Fzd3 and Celsr3 mutant animals and it is likely to reflect the specific responses of mutant neurons *in vitro*.

### 4.1.6 Axonal guidance is specifically impaired in mutants *in vivo*

We have shown that, in *Fzd3*$^{-/-}$ and *Celsr3*$^{-/-}$ guts, ENCCs are able to proliferate and to differentiate into neurons with the intrinsic capability to develop normal processes and morphologies. This suggests that the defect in tract formation observed in mutant samples appears to reflect a defect in interaction between neuronal processes and their surrounding environment *in vivo*. To examine this hypothesis further, we had to employ a strategy capable of identifying individual neurons and their processes *in situ.* Within the mature and developing ENS, neurons and neuronal processes do not form identifiable structural units of morphologically, functionally and biochemically similar neuronal subtypes, thus limiting the accessibility of the system to the study of single cell morphology and function. To overcome this limitation, we decided to take advantage of an inducible genetic fate mapping strategy to permanently label individual cells *in vivo* at a given developmental stage. For this, we used a

*Sox10iCreER$^{T2}$* transgenic line, which has been generated previously (Laranjeira, 2010). The CreER$^{T2}$ chimeric protein is a product of the fusion between the catalytic domain of the bacterial Cre recombinase and the mutated ligand-binding domain of the human estrogen receptor (ER$^{T2}$). When expressed, the chimeric protein CreER$^{T2}$ is sequestered in the cytoplasm and it is only able to translocate into the nucleus and to catalyse recombination after the synthetic ligand Tamoxifen (TM) or its metabolite 4-hydroxytamoxifen (4-OHT) are bound to the ER$^{T2}$ domain (Danielian *et al.*, 1998). In the *Sox10iCreER$^{T2}$* transgenic line, it has been shown that the CreER$^{T2}$ protein is able to catalyse recombination of the *R26ReYFP* locus within 24 hrs after 4-OHT administration, while the efficiency of recombination shows a linear correspondence with the dosage of ligand administered (Laranjeira, 2010). In this particular occasion, moreover, the chimeric protein is expressed under the control of regulatory regions of the *Sox10* promoter, where Sox10 is a transcription factor expressed in all ENS progenitors that give rise to neurons and glia within the ENS (Anderson *et al.*, 2006; Laranjeira, 2010; Southard-Smith *et al.*, 1998). Thus, we expected that by using the *Sox10iCreER$^{T2}$;R26ReYFP* at its lowest efficiency, we would be able to visualise by YFP fluorescence single neurons within the developing ENS network. To do that, we first established that 4-OHT needed to be administered to pregnant females approximately 48 hrs before the intended time of analysis, so that sufficient time would be given to Sox10$^{+}$ progenitor cells to recombine their *R26ReYFP* locus and differentiate morphologically into neurons (i.e. develop identifiable neurites) *in vivo.* Secondly, we empirically found that administration of 3 μg/g of 4-OHT in E10.5 pregnant females was able to produce a sufficiently sparse population of YFP-labelled neurons in embryos harvested at E12.5.

Following this experimental protocol, we analysed E12.5 guts from *Sox10iCreER$^{T2}$;R26ReYFP* embryos immunolabelled for GFP and TuJ1 (Fig. 4.9). In these guts, solitary GFP$^{+}$ ENCCs were labelled throughout the entire length of the intestinal tube (Fig. 4.9 A). Furthermore, a small percentage of GFP$^{+}$ cells showed a clear neuronal morphology with a prominent process extending from their cell body and they were confirmed to be neurons by TuJ1 immunoreactivity (Fig. 4.9 B-D).

Similarly, when the *Sox10iCreER$^{T2}$;R26ReYFP* transgenes were introduced into the Fzd3 and Celsr3 mutant backgrounds, we were still able to genetically label single ENCCs and identify neurons bearing well defined processes (Fig. 4.9 E-F). However, within the Celsr3 null background, recombination efficiency was significantly reduced compared to that of controls (Fig. 4.9 F).

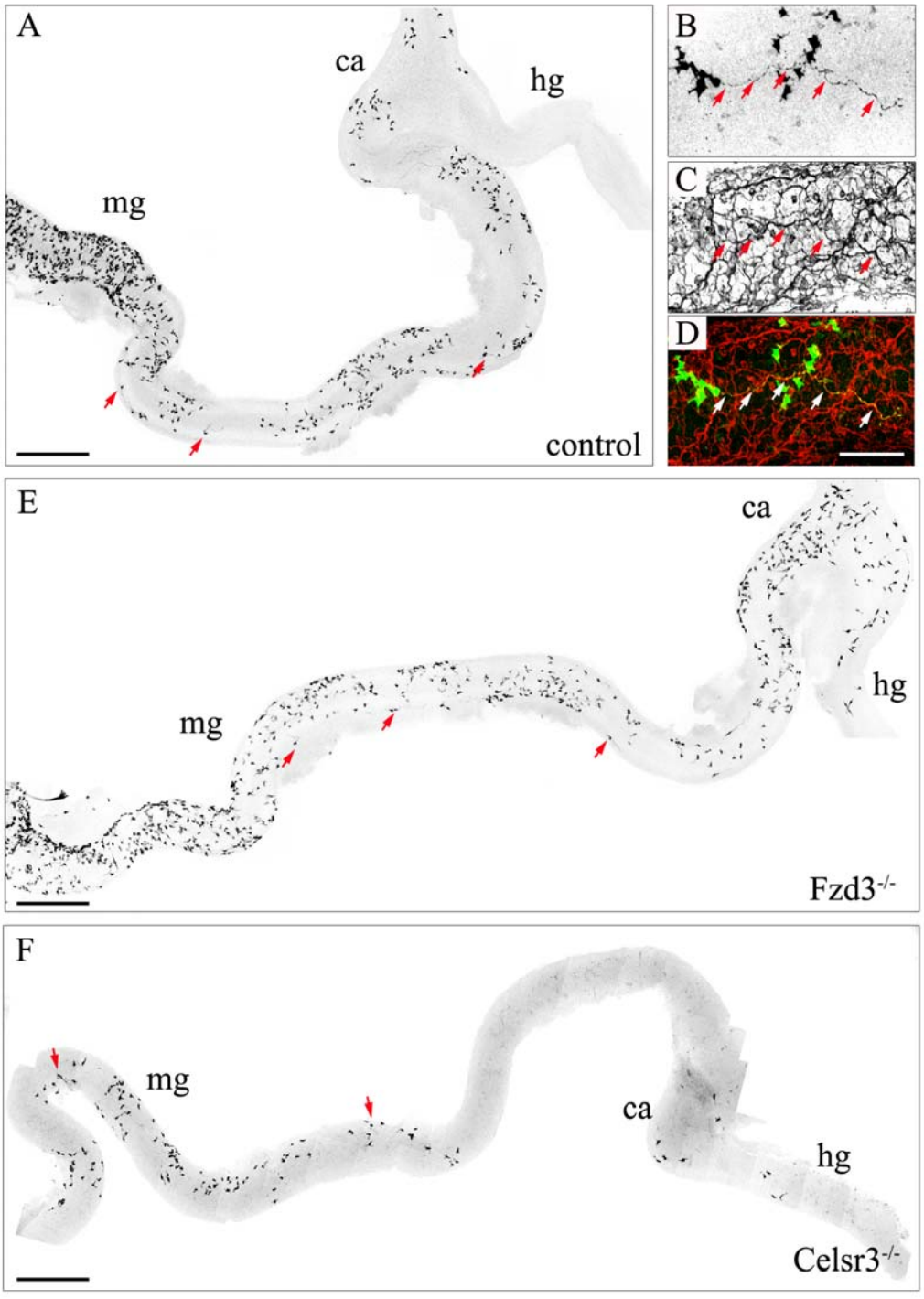


**Figure 4.9 (legend next page)**

**Figure 4.9 Genetic inducible fate mapping to label individual neurons in whole mount preparations of E12.5 guts**

The transgenic line *Sox10iCreER$^{T2}$* has been used to specifically recombine the reporter allele *R26ReYFP* within Sox10$^{+}$ ENS progenitors and follow up the morphology of their neuronal derivatives *in vivo*. 3 μg/g of 4-OHT was administered intraperitoneally to E10.5 pregnant females and embryos were harvested at E12.5. Whole mount preparations of E12.5 guts were then processed for GFP and TuJ1 immunolabelling. (**A**) Inverted confocal image of whole mount gut preparation immunolabelled for GFP. A sparse population of GFP$^{+}$ cells (dark grey) can be observed through the length of the midgut. Neurons can also be readily identified by the presence of one or more neurites (red arrows). Scale bar 200 μm. (**B-D**) Representative image of a GFP labelled neuron (B) also immunoreactive for TuJ1 (C). Merged image of panel B (GFP, green) and C (TuJ1, red) is shown in D. (**E-F**) *Sox10iCreER$^{T2}$;R26ReYFP* transgenes were introduced into the Fzd3 and Celsr3 KO background to label single cells *in vivo*. Individual GFP cells (dark grey) were found both in Fzd3 (E) and Celsr3 (F) mutant E12.5 gut preparations upon administration of 4-OHT *in vivo*. However, efficiency of recombination of the *R26ReYFP* reporter allele was lower in *Celsr3$^{-/-}$* guts, thus leading to less GFP cells in these samples (F) compared to *Fzd3$^{-/-}$* (E) and control (A) guts. Scale bars 200 μm (A, E, F) and 100 μm (B-D). Ca, caecum; hg, hindgut; mg, midgut.

We examined in detail the projection pattern of the labelled GFP$^{+}$ neurons found throughout the midgut region of control and mutant E12.5 guts (Fig. 4.10). To define the orientation of neuronal processes we drew an axis from the region of the cell body where the processes emerged to the end of their tip and measured the angle formed by this axis to the main axis of the gut. We found that 92% of control neurons were projecting caudally with their processes forming an angle between 45º and 315º to the main axis of the gut (N=25. Fig. 4.10 A-C). The remaining neurons were found to project circumferentially (8% between 45º and 75º). No processes were found oriented toward the oral side of the gut. Strikingly, Fzd3 mutant neurons showed a variety of orientation patterns. Neuronal processes projecting caudally were reduced to 39.2%, while those running circumferentially were increased to 41.2% and, surprisingly, 19.2% of neurons had oral projections (N=51. Fig. 4.10 D-F). Additionally, by measuring the average length of the longest neurite per neuron, we found that *Fzd3$^{-/-}$* neurons had neurites significantly shorter than controls (control 215.4±26.0 μm, *Fzd3$^{-/-}$* 133.4±12.8 μm. $P<0.01$. $N\geq25$. Fig. 4.10 I).

In Celsr3-null preparations, we found that neurons had a tendency to project aberrantly and have short neurites similar to Fzd3 mutant embryos (Fig. 4.10 G-H), but due to low recombination efficiency, we were unable to analyse a sufficient number of neurons to have definite percentages.

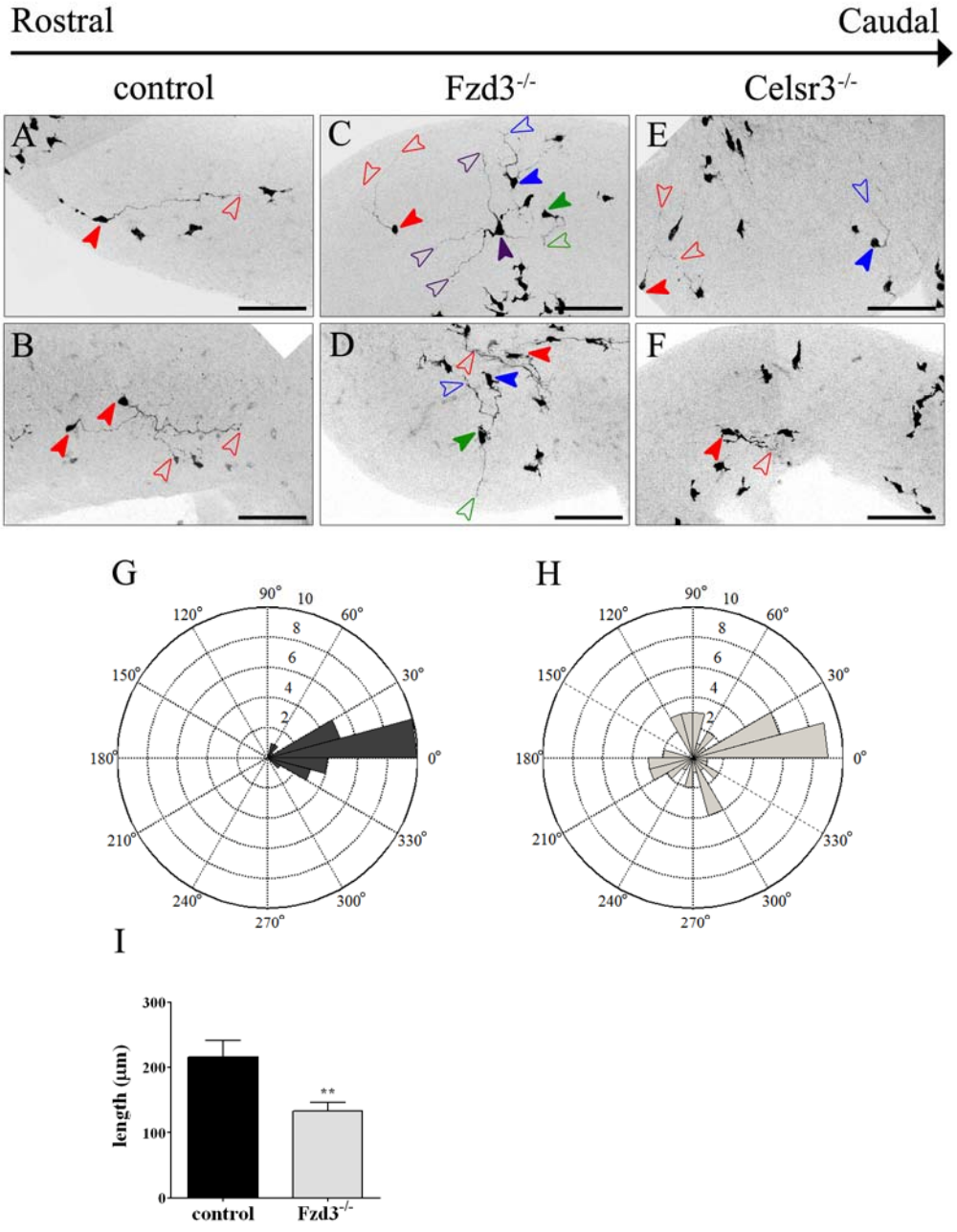


**Figure 4.10 (legend next page)**

**Figure 4.10 Defects in patterning of individual neurons in Fzd3 mutants *in vivo***
Analysis of individual neuronal processes in whole mount preparations of E12.5 guts from embryos carrying the *Sox10iCreER$^{T2}$;R26ReYFP* double transgene and Fzd3- or Celsr3-null alleles. (**A-F**) Representative inverted confocal images of GFP$^{+}$ labelled neurons. Enteric neurons in control guts (A-B) have generally a single longitudinal projection which is caudally directed. In contrast, neuronal projections in *Fzd3* (C-D) and *Celsr3* (E-F) mutant embryos are often directed circumferentially. Filled arrowheads indicate cell bodies and empty arrowheads the tips of the projections; different colours mark different neurons. Scale bars 100 μm. (**G-H**) Rose plots showing the distribution of angles formed by the nascent neuronal projections and the long axis of the gut in control (G) and Fzd3 mutant (H) guts. The area of each bin represents the number of projections oriented in that direction (control N=51, *Fzd3*$^{-/-}$ N=26). (**I**) Analysis of neurite length of individual GFP$^{+}$ labelled neurons shows that *Fzd3*$^{-/-}$ processes are shorter than controls *in vivo*. Control N=26, *Fzd3*$^{-/-}$ N=51. ** indicates P<0.01. Error bars, SEM.

These data show that ablation of *Fzd3* and *Celsr3* results in changes in directionality of neuronal processes *in vivo*. In mutant animals, the guidance of longitudinal processes appears to be affected, thus resulting in aberrant patterning and growth of developing neuronal projections.

### 4.1.7 Response to GDNF is unaffected in *Fzd3*$^{-/-}$ and *Celsr3*$^{-/-}$ explants

Our data suggest a change in orientation of processes of enteric neurons in *Fzd3*$^{-/-}$ and *Celsr3*$^{-/-}$ animals. One reason for that might be a change in the response of neuronal processes to their environment. A molecule that has been shown to be expressed in the gut mesenchyme while ENCCs colonise the gut and to promote axonal outgrowth and neurite attraction of enteric neurons *in vitro* is GDNF (Natarajan *et al.*, 2002; Young *et al.*, 2001). GDNF has been also suggested to be able to control patterning and organisation of enteric neurons (Wang *et al.*, 2010). Therefore, we wished to examine whether the altered patterning observed in Fzd3 and Celsr3-deficient neuronal processes could be a result of a change in the response of ENCCs and enteric neurons to GDNF. To test this hypothesis, we used an assay that has been previously used to test GDNF response in embryonic gut *in vitro*. E12.5 midgut explants from *Wnt1Cre;R26ReYFP;Fzd3* or *Celsr3* mice where incorporated in a three-dimensional collagen matrix and cultured for 24 hrs in presence of GDNF (Fig. 4.11). In these conditions control

explants showed a massive invasion of the matrix from both undifferentiated ENCC cell bodies ($YFP^{+}TuJ1^{-}$) and neuronal processes ($YFP^{+}TuJ1^{+}$) (Fig. 4.11 A-A"). In *Fzd3*$^{-/-}$ and *Celsr3*$^{-/-}$ explants, ENCCs and neuronal processes invaded the collagen matrix in similar numbers and at comparable distance relative to control (Fig. 4.11 B-B", C-C"), indicating that GDNF response is not affected in Fzd3 and Celsr3 mutant guts.

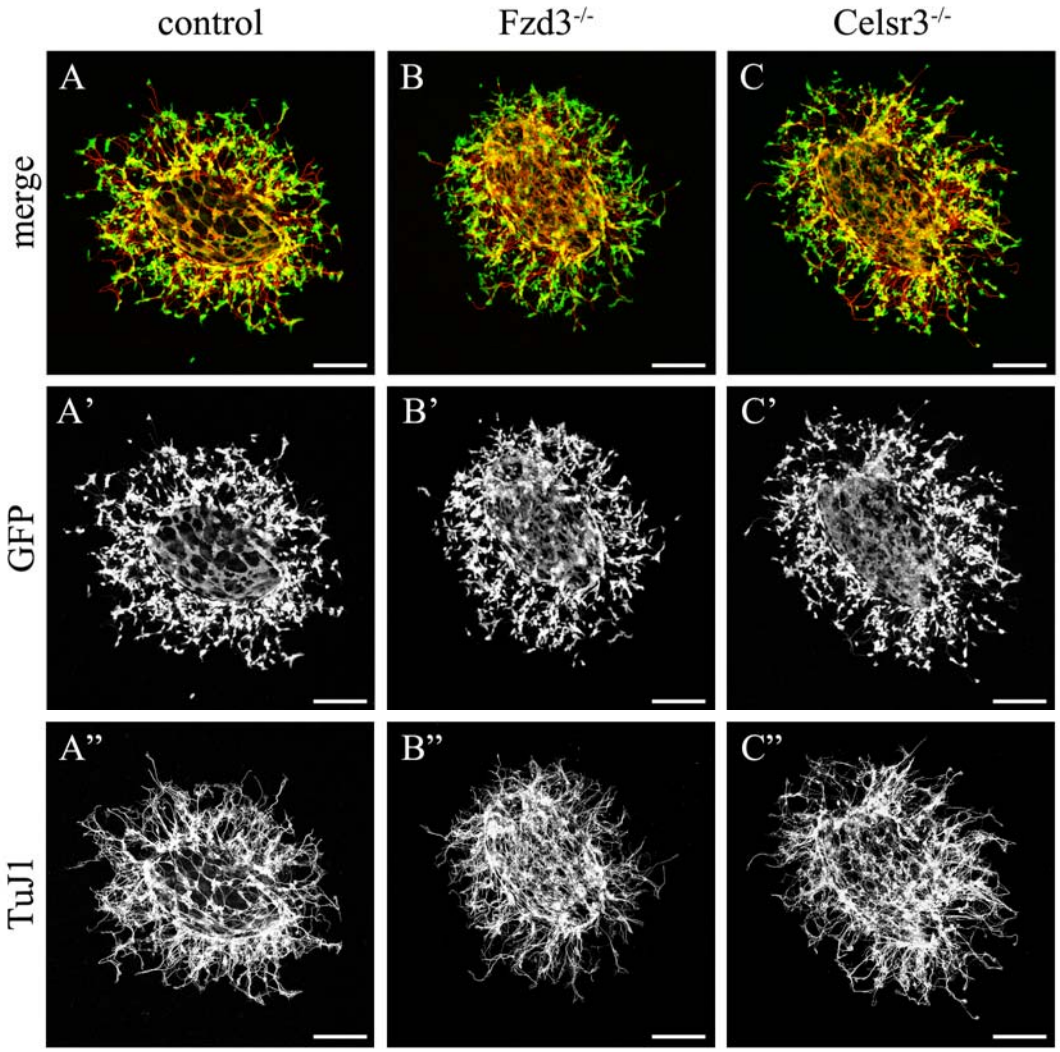


**Figure 4.11 GDNF response is normal in gut explants from *Fzd3*$^{-/-}$ and *Celsr3*$^{-/-}$ embryos**

(**A-C**) E12.5 gut explants were set in a 3D collagen matrix, cultured in presence of GDNF for 24 hrs and immunostained for GFP (green) to identify ENCCs and TuJ1 (red) to label neuronal processes. (**A'-C'**) Greyscale panels for the green channel (GFP) shown in A-E. (**A"-C"**) Greyscale panels for the red channel (TuJ1) shown in A-E. Number and distance migrated into the collagen matrix by ENCCs and neuronal processes is similar in control (A-A"), *Fzd3*$^{-/-}$ (B-B") and *Celsr3*$^{-/-}$ (C-C") explants. Scale bars 200 μm.

These observations suggest that patterning of enteric processes is likely to be controlled by Fzd3 and Celsr3 through a GDNF-independent mechanism.

### 4.1.8 Generation of conditional Celsr3 mutants reveals morphological and functional intestinal abnormalities

Correct wiring of the ENS is essential for normal intestinal motility and digestion. We showed that in *Fzd3*$^{-/-}$ and *Celsr3*$^{-/-}$ guts, as early as E12.5, specific defects in neuronal tract formation and axonal patterning can be detected. Therefore, we wanted to investigate whether defective wiring during embryonic development could underlie specific defects in the function of the mature ENS. To explore this, we aimed to overcome the perinatal lethality of the constitutive ablation of *Fzd3* and *Celsr3* by targeting the mutation only within the neural crest cell lineage. Hence, we obtained a conditional mutant allele of *Celsr3* (*Celsr3f*), generated previously by flanking exons 19 to 27 of the Celsr3 locus by loxP sites (Zhou *et al.*, 2008). Mice with inactivation of the Celsr3 gene within NCCs were produced by crossing *Wnt1*$^{+/Cre}$*;Celsr3*$^{+/-}$ mice with homozygous *Celsr3*$^{f/f}$ animals, thus obtaining *Wnt1*$^{+/Cre}$*;Celsr3*$^{f/-}$ mutant genotypes, which, for simplicity, we will define as Celsr3|Wnt1. To date, no conditional alleles for *Fzd3* have been generated, so we focused our analysis only on Celsr3 conditional mutants.

At weaning (P21) all genotypes were found close at the expected mendelian ratio of 1:1:1:1 (*Wnt1*$^{Cre/+}$*;Celsr3*$^{f/+}$ 26.8±4.8%, *Wnt1*$^{Cre/+}$*;Celsr3*$^{f/-}$ 26.24±4.9%, *Wnt1*$^{+/+}$*;Celsr3*$^{f/+}$ 27.22±7.3%, *Wnt1*$^{+/+}$*;Celsr3*$^{f/-}$ 19.7±3.8%. N=86. Fig. 4.12 A). However, within 3 weeks from weaning, the survival rate of Celsr3|Wnt1 animals rapidly dropped to about 50% (55.5% at P42. N=68. Fig. 4.12 B) and it then steadily decreased further in the following weeks (47.6% at P84, 39.6% at P105, 31.7% at P125. N=86. Fig. 4.12 B). Death of Celsr3|Wnt1 mice was usually sudden and the main cause is still unknown. Mutant weaners appeared smaller than littermates; nevertheless, they did not seem to have problems in feeding, locomotion or social behaviour. We monitored the growth rate of male and female mice over the period of 9 weeks from weaning and we found that the body weight of Celsr3|Wnt1 mice was significantly and consistently lower

compared to littermates in both sexes and at any time point considered (Fig. 4.12 C-D). Moreover, mutant weaners appeared already significantly lighter than controls at P21, suggesting that the decreased body weight is not due to hormonal imbalance which usually becomes evident only after weaning.

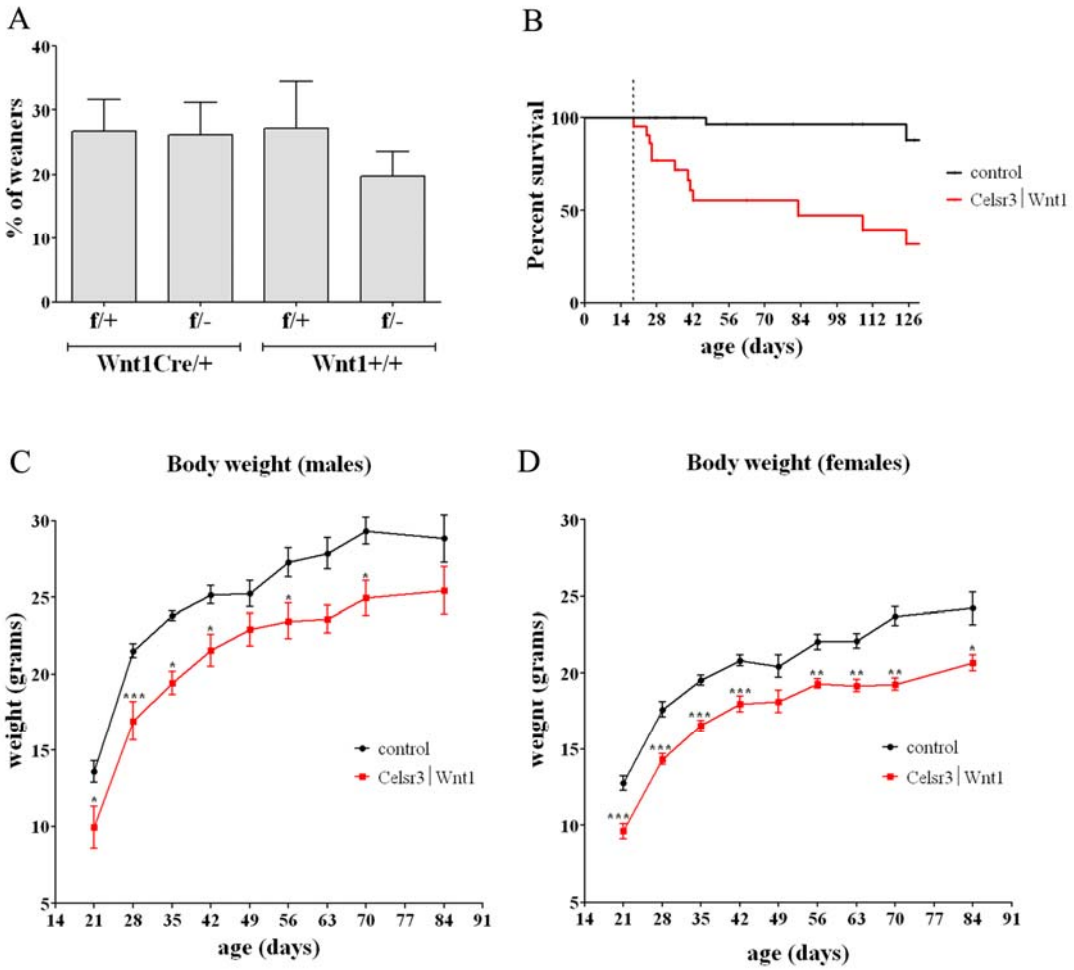


**Figure 4.12 Impaired survival and growth in NC-specific Celsr3 mutants**

Celsr3 gene is specifically inactivated within neural crest cells by using a *Wnt1Cre*;*Celsr3flox* mouse line (Wnt1|Celsr3). (**A**) Proportion of genotypes of animals retrieved at weaning (P21) from the experimental crossings. All the experimental genotypes are retrieved in the expected proportions (1:1:1:1) (**B**) Survival rate of mutant animals (red line) compared to control littermates (black line) shows that survival of Celsr3|Wnt1 animals is normal until weaning (P21, dashed line) and then it is drastically reduced within 4 weeks. (**C-D**) Body weight of Wnt1|Celsr3 animals over a period of 9 weeks in males (C) and females (D). Conditional Celsr3 mutant animals (red lines) have a significantly lower body weight compared to control littermates (black lines) for both sexes and at any stage considered. N=22. * indicates P <0.05, ** indicates P<0.01, *** indicates P<0.001. Error bars, SEM.

Lethality after weaning and decreased body weight might be indications of an underlying digestive problem in Celsr3|Wnt1 mice, thus we investigated whether any abnormality could be detected directly by anatomical examination of the gastrointestinal tract of P21 and P35 mutant animals (Fig. 4.13). We examined the gastrointestinal tracts of Celsr3|Wnt1 animals before and immediately after death and we compared them to that of control littermates. We found no changes in the gross anatomy of the intestinal tube in mutant animals, such as all the anatomical compartments (i.e. stomach, small intestine, caecum and colon) which were still clearly identifiable. However, in mutant samples, the muscular tone was often altered, revealing an alternation of contracted and distended bowel regions, associated with abnormal accumulation of intestinal contents (Fig. 4.13 B-C, E-F). The phenotype was more severe in post-mortem samples, suggesting that the altered physiology of the intestinal tube might contribute to the death of mutant animals (Fig. 4.13 C, F). Furthermore, we noticed that corresponding regions were affected by variable phenotypes, such as, for example, the stomach in P21 and P34 mutants, which was extremely contracted and distended respectively. Additionally, at any stage considered, the normal pattern of fecal pellets (size, number and repetition) seen in the colon of control animals was consistently lost in mutants. In fact, control stool pattern appeared highly regular, with the presence of few (4-5) big pellets, usually well distanced throughout the whole length of the colon (Fig. 4.13 A, D asterisks). Conversely, in Celsr3|Wnt1 colons, we found several (6-15) small pellets, irregularly spaced and, often overlying on each other (Fig. 4.13 B-C, E-F).

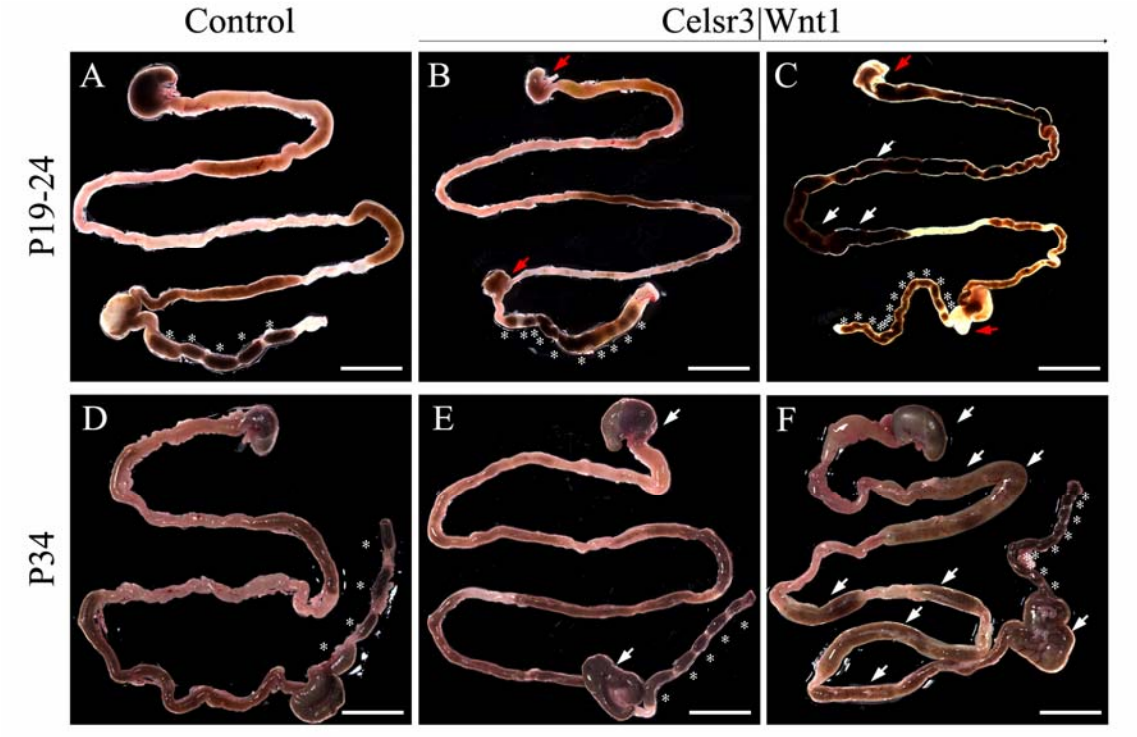


**Figure 4.13 Intestinal tracts of Celsr3|Wnt1 animals present altered muscular tone and pattern of intestinal contents**

Gross anatomy of the gastrointestinal tract in control (**A**, **D**) and mutant animals alive (**B**, **E**) and post-mortem (**C**, **F**) investigated at P19-24 (**A-C**) and P34 (**D-F**). In mutant samples muscular tone is often altered revealing contracted (red arrowheads) and distended areas (white arrowheads) associated with accumulation of intestinal contents. Additionally, the colonic stool pattern (size, number and repetition, asterisks) seen in controls (A,D) is altered in mutants (B-C, E-F). Scale bars 1 cm.

These data indicate a pseudo-obstructive impairment in intestinal motility in Celsr3|Wnt1 mice. Thus, we decided to investigate any underlying ENS abnormality in preparations of longitudinal muscle and myenteric plexus from the small intestine of P21 mice (Fig. 4.14). Preliminary results deriving from immunofluorescence staining for neuronal markers such as PGP and TuJ1, revealed a decreased number of interganglionic strands and secondary plexus fibres in P21 mutants. Additionally, in Celsr3|Wnt1 plexuses, the remaining interganglionic fibres appeared thinner creating gaps in between ganglia often larger than in the control neuronal plexus (Fig. 4.14 B-D). To explore whether the altered pattern of neuronal fibres in mutants could be due to specific defects in subclasses of enteric neurons, we assessed the presence of two of the main classes of enteric neurons, $nNOS^+$ and $ACh^+$ neurons, by immunofluorescence and AChE staining, respectively. Interestingly, we found a reduction in $nNOS^+$ intergangliar and secondary plexus fibres; however, we did not notice a dramatic reduction in the overall number of $nNOS^+$ cell bodies (Fig. 4.14 E-F). Conversely, when we processed mutant samples for AChE staining, we could not observe such a dramatic phenotype and organisation and morphology of $AChE^+$ fibres appeared similar to controls (Fig. 4.14 G-H). This suggests that the reduction in thickness and number of fibres in the myenteric plexus of Celsr3|Wnt1 mutants could be due to a specific defect in $NOS^+$ fibres.

**Figure 4.14 Conditional Celsr3 mutants have abnormal plexus morphology (image next page)**

(**A-F**) Strips of muscle with adherent myenteric plexus in P21 animals immunolabelled for the pan-neuronal markers (PGP, A-B, and TuJ1, C-D) and subtype specific marker (nNOS, E-F). Images are shown in greyscale. In the myenteric plexus of conditional mutant Celsr3 animals (B, D, F), interganglionic neuronal strands (arrows) appear thinner and the interganglionic gaps are bigger compared to control preparations (A, C, E). In addition, mutants have also a reduced density of secondary neuronal fibres (arrowheads). nNOS immunofluorescence (**E-F**) confirmed a similar aberrancy in mutant samples (F), where number of $nNOS^+$ fibres (and not of $nNOS^+$ cell bodies) seems affected. Scale bars 150 μm. (**G-H**) AChE staining of strips of muscle with adherent myenteric plexus in P21 animals. AChE reactivity (blue) shows a similar organisation and density of fibres between control (G) and mutant (H) preparations. Scale bars 50 μm.

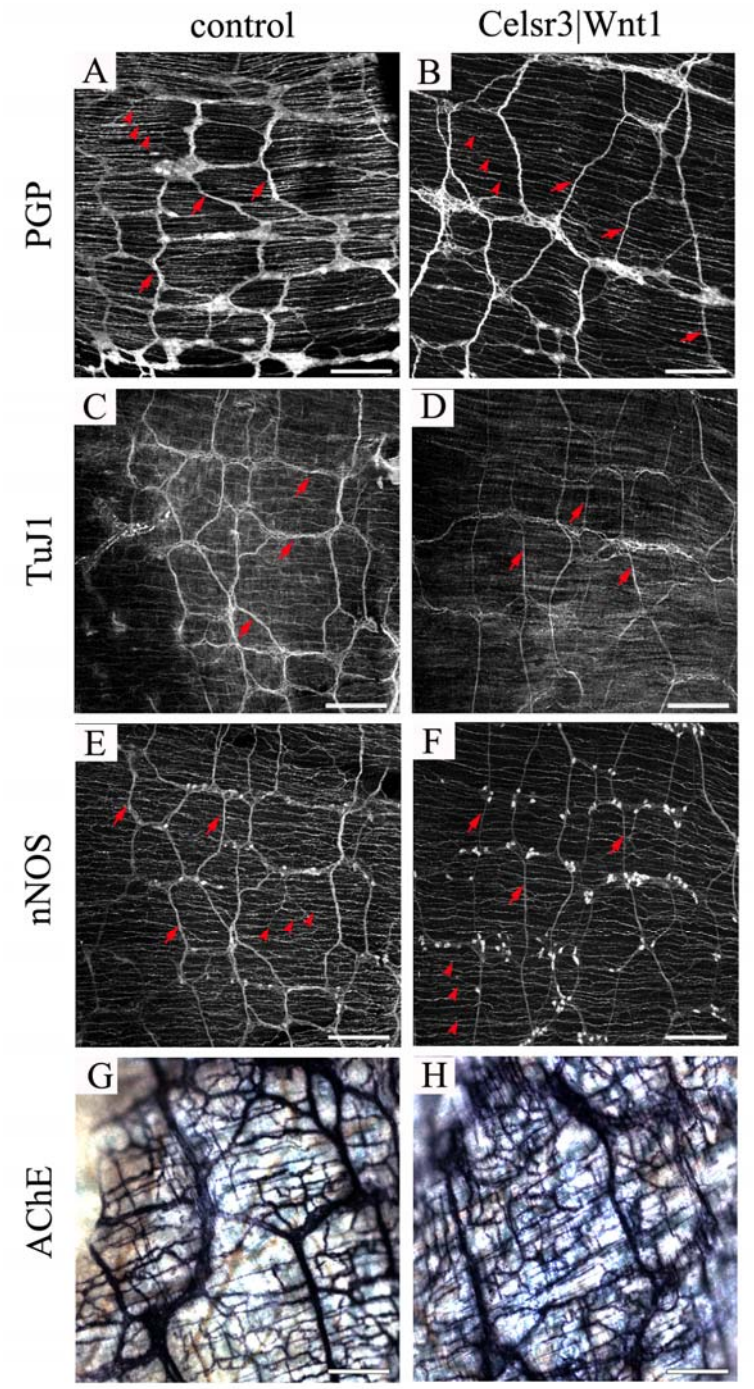


**Figure 4.14 (legend previous page)**

These data indicate that Celsr3 function is required for the formation and organisation of enteric neuronal processes of the mature ENS. In addition, Celsr3 conditional mutant animals fail to thrive and their intestinal function is likely to be compromised, thus suggesting that Celsr3 function is necessary for enteric neural circuit formation and function.

## 4.2 Discussion

The organization of enteric neurons is critical for the motor and secretory output of the gut during normal digestive function and underlies the homeostatic response of the gut in disease situations. Some organizational features of the mammalian ENS (such as the predominantly anal direction of axons of the early enteric neurons) are evident during embryogenesis. Nevertheless, the extent to which the organization of ENS circuitry is genetically controlled or reflects the adjustment of the ENS to emerging functional needs is currently unclear.

Bundles of longitudinal processes oriented caudally represent one of the first stereotypical patterns of ENS circuitry formation, although their function and relevance for later stages of network formation is still unknown. Here we demonstrate for the first time that Fzd3 and Celsr3 are expressed in the developing ENS and deletion of either gene *in vivo* leads to characteristic (and similar) defects in patterning of longitudinal fibres, without apparently affecting the migration, proliferation and neuronal differentiation of ENCCs.

### 4.2.1 Role of PCP genes in patterning of neuronal projections

Frizzled receptors and Celsr protocadherins are membrane bound molecules which are involved in several developmental processes regulating tissue morphogenesis. However, recent evidences have begun to unravel new broader roles for these molecules in neuronal circuitry formation. In *Drosophila*, for example, null mutations in *flamingo* (*fmi*, the fly orthologue of Celsr) produce defective axonal tracts in the CNS (Usui *et al.*, 1999). Fzd3 and Celsr3 KO animals show a complete loss of several longitudinal axonal bundles in the forebrain such as the thalamocortical, corticothalamic and nigrostriatal tracts and the anterior commissure (Tissir *et al.*, 2005; Wang *et al.*, 2002) Furthermore, recent studies in mammals have shown that Fzd3 and Celsr3 deficiency results in aberrant patterning of axons and cell bodies of monoaminergic neurons in the brainstem (Fenstermaker *et al.*, 2010). This suggests that there is a conserved role for Celsr3 and Fzd3 in developing neurons to promote the correct orientation of their projections.

To prove this hypothesis true also in the forming enteric neuronal circuits, we developed a novel approach to study the morphology and projection pattern of enteric neurons *in vivo*. Identification of individual neuronal projections within the enteric neuronal network has been attempted previously by DiI tracing or by immunolabeling for neurotransmitters expressed in specific neuronal subtypes, such as TH and NOS (Young *et al.*, 2002). However, these approaches, either individually or combined, presented several limitations including the high number of neurons labeled and the restricted timing of analysis. Our approach uses instead a genetic inducible fate mapping system (i.e. *Sox10iCreER$^{T2}$;R26ReYFP*) to permanently label single ENS progenitors and follow the morphology and fate of their neuronal derivatives in whole mount preparations of embryonic gut. By using this tool we have been able to observe a reduction of individual neuronal processes oriented longitudinally and caudally in Fzd3 and Celsr3 mutant guts, and also a concomitant increase in neuronal processes oriented aberrantly, providing strong evidence for specific guidance defects in mutant enteric neurons. In addition, our analysis also revealed that *Fzd3$^{-/-}$* neurites are shorter relative to controls *in vivo*. This growth defect may involve inhibitory or adhesive interactions with ECM components which are relieved in the presence of Fzd3 (and Celsr3) or, alternatively, it is possible that the same cues guiding growth cones may also be trophic cues for axons and promote concomitantly patterning and growth.

Hence, our data strongly suggest that Fzd3 and Celsr3 mediate the *in vivo* interaction of enteric neuronal processes with their environment along the longitudinal axis of the gut. This hypothesis is also corroborated by data showing that the reduction in neuronal tracts in Fzd3 and Celsr3 mutant guts is not due to neuronal loss and indicates that mutant enteric neurons maintain the intrinsic capability to differentiate into appropriate subtypes and produce normal neurites and morphologies when cultured *in vitro*.

### 4.2.2 Models for Fzd3 and Celsr3 function in axonal guidance

Given the similarities between the phenotypes observed in Fzd3- and Celsr3-dificient animals in the developing CNS and ENS, it is likely that both genes participate in a common genetic pathway regulating axon guidance in mammals.

In flies, flamingo (*fmi*), frizzled (*fz*), dishevelled (*dsh*), vang gogh (*vang*) and prickle (*pk*) form the core genes of the PCP pathway, a non-canonical Wnt signalling pathway (Uemura & Shimada, 2003). PCP interactions control tissue polarity of epithelial structures by driving localised actin polymerisation and promoting oriented growth of cuticle hairs and sensory bristles (Adler, 2002). In vertebrates, similar components and interactions are found during convergent extension and cochlear hair cell orientation (Uemura & Shimada, 2003). Interestingly, Wnt ligands seem dispensable in PCP signalling in *Drosophila*, whereas, in vertebrates, Wnt11 and Wnt5a are required for cell movement and intercalation during A-P elongation (Heisenberg *et al.*, 2000; Kilian *et al.*, 2003), and Wnt7a and Wnt5a have been implicated in orientation of stereociliary bundles (Dabdoub *et al.*, 2003; Qian *et al.*, 2007).

The discovery that some of these core PCP components are co-expressed in developing neurons and are required for their development, leads to the intriguing possibility that PCP-like interactions could also be used in other aspects of embryonic development other than epithelial tissue polarity. Therefore, PCP components could regulate coordinated cell and cytoskeletal polarity of neurons and growth cones in a manner analogous to the actions described in the plane of the epithelium. Alternatively, they may possess new context-dependent functions that exploit some of the properties fundamental to PCP signalling (cytoskeleton remodelling) or that converge with other cellular pathways (growth factors signalling, etc.). Unfortunately, up to now, our understanding of the role of PCP genes in nervous system development is limited to the description of phenotypes; however, several molecular mechanisms have been suggested.

In *Drosophila*, it has been shown that *fmi*-mediated homophilic interactions regulate CNS neuronal tract formation through a *fz*-dependent mechanism (Usui *et al.*, 1999), but at the same time, the same interactions are able to control photoreceptor axon targeting (Chen &

Clandinin, 2008) and dendritic development (Gao *et al.*, 2000) independently from the other PCP core genes and Wnt ligands. It appears therefore that fmi is able to activate the PCP pathway or to require only a subset of PCP machinery in a context-dependent manner.

In vertebrate neuronal development, the transcripts for *Celsr3* and *Fzd3*, vertebrate orthologues of *fmi* and *fz*, are co-expressed in the same developing neurons (Fenstermaker *et al.*, 2010; Tissir & Goffinet, 2006), together with other PCP core components, such as Dvl and Prickle (Tissir & Goffinet, 2006) and Vang Gogh-like (Fenstermaker *et al.*, 2010). This indicates that PCP-like interactions might have been maintained in the control of axon guidance, in which, for example, Celsr3 has been suggested to mediate homophilic interactions between growth cones and guidepost cells, allowing the further interaction of Fzd3 and Vangl2 expressed on opposing membranes, which in turn triggers an intracellular cascade promoting the directed growth of axons (Zhou *et al.*, 2008). However, other studies have shown that along with PCP components, also gradients of Wnt ligands, such as Wnt7a and Wnt5a, are required for axon guidance (Fenstermaker *et al.*, 2010). Indeed, the Wnt-Fzd signalling system has been suggested to direct patterning of axonal projections in the spinal cord, where, in particular, Fzd3 is able to mediate the attraction of Wnt4 and Wnt7b gradients on post-crossing axons (Lyuksyutova *et al.*, 2003). Thus, it is still unclear how Wnt-Fzd signalling integrates within or concomitantly to PCP signalling and what is the relative significance of all the components.

It is therefore possible that, in the developing ENS, Celsr3 mediates the adhesion between individual enteric neuronal processes or between processes and undifferentiated ENCCs, which might act as enteric guidepost cells. The Celsr3-mediated adhesion, then, might be a sufficient condition for activation of a PCP-like pathway within enteric neurons or, alternately, a necessary step in order for growth cones to respond to appropriate extrinsic organizational cues, such as GDNF or Wnt proteins. GDNF-RET signalling is able to promote outgrowth of neuronal processes from gut explants *in vitro* and it has been suggested to act as a chemoattractive cue for developing axons (Natarajan *et al.*, 2002; Young *et al.*, 2001). However, our results showed that Fzd3 and Celsr3 mutant neuronal processes (and ENCCs) have a normal response to GDNF in collagen matrix assays, thus excluding the idea that the function of Fzd3 and Celsr3 is GDNF-

dependent. On the other hand, Fzd ligands, Wnt proteins, are attractive candidates, since several members such as Wnt5a and Wnt11 are expressed in the developing gut mesoderm (Lickert *et al.*, 2001). However, to date, no studies have shown the involvement of these molecules in any aspect of ENS development.

### 4.2.3 Functional relevance of Celsr3 mutation in the ENS

The early steps of connectivity affected in the Fzd3 and Cels3 mutants are likely to be critical for later events that determine the connectivity and function of neuronal networks in the gut. Consistent with this view, the generation of NC-specific conditional Celsr3 mutants showed that animals fail to thrive and their intestinal function is likely to be compromised. Gastrointestinal tracts of mutant animals showed alternation of contracted and distended regions, suggestive of altered neural innervation of the intestinal smooth muscle. In addition, the stereotypical pattern of fecal pellets seen in the colon of control animals was lost in mutant samples, showing an irregular number of small size pellets, but also accumulation of contents. This phenotype suggests that pseudo-obstructive events might have taken place in the intestinal tract of mutant animals as a consequence of altered peristalsis. Interestingly, several idiopathic enteric neuropathies in humans are characterised by similar pathophysiological features such as pseudo-obstruction and slow intestinal transit (Di Nardo *et al.*, 2008).

Notably, we have been able to connect these pathoanatomical findings with altered morphology of the mature myenteric plexus. We found that the major neuronal fibres connecting ganglia (internodal fibres) and secondary fibres in the myenteric plexus of mutant animals are reduced in thickness and number. Interestingly, this defect appears to involve mainly the nitrinergic innervation of the gut. NOS neurons are among the first neurons to be born in the developing gut (Baetge & Gershon, 1989) and, as soon as they differentiate, they possess a single long process oriented longitudinally and projecting caudally (Young *et al.*, 2002). Taking into account the effect of Fzd3 and Celsr3 mutations on the formation of longitudinal processes at early stages of development, it is, therefore, likely that these genes have a specific function in

guidance and patterning of NOS enteric neurons. This also provides evidence for the existence of a genetic hardwiring of axons during ENS circuitry formation, where patterning of neuronal projections is a process that is controlled by a defined set of genes at early stages of development.

These findings also represent a step towards the understanding of the etiological features of several neuropathies affecting the motor function of the gastrointestinal tract. With a few exemptions, the mechanisms through which alterations in enteric neurons cause abnormal intestinal motility remain poorly understood. Current evidence shows that absence (such as in Hirschsprung's disease), degeneration (such as during aging) or functional impairment (such as in Achalasia or CHP) of enteric neurons is associated with uncoordinated motor activities, which result in altered transit of intestinal contents (De Giorgio & Camilleri, 2004; Di Nardo *et al.*, 2008). Several genes have been associated with some of these human conditions and they play important developmental roles in regulating the migration, proliferation and differentiation of neural crest cell progenitors of the ENS (Heanue & Pachnis, 2007; Newgreen & Young, 2002). However, very little is known about genes affecting the circuitry formation and how defects in patterning of enteric projections can affect the normal motor output of the mature ENS. Our data suggest that members of the PCP pathway, Fzd3 and Celsr3, represent a novel class of molecules that are required specifically for the formation of functional neuronal networks without affecting major developmental processes, such as migration and differentiation of neural crest cells, and, they might represent the basis for further investigation of molecular mechanisms underlying human enteric neuropathies.

# Chapter 5

# Concluding remarks

## 5.1 Genetic hardwiring of the ENS

Over the last several years, studies on the development of the ENS have put a great emphasis on the dissection of the genetic and molecular mechanisms controlling the colonisation of the gut by neural crest cells (Heanue & Pachnis, 2007; Newgreen & Young, 2002). This led to the identification of a number of genes involved in migration, proliferation and neuronal specification of ENCCs, but, also, it provided new insights into the genetics of the multigenic human enteric neuropathy Hirschsprung's disease. However, very little is known about the genetic mechanisms that control other features of ENS development, such as the formation of the enteric neuronal circuit. The understanding of this process is fundamental in light of increasing evidence suggesting that the aetiology of several idiopathic enteric neuropathies might be related to subtle defects in ENS innervation, rather than obvious morphological defects (i.e. loss or reduction of enteric neurons). Furthermore, the unravelling of defects in enteric circuitry might also explain other clinical conditions, such as the persistent dismotility patterns recorded in normoganglionic regions of some HSCR patients, even after successful surgical resection of the aganglionic area.

Considerable progress has been made in the understanding of the normal organisation and function of the ENS in the recent years (Furness, 2006). It is clear now that the regular, repetitive and controlled pattern of intestinal motility is the result of a stereotypical organisation of neurons of different morphological, physio-biochemical and functional properties. Different subtypes of enteric neurons form basic units of connectivity and these units are then repeated around and along the entire length of the gastrointestinal tract, thus producing complex intrinsic reflexes which regulate and control the muscular motor output of the ENS. Nevertheless, it is still not known whether this precise organisation of the ENS circuitry is genetically controlled or it results from the adjustment of the ENS to emerging functional needs.

Although the answer is likely to lie in between these two hypotheses, our data strongly support the idea that genetic factors control the organisation and connectivity of neuronal processes of the ENS. In fact, for the first time, we demonstrated that basic modules of ENS

patterning depend on the function of two classes of genes, Rac GTPases and PCP core genes, where the latter are able to control specifically the patterning of enteric neurons without affecting the normal colonisation or differentiation of the ENS. However, several questions still remain to be answered: (1) what is the molecular mechanism underlying the function of these genes? (2) What is the relevance of early patterning of enteric neurons to later events of circuit formation? (3) What are the functional consequences of specific defects in ENS circuitry?

Answering such questions will provide a better understanding of the function of the largest part of the PNS, but it will also help us uncovering the pathogenesis and, possible treatment targets, of those intestinal conditions, such as chronic pseudo-obstruction, slow transit constipation, post-operative HSCR, for which clinical management is at the moment mainly palliative.

## 5.2 Importance of the PCP pathway

Planar Cell Polarity is a term that refers to the coordinated orientation of a population of cells within a single epithelial plane (Adler, 2002; Uemura & Shimada, 2003). This process creates molecular asymmetries that are capable of aligning neighbouring cells and that are essential for development of higher order structures such as the neural tube and the inner ear. However, recent findings have supported the idea that PCP-interactions are not only confined to the polarity of epithelia but they might control broader developmental processes involving cell polarisation, such as cell migration and directed axon and dendritic outgrowth (Montcouquiol *et al.*, 2006).

Our findings support this idea and they demonstrate a direct role for PCP core genes (i.e. Fzd3 and Celsr3) in patterning of enteric neuronal processes. Nevertheless, the molecular mechanism involving these genes in the developing nervous system is still unknown. Our data suggest that PCP genes control interaction of neuronal processes with their environment, as well as their fasciculation. Further studies will be necessary to characterise the mechanisms by which these two events are able to direct growth of axons/neurites *in vivo*.

The activity of PCP genes has a direct effect on cytoskeletal dynamics and, therefore, it is likely to involve the activation of specific intracellular mediators, such as the small Rho GTPases. Accordingly, Rac function is required for patterning of neuronal processes and correct orientation of migrating cells at early stages of gut colonisation. However, it is still unclear whether the patterning defects observed in Rac mutants are equivalent to those found in Fzd3 and Celsr3 mutants. In the former, we found that neuronal tracts at the front of migration were misoriented, while, in the latter, we observed a lack of longitudinal bundles running along the entire length of the midgut. There is a possibility that, since different stages of development were analysed, the two phenotypes reflect the same type of defects in axonal patterning. In fact, the neuronal tracts at the front of migration might act as an initial backbone for further neuronal processes to build on and form thick bundles along the developing midgut and, if this is true, we should expect to fail to find longitudinal tracts in the midgut of Rac mutants and at the front of Fzd3 and Celsr3 mutants at appropriate developmental ages. Alternatively, it is possible that the two groups of genes are targeting independent patterning events and, therefore, Rac function, for example, might control the orientation of neuronal tracts by concomitantly affecting migration and orientation of ENCCs. Further investigation into the common features of the two groups of mutations will hopefully clarify this issue.

Unlike invertebrates, vertebrates seem to have retained a role for Wnt proteins in the PCP pathway. It is unclear whether Wnt proteins (and possibly gradients of them) are required to break the initial cellular symmetry and trigger PCP interactions, or whether they are instead needed to stabilise PCP-mediated cellular interactions once these have already been initiated. Interestingly, Wnt4, Wnt5a and Wnt11 appear to be the only Wnt proteins to signal exclusively through a non-canonical Wnt/PCP pathway. Intriguingly, transcripts for these three genes are expressed in the developing gut. In particular, Wnt5a expression appears to be consistent with ENCC localisation and timing of invasion of the gut mesenchyme (Cervantes *et al.*, 2009; Lickert *et al.*, 2001). In the future, it will be of great interest to test whether this molecule has a specific effect on ENS patterning and whether it interacts with the PCP core genes discovered in our study.

## 5.3 New understanding of enteric neuropathies

Enteric neuropathies represent a significant clinical challenge due to the high morbidity and mortality resulting from the still inadequate treatment of the pathophysiological consequences on gut function. Evidence has been accumulated showing that genetic factors play a relevant role on the onset of enteric neuronal diseases and that a better understanding of the molecular mechanisms controlling the formation of a functional ENS represents a step towards the better understanding of the genetic basis of intestinal motility (and dysmotility) (De Giorgio *et al.*, 2004; Di Nardo *et al.*, 2008).

Our data support this idea and demonstrate, for the first time, that basic patterns of connectivity, established as early as the first enteric neurons differentiate within the developing gut, are fundamental for the appropriate function of the mature ENS. In particular, from the preliminary study of conditional Celsr3 mutants, we propose that the impaired formation of longitudinal tracts during fetal life might relate to a reduced number of $NOS^+$ fibres in the adult myenteric plexus, thus resulting in altered intestinal motility. Nevertheless, further studies will be necessary to elucidate, and correlate, the effects of the mutation on: (1) the morphology and organisation of the ENS plexus and (2) the physiology of the gastrointestinal tract. If a correlation is found between these features, conditional Celsr3 mutant mice might represent one of the first models of enteric dysmotility with specific defects in circuitry formation. It will therefore be of great interest to determine whether mutations in Celsr3 (and Fzd3) are indeed implicated in the aetiology of congenital or sporadic human enteric neuropathies.

## 5.4 Technical advances

*In situ* investigation of single cell morphology has always been an approach that is as appealing as it is prohibitive for the understanding of complex cellular systems such as the nervous system. In particular, in the ENS, the lack of specific markers for subclasses of neurons and the lack of distinct anatomical divisions have always represented a great obstacle in developing useful tools to study the morphology of individual neurons within the ENS network.

Recent technical advances have shown how genetic tools can be used to specifically and permanently trace, with fluorescent tags, single neurons within the CNS in several systems (Lee & Luo, 2001; Livet *et al.*, 2007; Rotolo *et al.*, 2008; Sato *et al.*, 2007). Analogously, in our study, we have devised a novel method to specifically identify isolated enteric neurons in whole mount preparations of embryonic guts by using the genetic inducible fate mapping system *Sox10iCreER$^{T2}$;R26ReYFP*. Inducible recombination of the *R26ReYFP* locus allowed us to specifically titre the efficiency and timing of recombination, thus leading to an efficient single-cell YFP labelling of enteric neurons at an appropriate developmental age (i.e. E12.5). Further developments of this tool and its wider use will be particularly useful to study individual neurons at different developmental ages and in the adult ENS, thus providing a better understanding of the mechanisms controlling the patterning of enteric neurons, the formation of connectivity modules and the function of enteric neuronal circuitry.

Finally, with our work we aim to produce a holistic approach into the study of ENS development, which can combine genetics, anatomy/morphology and physiology and that can lead to a better understanding of the normal and pathological development of this nervous system.

# References

**Adler, P. N. (2002).** Planar signaling and morphogenesis in Drosophila. *Dev Cell* **2**, 525-535.

**Albertinazzi, C., Gilardelli, D., Paris, S., Longhi, R. & de Curtis, I. (1998).** Overexpression of a neural-specific rho family GTPase, cRac1B, selectively induces enhanced neuritogenesis and neurite branching in primary neurons. *J Cell Biol* **142**, 815-825.

**Anderson, R. B., Stewart, A. L. & Young, H. M. (2006).** Phenotypes of neural-crest-derived cells in vagal and sacral pathways. *Cell Tissue Res* **323**, 11-25.

**Anderson, R. B., Turner, K. N., Nikonenko, A. G., Hemperly, J., Schachner, M. & Young, H. M. (2006).** The cell adhesion molecule l1 is required for chain migration of neural crest cells in the developing mouse gut. *Gastroenterology* **130**, 1221-1232.

**Anderson, R. B., Bergner, A. J., Taniguchi, M., Fujisawa, H., Forrai, A., Robb, L. & Young, H. M. (2007).** Effects of different regions of the developing gut on the migration of enteric neural crest-derived cells: a role for Sema3A, but not Sema3F. *Dev Biol* **305**, 287-299.

**Anlauf, M., Schafer, M. K., Eiden, L. & Weihe, E. (2003).** Chemical coding of the human gastrointestinal nervous system: cholinergic, VIPergic, and catecholaminergic phenotypes. *J Comp Neurol* **459**, 90-111.

**Asai, N., Fukuda, T., Wu, Z., Enomoto, A., Pachnis, V., Takahashi, M. & Costantini, F. (2006).** Targeted mutation of serine 697 in the Ret tyrosine kinase causes migration defect of enteric neural crest cells. *Development* **133**, 4507-4516.

**Aube, A. C., Cabarrocas, J., Bauer, J., Philippe, D., Aubert, P., Doulay, F., Liblau, R., Galmiche, J. P. & Neunlist, M. (2006).** Changes in enteric neurone phenotype and intestinal functions in a transgenic mouse model of enteric glia disruption. *Gut* **55**, 630-637.

**Awasaki, T., Saito, M., Sone, M., Suzuki, E., Sakai, R., Ito, K. & Hama, C. (2000).** The Drosophila trio plays an essential role in patterning of axons by regulating their directional extension. *Neuron* **26**, 119-131.

**Aziz, Q. & Thompson, D. G. (1998).** Brain-gut axis in health and disease. *Gastroenterology* **114**, 559-578.

**Baetge, G. & Gershon, M. D. (1989).** Transient catecholaminergic (TC) cells in the vagus nerves and bowel of fetal mice: relationship to the development of enteric neurons. *Dev Biol* **132**, 189-211.

**Baillie, C. T., Kenny, S. E., Rintala, R. J., Booth, J. M. & Lloyd, D. A. (1999).** Long-term outcome and colonic motility after the Duhamel procedure for Hirschsprung's disease. *J Pediatr Surg* **34**, 325-329.

**Baloh, R. H., Enomoto, H., Johnson, E. M., Jr. & Milbrandt, J. (2000).** The GDNF family ligands and receptors - implications for neural development. *Curr Opin Neurobiol* **10**, 103-110.

**Barlow, A., de Graaff, E. & Pachnis, V. (2003).** Enteric nervous system progenitors are coordinately controlled by the G protein-coupled receptor EDNRB and the receptor tyrosine kinase RET. *Neuron* **40**, 905-916.

**Barlow, A. J., Wallace, A. S., Thapar, N. & Burns, A. J. (2008).** Critical numbers of neural crest cells are required in the pathways from the neural tube to the foregut to ensure complete enteric nervous system formation. *Development* **135**, 1681-1691.

**Bass, M. D., Roach, K. A., Morgan, M. R., Mostafavi-Pour, Z., Schoen, T., Muramatsu, T., Mayer, U., Ballestrem, C., Spatz, J. P. & Humphries, M. J. (2007).** Syndecan-4-dependent Rac1 regulation determines directional migration in response to the extracellular matrix. *J Cell Biol* **177**, 527-538.

**Bassotti, G. & Villanacci, V. (2006).** Slow transit constipation: a functional disorder becomes an enteric neuropathy. *World J Gastroenterol* **12**, 4609-4613.

**Bateman, J., Shu, H. & Van Vactor, D. (2000).** The guanine nucleotide exchange factor trio mediates axonal development in the Drosophila embryo. *Neuron* **26**, 93-106.

**Baynash, A. G., Hosoda, K., Giaid, A., Richardson, J. A., Emoto, N., Hammer, R. E. & Yanagisawa, M. (1994).** Interaction of endothelin-3 with endothelin-B receptor is essential for development of epidermal melanocytes and enteric neurons. *Cell* **79**, 1277-1285.

**Bernards, A. & Settleman, J. (2004).** GAP control: regulating the regulators of small GTPases. *Trends Cell Biol* **14**, 377-385.

**Berseth, C. L. (1996).** Gastrointestinal motility in the neonate. *Clin Perinatol* **23**, 179-190.

**Bingham, S., Higashijima, S., Okamoto, H. & Chandrasekhar, A. (2002).** The Zebrafish trilobite gene is essential for tangential migration of branchiomotor neurons. *Dev Biol* **242**, 149-160.

**Bjorklund, H., Dahl, D. & Seiger, A. (1984).** Neurofilament and glial fibrillary acid protein-related immunoreactivity in rodent enteric nervous system. *Neuroscience* **12**, 277-287.

**Blaugrund, E., Pham, T. D., Tennyson, V. M., Lo, L., Sommer, L., Anderson, D. J. & Gershon, M. D. (1996).** Distinct subpopulations of enteric neuronal progenitors defined by time of development, sympathoadrenal lineage markers and Mash-1-dependence. *Development* **122**, 309-320.

**Bodmer, D., Levine-Wilkinson, S., Richmond, A., Hirsh, S. & Kuruvilla, R. (2009).** Wnt5a mediates nerve growth factor-dependent axonal branching and growth in developing sympathetic neurons. *J Neurosci* **29**, 7569-7581.

**Bolis, A., Corbetta, S., Cioce, A. & de Curtis, I. (2003).** Differential distribution of Rac1 and Rac3 GTPases in the developing mouse brain: implications for a role of Rac3 in Purkinje cell differentiation. *Eur J Neurosci* **18**, 2417-2424.

**Bondurand, N., Natarajan, D., Thapar, N., Atkins, C. & Pachnis, V. (2003).** Neuron and glia generating progenitors of the mammalian enteric nervous system isolated from foetal and postnatal gut cultures. *Development* **130**, 6387-6400.

**Bondurand, N., Natarajan, D., Barlow, A., Thapar, N. & Pachnis, V. (2006).** Maintenance of mammalian enteric nervous system progenitors by SOX10 and endothelin 3 signalling. *Development* **133**, 2075-2086.

**Bornstein, J. C. (2009).**Autonomic Nervous System: Gastrointestinal Control. In *Encyclopedia of Neuroscience*, pp. 929-939. Edited by L. R. Squire. Oxford: Academic Press.

**Bowles, J., Schepers, G. & Koopman, P. (2000).** Phylogeny of the SOX family of developmental transcription factors based on sequence and structural indicators. *Dev Biol* **227**, 239-255.

**Bradley, J. S., Jr., Parr, E. J. & Sharkey, K. A. (1997).** Effects of inflammation on cell proliferation in the myenteric plexus of the guinea-pig ileum. *Cell Tissue Res* **289**, 455-461.

**Branchek, T. A. & Gershon, M. D. (1989).** Time course of expression of neuropeptide Y, calcitonin gene-related peptide, and NADPH diaphorase activity in neurons of the developing murine bowel and the appearance of 5-hydroxytryptamine in mucosal enterochromaffin cells. *J Comp Neurol* **285**, 262-273.

**Breau, M. A., Pietri, T., Eder, O., Blanche, M., Brakebusch, C., Fassler, R., Thiery, J. P. & Dufour, S. (2006).** Lack of beta1 integrins in enteric neural crest cells leads to a Hirschsprung-like phenotype. *Development* **133**, 1725-1734.

**Breau, M. A., Dahmani, A., Broders-Bondon, F., Thiery, J. P. & Dufour, S. (2009).** Beta1 integrins are required for the invasion of the caecum and proximal hindgut by enteric neural crest cells. *Development* **136**, 2791-2801.

**Brehmer, A. (2006).** Structure of enteric neurons. *Adv Anat Embryol Cell Biol* **186**, 1-91.

**Briancon-Marjollet, A., Ghogha, A., Nawabi, H., Triki, I., Auziol, C., Fromont, S., Piche, C., Enslen, H., Chebli, K., Cloutier, J. F., Castellani, V., Debant, A. & Lamarche-Vane, N. (2008).** Trio mediates netrin-1-induced Rac1 activation in axon outgrowth and guidance. *Mol Cell Biol* **28**, 2314-2323.

**Britsch, S., Goerich, D. E., Riethmacher, D., Peirano, R. I., Rossner, M., Nave, K. A., Birchmeier, C. & Wegner, M. (2001).** The transcription factor Sox10 is a key regulator of peripheral glial development. *Genes Dev* **15**, 66-78.

**Brookes, S. J. (2001).** Classes of enteric nerve cells in the guinea-pig small intestine. *Anat Rec* **262**, 58-70.

**Brooks, A. S., Oostra, B. A. & Hofstra, R. M. (2005).** Studying the genetics of Hirschsprung's disease: unraveling an oligogenic disorder. *Clin Genet* **67**, 6-14.

**Burns, A. J. & Douarin, N. M. (1998).** The sacral neural crest contributes neurons and glia to the post-umbilical gut: spatiotemporal analysis of the development of the enteric nervous system. *Development* **125**, 4335-4347.

**Burns, A. J., Champeval, D. & Le Douarin, N. M. (2000).** Sacral neural crest cells colonise aganglionic hindgut in vivo but fail to compensate for lack of enteric ganglia. *Dev Biol* **219**, 30-43.

**Burns, A. J. & Le Douarin, N. M. (2001).** Enteric nervous system development: analysis of the selective developmental potentialities of vagal and sacral neural crest cells using quail-chick chimeras. *Anat Rec* **262**, 16-28.

**Burns, A. J., Delalande, J. M. & Le Douarin, N. M. (2002).** In ovo transplantation of enteric nervous system precursors from vagal to sacral neural crest results in extensive hindgut colonisation. *Development* **129**, 2785-2796.

**Burns, A. J. (2005).** Migration of neural crest-derived enteric nervous system precursor cells to and within the gastrointestinal tract. *Int J Dev Biol* **49**, 143-150.

**Bush, T. G., Savidge, T. C., Freeman, T. C., Cox, H. J., Campbell, E. A., Mucke, L., Johnson, M. H. & Sofroniew, M. V. (1998).** Fulminant jejuno-ileitis following ablation of enteric glia in adult transgenic mice. *Cell* **93**, 189-201.

**Cacalano, G., Farinas, I., Wang, L. C., Hagler, K., Forgie, A., Moore, M., Armanini, M., Phillips, H., Ryan, A. M., Reichardt, L. F., Hynes, M., Davies, A. & Rosenthal, A. (1998).** GFRalpha1 is an essential receptor component for GDNF in the developing nervous system and kidney. *Neuron* **21**, 53-62.

**Cadigan, K. M. & Liu, Y. I. (2006).** Wnt signaling: complexity at the surface. *J Cell Sci* **119**, 395-402.

**Cantrell, V. A., Owens, S. E., Chandler, R. L., Airey, D. C., Bradley, K. M., Smith, J. R. & Southard-Smith, E. M. (2004).** Interactions between Sox10 and EdnrB modulate penetrance and severity of aganglionosis in the Sox10Dom mouse model of Hirschsprung disease. *Hum Mol Genet* **13**, 2289-2301.

**Carmona-Fontaine, C., Matthews, H. K., Kuriyama, S., Moreno, M., Dunn, G. A., Parsons, M., Stern, C. D. & Mayor, R. (2008).** Contact inhibition of locomotion in vivo controls neural crest directional migration. *Nature* **456**, 957-961.

**Carreira-Barbosa, F., Concha, M. L., Takeuchi, M., Ueno, N., Wilson, S. W. & Tada, M. (2003).** Prickle 1 regulates cell movements during gastrulation and neuronal migration in zebrafish. *Development* **130**, 4037-4046.

**Causeret, F., Hidalgo-Sanchez, M., Fort, P., Backer, S., Popoff, M. R., Gauthier-Rouviere, C. & Bloch-Gallego, E. (2004).** Distinct roles of Rac1/Cdc42 and Rho/Rock for axon outgrowth and nucleokinesis of precerebellar neurons toward netrin 1. *Development* **131**, 2841-2852.

**Cervantes, S., Yamaguchi, T. P. & Hebrok, M. (2009).** Wnt5a is essential for intestinal elongation in mice. *Dev Biol* **326**, 285-294.

**Chae, T., Kwon, Y. T., Bronson, R., Dikkes, P., Li, E. & Tsai, L. H. (1997).** Mice lacking p35, a neuronal specific activator of Cdk5, display cortical lamination defects, seizures, and adult lethality. *Neuron* **18**, 29-42.

**Chae, J., Kim, M. J., Goo, J. H., Collier, S., Gubb, D., Charlton, J., Adler, P. N. & Park, W. J. (1999).** The Drosophila tissue polarity gene starry night encodes a member of the protocadherin family. *Development* **126**, 5421-5429.

**Chakravarti, A. (2001).** Hirschsprung Disease. In *The Metabolic and Molecular Basis of Inherited Diseases*, pp. 6231-6255. Edited by C. R. Scriver, W. S. Sly & B. Childs. New York: McGraw-Hill.

**Chalazonitis, A., Rothman, T. P., Chen, J. & Gershon, M. D. (1998).** Age-dependent differences in the effects of GDNF and NT-3 on the development of neurons and glia from neural crest-derived precursors immunoselected from the fetal rat gut: expression of GFRalpha-1 in vitro and in vivo. *Dev Biol* **204**, 385-406.

**Chalazonitis, A., Pham, T. D., Rothman, T. P., DiStefano, P. S., Bothwell, M., Blair-Flynn, J., Tessarollo, L. & Gershon, M. D. (2001).** Neurotrophin-3 is required for the survival-differentiation of subsets of developing enteric neurons. *J Neurosci* **21**, 5620-5636.

**Chalazonitis, A., D'Autreaux, F., Guha, U., Pham, T. D., Faure, C., Chen, J. J., Roman, D., Kan, L., Rothman, T. P., Kessler, J. A. & Gershon, M. D. (2004).** Bone morphogenetic protein-2 and -4 limit the number of enteric neurons but promote development of a TrkC-expressing neurotrophin-3-dependent subset. *J Neurosci* **24**, 4266-4282.

**Chalazonitis, A., Pham, T. D., Li, Z., Roman, D., Guha, U., Gomes, W., Kan, L., Kessler, J. A. & Gershon, M. D. (2008).** Bone morphogenetic protein regulation of enteric neuronal phenotypic diversity: relationship to timing of cell cycle exit. *J Comp Neurol* **509**, 474-492.

**Chandrasekhar, A. (2004).** Turning heads: development of vertebrate branchiomotor neurons. *Dev Dyn* **229**, 143-161.

**Chen, L., Liao, G., Waclaw, R. R., Burns, K. A., Linquist, D., Campbell, K., Zheng, Y. & Kuan, C. Y. (2007).** Rac1 controls the formation of midline commissures and the competency of tangential migration in ventral telencephalic neurons. *J Neurosci* **27**, 3884-3893.

**Chen, P. L. & Clandinin, T. R. (2008).** The cadherin Flamingo mediates level-dependent interactions that guide photoreceptor target choice in Drosophila. *Neuron* **58**, 26-33.

**Chen, W. S., Antic, D., Matis, M., Logan, C. Y., Povelones, M., Anderson, G. A., Nusse, R. & Axelrod, J. D. (2008).** Asymmetric homotypic interactions of the atypical cadherin flamingo mediate intercellular polarity signaling. *Cell* **133**, 1093-1105.

**Chitkara, D. K. & Di Lorenzo, C. (2006).** From the bench to the 'crib'-side: implications of scientific advances to paediatric neurogastroenterology and motility. *Neurogastroenterol Motil* **18**, 251-262.

**Cho, Y. J., Zhang, B., Kaartinen, V., Haataja, L., de Curtis, I., Groffen, J. & Heisterkamp, N. (2005).** Generation of rac3 null mutant mice: role of Rac3 in Bcr/Abl-caused lymphoblastic leukemia. *Mol Cell Biol* **25**, 5777-5785.

**Christensen, J. & Rick, G. A. (1985).** Nerve cell density in submucous plexus throughout the gut of cat and opossum. *Gastroenterology* **89**, 1064-1069.

**Chrostek, A., Wu, X., Quondamatteo, F., Hu, R., Sanecka, A., Niemann, C., Langbein, L., Haase, I. & Brakebusch, C. (2006).** Rac1 is crucial for hair follicle integrity but is not essential for maintenance of the epidermis. *Mol Cell Biol* **26**, 6957-6970.

**Ciani, L. & Salinas, P. C. (2005).** WNTs in the vertebrate nervous system: from patterning to neuronal connectivity. *Nat Rev Neurosci* **6**, 351-362.

**Clarke, R. W. & Harris, J. (2004).** The organization of motor responses to noxious stimuli. *Brain Res Brain Res Rev* **46**, 163-172.

**Corbetta, S., Gualdoni, S., Albertinazzi, C., Paris, S., Croci, L., Consalez, G. G. & de Curtis, I. (2005).** Generation and characterization of Rac3 knockout mice. *Mol Cell Biol* **25**, 5763-5776.

**Corbetta, S., D'Adamo, P., Gualdoni, S., Braschi, C., Berardi, N. & de Curtis, I. (2008).** Hyperactivity and novelty-induced hyperreactivity in mice lacking Rac3. *Behav Brain Res* **186**, 246-255.

**Corbetta, S., Gualdoni, S., Ciceri, G., Monari, M., Zuccaro, E., Tybulewicz, V. L. & de Curtis, I. (2009).** Essential role of Rac1 and Rac3 GTPases in neuronal development. *FASEB J*.

**Cornet, A., Savidge, T. C., Cabarrocas, J., Deng, W. L., Colombel, J. F., Lassmann, H., Desreumaux, P. & Liblau, R. S. (2001).** Enterocolitis induced by autoimmune targeting of enteric glial cells: a possible mechanism in Crohn's disease? *Proc Natl Acad Sci U S A* **98**, 13306-13311.

**Corpening, J. C., Cantrell, V. A., Deal, K. K. & Southard-Smith, E. M. (2008).** A Histone2BCerulean BAC transgene identifies differential expression of Phox2b in migrating enteric neural crest derivatives and enteric glia. *Dev Dyn* **237**, 1119-1132.

**Cortesini, C., Cianchi, F., Infantino, A. & Lise, M. (1995).** Nitric oxide synthase and VIP distribution in enteric nervous system in idiopathic chronic constipation. *Dig Dis Sci* **40**, 2450-2455.

**Coulie, B. & Camilleri, M. (1999).** Intestinal pseudo-obstruction. *Annu Rev Med* **50**, 37-55.

**Dabdoub, A., Donohue, M. J., Brennan, A., Wolf, V., Montcouquiol, M., Sassoon, D. A., Hseih, J. C., Rubin, J. S., Salinas, P. C. & Kelley, M. W. (2003).** Wnt signaling mediates reorientation of outer hair cell stereociliary bundles in the mammalian cochlea. *Development* **130**, 2375-2384.

**Danielian, P. S., Muccino, D., Rowitch, D. H., Michael, S. K. & McMahon, A. P. (1998).** Modification of gene activity in mouse embryos in utero by a tamoxifen-inducible form of Cre recombinase. *Curr Biol* **8**, 1323-1326.

**D'Autreaux, F., Morikawa, Y., Cserjesi, P. & Gershon, M. D. (2007).** Hand2 is necessary for terminal differentiation of enteric neurons from crest-derived precursors but not for their migration into the gut or for formation of glia. *Development* **134**, 2237-2249.

**De Calisto, J., Araya, C., Marchant, L., Riaz, C. F. & Mayor, R. (2005).** Essential role of non-canonical Wnt signalling in neural crest migration. *Development* **132**, 2587-2597.

**de Curtis, I. (2008).** Functions of Rac GTPases during neuronal development. *Dev Neurosci* **30**, 47-58.

**De Giorgio, R., Stanghellini, V., Barbara, G., Corinaldesi, R., De Ponti, F., Tonini, M., Bassotti, G. & Sternini, C. (2000).** Primary enteric neuropathies underlying gastrointestinal motor dysfunction. *Scand J Gastroenterol* **35**, 114-122.

**De Giorgio, R., Seri, M., Cogliandro, R., Cusano, R., Fava, M., Caroli, F., Panetta, D., Forabosco, P., Barbara, G., Ravazzolo, R., Ceccherini, I., Corinaldesi, R. & Stanghellini, V. (2001).** Analysis of candidate genes for intrinsic neuropathy in a family with chronic idiopathic intestinal pseudo-obstruction. *Clin Genet* **59**, 131-133.

**De Giorgio, R. & Camilleri, M. (2004).** Human enteric neuropathies: morphology and molecular pathology. *Neurogastroenterol Motil* **16**, 515-531.

**De Giorgio, R., Guerrini, S., Barbara, G., Cremon, C., Stanghellini, V. & Corinaldesi, R. (2004).** New insights into human enteric neuropathies. *Neurogastroenterol Motil* **16 Suppl 1**, 143-147.

**Deglincerti, A., De Giorgio, R., Cefle, K., Devoto, M., Pippucci, T., Castegnaro, G., Panza, E., Barbara, G., Cogliandro, R. F., Mungan, Z., Palanduz, S., Corinaldesi, R., Romeo, G., Seri, M. & Stanghellini, V. (2007).** A novel locus for syndromic chronic idiopathic intestinal pseudo-obstruction maps to chromosome 8q23-q24. *Eur J Hum Genet* **15**, 889-897.

**Delalande, J. M., Barlow, A. J., Thomas, A. J., Wallace, A. S., Thapar, N., Erickson, C. A. & Burns, A. J. (2008).** The receptor tyrosine kinase RET regulates hindgut colonization by sacral neural crest cells. *Dev Biol* **313**, 279-292.

**Di Lorenzo, C. (1999).** Pseudo-obstruction: current approaches. *Gastroenterology* **116**, 980-987.

**Di Nardo, G., Blandizzi, C., Volta, U., Colucci, R., Stanghellini, V., Barbara, G., Del Tacca, M., Tonini, M., Corinaldesi, R. & De Giorgio, R. (2008).** Review article: molecular, pathological and therapeutic features of human enteric neuropathies. *Aliment Pharmacol Ther* **28**, 25-42.

**Dickson, B. J. (2001).** Rho GTPases in growth cone guidance. *Curr Opin Neurobiol* **11**, 103-110.

**Druckenbrod, N. R. & Epstein, M. L. (2005).** The pattern of neural crest advance in the cecum and colon. *Dev Biol* **287**, 125-133.

**Druckenbrod, N. R. & Epstein, M. L. (2007).** Behavior of enteric neural crest-derived cells varies with respect to the migratory wavefront. *Dev Dyn* **236**, 84-92.

**Druckenbrod, N. R., Powers, P. A., Bartley, C. R., Walker, J. W. & Epstein, M. L. (2008).** Targeting of endothelin receptor-B to the neural crest. *Genesis* **46**, 396-400.

**Druckenbrod, N. R. & Epstein, M. L. (2009).** Age-dependent changes in the gut environment restrict the invasion of the hindgut by enteric neural progenitors. *Development* **136**, 3195-3203.

**Du, S. J., Purcell, S. M., Christian, J. L., McGrew, L. L. & Moon, R. T. (1995).** Identification of distinct classes and functional domains of Wnts through expression of wild-type and chimeric proteins in Xenopus embryos. *Mol Cell Biol* **15**, 2625-2634.

**Durbec, P. L., Larsson-Blomberg, L. B., Schuchardt, A., Costantini, F. & Pachnis, V. (1996).** Common origin and developmental dependence on c-ret of subsets of enteric and sympathetic neuroblasts. *Development* **122**, 349-358.

**Durbec, P. & Cremer, H. (2001).** Revisiting the function of PSA-NCAM in the nervous system. *Mol Neurobiol* **24**, 53-64.

**Echelard, Y., Vassileva, G. & McMahon, A. P. (1994).** Cis-acting regulatory sequences governing Wnt-1 expression in the developing mouse CNS. *Development* **120**, 2213-2224.

**Elworthy, S., Pinto, J. P., Pettifer, A., Cancela, M. L. & Kelsh, R. N. (2005).** Phox2b function in the enteric nervous system is conserved in zebrafish and is sox10-dependent. *Mech Dev* **122**, 659-669.

**Enomoto, H., Araki, T., Jackman, A., Heuckeroth, R. O., Snider, W. D., Johnson, E. M., Jr. & Milbrandt, J. (1998).** GFR alpha1-deficient mice have deficits in the enteric nervous system and kidneys. *Neuron* **21**, 317-324.

**Epstein, M. L., Mikawa, T., Brown, A. M. & McFarlin, D. R. (1994).** Mapping the origin of the avian enteric nervous system with a retroviral marker. *Dev Dyn* **201**, 236-244.

**Erickson, C. A. & Goins, T. L. (2000).** Sacral neural crest cell migration to the gut is dependent upon the migratory environment and not cell-autonomous migratory properties. *Dev Biol* **219**, 79-97.

**Etienne-Manneville, S. & Hall, A. (2002).** Rho GTPases in cell biology. *Nature* **420**, 629-635.

**Etienne-Manneville, S. (2004).** Cdc42--the centre of polarity. *J Cell Sci* **117**, 1291-1300.

**Facer, P., Knowles, C. H., Thomas, P. K., Tam, P. K., Williams, N. S. & Anand, P. (2001).** Decreased tyrosine kinase C expression may reflect developmental abnormalities in Hirschsprung's disease and idiopathic slow-transit constipation. *Br J Surg* **88**, 545-552.

**Farndon, P. A. & Bianchi, A. (1983).** Waardenburg's syndrome associated with total aganglionosis. *Arch Dis Child* **58**, 932-933.

**Fenstermaker, A. G., Prasad, A. A., Bechara, A., Adolfs, Y., Tissir, F., Goffinet, A., Zou, Y. & Pasterkamp, R. J. (2010).** Wnt/planar cell polarity signaling controls the anterior-posterior organization of monoaminergic axons in the brainstem. *J Neurosci* **30**, 16053-16064.

**Ferri, G. L., Probert, L., Cocchia, D., Michetti, F., Marangos, P. J. & Polak, J. M. (1982).** Evidence for the presence of S-100 protein in the glial component of the human enteric nervous system. *Nature* **297**, 409-410.

**Fletcher, E. L., Clark, M. J. & Furness, J. B. (2002).** Neuronal and glial localization of GABA transporter immunoreactivity in the myenteric plexus. *Cell Tissue Res* **308**, 339-346.

**Fu, M., Vohra, B. P., Wind, D. & Heuckeroth, R. O. (2006).** BMP signaling regulates murine enteric nervous system precursor migration, neurite fasciculation, and patterning via altered Ncam1 polysialic acid addition. *Dev Biol* **299**, 137-150.

**Fu, M., Sato, Y., Lyons-Warren, A., Zhang, B., Kane, M. A., Napoli, J. L. & Heuckeroth, R. O. (2010).** Vitamin A facilitates enteric nervous system precursor migration by reducing Pten accumulation. *Development* **137**, 631-640.

**Fuchs, S., Herzog, D., Sumara, G., Buchmann-Moller, S., Civenni, G., Wu, X., Chrostek-Grashoff, A., Suter, U., Ricci, R., Relvas, J. B., Brakebusch, C. & Sommer, L. (2009).** Stage-specific control of neural crest stem cell proliferation by the small rho GTPases Cdc42 and Rac1. *Cell Stem Cell* **4**, 236-247.

**Fukuda, T., Kiuchi, K. & Takahashi, M. (2002).** Novel mechanism of regulation of Rac activity and lamellipodia formation by RET tyrosine kinase. *J Biol Chem* **277**, 19114-19121.

**Furness, J. B., Young, H. M., Pompolo, S., Bornstein, J. C., Kunze, W. A. & McConalogue, K. (1995).** Plurichemical transmission and chemical coding of neurons in the digestive tract. *Gastroenterology* **108**, 554-563.

**Furness, J. B. (2000).** Types of neurons in the enteric nervous system. *J Auton Nerv Syst* **81**, 87-96.

**Furness, J. B., Clerc, N., Lomax, A. E., Bornstein, J. C. & Kunze, W. A. (2000).** Shapes and projections of tertiary plexus neurons of the guinea-pig small intestine. *Cell Tissue Res* **300**, 383-387.

**Furness, J. B. (2006).** *The Enteric Nervous System*. Oxford: Blackwell Publishing.

**Furness, J. B. (2009).**Enteric Nervous System: Neural Circuits and Chemical Coding. In *Encyclopedia of Neuroscience*, pp. 1089-1095. Edited by L. R. Squire. Oxford: Academic Press.

**Gabella, G. (1972).** Fine structure of the myenteric plexus in the guinea-pig ileum. *J Anat* **111**, 69-97.

**Gabella, G. (1981).** Ultrastructure of the nerve plexuses of the mammalian intestine: the enteric glial cells. *Neuroscience* **6**, 425-436.

**Gabella, G. (1987).** The number of neurons in the small intestine of mice, guinea-pigs and sheep. *Neuroscience* **22**, 737-752.

**Gabella, G. (1990).** On the plasticity of form and structure of enteric ganglia. *J Auton Nerv Syst* **30 Suppl**, S59-66.

**Gao, F. B., Kohwi, M., Brenman, J. E., Jan, L. Y. & Jan, Y. N. (2000).** Control of dendritic field formation in Drosophila: the roles of flamingo and competition between homologous neurons. *Neuron* **28**, 91-101.

**Gargiulo, A., Auricchio, R., Barone, M. V., Cotugno, G., Reardon, W., Milla, P. J., Ballabio, A., Ciccodicola, A. & Auricchio, A. (2007).** Filamin A is mutated in X-linked chronic idiopathic intestinal pseudo-obstruction with central nervous system involvement. *Am J Hum Genet* **80**, 751-758.

**Gariepy, C. E., Williams, S. C., Richardson, J. A., Hammer, R. E. & Yanagisawa, M. (1998).** Transgenic expression of the endothelin-B receptor prevents congenital intestinal aganglionosis in a rat model of Hirschsprung disease. *J Clin Invest* **102**, 1092-1101.

**Gariepy, C. E. (2004).** Developmental disorders of the enteric nervous system: genetic and molecular bases. *J Pediatr Gastroenterol Nutr* **39**, 5-11.

**Gershon, M. D. & Rothman, T. P. (1991).** Enteric glia. *Glia* **4**, 195-204.

**Gershon, M. D. (1998).** *The Second Brain*. New York: Harper Collins.

**Gianino, S., Grider, J. R., Cresswell, J., Enomoto, H. & Heuckeroth, R. O. (2003).** GDNF availability determines enteric neuron number by controlling precursor proliferation. *Development* **130**, 2187-2198.

**Glogauer, M., Marchal, C. C., Zhu, F., Worku, A., Clausen, B. E., Foerster, I., Marks, P., Downey, G. P., Dinauer, M. & Kwiatkowski, D. J. (2003).** Rac1 deletion in mouse neutrophils has selective effects on neutrophil functions. *J Immunol* **170**, 5652-5657.

**Goldberg, E. L. (1984).** An epidemiological study of Hirschsprung's disease. *Int J Epidemiol* **13**, 479-485.

**Goodrich, L. V. (2008).** The plane facts of PCP in the CNS. *Neuron* **60**, 9-16.

**Govek, E. E., Newey, S. E. & Van Aelst, L. (2005).** The role of the Rho GTPases in neuronal development. *Genes Dev* **19**, 1-49.

**Gualdoni, S., Albertinazzi, C., Corbetta, S., Valtorta, F. & de Curtis, I. (2007).** Normal levels of Rac1 are important for dendritic but not axonal development in hippocampal neurons. *Biol Cell* **99**, 455-464.

**Haataja, L., Groffen, J. & Heisterkamp, N. (1997).** Characterization of RAC3, a novel member of the Rho family. *J Biol Chem* **272**, 20384-20388.

**Hajdo-Milasinovic, A., Ellenbroek, S. I., van Es, S., van der Vaart, B. & Collard, J. G. (2007).** Rac1 and Rac3 have opposing functions in cell adhesion and differentiation of neuronal cells. *J Cell Sci* **120**, 555-566.

**Hajdo-Milasinovic, A., van der Kammen, R. A., Moneva, Z. & Collard, J. G. (2009).** Rac3 inhibits adhesion and differentiation of neuronal cells by modifying GIT1 downstream signaling. *J Cell Sci* **122**, 2127-2136.

**Hamilton, J. & Bodurtha, J. N. (1989).** Congenital central hypoventilation syndrome and Hirschsprung's disease in half sibs. *J Med Genet* **26**, 272-274.

**Hamoudi, A. B., Reiner, C. B., Boles, E. T., Jr., McClung, H. J. & Kerzner, B. (1982).** Acetylthiocholinesterase staining activity of rectal mucosa. Its use in the diagnosis of Hirschsprung's disease. *Arch Pathol Lab Med* **106**, 670-672.

**Hanani, M. & Reichenbach, A. (1994).** Morphology of horseradish peroxidase (HRP)-injected glial cells in the myenteric plexus of the guinea-pig. *Cell Tissue Res* **278**, 153-160.

**Hao, M. M., Anderson, R. B., Kobayashi, K., Whitington, P. M. & Young, H. M. (2008).** The migratory behavior of immature enteric neurons. *Dev Neurobiol*.

**Hao, M. M. & Young, H. M. (2009).** Development of enteric neuron diversity. *J Cell Mol Med* **13**, 1193-1210.

**Haricharan, R. N. & Georgeson, K. E. (2008).** Hirschsprung disease. *Semin Pediatr Surg* **17**, 266-275.

**Heanue, T. A. & Pachnis, V. (2007).** Enteric nervous system development and Hirschsprung's disease: advances in genetic and stem cell studies. *Nat Rev Neurosci* **8**, 466-479.

**Hearn, C. J., Murphy, M. & Newgreen, D. (1998).** GDNF and ET-3 differentially modulate the numbers of avian enteric neural crest cells and enteric neurons in vitro. *Dev Biol* **197**, 93-105.

**Heasman, S. J. & Ridley, A. J. (2008).** Mammalian Rho GTPases: new insights into their functions from in vivo studies. *Nat Rev Mol Cell Biol* **9**, 690-701.

**Heisenberg, C. P., Tada, M., Rauch, G. J., Saude, L., Concha, M. L., Geisler, R., Stemple, D. L., Smith, J. C. & Wilson, S. W. (2000).** Silberblick/Wnt11 mediates convergent extension movements during zebrafish gastrulation. *Nature* **405**, 76-81.

**Hendershot, T. J., Liu, H., Sarkar, A. A., Giovannucci, D. R., Clouthier, D. E., Abe, M. & Howard, M. J. (2007).** Expression of Hand2 is sufficient for neurogenesis and cell type-specific gene expression in the enteric nervous system. *Dev Dyn* **236**, 93-105.

**Hendzel, M. J., Wei, Y., Mancini, M. A., Van Hooser, A., Ranalli, T., Brinkley, B. R., Bazett-Jones, D. P. & Allis, C. D. (1997).** Mitosis-specific phosphorylation of histone H3 initiates primarily within pericentromeric heterochromatin during G2 and spreads in an ordered fashion coincident with mitotic chromosome condensation. *Chromosoma* **106**, 348-360.

**Herbarth, B., Pingault, V., Bondurand, N., Kuhlbrodt, K., Hermans-Borgmeyer, I., Puliti, A., Lemort, N., Goossens, M. & Wegner, M. (1998).** Mutation of the Sry-related Sox10 gene in Dominant megacolon, a mouse model for human Hirschsprung disease. *Proc Natl Acad Sci U S A* **95**, 5161-5165.

**Heuckeroth, R. O., Lampe, P. A., Johnson, E. M. & Milbrandt, J. (1998).** Neurturin and GDNF promote proliferation and survival of enteric neuron and glial progenitors in vitro. *Dev Biol* **200**, 116-129.

**Heuckeroth, R. O., Enomoto, H., Grider, J. R., Golden, J. P., Hanke, J. A., Jackman, A., Molliver, D. C., Bardgett, M. E., Snider, W. D., Johnson, E. M., Jr. & Milbrandt, J. (1999).** Gene targeting reveals a critical role for neurturin in the development and maintenance of enteric, sensory, and parasympathetic neurons. *Neuron* **22**, 253-263.

**Hofstra, R. M., Osinga, J., Tan-Sindhunata, G., Wu, Y., Kamsteeg, E. J., Stulp, R. P., van Ravenswaaij-Arts, C., Majoor-Krakauer, D., Angrist, M., Chakravarti, A., Meijers, C. & Buys, C. H. (1996).** A homozygous mutation in the endothelin-3 gene associated with a combined Waardenburg type 2 and Hirschsprung phenotype (Shah-Waardenburg syndrome). *Nat Genet* **12**, 445-447.

**Holmberg, A., Olsson, C. & Holmgren, S. (2006).** The effects of endogenous and exogenous nitric oxide on gut motility in zebrafish Danio rerio embryos and larvae. *J Exp Biol* **209**, 2472-2479.

**Horstadius, S. (1950).** *The Neural Crest*. Cambridge: Cambridge University Press.

**Hosoda, K., Hammer, R. E., Richardson, J. A., Baynash, A. G., Cheung, J. C., Giaid, A. & Yanagisawa, M. (1994).** Targeted and natural (piebald-lethal) mutations of endothelin-B receptor gene produce megacolon associated with spotted coat color in mice. *Cell* **79**, 1267-1276.

**Hotta, R., Anderson, R. B., Kobayashi, K., Newgreen, D. F. & Young, H. M. (2010).** Effects of tissue age, presence of neurones and endothelin-3 on the ability of enteric neurone precursors to colonize recipient gut: implications for cell-based therapies. *Neurogastroenterol Motil* **22**, 331-e386.

**Inoue, A., Yanagisawa, M., Kimura, S., Kasuya, Y., Miyauchi, T., Goto, K. & Masaki, T. (1989).** The human endothelin family: three structurally and pharmacologically distinct isopeptides predicted by three separate genes. *Proc Natl Acad Sci U S A* **86**, 2863-2867.

**Jaffe, A. B. & Hall, A. (2005).** Rho GTPases: biochemistry and biology. *Annu Rev Cell Dev Biol* **21**, 247-269.

**Jessen, K. R. & Mirsky, R. (1980).** Glial cells in the enteric nervous system contain glial fibrillary acidic protein. *Nature* **286**, 736-737.

**Jessen, K. R. & Mirsky, R. (1983).** Astrocyte-like glia in the peripheral nervous system: an immunohistochemical study of enteric glia. *J Neurosci* **3**, 2206-2218.

**Jessen, J. R., Topczewski, J., Bingham, S., Sepich, D. S., Marlow, F., Chandrasekhar, A. & Solnica-Krezel, L. (2002).** Zebrafish trilobite identifies new roles for Strabismus in gastrulation and neuronal movements. *Nat Cell Biol* **4**, 610-615.

**Jiang, Y., Liu, M. T. & Gershon, M. D. (2003).** Netrins and DCC in the guidance of migrating neural crest-derived cells in the developing bowel and pancreas. *Dev Biol* **258**, 364-384.

**Jing, S., Wen, D., Yu, Y., Holst, P. L., Luo, Y., Fang, M., Tamir, R., Antonio, L., Hu, Z., Cupples, R., Louis, J. C., Hu, S., Altrock, B. W. & Fox, G. M. (1996).** GDNF-induced activation of the ret protein tyrosine kinase is mediated by GDNFR-alpha, a novel receptor for GDNF. *Cell* **85**, 1113-1124.

**Kapur, R. P., Yost, C. & Palmiter, R. D. (1992).** A transgenic model for studying development of the enteric nervous system in normal and aganglionic mice. *Development* **116**, 167-175.

**Kapur, R. P., Sweetser, D. A., Doggett, B., Siebert, J. R. & Palmiter, R. D. (1995).** Intercellular signals downstream of endothelin receptor-B mediate colonization of the large intestine by enteric neuroblasts. *Development* **121**, 3787-3795.

**Kapur, R. P. (1999).** Early death of neural crest cells is responsible for total enteric aganglionosis in Sox10(Dom)/Sox10(Dom) mouse embryos. *Pediatr Dev Pathol* **2**, 559-569.

**Kapur, R. P. (2000).** Colonization of the murine hindgut by sacral crest-derived neural precursors: experimental support for an evolutionarily conserved model. *Dev Biol* **227**, 146-155.

**Kapur, R. P. & Correa, H. (2009).** Architectural malformation of the muscularis propria as a cause for intestinal pseudo-obstruction: two cases and a review of the literature. *Pediatr Dev Pathol* **12**, 156-164.

**Kassai, H., Terashima, T., Fukaya, M., Nakao, K., Sakahara, M., Watanabe, M. & Aiba, A. (2008).** Rac1 in cortical projection neurons is selectively required for midline crossing of commissural axonal formation. *Eur J Neurosci* **28**, 257-267.

**Kaufmann, N., Wills, Z. P. & Van Vactor, D. (1998).** Drosophila Rac1 controls motor axon guidance. *Development* **125**, 453-461.

**Kawauchi, T., Chihama, K., Nabeshima, Y. & Hoshino, M. (2003).** The in vivo roles of STEF/Tiam1, Rac1 and JNK in cortical neuronal migration. *EMBO J* **22**, 4190-4201.

**Keeble, T. R., Halford, M. M., Seaman, C., Kee, N., Macheda, M., Anderson, R. B., Stacker, S. A. & Cooper, H. M. (2006).** The Wnt receptor Ryk is required for Wnt5a-mediated axon guidance on the contralateral side of the corpus callosum. *J Neurosci* **26**, 5840-5848.

**Kilian, B., Mansukoski, H., Barbosa, F. C., Ulrich, F., Tada, M. & Heisenberg, C. P. (2003).** The role of Ppt/Wnt5 in regulating cell shape and movement during zebrafish gastrulation. *Mech Dev* **120**, 467-476.

**Kim, J., Lo, L., Dormand, E. & Anderson, D. J. (2003).** SOX10 maintains multipotency and inhibits neuronal differentiation of neural crest stem cells. *Neuron* **38**, 17-31.

**Kohn, A. D. & Moon, R. T. (2005).** Wnt and calcium signaling: beta-catenin-independent pathways. *Cell Calcium* **38**, 439-446.

**Kondyli, M., Varakis, J. & Assimakopoulou, M. (2005).** Expression of p75NTR and Trk neurotrophin receptors in the enteric nervous system of human adults. *Anat Sci Int* **80**, 223-228.

**Krishnamurthy, S., Schuffler, M. D., Rohrmann, C. A. & Pope, C. E., 2nd (1985).** Severe idiopathic constipation is associated with a distinctive abnormality of the colonic myenteric plexus. *Gastroenterology* **88**, 26-34.

**Kruger, G. M., Mosher, J. T., Tsai, Y. H., Yeager, K. J., Iwashita, T., Gariepy, C. E. & Morrison, S. J. (2003).** Temporally distinct requirements for endothelin receptor B in the generation and migration of gut neural crest stem cells. *Neuron* **40**, 917-929.

**Kuhlbrodt, K., Herbarth, B., Sock, E., Hermans-Borgmeyer, I. & Wegner, M. (1998).** Sox10, a novel transcriptional modulator in glial cells. *J Neurosci* **18**, 237-250.

**Landman, K. A., Simpson, M. J. & Newgreen, D. F. (2007).** Mathematical and experimental insights into the development of the enteric nervous system and Hirschsprung's disease. *Dev Growth Differ* **49**, 277-286.

**Lane, P. W. & Liu, H. M. (1984).** Association of megacolon with a new dominant spotting gene (Dom) in the mouse. *J Hered* **75**, 435-439.

**Lang, D., Chen, F., Milewski, R., Li, J., Lu, M. M. & Epstein, J. A. (2000).** Pax3 is required for enteric ganglia formation and functions with Sox10 to modulate expression of c-ret. *J Clin Invest* **106**, 963-971.

**Lang, D. & Epstein, J. A. (2003).** Sox10 and Pax3 physically interact to mediate activation of a conserved c-RET enhancer. *Hum Mol Genet* **12**, 937-945.

**Laranjeira, C. S. (2010).** In vivo identification of neural stem cells in the enteric nervous system. Unpublished PhD thesis: University College London, UK.

**Le Douarin, N. (1973).** A biological cell labeling technique and its use in expermental embryology. *Dev Biol* **30**, 217-222.

**Le Douarin, N. M. & Teillet, M. A. (1973).** The migration of neural crest cells to the wall of the digestive tract in avian embryo. *J Embryol Exp Morphol* **30**, 31-48.

**Le Douarin, N. M. & Teillet, M. A. (1974).** Experimental analysis of the migration and differentiation of neuroblasts of the autonomic nervous system and of neurectodermal mesenchymal derivatives, using a biological cell marking technique. *Dev Biol* **41**, 162-184.

**Le Douarin, N. M., Renaud, D., Teillet, M. A. & Le Douarin, G. H. (1975).** Cholinergic differentiation of presumptive adrenergic neuroblasts in interspecific chimeras after heterotopic transplantations. *Proc Natl Acad Sci U S A* **72**, 728-732.

**Le Douarin, N. M. & Kalcheim, C. (1999).** *The Neural Crest*, second edn. Cambridge: Cambridge University Press.

**Lee, T. & Luo, L. (2001).** Mosaic analysis with a repressible cell marker (MARCM) for Drosophila neural development. *Trends Neurosci* **24**, 251-254.

**Lee, R. C., Clandinin, T. R., Lee, C. H., Chen, P. L., Meinertzhagen, I. A. & Zipursky, S. L. (2003).** The protocadherin Flamingo is required for axon target selection in the Drosophila visual system. *Nat Neurosci* **6**, 557-563.

**Leibl, M. A., Ota, T., Woodward, M. N., Kenny, S. E., Lloyd, D. A., Vaillant, C. R. & Edgar, D. H. (1999).** Expression of endothelin 3 by mesenchymal cells of embryonic mouse caecum. *Gut* **44**, 246-252.

**Li, Z. S., Pham, T. D., Tamir, H., Chen, J. J. & Gershon, M. D. (2004).** Enteric dopaminergic neurons: definition, developmental lineage, and effects of extrinsic denervation. *J Neurosci* **24**, 1330-1339.

**Li, L., Hutchins, B. I. & Kalil, K. (2009).** Wnt5a induces simultaneous cortical axon outgrowth and repulsive axon guidance through distinct signaling mechanisms. *J Neurosci* **29**, 5873-5883.

**Lickert, H., Kispert, A., Kutsch, S. & Kemler, R. (2001).** Expression patterns of Wnt genes in mouse gut development. *Mech Dev* **105**, 181-184.

**Liebl, E. C., Forsthoefel, D. J., Franco, L. S., Sample, S. H., Hess, J. E., Cowger, J. A., Chandler, M. P., Shupert, A. M. & Seeger, M. A. (2000).** Dosage-sensitive, reciprocal genetic interactions between the Abl tyrosine kinase and the putative GEF trio reveal trio's role in axon pathfinding. *Neuron* **26**, 107-118.

**Liu, Y., Shi, J., Lu, C. C., Wang, Z. B., Lyuksyutova, A. I., Song, X. J. & Zou, Y. (2005).** Ryk-mediated Wnt repulsion regulates posterior-directed growth of corticospinal tract. *Nat Neurosci* **8**, 1151-1159.

**Livet, J., Weissman, T. A., Kang, H., Draft, R. W., Lu, J., Bennis, R. A., Sanes, J. R. & Lichtman, J. W. (2007).** Transgenic strategies for combinatorial expression of fluorescent proteins in the nervous system. *Nature* **450**, 56-62.

**Lo, L. C., Johnson, J. E., Wuenschell, C. W., Saito, T. & Anderson, D. J. (1991).** Mammalian achaete-scute homolog 1 is transiently expressed by spatially restricted subsets of early neuroepithelial and neural crest cells. *Genes Dev* **5**, 1524-1537.

**Lomax, A. E., Sharkey, K. A. & Furness, J. B. (2010).** The participation of the sympathetic innervation of the gastrointestinal tract in disease states. *Neurogastroenterol Motil* **22**, 7-18.

**Luo, L., Liao, Y. J., Jan, L. Y. & Jan, Y. N. (1994).** Distinct morphogenetic functions of similar small GTPases: Drosophila Drac1 is involved in axonal outgrowth and myoblast fusion. *Genes Dev* **8**, 1787-1802.

**Luo, L., Hensch, T. K., Ackerman, L., Barbel, S., Jan, L. Y. & Jan, Y. N. (1996).** Differential effects of the Rac GTPase on Purkinje cell axons and dendritic trunks and spines. *Nature* **379**, 837-840.

**Lyuksyutova, A. I., Lu, C. C., Milanesio, N., King, L. A., Guo, N., Wang, Y., Nathans, J., Tessier-Lavigne, M. & Zou, Y. (2003).** Anterior-posterior guidance of commissural axons by Wnt-frizzled signaling. *Science* **302**, 1984-1988.

**Malosio, M. L., Gilardelli, D., Paris, S., Albertinazzi, C. & de Curtis, I. (1997).** Differential expression of distinct members of Rho family GTP-binding proteins during neuronal development: identification of Rac1B, a new neural-specific member of the family. *J Neurosci* **17**, 6717-6728.

**Manié, S., Santoro, M., Fusco, A. & Billaud, M. (2001).** The RET receptor: function in development and dysfunction in congenital malformation. *Trends in Genetics* **17**, 580-589.

**Mashimo, H., Kjellin, A. & Goyal, R. K. (2000).** Gastric stasis in neuronal nitric oxide synthase-deficient knockout mice. *Gastroenterology* **119**, 766-773.

**Matsuoka, T., Ahlberg, P. E., Kessaris, N., Iannarelli, P., Dennehy, U., Richardson, W. D., McMahon, A. P. & Koentges, G. (2005).** Neural crest origins of the neck and shoulder. *Nature* **436**, 347-355.

**Matthews, H. K., Marchant, L., Carmona-Fontaine, C., Kuriyama, S., Larrain, J., Holt, M. R., Parsons, M. & Mayor, R. (2008).** Directional migration of neural crest cells in vivo is regulated by Syndecan-4/Rac1 and non-canonical Wnt signaling/RhoA. *Development* **135**, 1771-1780.

**McKeown, S. J., Chow, C. W. & Young, H. M. (2001).** Development of the submucous plexus in the large intestine of the mouse. *Cell Tissue Res* **303**, 301-305.

**Meier-Ruge, W. (1974).** Hirschsprung's disease: its aetiology, pathogenesis and differential diagnosis. *Curr Top Pathol* **59**, 131-179.

**Meier-Ruge, W. (1992).** Epidemiology of congenital innervation defects of the distal colon. *Virchows Arch A Pathol Anat Histopathol* **420**, 171-177.

**Mlodzik, M. (2002).** Planar cell polarization: do the same mechanisms regulate Drosophila tissue polarity and vertebrate gastrulation? *Trends Genet* **18**, 564-571.

**Moll, J., Sansig, G., Fattori, E. & van der Putten, H. (1991).** The murine rac1 gene: cDNA cloning, tissue distribution and regulated expression of rac1 mRNA by disassembly of actin microfilaments. *Oncogene* **6**, 863-866.

**Montcouquiol, M., Crenshaw, E. B., 3rd & Kelley, M. W. (2006).** Noncanonical Wnt signaling and neural polarity. *Annu Rev Neurosci* **29**, 363-386.

**Moore, M. W., Klein, R. D., Farinas, I., Sauer, H., Armanini, M., Phillips, H., Reichardt, L. F., Ryan, A. M., Carver-Moore, K. & Rosenthal, A. (1996).** Renal and neuronal abnormalities in mice lacking GDNF. *Nature* **382**, 76-79.

**Morgan, M. R., Humphries, M. J. & Bass, M. D. (2007).** Synergistic control of cell adhesion by integrins and syndecans. *Nat Rev Mol Cell Biol* **8**, 957-969.

**Muller, D., Djebbara-Hannas, Z., Jourdain, P., Vutskits, L., Durbec, P., Rougon, G. & Kiss, J. Z. (2000).** Brain-derived neurotrophic factor restores long-term potentiation in polysialic acid-neural cell adhesion molecule-deficient hippocampus. *Proc Natl Acad Sci U S A* **97**, 4315-4320.

**Nagahama, M., Semba, R., Tsuzuki, M. & Aoki, E. (2001).** L-arginine immunoreactive enteric glial cells in the enteric nervous system of rat ileum. *Biol Signals Recept* **10**, 336-340.

**Nataf, V., Lecoin, L., Eichmann, A. & Le Douarin, N. M. (1996).** Endothelin-B receptor is expressed by neural crest cells in the avian embryo. *Proc Natl Acad Sci U S A* **93**, 9645-9650.

**Natarajan, D., Grigoriou, M., Marcos-Gutierrez, C. V., Atkins, C. & Pachnis, V. (1999).** Multipotential progenitors of the mammalian enteric nervous system capable of colonising aganglionic bowel in organ culture. *Development* **126**, 157-168.

**Natarajan, D., Marcos-Gutierrez, C., Pachnis, V. & de Graaff, E. (2002).** Requirement of signalling by receptor tyrosine kinase RET for the directed migration of enteric nervous system progenitor cells during mammalian embryogenesis. *Development* **129**, 5151-5160.

**Newgreen, D. & Thiery, J. P. (1980).** Fibronectin in early avian embryos: synthesis and distribution along the migration pathways of neural crest cells. *Cell Tissue Res* **211**, 269-291.

**Newgreen, D. & Young, H. M. (2002).** Enteric nervous system: development and developmental disturbances--part 1. *Pediatr Dev Pathol* **5**, 224-247.

**Newsome, T. P., Schmidt, S., Dietzl, G., Keleman, K., Asling, B., Debant, A. & Dickson, B. J. (2000).** Trio combines with dock to regulate Pak activity during photoreceptor axon pathfinding in Drosophila. *Cell* **101**, 283-294.

**Ng, J., Nardine, T., Harms, M., Tzu, J., Goldstein, A., Sun, Y., Dietzl, G., Dickson, B. J. & Luo, L. (2002).** Rac GTPases control axon growth, guidance and branching. *Nature* **416**, 442-447.

**Nikolic, M., Chou, M. M., Lu, W., Mayer, B. J. & Tsai, L. H. (1998).** The p35/Cdk5 kinase is a neuron-specific Rac effector that inhibits Pak1 activity. *Nature* **395**, 194-198.

**Nusse, R. (2005).** Wnt signaling in disease and in development. *Cell Res* **15**, 28-32.

**O'Brien, S. P., Seipel, K., Medley, Q. G., Bronson, R., Segal, R. & Streuli, M. (2000).** Skeletal muscle deformity and neuronal disorder in Trio exchange factor-deficient mouse embryos. *Proc Natl Acad Sci U S A* **97**, 12074-12078.

**Okamura, Y. & Saga, Y. (2008).** Notch signaling is required for the maintenance of enteric neural crest progenitors. *Development* **135**, 3555-3565.

**O'Kane, E. M., Stone, T. W. & Morris, B. J. (2003).** Distribution of Rho family GTPases in the adult rat hippocampus and cerebellum. *Brain Res Mol Brain Res* **114**, 1-8.

**Pachnis, V., Mankoo, B. & Costantini, F. (1993).** Expression of the c-ret proto-oncogene during mouse embryogenesis. *Development* **119**, 1005-1017.

**Pankov, R., Endo, Y., Even-Ram, S., Araki, M., Clark, K., Cukierman, E., Matsumoto, K. & Yamada, K. M. (2005).** A Rac switch regulates random versus directionally persistent cell migration. *J Cell Biol* **170**, 793-802.

**Paratore, C., Goerich, D. E., Suter, U., Wegner, M. & Sommer, L. (2001).** Survival and glial fate acquisition of neural crest cells are regulated by an interplay between the transcription factor Sox10 and extrinsic combinatorial signaling. *Development* **128**, 3949-3961.

**Paratore, C., Eichenberger, C., Suter, U. & Sommer, L. (2002).** Sox10 haploinsufficiency affects maintenance of progenitor cells in a mouse model of Hirschsprung disease. *Hum Mol Genet* **11**, 3075-3085.

**Park, M. & Moon, R. T. (2002).** The planar cell-polarity gene stbm regulates cell behaviour and cell fate in vertebrate embryos. *Nat Cell Biol* **4**, 20-25.

**Park, W. & Vaezi, M. F. (2005).** Etiology and Pathogenesis of Achalasia: The Current Understanding. *Am J Gastroenterol* **100**, 1404-1414.

**Pattyn, A., Morin, X., Cremer, H., Goridis, C. & Brunet, J. F. (1997).** Expression and interactions of the two closely related homeobox genes Phox2a and Phox2b during neurogenesis. *Development* **124**, 4065-4075.

**Pattyn, A., Morin, X., Cremer, H., Goridis, C. & Brunet, J. F. (1999).** The homeobox gene Phox2b is essential for the development of autonomic neural crest derivatives. *Nature* **399**, 366-370.

**Peters-van der Sanden, M. J., Kirby, M. L., Gittenberger-de Groot, A., Tibboel, D., Mulder, M. P. & Meijers, C. (1993).** Ablation of various regions within the avian vagal neural crest has differential effects on ganglion formation in the fore-, mid- and hindgut. *Dev Dyn* **196**, 183-194.

**Pham, T. D., Gershon, M. D. & Rothman, T. P. (1991).** Time of origin of neurons in the murine enteric nervous system: sequence in relation to phenotype. *J Comp Neurol* **314**, 789-798.

**Pichel, J. G., Shen, L., Sheng, H. Z., Granholm, A. C., Drago, J., Grinberg, A., Lee, E. J., Huang, S. P., Saarma, M., Hoffer, B. J., Sariola, H. & Westphal, H. (1996).** Defects in enteric innervation and kidney development in mice lacking GDNF. *Nature* **382**, 73-76.

**Pingault, V., Bondurand, N., Kuhlbrodt, K., Goerich, D. E., Prehu, M. O., Puliti, A., Herbarth, B., Hermans-Borgmeyer, I., Legius, E., Matthijs, G., Amiel, J., Lyonnet, S., Ceccherini, I., Romeo, G., Smith, J. C., Read, A. P., Wegner, M. & Goossens, M. (1998).** SOX10 mutations in patients with Waardenburg-Hirschsprung disease. *Nat Genet* **18**, 171-173.

**Porter, A. J., Wattchow, D. A., Hunter, A. & Costa, M. (1998).** Abnormalities of nerve fibers in the circular muscle of patients with slow transit constipation. *Int J Colorectal Dis* **13**, 208-216.

**Powley, T. L. (2000).** Vagal input to the enteric nervous system. *Gut* **47 Suppl 4**, iv30-32; discussion iv36.

**Puffenberger, E. G., Hosoda, K., Washington, S. S., Nakao, K., deWit, D., Yanagisawa, M. & Chakravart, A. (1994).** A missense mutation of the endothelin-B receptor gene in multigenic Hirschsprung's disease. *Cell* **79**, 1257-1266.

**Qian, D., Jones, C., Rzadzinska, A., Mark, S., Zhang, X., Steel, K. P., Dai, X. & Chen, P. (2007).** Wnt5a functions in planar cell polarity regulation in mice. *Dev Biol* **306**, 121-133.

**Qu, Z. D., Thacker, M., Castelucci, P., Bagyanszki, M., Epstein, M. L. & Furness, J. B. (2008).** Immunohistochemical analysis of neuron types in the mouse small intestine. *Cell Tissue Res* **334**, 147-161.

**Qu, Y., Glasco, D. M., Zhou, L., Sawant, A., Ravni, A., Fritzsch, B., Damrau, C., Murdoch, J. N., Evans, S., Pfaff, S. L., Formstone, C., Goffinet, A. M., Chandrasekhar, A. & Tissir, F. (2010).** Atypical cadherins Celsr1-3 differentially regulate migration of facial branchiomotor neurons in mice. *J Neurosci* **30**, 9392-9401.

**Rauch, U., Klotz, M., Maas-Omlor, S., Wink, E., Hansgen, A., Hagl, C., Holland-Cunz, S. & Schafer, K. H. (2006).** Expression of intermediate filament proteins and neuronal markers in the human fetal gut. *J Histochem Cytochem* **54**, 39-46.

**Ridley, A. J., Schwartz, M. A., Burridge, K., Firtel, R. A., Ginsberg, M. H., Borisy, G., Parsons, J. T. & Horwitz, A. R. (2003).** Cell migration: integrating signals from front to back. *Science* **302**, 1704-1709.

**Roberts, A. W., Kim, C., Zhen, L., Lowe, J. B., Kapur, R., Petryniak, B., Spaetti, A., Pollock, J. D., Borneo, J. B., Bradford, G. B., Atkinson, S. J., Dinauer, M. C. & Williams, D. A. (1999).** Deficiency of the hematopoietic cell-specific Rho family GTPase Rac2 is characterized by abnormalities in neutrophil function and host defense. *Immunity* **10**, 183-196.

**Roberts, R. R., Murphy, J. F., Young, H. M. & Bornstein, J. C. (2007).** Development of colonic motility in the neonatal mouse-studies using spatiotemporal maps. *Am J Physiol Gastrointest Liver Physiol* **292**, G930-938.

**Roberts, R. R., Bornstein, J. C., Bergner, A. J. & Young, H. M. (2008).** Disturbances of colonic motility in mouse models of Hirschsprung's disease. *Am J Physiol Gastrointest Liver Physiol* **294**, G996-G1008.

**Roberts, R. R., Ellis, M., Gwynne, R. M., Bergner, A. J., Lewis, M. D., Beckett, E. A., Bornstein, J. C. & Young, H. M. (2010).** The first intestinal motility patterns in fetal mice are not mediated by neurons or interstitial cells of Cajal. *J Physiol* **588**, 1153-1169.

**Rossi, J., Luukko, K., Poteryaev, D., Laurikainen, A., Sun, Y. F., Laakso, T., Eerikainen, S., Tuominen, R., Lakso, M., Rauvala, H., Arumae, U., Pasternack, M., Saarma, M. & Airaksinen, M. S. (1999).** Retarded growth and deficits in the enteric and parasympathetic nervous system in mice lacking GFR alpha2, a functional neurturin receptor. *Neuron* **22**, 243-252.

**Rosso, S. B., Sussman, D., Wynshaw-Boris, A. & Salinas, P. C. (2005).** Wnt signaling through Dishevelled, Rac and JNK regulates dendritic development. *Nat Neurosci* **8**, 34-42.

**Rothman, T. P. & Gershon, M. D. (1982).** Phenotypic expression in the developing murine enteric nervous system. *J Neurosci* **2**, 381-393.

**Rothman, T. P., Nilaver, G. & Gershon, M. D. (1984).** Colonization of the developing murine enteric nervous system and subsequent phenotypic expression by the precursors of peptidergic neurons. *J Comp Neurol* **225**, 13-23.

**Rothman, T. P., Tennyson, V. M. & Gershon, M. D. (1986).** Colonization of the bowel by the precursors of enteric glia: studies of normal and congenitally aganglionic mutant mice. *J Comp Neurol* **252**, 493-506.

**Rothman, T. P., Chen, J., Howard, M. J., Costantini, F., Schuchardt, A., Pachnis, V. & Gershon, M. D. (1996).** Increased expression of laminin-1 and collagen (IV) subunits in the aganglionic bowel of ls/ls, but not c-ret -/- mice. *Dev Biol* **178**, 498-513.

**Rotolo, T., Smallwood, P. M., Williams, J. & Nathans, J. (2008).** Genetically-directed, cell type-specific sparse labeling for the analysis of neuronal morphology. *PLoS One* **3**, e4099.

**Ruhl, A., Franzke, S., Collins, S. M. & Stremmel, W. (2001).** Interleukin-6 expression and regulation in rat enteric glial cells. *Am J Physiol Gastrointest Liver Physiol* **280**, G1163-1171.

**Ruhl, A., Franzke, S. & Stremmel, W. (2001).** IL-1beta and IL-10 have dual effects on enteric glial cell proliferation. *Neurogastroenterol Motil* **13**, 89-94.

**Ruhl, A. (2005).** Glial cells in the gut. *Neurogastroenterol Motil* **17**, 777-790.

**Sanchez, M. P., Silos-Santiago, I., Frisen, J., He, B., Lira, S. A. & Barbacid, M. (1996).** Renal agenesis and the absence of enteric neurons in mice lacking GDNF. *Nature* **382**, 70-73.

**Sanders, K. M. (2006).** Interstitial cells of Cajal at the clinical and scientific interface. *J Physiol* **576**, 683-687.

**Sandgren, K., Larsson, L. T. & Ekblad, E. (2002).** Widespread changes in neurotransmitter expression and number of enteric neurons and interstitial cells of Cajal in lethal spotted mice: an explanation for persisting dysmotility after operation for Hirschsprung's disease? *Dig Dis Sci* **47**, 1049-1064.

**Sato, T., Hamaoka, T., Aizawa, H., Hosoya, T. & Okamoto, H. (2007).** Genetic single-cell mosaic analysis implicates ephrinB2 reverse signaling in projections from the posterior tectum to the hindbrain in zebrafish. *J Neurosci* **27**, 5271-5279.

**Sato, Y. & Heuckeroth, R. O. (2008).** Retinoic acid regulates murine enteric nervous system precursor proliferation, enhances neuronal precursor differentiation, and reduces neurite growth in vitro. *Dev Biol* **320**, 185-198.

**Savidge, T. C., Newman, P., Pothoulakis, C., Ruhl, A., Neunlist, M., Bourreille, A., Hurst, R. & Sofroniew, M. V. (2007).** Enteric glia regulate intestinal barrier function and inflammation via release of S-nitrosoglutathione. *Gastroenterology* **132**, 1344-1358.

**Schaeren-Wiemers, N. & Gerfin-Moser, A. (1993).** A single protocol to detect transcripts of various types and expression levels in neural tissue and cultured cells: in situ hybridization using digoxigenin-labelled cRNA probes. *Histochemistry* **100**, 431-440.

**Schiltz, C. A., Benjamin, J. & Epstein, M. L. (1999).** Expression of the GDNF receptors ret and GFRalpha1 in the developing avian enteric nervous system. *J Comp Neurol* **414**, 193-211.

**Schlessinger, K., Hall, A. & Tolwinski, N. (2009).** Wnt signaling pathways meet Rho GTPases. *Genes Dev* **23**, 265-277.

**Schmidt, A. & Hall, A. (2002).** Guanine nucleotide exchange factors for Rho GTPases: turning on the switch. *Genes Dev* **16**, 1587-1609.

**Schuchardt, A., D'Agati, V., Larsson-Blomberg, L., Costantini, F. & Pachnis, V. (1994).** Defects in the kidney and enteric nervous system of mice lacking the tyrosine kinase receptor Ret. *Nature* **367**, 380-383.

**Seabra, M. C. (1998).** Membrane association and targeting of prenylated Ras-like GTPases. *Cell Signal* **10**, 167-172.

**Serbedzija, G. N., Burgan, S., Fraser, S. E. & Bronner-Fraser, M. (1991).** Vital dye labelling demonstrates a sacral neural crest contribution to the enteric nervous system of chick and mouse embryos. *Development* **111**, 857-866.

**Sharkey, K. A., Parr, E. J. & Keenan, C. M. (1999).** Immediate-early gene expression in the inferior mesenteric ganglion and colonic myenteric plexus of the guinea pig. *J Neurosci* **19**, 2755-2764.

**Shepherd, I. T. & Raper, J. A. (1999).** Collapsin-1/semaphorin D is a repellent for chick ganglion of Remak axons. *Dev Biol* **212**, 42-53.

**Shima, Y., Kengaku, M., Hirano, T., Takeichi, M. & Uemura, T. (2004).** Regulation of dendritic maintenance and growth by a mammalian 7-pass transmembrane cadherin. *Dev Cell* **7**, 205-216.

**Shima, Y., Kawaguchi, S. Y., Kosaka, K., Nakayama, M., Hoshino, M., Nabeshima, Y., Hirano, T. & Uemura, T. (2007).** Opposing roles in neurite growth control by two seven-pass transmembrane cadherins. *Nat Neurosci* **10**, 963-969.

**Shirsat, N. V., Pignolo, R. J., Kreider, B. L. & Rovera, G. (1990).** A member of the ras gene superfamily is expressed specifically in T, B and myeloid hemopoietic cells. *Oncogene* **5**, 769-772.

**Shnitsar, I. & Borchers, A. (2008).** PTK7 recruits dsh to regulate neural crest migration. *Development* **135**, 4015-4024.

**Simpson, M. J., Zhang, D. C., Mariani, M., Landman, K. A. & Newgreen, D. F. (2007).** Cell proliferation drives neural crest cell invasion of the intestine. *Dev Biol* **302**, 553-568.

**Smith, J., Cochard, P. & Le Douarin, N. M. (1977).** Development of choline acetyltransferase and cholinesterase activities in enteric ganglia derives from presumptive adrenergic and cholinergic levels of the neural crest. *Cell Differ* **6**, 199-216.

**Southard-Smith, E. M., Kos, L. & Pavan, W. J. (1998).** Sox10 mutation disrupts neural crest development in Dom Hirschsprung mouse model. *Nat Genet* **18**, 60-64.

**Srinivas, S., Watanabe, T., Lin, C. S., William, C. M., Tanabe, Y., Jessell, T. M. & Costantini, F. (2001).** Cre reporter strains produced by targeted insertion of EYFP and ECFP into the ROSA26 locus. *BMC Dev Biol* **1**, 4.

**Stach, W. (1989).** A revised morphological classification of neurons in the enteric nervous system. In *Nerves and the Gastrointestinal Tract*, pp. 29-45. Edited by M. V. Singer & H. Goebell. Lancaster, UK: MTP Press.

**Stach, W., Krammer, H. J. & Brehmer, A. (2000).** Structural organisation of enteric nerve cells in large mammals including man. In *Neurogastroenterology from the Basics to the Clinics*. Edited by H. J. Krammer & M. V. Singer. Dordrecht, Netherlands: Kluwer Academic Publishers.

**Stanchina, L., Baral, V., Robert, F., Pingault, V., Lemort, N., Pachnis, V., Goossens, M. & Bondurand, N. (2006).** Interactions between Sox10, Edn3 and Ednrb during enteric nervous system and melanocyte development. *Dev Biol* **295**, 232-249.

**Stemple, D. L. & Anderson, D. J. (1992).** Isolation of a stem cell for neurons and glia from the mammalian neural crest. *Cell* **71**, 973-985.

**Stewart, A. L., Young, H. M., Popoff, M. & Anderson, R. B. (2007).** Effects of pharmacological inhibition of small GTPases on axon extension and migration of enteric neural crest-derived cells. *Dev Biol* **307**, 92-104.

**Sugihara, K., Nakatsuji, N., Nakamura, K., Nakao, K., Hashimoto, R., Otani, H., Sakagami, H., Kondo, H., Nozawa, S., Aiba, A. & Katsuki, M. (1998).** Rac1 is required for the formation of three germ layers during gastrulation. *Oncogene* **17**, 3427-3433.

**Sundqvist, M. & Holmgren, S. (2006).** Ontogeny of excitatory and inhibitory control of gastrointestinal motility in the African clawed frog, Xenopus laevis. *Am J Physiol Regul Integr Comp Physiol* **291**, R1138-1144.

**Taraviras, S., Marcos-Gutierrez, C. V., Durbec, P., Jani, H., Grigoriou, M., Sukumaran, M., Wang, L. C., Hynes, M., Raisman, G. & Pachnis, V. (1999).** Signalling by the RET receptor tyrosine kinase and its role in the development of the mammalian enteric nervous system. *Development* **126**, 2785-2797.

**Taylor, M. K., Yeager, K. & Morrison, S. J. (2007).** Physiological Notch signaling promotes gliogenesis in the developing peripheral and central nervous systems. *Development* **134**, 2435-2447.

**Tennyson, V. M., Pham, T. D., Rothman, T. P. & Gershon, M. D. (1986).** Abnormalities of smooth muscle, basal laminae, and nerves in the aganglionic segments of the bowel of lethal spotted mutant mice. *Anat Rec* **215**, 267-281.

**Thapar, N. (2009).** New frontiers in the treatment of Hirschsprung disease. *J Pediatr Gastroenterol Nutr* **48 Suppl 2**, S92-94.

**Theveneau, E., Marchant, L., Kuriyama, S., Gull, M., Moepps, B., Parsons, M. & Mayor, R. (2010).** Collective chemotaxis requires contact-dependent cell polarity. *Dev Cell* **19**, 39-53.

**Thomas, P. S., Kim, J., Nunez, S., Glogauer, M. & Kaartinen, V. (2010).** Neural crest cell-specific deletion of Rac1 results in defective cell-matrix interactions and severe craniofacial and cardiovascular malformations. *Dev Biol* **340**, 613-625.

**Threadgill, R., Bobb, K. & Ghosh, A. (1997).** Regulation of dendritic growth and remodeling by Rho, Rac, and Cdc42. *Neuron* **19**, 625-634.

**Timmermans, J. P., Barbiers, M., Scheuermann, D. W., Bogers, J. J., Adriaensen, D., Fekete, E., Mayer, B., Van Marck, E. A. & De Groodt-Lasseel, M. H. (1994).** Nitric oxide synthase immunoreactivity in the enteric nervous system of the developing human digestive tract. *Cell Tissue Res* **275**, 235-245.

**Timmermans, J. P., Hens, J. & Adriaensen, D. (2001).** Outer submucous plexus: an intrinsic nerve network involved in both secretory and motility processes in the intestine of large mammals and humans. *Anat Rec* **262**, 71-78.

**Tissir, F., De-Backer, O., Goffinet, A. M. & Lambert de Rouvroit, C. (2002).** Developmental expression profiles of Celsr (Flamingo) genes in the mouse. *Mech Dev* **112**, 157-160.

**Tissir, F., Bar, I., Jossin, Y., De Backer, O. & Goffinet, A. M. (2005).** Protocadherin Celsr3 is crucial in axonal tract development. *Nat Neurosci* **8**, 451-457.

**Tissir, F. & Goffinet, A. M. (2006).** Expression of planar cell polarity genes during development of the mouse CNS. *Eur J Neurosci* **23**, 597-607.

**Torihashi, S., Ward, S. M. & Sanders, K. M. (1997).** Development of c-Kit-positive cells and the onset of electrical rhythmicity in murine small intestine. *Gastroenterology* **112**, 144-155.

**Uemura, T. & Shimada, Y. (2003).** Breaking cellular symmetry along planar axes in Drosophila and vertebrates. *J Biochem* **134**, 625-630.

**Uesaka, T., Jain, S., Yonemura, S., Uchiyama, Y., Milbrandt, J. & Enomoto, H. (2007).** Conditional ablation of GFRalpha1 in postmigratory enteric neurons triggers unconventional neuronal death in the colon and causes a Hirschsprung's disease phenotype. *Development* **134**, 2171-2181.

**Usui, T., Shima, Y., Shimada, Y., Hirano, S., Burgess, R. W., Schwarz, T. L., Takeichi, M. & Uemura, T. (1999).** Flamingo, a seven-pass transmembrane cadherin, regulates planar cell polarity under the control of Frizzled. *Cell* **98**, 585-595.

**Vanderwinden, J. M., Mailleux, P., Schiffmann, S. N., Vanderhaeghen, J. J. & De Laet, M. H. (1992).** Nitric oxide synthase activity in infantile hypertrophic pyloric stenosis. *N Engl J Med* **327**, 511-515.

**Vanderwinden, J. M. & Rumessen, J. J. (1999).** Interstitial cells of Cajal in human gut and gastrointestinal disease. *Microsc Res Tech* **47**, 344-360.

**Vannucchi, M. G. & Faussone-Pellegrini, M. S. (1996).** Differentiation of cholinergic cells in the rat gut during pre- and postnatal life. *Neurosci Lett* **206**, 105-108.

**Vannucchi, M. G. & Faussone-Pellegrini, M. S. (2000).** Synapse formation during neuron differentiation: an in situ study of the myenteric plexus during murine embryonic life. *J Comp Neurol* **425**, 369-381.

**Vastrik, I., Eickholt, B. J., Walsh, F. S., Ridley, A. & Doherty, P. (1999).** Sema3A-induced growth-cone collapse is mediated by Rac1 amino acids 17-32. *Curr Biol* **9**, 991-998.

**Veeman, M. T., Axelrod, J. D. & Moon, R. T. (2003).** A second canon. Functions and mechanisms of beta-catenin-independent Wnt signaling. *Dev Cell* **5**, 367-377.

**Vigorito, E., Bell, S., Hebeis, B. J., Reynolds, H., McAdam, S., Emson, P. C., McKenzie, A. & Turner, M. (2004).** Immunological function in mice lacking the Rac-related GTPase RhoG. *Mol Cell Biol* **24**, 719-729.

**Vincent, S., Jeanteur, P. & Fort, P. (1992).** Growth-regulated expression of rhoG, a new member of the ras homolog gene family. *Mol Cell Biol* **12**, 3138-3148.

**Vivancos, V., Chen, P., Spassky, N., Qian, D., Dabdoub, A., Kelley, M., Studer, M. & Guthrie, S. (2009).** Wnt activity guides facial branchiomotor neuron migration, and involves the PCP pathway and JNK and ROCK kinases. *Neural Dev* **4**, 7.

**Vohra, B. P., Fu, M. & Heuckeroth, R. O. (2007).** Protein kinase Czeta and glycogen synthase kinase-3beta control neuronal polarity in developing rodent enteric neurons, whereas SMAD specific E3 ubiquitin protein ligase 1 promotes neurite growth but does not influence polarity. *J Neurosci* **27**, 9458-9468.

**Wada, H., Tanaka, H., Nakayama, S., Iwasaki, M. & Okamoto, H. (2006).** Frizzled3a and Celsr2 function in the neuroepithelium to regulate migration of facial motor neurons in the developing zebrafish hindbrain. *Development* **133**, 4749-4759.

**Wada, H. & Okamoto, H. (2009).** Roles of planar cell polarity pathway genes for neural migration and differentiation. *Dev Growth Differ* **51**, 233-240.

**Wahl, S., Barth, H., Ciossek, T., Aktories, K. & Mueller, B. K. (2000).** Ephrin-A5 induces collapse of growth cones by activating Rho and Rho kinase. *J Cell Biol* **149**, 263-270.

**Wallace, A. S. & Burns, A. J. (2005).** Development of the enteric nervous system, smooth muscle and interstitial cells of Cajal in the human gastrointestinal tract. *Cell Tissue Res* **319**, 367-382.

**Walmsley, M. J., Ooi, S. K., Reynolds, L. F., Smith, S. H., Ruf, S., Mathiot, A., Vanes, L., Williams, D. A., Cancro, M. P. & Tybulewicz, V. L. (2003).** Critical roles for Rac1 and Rac2 GTPases in B cell development and signaling. *Science* **302**, 459-462.

**Walters, J. R., Bishop, A. E., Facer, P., Lawson, E. M., Rogers, J. H. & Polak, J. M. (1993).** Calretinin and calbindin-D28k immunoreactivity in the human gastrointestinal tract. *Gastroenterology* **104**, 1381-1389.

**Wang, Y., Thekdi, N., Smallwood, P. M., Macke, J. P. & Nathans, J. (2002).** Frizzled-3 is required for the development of major fiber tracts in the rostral CNS. *J Neurosci* **22**, 8563-8573.

**Wang, Y., Guo, N. & Nathans, J. (2006).** The role of Frizzled3 and Frizzled6 in neural tube closure and in the planar polarity of inner-ear sensory hair cells. *J Neurosci* **26**, 2147-2156.

**Wang, Y. & Nathans, J. (2007).** Tissue/planar cell polarity in vertebrates: new insights and new questions. *Development* **134**, 647-658.

**Wang, H., Hughes, I., Planer, W., Parsadanian, A., Grider, J. R., Vohra, B. P., Keller-Peck, C. & Heuckeroth, R. O. (2010).** The timing and location of glial cell line-derived neurotrophic factor expression determine enteric nervous system structure and function. *J Neurosci* **30**, 1523-1538.

**Weber, A., Wienker, T. F., Jung, M., Easton, D., Dean, H. J., Heinrichs, C., Reis, A. & Clark, A. J. (1996).** Linkage of the gene for the triple A syndrome to chromosome 12q13 near the type II keratin gene cluster. *Hum Mol Genet* **5**, 2061-2066.

**Wells, C. M., Walmsley, M., Ooi, S., Tybulewicz, V. & Ridley, A. J. (2004).** Rac1-deficient macrophages exhibit defects in cell spreading and membrane ruffling but not migration. *J Cell Sci* **117**, 1259-1268.

**Wilson, Y. M., Richards, K. L., Ford-Perriss, M. L., Panthier, J. J. & Murphy, M. (2004).** Neural crest cell lineage segregation in the mouse neural tube. *Development* **131**, 6153-6162.

**Wood, J. D. (1981).** Intrinsic neural control of intestinal motility. *Annu Rev Physiol* **43**, 33-51.

**Woodward, M. N., Kenny, S. E., Vaillant, C., Lloyd, D. A. & Edgar, D. H. (2000).** Time-dependent effects of endothelin-3 on enteric nervous system development in an organ culture model of Hirschsprung's disease. *J Pediatr Surg* **35**, 25-29.

**Wu, J. J., Chen, J. X., Rothman, T. P. & Gershon, M. D. (1999).** Inhibition of in vitro enteric neuronal development by endothelin-3: mediation by endothelin B receptors. *Development* **126**, 1161-1173.

**Yin, X., Watanabe, M. & Rutishauser, U. (1995).** Effect of polysialic acid on the behavior of retinal ganglion cell axons during growth into the optic tract and tectum. *Development* **121**, 3439-3446.

**Ying, G., Wu, S., Hou, R., Huang, W., Capecchi, M. R. & Wu, Q. (2009).** The protocadherin gene Celsr3 is required for interneuron migration in the mouse forebrain. *Mol Cell Biol* **29**, 3045-3061.

**Yntema, C. L. & Hammond, W. S. (1954).** The origin of intrinsic ganglia of trunk viscera from vagal neural crest in the chick embryo. *J Comp Neurol* **101**, 515-541.

**Yoshikawa, S., McKinnon, R. D., Kokel, M. & Thomas, J. B. (2003).** Wnt-mediated axon guidance via the Drosophila Derailed receptor. *Nature* **422**, 583-588.

**Young, H. M., Hearn, C. J., Ciampoli, D., Southwell, B. R., Brunet, J. F. & Newgreen, D. F. (1998).** A single rostrocaudal colonization of the rodent intestine by enteric neuron precursors is revealed by the expression of Phox2b, Ret, and p75 and by explants grown under the kidney capsule or in organ culture. *Dev Biol* **202**, 67-84.

**Young, H. M., Torihashi, S., Ciampoli, D. & Sanders, K. M. (1998).** Identification of neurons that express stem cell factor in the mouse small intestine. *Gastroenterology* **115**, 898-908.

**Young, H. M., Ciampoli, D., Hsuan, J. & Canty, A. J. (1999).** Expression of Ret-, p75(NTR)-, Phox2a-, Phox2b-, and tyrosine hydroxylase-immunoreactivity by undifferentiated neural crest-derived cells and different classes of enteric neurons in the embryonic mouse gut. *Dev Dyn* **216**, 137-152.

**Young, H. M., Hearn, C. J., Farlie, P. G., Canty, A. J., Thomas, P. Q. & Newgreen, D. F. (2001).** GDNF is a chemoattractant for enteric neural cells. *Dev Biol* **229**, 503-516.

**Young, H. M. & Newgreen, D. (2001).** Enteric neural crest-derived cells: origin, identification, migration, and differentiation. *Anat Rec* **262**, 1-15.

**Young, H. M., Jones, B. R. & McKeown, S. J. (2002).** The projections of early enteric neurons are influenced by the direction of neural crest cell migration. *J Neurosci* **22**, 6005-6018.

**Young, H. M., Bergner, A. J. & Muller, T. (2003).** Acquisition of neuronal and glial markers by neural crest-derived cells in the mouse intestine. *J Comp Neurol* **456**, 1-11.

**Young, H. M., Bergner, A. J., Anderson, R. B., Enomoto, H., Milbrandt, J., Newgreen, D. F. & Whitington, P. M. (2004).** Dynamics of neural crest-derived cell migration in the embryonic mouse gut. *Dev Biol* **270**, 455-473.

**Young, H. M., Turner, K. N. & Bergner, A. J. (2005).** The location and phenotype of proliferating neural-crest-derived cells in the developing mouse gut. *Cell Tissue Res* **320**, 1-9.

**Young, H. M. (2008).** On the outside looking in: longitudinal muscle development in the gut. *Neurogastroenterol Motil* **20**, 431-433.

**Zalcman, G., Dorseuil, O., Garcia-Ranea, J. A., Gacon, G. & Camonis, J. (1999).** RhoGAPs and RhoGDIs, (His)stories of two families. *Prog Mol Subcell Biol* **22**, 85-113.

**Zallen, J. A. (2007).** Planar polarity and tissue morphogenesis. *Cell* **129**, 1051-1063.

**Zhang, W., Segura, B. J., Lin, T. R., Hu, Y. & Mulholland, M. W. (2003).** Intercellular calcium waves in cultured enteric glia from neonatal guinea pig. *Glia* **42**, 252-262.

**Zhang, X., Zhu, J., Yang, G. Y., Wang, Q. J., Qian, L., Chen, Y. M., Chen, F., Tao, Y., Hu, H. S., Wang, T. & Luo, Z. G. (2007).** Dishevelled promotes axon differentiation by regulating atypical protein kinase C. *Nat Cell Biol* **9**, 743-754.

**Zhou, L., Bar, I., Achouri, Y., Campbell, K., De Backer, O., Hebert, J. M., Jones, K., Kessaris, N., de Rouvroit, C. L., O'Leary, D., Richardson, W. D., Goffinet, A. M. & Tissir, F. (2008).** Early forebrain wiring: genetic dissection using conditional Celsr3 mutant mice. *Science* **320**, 946-949.

**Zhu, L., Lee, H. O., Jordan, C. S., Cantrell, V. A., Southard-Smith, E. M. & Shin, M. K. (2004).** Spatiotemporal regulation of endothelin receptor-B by SOX10 in neural crest-derived enteric neuron precursors. *Nat Genet* **36**, 732-737.

**Zipkin, I. D., Kindt, R. M. & Kenyon, C. J. (1997).** Role of a new Rho family member in cell migration and axon guidance in C. elegans. *Cell* **90**, 883-894.

**Zou, Y. & Lyuksyutova, A. I. (2007).** Morphogens as conserved axon guidance cues. *Curr Opin Neurobiol* **17**, 22-28.